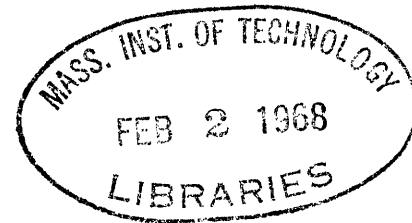A PRELIMINARY INVESTIGATION OF
THE FORMATION OF CARBON BLACK
BY THE PYROLYSIS OF RESIDUAL FUEL OIL

by

Alvin E. Witt

B,S., Michigan State University
(1960)

S. M., Massachusetts Institute of Technology
(1966)

Submitted in Partial Fulfillment

of the Requirements for the

Degree of Doctor of Science

at the

MASSACHUSETTS INSTITUTE OF TECHNOLOGY

January 8, 1968

Signature of Author:____
Department of Chemical Engineering
January 8, 1968

Certified by
'Thesis 'Supervisors

Accepted by:____
Chairman,
Departmental Committee on Graduate Theses

ABSTRACT

A PRELIMINARY INVESTIGATION OF
THE FORMATION OF CARBON BLACK
BY THE PYROLYSIS OF RESIDUAL FUEL OIL

by

Alvin E. Witt

Submitted to the Department of Chemical Engineering in partial fulfillment of the requirements for the degree of Doctor of Science.

The objectives of this investigation were to study the process of carbon black formation and to determine the important process parameters and their influence on carbon black properties. These goals were accomplished in a series of experiments in which process parameters were systematically varied. The parameters included the reactor temperature (2000 to 2900°F), the residence time (40 to 100 milliseconds), and the drop size of the feed material (28 to 100 microns). Feed materials consisted of two commercial carbon black oils and Naphthalene. This program demonstrated how processing conditions affect the size and structure of the carbon black particles.

The formation of carbon black can be considered as a nucleation step followed by simultaneous gas phase and surface reactions. The nucleation step has a high activation energy and is the most important step in the formation process. The size and structure of the carbon black are strongly influenced by the conditions of nucleation.

The gas phase reaction generates species which add to the carbon nuclei. The activation energy for this process depends on the feed stock and was between 35 and 45 Kcal per mole for the materials used in this study.

The surface growth reaction and an apparent activation energy of 3 and 6 Kcal per mole for the two residual oils and 7 Kcal per mole for the Naphthalene.

This study indicates that the process of nucleation must be studied in depth before one can optimize the conditions for carbon black production.

Thesis Supervisors: Hoyt C. Hottel
Professor of Fuel Engineering

Glenn C. Williams
Professor of Chemical Engineering

William H. Dalzell
Professor of Chemical Engineering

Department of Chemical Engineering
Massachusetts Institute of Technology
Cambridge, Massachusetts 02139
January 8, 1968

Professor Edward N. Hartley
Secretary of the Faculty
Massachusetts Institute of Technology
Cambridge, Massachusetts 02139

Dear Professor Hartley:

In accordance with the regulations of the Faculty, I herewith
submit a thesis, entitled "A Preliminary Investigation of the
Formation of Carbon Black by the Pyrolysis of Residual Fuel Oil"
in partial fulfillment of the requirements for the degree of Doctor
of Science in Chemical Engineering at the Massachusetts Institute of
Technology.

Respectfully submitted,

Alvin E. Witt

AEW/lkp

Acknowledgements

The subject of this study was suggested to the author by his thesis supervisor, Professor G. C. Williams. His moral support and interest during the period of this investigation was greatly appreciated. The interest and guidance of my other thesis supervisors, Professors Hottel and Dalzell was very much appreciated.

The interest of Professor J. B. Howard in carbon formation and the resultant long hours of discussion will always be remembered.

The value of the financial and technical assistance, as well as the comradeship, that the author received from the personnel of Cabot Corporation is immeasurable. Special thanks are due to R. Antonsen for his efforts and interest throughout the program, to D. Harling for electron microscope pictures and their interpretation, and to L. Doppler and his associates for the solids analyses and their subsequent interpretation, and finally, to Dr. A. C. Morgan and all his associates at Cabot's Billreca Laboratories for their interest and assistance.

Thanks are due to Herb Passler for his many helpful suggestions and his aid in construction of the apparatus.

The many useful discussions and the comradeship of my fellow researchers, R. Gurnitz, G. Kwentus, E. Matulevicius, J. Noble, D. Reed and I. Vasalos will long be remembered.

Financial support for this project was supplied by Cabot Corporation and the author received personal support from a National Science Foundation Traineeship.

Table of Contents

Index to Figures

Index to Tables

I. SUMMARY

Historically, the existence of carbon black or soot has been both
a blessing and a problem. The ancients collected carbon black from
flames and used it in inks and paints. Flames containing soot have
long been used as light sources or to increase heat transfer by radiation,
but improper conditions caused carbon to deposit in undesirable locations.
Even today, carbon is deposited in internal comustion engines or goes up
smoke stacks, where it becomes a major source of air pollution.
Currently, carbon black uses range from a filler in rubber (where it
increases tire life) to a filter for the clarification of fine wines.
These applications require the production of billions of pounds per year
of carbon black. Both the control of soot and the production of carbon
black require a solid understanding of the formation and growth process.

It was the objective of the present work to study the variables
which control the rate of formation and the quantities of carbon black
derived from residual fuel oils and from the results of these studies to
try to clarify and add to the current models which attempt to describe
the complex carbon formation process. From a practical viewpoint, it
is desirable to learn the relative importance of process parameters
and to understand how these variable alter the physical properties of
the carbon black. In addition, an understanding of the formation
process should permit better control of carbon formation and allow the
optimization of the process.

The above objective was accomplished by an experimental program
in which the range of the controlled experimental variables encompassed
most production operating conditions. The controlled variables were
the type of oil, the fineness of the oil atomization, and the reactor

temperature and residence time. The black making characteristics of two slightly different commercial residual fuel oils Cosden Tar (CT) and Aromatic Concentrate (AC) were compared to those of pure Naphthalene (N). These materials were disintegrated into uniformly sized drops on a spinning disk atomizer. Drops with diameters of either 28, 64 or 100 microns were mixed with the combustion products of a natural gas-air flame. These hot gases supplied the energy to vaporize and pyrolyze the feed materials. The combustion gases and oil were reacted in a laminar flow reactor which was operated at temperatures of from 2000 to 2900°F. The reaction time or residence time was varied from 40 to 100 milliseconds. After the desired time, the reaction mixture was quenched with steam and the gas and solid samples were collected. These samples were analyzed and variations between samples were studied as a function of the processing conditions.

The most important responses to process variations were the yield of carbon black and the particle size of the carbon black. The latter was determined from electron micrographs. In addition to these responses, the samples were analyzed for surface area, absorptivity (scale), hiding power (tint), and the percent extractable. These analyses are all important industrial quality control tests.

In the following discussions, it is assumed that "the ideal carbon black process" has a high yield and produces a material with a high surface area, a high absorptivity, a short chain length, a small diameter, and with a low concentration of extractables. It is important to note that the carbon black produced during this study was similar in morphology and microstructure to production blacks of the larger particle sizes. But poor nucleation conditions prevented

the production of small particle size, low extract carbon blacks in this experimental equipment.

The process of carbon formation can be considered as a nucleation step followed by simultaneous gas phase and surface reactions. Nucleation is the most important step in the formation process. The nucleation conditions determine the size and number of the original particles, which in turn affect the final size, surface area, chain length, and percent extractable of the carbon black particles. After the appearance of nuclei, growth occurs by the rapid surface addition of the species which were produced by gas phase reactions.

The most extensive studies of the nucleation process are those of Tesner (1) on toluene and a higher aromatic similar to kerosene in volatility. Tesner's flow system was turbulent, the present is laminar; he was able to sample in the nucleation period, in the present apparatus nucleation was distributed over a time period 10 to 20 times that observed by Tesner.

In addition, in the present apparatus nucleation occurred long before the first sampling point; however, it is still possible to make meaningful comparisons with Tesner's work. First, the nucleation process in both the present and in Tesner's work had an activation energy of over 100 Kcal per mole, and the rate data could be fitted by a free radical rate expression. Second, nucleation began very soon after the reactants were mixed and ceased when reactant concentrations were still high.

In the present experiments, the observed variation in the size of particles at the first sampling point was explained by the fact that the nucleation time was short (Tesner reports 10^{-4} seconds) compared

to the one to seven millisecond vaporization time of the drops and thus the first particles to form had a longer time to grow. The larger oil drops formed more particles because nucleation occurred in a region of higher concentration. The rapid agglomeration of these small particles combined with surface growth made it impossible to determine whether or not a secondary nucleation occurred.

In summary, nucleation is considered to be a high activation energy process with possible radical characteristics. It occurs very rapidly and terminates while reactant concentrations are still high. In terms of the "ideal black process", nucleation is then very important. A high temperature system with thorough rapid mixing (good nucleation conditions) produces large numbers of small particles. Extractable material can be rapidly boiled from these small particles, and, therfore, the reaction can be quenched after a short residence time. This can result in a high yield process which produces small, short chained particles.

Once the particles have nucleated, agglomeration and growth occur simultaneously. The former causes the number of particles to decrease and narrows the observed range of particle diameters. As the particles agglomerate, gas phase reactions generate species which add to the surface of the particles in a rapid surface reaction. Homann and Wagner (2), working with low pressure flames, have reported that in acetylene and benzene flames growth occurs by the surface decomposition of poly-acetylenes and polycyclic aromatics, respectively. In this program, differences were also observed in the growth process for the different feed materials.

The assumption that growth occurs mainly by collision between a gas molecule and a carbon particle sheds some light on the gas phase process.

Collision theory yields the following relationship for growth by a gas molecule collision with a carbon particle.

$$\frac{dC}{dt} = \text{constant} \ (Ns)^{1/3}(C)^{2/3} \ \frac{X}{T^{1/2}} \ \exp(^{-E}/RT) \qquad (1\text{-}1)$$

Here C is the concentration of carbon black and Ns is the number of particles. X is the mole fraction of fuel and in the simple treatment of Foster (3) it was assumed that the concentration of the actual adding species would be proportional to X. As mentioned previously, in the present experiments, nucleation occurred during the vaporization of the droplet; hence, during this time, nucleation, growth and agglomeration occurred simultaneously. Later in the process, only growth and agglomeration occurred. However, it is quite probable that the concentration of the adding species instead of being simply proportional to X may vary both in nature and in propertionality to X depending upon the conditions of nucleation. Then addording to the proposed three step formation model, for the present experiments the activation Energy (E) in equation (1-1) will be influenced by the nucleation reaction (En), the gas phase reaction (Eg), and the surface reaction (Es). Since the activation energy for nucleation was over 100 Kcal per mole, nucleation may strongly influence the value of E determined from this equation. When equation (1-1) was solved using the present experimental results for three different materials under similar conditions (64 micron drops), the values of E were 35 Kcal per mole (CT), 45 Kcal per mole (AC), and 41 Kcal per mole (N). The influence of the nucleation conditions was seen from the fact that for Cosden Tar (where the number of nuclei varied due to drop size), the values of E were 18, 35 and 50 Kcal per mole with increasing drop sizes of 28, 64 and 100 microns. All values of E were less than the 57.6 Kcal

per mole reported by Foster who used methane as a feed stock, but comparable to the 30-40 Kcal per mole reported by Homann (4).

Obviously, equation (1-1) cannot be expected to predict anything about particle growth if a major fraction of the growth process occurs by agglomeration. In this case, the apparent activation energy for particle growth would be expected to show little influence of the gas phase generation of adding species and would thus have a low value. The change in size of the particles with time fitted a volumetric growth law, i.e., the rate was proportional to the amount of material present. However, reasonable fits of the data were also obtained for a diffusional, or a surface-area limited process. The accuracy of particle size, as determined from electron micrographs, does not permit an absolute selection of a growth model. The activation energies determined from the variation of size with time and temperature were 3 Kcal per mole for the Cosden Tar, 6 Kcal per mole for the Aromatic Concentrate, and 7 Kcal per mole for the Naphthalene. These values are close to the 3-7 Kcal per mole reported by Tesner (5).

After the analysis of the formation process, it was possible to reach some conclusions regarding the variation of the other product characteristics. As one would predict for a growth process, the surface areas of the carbon black decreased with increased residence time. Since high surface area is desirable, it is important to quench the mixture as soon as the extractable had boiled off.

The scale is an industrially important parameter which is related to the absorptivity or blackness of the carbon particles. Industrially, this parameter is correlated with particle size. The correlation with size did not hold for this study. Regions of growth showed an increase in scale but not at a rate commensurate with the observed change in

size. In addition, particles with widely different diameters were observed
to have the same scale. These variations were probably due to variations
in chemical composition which will affect the particle absorptivity.

Industrially, the percent tint is considered as a measure of the
hiding power of the particles. It was found that the tint is a measure
of the particle chain length. This measure of chain length passed through
a minimum with residence time. This can be explained if one assumes that
the particle-to-particle bonds in the reactor are relatively weak and
depend on the amount of extractable, and then these bonds could be fractured
by collisions or chain movements. Initially, the particle cohesion is
due to the stickiness of the extractable material which is gradually
removed, thus weakening the bonding so that collisions at this stage
may rupture the chains; later in the process the colliding particles
are bonded by linkages similar in strength to those within the particles.

In conclusion, it has been shown that the carbon black formation
process can be considered as a process of nucleation, followed by gas
phase reaction and growth. The nucleation step is the most important
and needs to be investigated in depth to permit optimization of processing
conditions.

II. INTRODUCTION

The production of carbon black dates back to ancient Rome and
China where oil flames were impinged on cold surfaces to produce carbon
black for use in paints and inks. Since 1864 this industry has grown from
a few hundred pounds per year to the production of 2.7×10^9 pounds (6) in
1964. Of this total, the furnace process accounted for 2.3×10^9 pounds
while 0.201×10^9 and 0.245×10^9 pounds were made by the channel and
thermal processes, respectively. Roughly 95% of all carbon black is used
as a filler in rubber products, with one of the major uses being a filler
in automobile tires. Approximately 60 years ago it was discovered that
carbon black greatly increases the strength and wear resistance of natural
rubber products. It is carbon black that has increased the expected life
of a tire from 3,000 miles up to 30,000 to 40,000 miles. Today, approximately
one-third, by wieght, of an automobile tire is carbon black.

In addition to use in rubber industry, carbon black is used in paints,
radio resistors, inks, explosives, and as a filter for the clarification
of fine wines. It is widely used because it is relatively cheap, chemically
inert, and available in a wide range of sizes and properties with a consistent
quality.

2.1 Definition of the Problem

Historically, the carbon black industry has followed a pattern of
evolution. As researchers have developed new analytical techniques for
characterizing blacks and new processes, the production people have
installed the new process and varied processing parameters in an effort
to find the effect of processing parameters on black properties. However,
the main emphasis has always been on producing carbon black. This type of
progress, combined with increasing costs and decreasing availability of
natural gas led to the use of residual oil as a feed stock. Because the oil

process gave blacks with unique properties and higher yields than did the natural gas process. The production of oil blacks increases every year.

As competition increases, it is becoming more and more critical to determine optimum operating conditions and also to learn the effect of these parameters on the properties of carbon black. Even though, in the final analysis, the important fact will be how the carbon black affects its rubber partner and the process economics.

Close examination of Figure 2-1, which is a rough schematic of one type of oil black furnace, helps to point out the reasons why it is so difficult to optimize black properties and to determine the parameter interactions in a conventional furnace. In this furnace, the natural gas and air enter the reaction zone tangentially and form the primary fire. The atomized oil is injected into the center of the swirling blast gases. The mixture of combustion products and oil then flow through the 12 inch diameter by 12 foot long furnace. The oxygen content of the furnace gases is such that if the mixture were allowed to reach equilibrium all of the carbon would be gasified. At the end of the furnace, when the carbon black is fully developed, the reaction mixture is quenched to approximately 800°F with water. It is obvious that the time-temperature history of the oil or carbon black particle is very difficult to determine in this swirling turbulent gas. In addition, both bi-fluid and pressure atomizers produce a wide range of drop sizes, and this makes it difficult to determine the effect of the fineness of atomization on black structure.

Ideally, one desires to make a fine (small) carbon particle with a high degree of structure (chaining). High temperatures favor fine particles but also increase the rate of consumption of carbon by reactions (2-1) and (2-2).

$$C + H_2O \longrightarrow CO + H_2 \qquad\qquad (2-1)$$

$$C + CO_2 \longrightarrow 2CO \qquad\qquad (2-2)$$

OIL BLACK FURNACE

Figure 2-1

Oil →

Reaction Zone

Air Fuel

Water
Quench
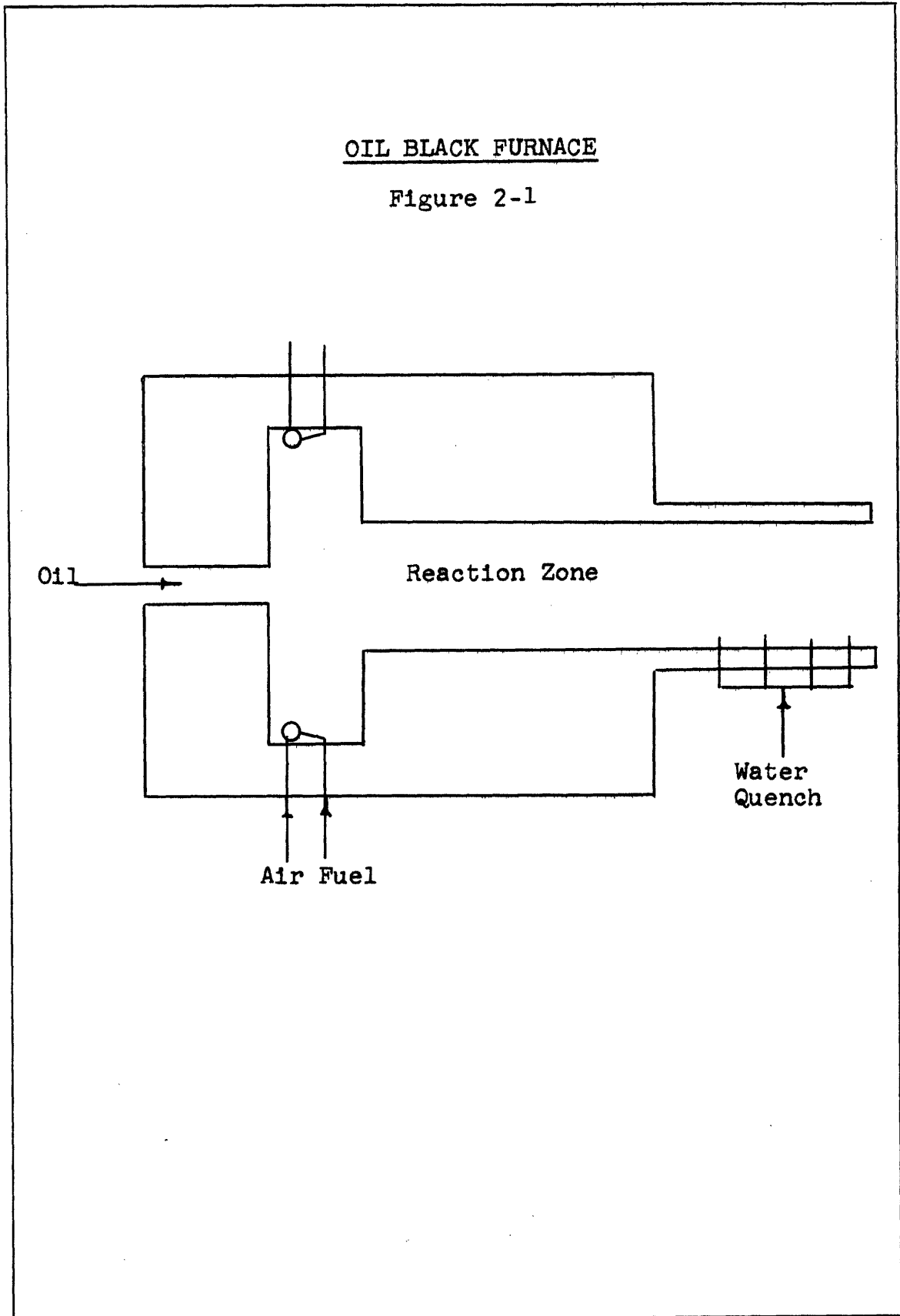
Therefore, one would like to determine optimum conditions for a high yield, a high degree of chaining and a small size. In addition, it is desirable to be able to predict the effect of changes in temperature, residence time, drop size and starting material on the physical and chemical properties of the black.

It was the purpose of this thesis to conduct a controlled experimental program in which the process variables of temperature, drop size, and residence time were systematically varied. From this work, general trends of the effect of process parameters on the black properties were determined, and more insight was gained into the formation process. These tests also defined areas that warrant more investigation. Before going into the experimental program in depth, it is first desirable to review the current state of the art.

2.2 Literature Survey

The subject of dispersed carbon formation is like a maze, with many plausible roads pointing the direction to truth. There are numerous theories on carbon formation, but as yet none of these are able to answer all of the questions on the mechanism of nucleation, growth or the origin of the final chain structure of the black. Because of the magnitude of the problem, only the highlights of carbon formation are covered in this section. First, the current picture of the physical and chemical properties of carbon black is discussed. This is followed by a review of the status of prominent theories on dispersed carbon formation. Next, a discussion of the commercial production of carbon black is given to place the goals of this thesis in their proper perspective. And finally, a brief survey of liquid atomization techniques is given.

2.21 Physical and Chemical Properties of Carbon Black

The nature of carbon black particles has been investigated using x-ray diffraction, light scattering, electron miscroscopy, and mass

spectrometry. (7) (8). A very simplified model of carbon black is shown in Figure 2-2. Electron micrographs have shown that in thermal blacks (the different black processes are described in section 2.231) there are often discrete spherical particles, while in channel blacks most of the particles are in a chain structure with very few discrete particles. Furnace blacks are the extreme case and are almost always fused into a peanut structure forming aggregates. Often it is very difficult to define a meaningful particle size in these large aggregates. In this experimental program the particle size is considered to be the diameter of the nodules, as indicated on the figure. In practice, this dimension can vary from 40 to 2,000 $\overset{o}{A}$ depending on the age (elapsed time from nucleation) of the particles. Each particle or nodule is composed of up to 10^4 crystallites with each crystallite contining from 5 to 10 layer planes of carbon atoms. These layer planes are identical to the layer planes in graphite. However, in contrast to graphite, the carbon atoms in adjoining layers are not stacked on top of each other. It is because of this structure that carbon black is not crystalline or amorphous but an intermediate state called "turbostratic". An average carbon nodule can contain in the layer plane structure as many as 10^5 to 10^6 carbon atoms. One important problem in defining a mechanism of carbon formation is to describe a route whereby simple fuel molecules, containing a few carbon atoms, can be converted in only fractions of a millisecond, into these large aggregates.

It has been found that hydrogen and oxygen are covalently bonded into the black structure. The chemical composition of the chain structure varies from 1/2 to 1-1/2% of hydrogen and up to 8% oxygen on a weight basis.

Another property which may be of use in this study is the complex refractive index which depends on the H/C ratio but is independent of size or state of aggregation (9). The complex refractive index of an absorbing

CARBON BLACK CHAIN

Figure 2-2

d
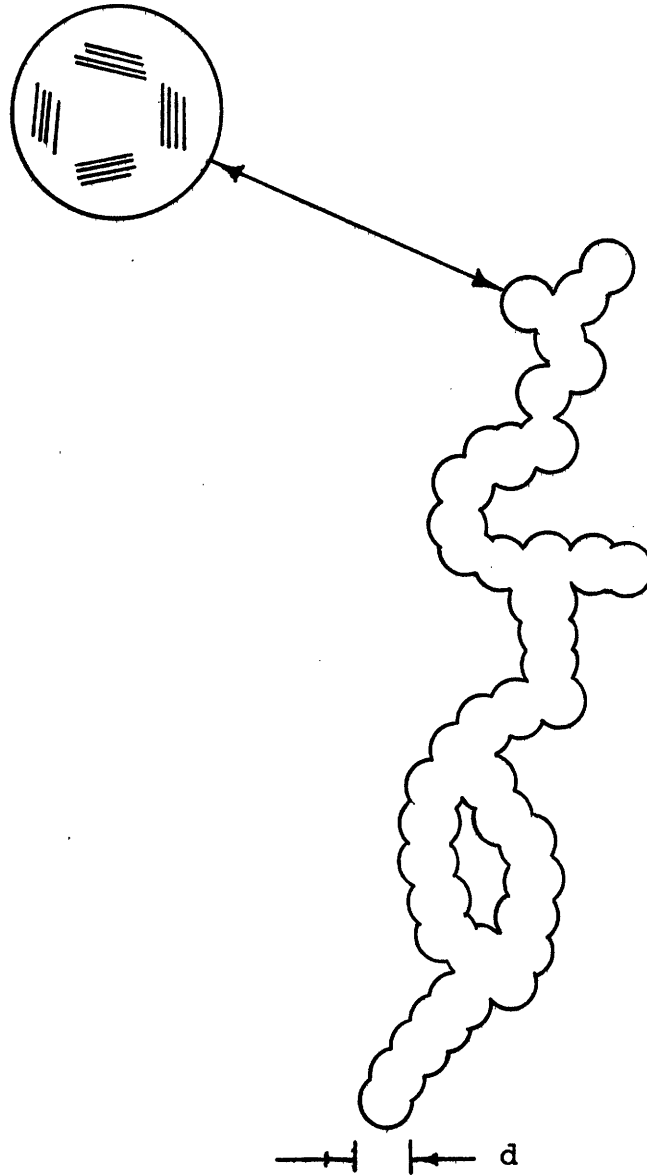
medium for light of a wavelength λ, is given by the following equation:

$$m = n_\lambda - in'_\lambda \tag{2-3}$$

Here n is the normal refractive index or the ratio of the velocity of light in a vacuum to the velocity in the medium, and n' is the absorption constant. This constant is related to the absorption coefficient by equation (2-4).

$$\gamma = 4\pi n'/\lambda \tag{2-4}$$

In addition to these more conventional methods of describing carbon black, the industry has many tests (10) for characterizing carbon black. The tests used in evaluating the product from this experimental program were scale, nitrogen surface area, tinting strength, and benzene extract. Specific details on some of these tests are given in Appendix C. Scale is a measure of the diffuse reflectance from a carbon black-varnish dispersion. For oil furnace blacks it varies from 83 to 96. Surface areas and benzene extracts for similar materials vary from 30 to 220 m^2/gram and from 0.02 to 6.0%, respectively. Generally, the percent extract is less than 0.1%. The tinting strength is a measure of the hiding power of the black and on an arbitrary scale varies from 83 to 250%.

This description on the morphology of carbon black, although brief, is adequate as a basis for discussion of carbon black formation.

2.22 Formation of Dispersed Carbon

A complete description of carbon formation in flames has not been produced, even though a large amount of work has been directed towards attaining an understanding of this process. The root of the difficulty lies in the fact that the whole process of carbon formation, which performs the feat of converting the carbon contained in gaseous hydrocarbon molecules into relatively large and neatly structured solid particles, occurs in a time of only about 10^{-4} seconds. To observe, let alone to measure the

details of such rapid events, is extremely difficult. Nevertheless,
a large number of experimental observations on the various aspects of carbon
formation have been compiled and are available for testing the various
hypothesis which might be proposed. The published literature is generally
concerned with carbon formation in flames and, therefore, in many cases
it will be necessary to try to extend this information into the region of
industrial oil black furnaces.

In the last section, the physical properties of carbon black were
described briefly. This structure should be kept in mind, since it is
this complex structure that makes it difficult to describe a mechanism
or a series of mechanisms for carbon black formation. Before discussing
the theories of carbon formation, it is first necessary to provide some
background information. In this section, we begin by reviewing ion
formation, ion identification and ion concentration in flames. In the
final analysis, all of these topics aid in model development. Then the
general phenomena which have been observed during carbon formation are
discussed. With these facts presented, several models of carbon black
formation are briefly outlined. Finally, recent pertinent experimental work
is both discussed in detail and summarized.

2.221 **Ion Formation in Flames** In recent years, van Tiggelen (11),
Calcote (12), and Thring (13), among others, have been trying to find
answers to the questions of: How are the ions formed? What is their
concentration? What is the nature of the ion? All three of these
problems are interconnected because the mechanism proposed for production
must be able to predict the number, as well as the type, of ions that
are found in the flame. The most obvious source of ions is thermal
ionization, i.e., ionization which is controlled by the concentration
of species of low ionization potential present in the flame. This

includes the ionization of (1) impurities (such as metallic species),
(2) equilibrium and non-equilibrium species present at flame temperatures,
and (3) carbon or soot particles. In many cases there are not enough
impurities present to produce a significant number of ions. Even if
there were, the ionization of impurities, as well as equilibrium and non-
equilibrium species, would be very dependent upon temperature and this
is not the case. As an example, large concentrations of ions are found
in relatively cool hydrocarbon flames. It was probably Stern (14) who
first suggested that the positively charged particles were carbon.
The reasoning behind this assumption is that most simple molecules and
atoms present in reacting systems, including free radicals, have ionization
potentials of over 10 electron volts. Since the most energetic hydro-
carbon flame reaction gives off only about 4 electron volts, chances of
ionization are small. On the other hand, carbon has a thermionic work
function of approximately 4 electron volts, and, therefore, it stands
a good chance of becoming ionized. Hence, carbon or soot probably comes
from the dehydrogenation and ionization of the hydrocarbon molecule.

    2.222 Ion Concentration. Thermal considerations alone do not
account for the large number of ions, i.e., 10^{11} to 10^{12} ions per cubic
centimeter that are found in flames. Nor can these considerations
account for the fact that the ion concentration is greater in the reaction
zone than in the hot gases. Chemi-ionization (15) has been proposed as a
mechanism for accounting for the remainder of the ions. It has been
shown that chemi-ionization is possible in flames, but it is very
complicated because of the presence of a large number of species. Some
proposed reactions that could account for some of the more prominent
positive ions, other than soot, are given in equations (2-5), (2-6)
and (2-7).

$$CH + 0 \rightleftharpoons CHO^+ + e^- \tag{2-5}$$

$$CHO^+ + H_2O \rightleftharpoons H_3O^+ + CO \tag{2-6}$$

$$H_3O^+ + e^- \rightleftharpoons H_2O + H \tag{2-7}$$
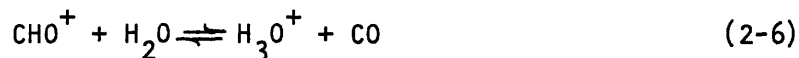
Additional ions will also be produced due to inelastic collisions if an electric field is imposed on the flame.

In summary, all ions are produced in the lower part of the flame by (1) ionization of carbon particles, (2) chemi-ionization, and (3) collisional exchange.

2.223 <u>Ion Identification</u>. Using a mass spectrometer and Langmuir probes, the positive ions in major concentrations, excluding soot, have been found to be H_3O^+, H_2O^+, CO^+, NO^+, COH^+, and $C_2HO_2^+$ [16] [17] [18] [19]. It was also found that the mass of the positive particle is much greater than the negative particles, and from a comparison of mobility data, a majority of the negative particles were identified as electrons. In a recent work, van Tiggelen and Feugier [20] have identified other negative ions of a methane-oxygen flame. These ions, in order of decreasing importance are CH^-, O^-, CH_3^-, $CO_3H_2^-$, H_2^-, $CO_3H_3^-$, $CO_2H_2^-$, and $C_2OH_3^-$.

2.224 <u>General Phenomena of Carbon Formation</u> [21]

2.2241 <u>Effect of Flame Type</u>. In general, the properties of the carbon are little affected by the type of flame, the nature of the fuel, or other conditions under which they are produced. But the tendency to form carbon and the extent of formation depend strongly on these factors. The simplest test for carbon in flames is luminosity. For a diffusion, the flame height where luminosity first appears is often an important experimental point.

Diffusion flames are often used for studying carbon formation since the fuel and oxygen meet only in the thin reaction zone. Mixing of

additional oxygen with the diffusion flame reduces carbon formation, and if enough oxygen is added, a premixed flame is obtained and no carbon is formed. In a diffusion flame, the amount of carbon formed depends strongly on the fuel. The extent of carbon formation decreases in the following order:

NAPHTHALENES $>$ BENZENES $>$ DIOLEFINS $>$ MONO-OLEFINS $>$ PARAFFINS

In most cases with a given series of organic compounds the tendency to form carbon decreases with increasing molecular weight. In general, the carbon-to-hydrogen ratio is one of the principal factors controlling carbon black formation. This fact will also hold for industrial production of carbon black. A lesser influence is exhibited by the compactness of the fuel molecules.

In premixed flames, efforts have been directed towards establishing the conditions of incipient carbon formation, i.e., the critical air-to-fuel ratio. In principle, carbon formation should not occur in mixtures containing more than enough oxygen to convert the carbon into its oxides. Equilibrium considerations indicate that carbon formation should occur only with a O/C atom ratio one or less. However, carbon particles have been observed in premixed flames with a O/C ratio of 1.45 to 2.14 (22). This occurs because the decomposition of hydrocarbons to carbon can proceed more rapidly than the oxidation reactions of the hydrocarbons or the reactions of the carbon with CO_2 or H_2O. For premixed flames, the tendency to form carbon as a function of fuel is:

NAPHTHLENES $>$ BENZENES $>$ ALCOHOLS $>$ PARAFFINS $>$ OFEFINS
ALDEHYDES, KETONES AND ETHERS $>$ ACETYLENE

Well-defined relationships exist between the carbon forming tendency and the structure of the fuel.

2.2242 <u>Effect of Pressure</u>. An increase in the pressure on a

diffusion flame causes an increase in the amount of carbon formed.

Parker and Wolfhard (<u>23</u>), studying the effect of pressure on carbon formation

found no carbon at a pressure of 25 mm of Hg. The first visible carbon

was found at a pressure of 180 mm of Hg. The possibility that the low

pressure diffusion flame actually burned as a premixed flame was excluded

by the fact that the low pressure limit for carbon formation was inde-

pendent of burner diameter. Therefore, they demonstrated that there is

a real effect of pressure on carbon formation.

A similar increase in carbon formation with pressure is found in

premixed flames. In addition, as pressure increases, the intensity of

the C_2 and CH bands decreases. This point will be used later in

discussing the proposed mechanisms of carbon black formation.

2.2243 <u>Effect of Diluents (gases added in large amounts)</u>. The

result of diluent addition depends on whether the flame is diffusional

or premixed. Street and Thomas (<u>24</u>) have found that for premixed flames,

dilution of combustion air with nitrogen increases carbon formation

while enrichment with oxygen decreases it. With diffusion flames, the

result is just the opposite. In the latter case, the addition of the

diluent would be similar to a reduction in pressure.

2.2244 <u>Effect of Additives (trace quantities)</u>. Generally additives

have only a small effect on carbon formation in a diffusion flame. It

is interesting to note that SO_3 and H_2 tend to decrease carbon formation

while bromine, chlorine and their organic compounds tend to increase

carbon formation.

As in diffusion flames, additives have only a small effect on

premixed flames. An exception is SO_3 which strongly increases carbon

formation. In contrast SO_2 and H_2 decrease formation, but much larger

amounts than that for SO_3 are required to produce a significant effect.

2.2245 <u>Effect of an Electric Field</u>. Many investigators have been

interested in this phenomena. Most of this work has been concerned with

premixed or Bunson burner types of flame. Calcote has studied both the effects

of transverse (25) and longitudinal (26) fields on the stability of burner

flames. His results indicate that the ionic concentration in the flame

is 10^{10} ions per cubic centimeter. It is important to note that even

though there is a large number of ions present, they do not appear to

play a significant role in the combustion process.

Weinberg and Payne, using primarily premixed flames, have studied

flame properties in an electric field (27). They have looked briefly at ion

motion, induced gas movement, changes in heat transfer and changes in

carbon deposition. They found that diffusion flames were significantly

more deflected than premixed flames. This would be expected since

diffusion flames contain more carbon. However, the presence of the

field did not seem to alter the primary mechanism of carbon formation.

Electron diffraction and electron microscope measurements showed no

field-induced change in either size or orientation of the collected

particles.

In a more recent work using more sophisticated equipment, Weinberg

and Place (28) have found that the electric field can affect the nucleation

and growth of the carbon black. This work adds considerable insight

into the carbon formation process. It was shown that with a large

flux of positive ions through the pyrolysis zone, the amount of carbon

produced increased while particle size decreased. This change in mass

resulted from an eightfold increase in the number of particles formed.

Since the only change was the number of positive ions entering the flame

zone, it seems likely that these ions act as nuclei for carbon formation.

In additional experiments, cesium was added to the flame. Cesium was

chosen because it ionizes readily at flame temperatures. This added

ion flux resulted in a 2 to 3 fold increase in the mass of carbon formed.

By manipulating the field, it was also possible to control carbon residence

time in the flame. In this manner, they found that by controlling

residence time they could control ultimate particle size.

The present author (29), using an electric field, collected carbon black

in the fuel rich zone of a diffusion flame as a function of position

above the burner. He fould the size of the particles to be uniform at

any one location in the flame. The first carbon particles to form were

approximately 50 $\overset{\circ}{A}$ in diameter. As samples were taken further from the

burner, particle size increased, but there was no indication that any

more small particles were formed, thus indicating that after the initial

nucleation, no new particles were formed.

2.225 <u>General Theories of Carbon Formation</u>. Theories of carbon

formation might better be classed as qualitative chemical models. In

the following section, a brief description will be given of a few of

these models. It is worthwhile to note that some are concerned primarily

with nucleation while others are concerned only with growth. It is to

be expected that these two processes would be controlled by different

laws.

2.2251 <u>C_2 Condensation Theory</u>. Smith (30) first suggested that solid

carbon results from the polymerization of C_2 molecules. This theory

is attractive since it is physically satisfying and C_2 absorption bands

are detected in flames. But the concentration of C_2 in premixed flames

appears to be insufficient to cause formation of significant amounts of carbon. Two other disturbing facts are that this polymerization reaction has a high energy of activation and in some flames carbon is found before C_2 band emission begins.

2.2252 The Hydrocarbon Polymerization Theory. This model postulates that solid carbon is the end product of a series of processes which include polymerization followed by dehydrogenation and graphitization. There are many alternative routes for this scheme. Gaydon and Wolfhard (31) suggest that carbon black may be formed in either of two ways: (1) very large, possibly unstable, molecules could be formed which graphitize from within; or (2) that the concentration of large hydrocarbons increases until the saturation pressure is reached, at which time they condense to form nuclei. They note that since sulfur trioxide is a chain initiator in polymerization reactions and since it increases carbon formation, possibly nucleation is a chain reaction.

The main argument against polymerization has been put forth by Porter (32) as an argument for the acetylene theory. He employed absolute reaction rate theory to show that at flame temperatures, polymerization rates would be much slower than depolymerization and decomposition reactions.

2.2253 The Acetylene Theory. In this scheme, Porter asserts that all carbon is formed more or less directly by simultaneous polymerization and dehydrogenation of acetylene. This is supported by the fact that above 1000°C many hydrocarbons decompose into smaller molecules, especially into methane and acetylene. Acetylene itself is easily decomposed into carbon and hydrogen. While this theory seems reasonable for the growth of particles, it does not explain the origin of the complex carbon nucleus.

2.2254 <u>Surface Deposition Theory</u>. According to Tesner [33][34], the carbon formation process can be divided into two parts. First is the nucleation of a new phase. In the second stage the particles grow but no new particles are formed. He postulates that growth occurs through the direct deposition of hydrocarbons on the particle surface [35].

2.226 <u>Pertinent Results of Experimental Investigations</u>. Bonne, Homann and Wagner [36] simultaneously followed the total concentration, number density, and particle size of the carbon black. They also measured C_2H_2, C_4H_2, C_6H_2, C_3H_2, $C_{10}H_2$ concentrations throughout the entire combustion zone. At the end of the reaction zone, where oxygen had been used up, the concentrations of higher acetylides passed through a maximum. They noted that as soon as carbon formation began, the acetylide concentrations decreased. At this time they found no other hydrocarbons present in sufficient amounts to account for growth. In addition, they found no correlation between CO concentration and carbon formation.

The first carbon they collected was 40 $\overset{\circ}{A}$ in diameter with an atomic C/H ratio of 2.0. Only after extended residence time in the flame did the black approach the normal black formula of C_8H. Bonne, et. al. consider growth as a combination of agglomeration and further addition of large polyacetylides.

In light of this work it would appear that Porter's [37] acetylene role could be modified and better named a polyacetylide model. Possibly acetylene yields polyacetylides, other polyunsaturates and related free radicals.

In a recent work, Homann and Wagner [38] reported on experiments on benzene and acetylene flames. In both types of flames they found three groups of hydrocarbons. These were:

1. Acetylene and polyacetylenes (mass range 26 to 146).

2. Polycyclic aromatic hydrocarbons (mass range 78 to 300).

3. Reactive polycyclic hydrocarbons, probably with side chains, containing more hydrogen than aromatics (mass range 150 to greater than 550).

For acetylene flames, they postulate a scheme of acetylene reactions with C_2H and C_2H_3 radicals to form polyacetylenes and polyacetylene radicals. More radical reactions lead to group 3 hydrocarbons with group 2 hydrocarbons being generated as a by-product. These reactive polycyclic materials (group 3) then add more polyacetylenes to form small active soot particles. Then agglomeration of small soot particles and addition of polyacetylenes yields large (250 Å) inactive soot particles which grow by a heterogeneous surface decomposition of C_2H_2 and polyacetylenes.

In benzene flames polyacetylenes are again present but they do not take an active part in soot formation. In contrast to acetylene flames, here the polycyclic aromatics are added to the radicals to form soot particles. These aromatics seem to be more efficient building bricks and hence more carbon black is formed in the benzene flame.

Foster and Narasimham (39), studying the pyrolysis of methane (turbulent flame), noted two regions of carbon formation. The first region includes a rapid precipitation of carbon black in less than 10 milliseconds. The second region is a growth region with no new particle formation. Initial particle sizes were 33 Å at 2,543°R to 230 Å at 3,173°R. The particle growth was correlated by the equation:

$$\frac{dC}{dt} = 3.87 \times 10^8 \left(\frac{X}{T^{0.5}}\right) C^{2/3} N_s^{1/3} \left(\ell^{\frac{-57,000}{RT}}\right) \qquad (2-8)$$

X = mol fraction CH_4

C = Soot concentration mg/ml

N_s = Number of soot particles/ml

The effect of flow and temperature on the structure of carbon black has been studied by Surovikin and Pokorskii (40). They pyrolyzed toluene and green oil in the combustion products of a diesel fuel-air flame. In one series, with toluene, they varied velocities from 130 to 985 ft/sec at 2,320°F. The degree of structure of the carbon black (oil absorption number) decreased from 1.18 to 0.8 with increasing velocity while the surface area remained constant at 100 square meters per gram. Hence, they conclude that the formation of structure is a molecular process which is not affected by the turbulent pulsations in the stream. They also found that at a velocity of 600 ft/sec green oil gave carbon black with surface areas increasing from 48 to 120 m^2/gr with increasing temperature from 2,200 to 2,530°F.

Surovikin (41) used a tubular reactor to determine the kinetics of the formation of carbon black from liquid hydrocarbons. Feed stocks were toluene and green oil. Temperatures in the reactor varied between 2,390°F and 2,418°F with contact times between 2.0×10^{-4} and 0.08 seconds. Over this time range, he found that surface area decreased with increasing time from 87 to 78 m^2/gm and 102 to 82 m^2/gm for green oil and toluene, respectively. This work showed a sharp maximum in the rate of particle formation, with most of the particles formed in 2 to 4×10^{-4} seconds. With toluene, an induction period of 13×10^{-4} second was measured. It was not possible to measure an induction period on the green oil, but it was less than 2×10^{-4} sec.

Tesner and co-workers (42) are currently studying the kinetics of carbon black production from liquid aromatic hydrocarbons. This work

again has demonstrated that the production of carbon black is a two-step process. These studies still do not allow one to identify the nature of the initial radical nuclei, but they do show that the appearance of highly unsaturated nuclei is required. The generation of these radicals requires the overcoming of a high energy barrier (120 Kcal/mole), and their formation is the start of an avalanche type of chain branching process. This process seems to be very similar to a branched chain explosion. The explosion is then rapidly terminated by a quadratic termination step, yielding a sharp maximum in the particle formation rate. For black formation, this step probably consists of radical loss on the surface of the carbon black. Activation energies for the growth process were found to be 6 to 7 Kcal/mole for toluene and 3 Kcal/mole for green oil.

Tesner and Surooinin (43) have studied the basic principles of the kinetics of carbon black formation under conditions where a highly atomized oil is injected into a stream of hot combustion products. In these studies, toluene and green oil were used as feed materials with reactor velocities of 120 to 984 ft/sec. With a change in gas velocity of an order of magnitude and with liquid or vapor feed the length of the induction period and the surface area of the carbon black remained constant. Hence under the experimental conditions, diffusion and heat transfer have no substantial influence on the formation of carbon black. Again an induction period was noted, with oxygen disappearing and large amounts of hydrogen appearing just before carbon black began to form. A large amount of tar-like resin was found to be present at the same time.

On a slightly different tack, Bass (44) used high speed photography to study the pyrolysis of green oil. With a reactor velocity of 32 to

66 ft/sec and a temperature of 1290-1300°C, he found the surface area
to vary with drop size. When drop size was decreased from 4.85 mm to
1.86 mm, the surface area increased from 68 to 120 m^2/gm. For smaller
drops, he also took photographs to study the shape of the flame envelope
around the particle. He observed tear-drop shaped flames similar to those
reported by Gerald and Chang.

Testing the dominant hypothesis against available data allows one
to improve the model of carbon black formation. First in the early stages,
one has the formation of polyacetylenes, polycyclic aromatics and reactive
hydrocarbons. The types and roles of these materials could depend strongly
on the types of feed materials used. Subsequently, these materials,
through radical reactions, nucleate solid carbon particles. As in other
types of nucleation reactions, the presence of very small particles or
ions will increase the number of nuclei formed for a given set of con-
ditions. These small particles then grow through heterogeneous surface
addition reactions. One point of confusion is: Are the black particles
chained at this point? If so, why isn't the chain structure damped out
with increasing size. If the particles are not chained, when does it
occur and how? These are just a few of the questions that must be
answered in order to obtain a firm picture of the mechanism of carbon
black formation. With a picture of the theoretical problems associated
with carbon formation, a discussion of current production techniques
should point out some of the experimental facts and problems.

2.23 Carbon Black Production

2.231 <u>History</u>. In discussing carbon black production, one must
remember that this industry is not new but on the contrary it has
evolved from a small plant built in New Cumberland, West Virginia

in 1864. It is only in recent years that modern instrumentation and analytical techniques have begun to transform this very complex art into a more controlled science. Because of this fact, most published material is directed towards production and very little fundamental information is available in the open literature.

The first plant for the successful manufacture of carbon black was built in New Cumberland, West Viriginia in the year 1864 (45). In this plant, the forerunner of the contact or channel process, a natural gas air flame, was impinged on a soapstone slab. The deposited product was then scraped from the slabs. In the modern contact process (46) the natural gas is first treated to remove its gasoline. Next, the gas is burned with an insufficient supply of air. The luminous flame impinges on the underside of mild steel channels where black deposits. The black is then scraped from the channels. Rising costs of natural gas combined with a low efficiency and an increasing national interest in air pollution are slowly forcing this process out of the picture.

In 1916 the thermal process went into production. In this cyclic operation, combustion gases first heat brick checkerwork to 3,000°F, then methane is pyrolyzed into carbon and hydrogen on the hot surface. This process is more efficient than the contact process but the particles are larger and do not reinforce rubber as well. These particles are generally not chained but occur as discrete spheroids.

The furnace process, developed in 1928, is a result of effort aimed at producing finer particles at a higher yield. In this process, natural gas and 50% stoichiometric air are burned inside a refractory furnace. The temperature is approximately 2500°F. As the price of natural gas increased in the early 1940's, the industry began to feed oil into the

hot blast gases formed from a natural gas and air fire. In this case,
the oil is the source of the carbon in the carbon black. This process
gives improved yields and a product with good reinforcing properties.
Table I gives the relative importance of the different types of processes.

Table I (47)

Carbon Black Production

Process	Production in 1964 (pounds)
Furnace	2.3×10^9
Channel	0.2×10^9
Thermal	0.245×10^9
TOTAL	2.745×10^9

Of the output of carbon black, 95% is used as a rubber filler.

2.232 <u>Current Production of Oil Blacks</u>. Nelson (48) describes
oils that are good for carbon black manufacture as being composed of 4%
to 40% paraffins, 8% to 52% aromatics and 38% to 60% unsaturates. In
Summary, these oils have between 60% to 96% paraffins, aromatics and
unsaturates. He classes black-making oils by a characterization factor
which is defined by:

$$CF = \frac{(\text{Mean Boiling Point } °F)^{1/3}}{\text{sp. gr.}} \qquad (2-9)$$

Figure 2-3 gives Nelson's plot of percent yield from one furnace process
against characterization factor. The yield is based on a 100% yield
from an oil with a characterization factor (CF) of 10.84. On this basis,
the feed stocks used for this experimental program, which have charac-
terization factors of from 0.87 to 0.94, should give high yields.

One current source of oil is thermally cracked recycle oil with a
high aromatic content. Currently, yields for oil blacks run as high as
60% of the carbon available in the oil (49).

Figure 2-3
EFFECT OF CHACTERIZATION FACTOR ON YIELD
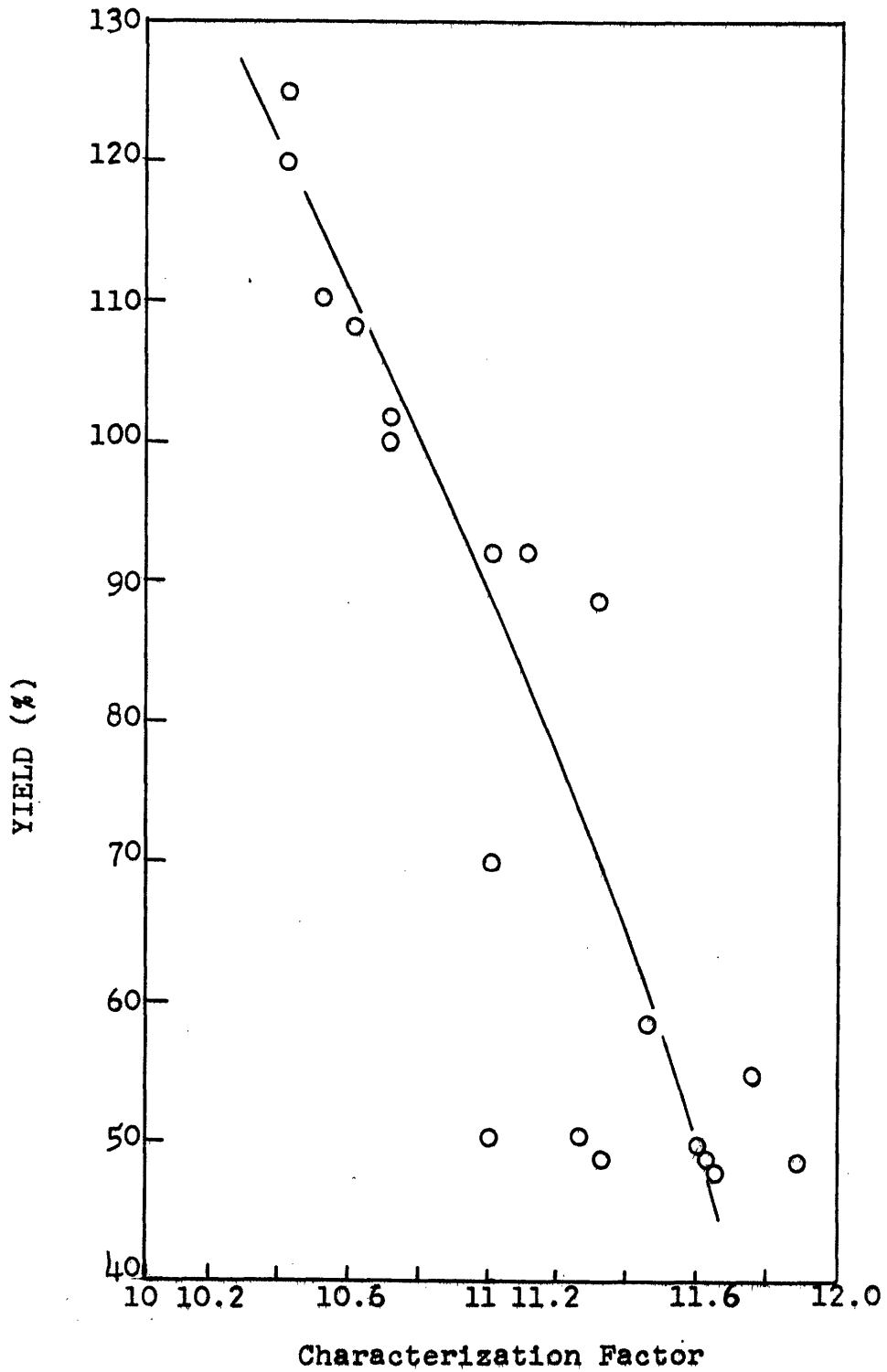
A typical process is the Continental oil black process (50) which begins with thermally cracked recycle oil containing a high percentage of aromatics. This oil is vaporized between 375 and 400°F and injected directly into the furnace as shown in Figure 2-4. Heat for cracking is supplied by the combustion of gas and air which enter the furnace tangentially. This 12 foot furnace has a 12 inch diameter reaction zone which is kept under 2600°F by controlling the air-to-fuel ratio. The product is then quenched with water to stop the carbon depleting reactions. After further cooling, the carbon is collected and either further processed or packaged for sale. Continental Carbon runs a similar process (51) but they start with an aromatic oil cut from the cat cracker. This material has a high boiling point and, therefore, it is pressure atomized into the center of the furnace. They have obtained yields up to 60% and have found that the temperature history of the material is critical in determining the quality and type of black.

Several general statements can be made on the important parameters in oil black manufacture (52). First, the oil should have a H/C ratio of 0.75 to 1.25 and secondly a mean molecular weight of 225 to 550.

High boiling oils are generally preheated and atomized with a bi-fluid atomizer (30-100 microns diameter drops) and then fed to the furnace with enough oxygen for 25% to 50% combustion of the total carbon (carbon in natural gas plus carbon in oil). With these conditions, it has been found that particle size is dependent on the velocity of the gas in the furnace and the residence time. Factors which favor small particles are the addition of diluents, high temperatures, and short residence times. Black properties are also improved by the addition of trace amounts of easily ionized material, i.e., cesium (53).
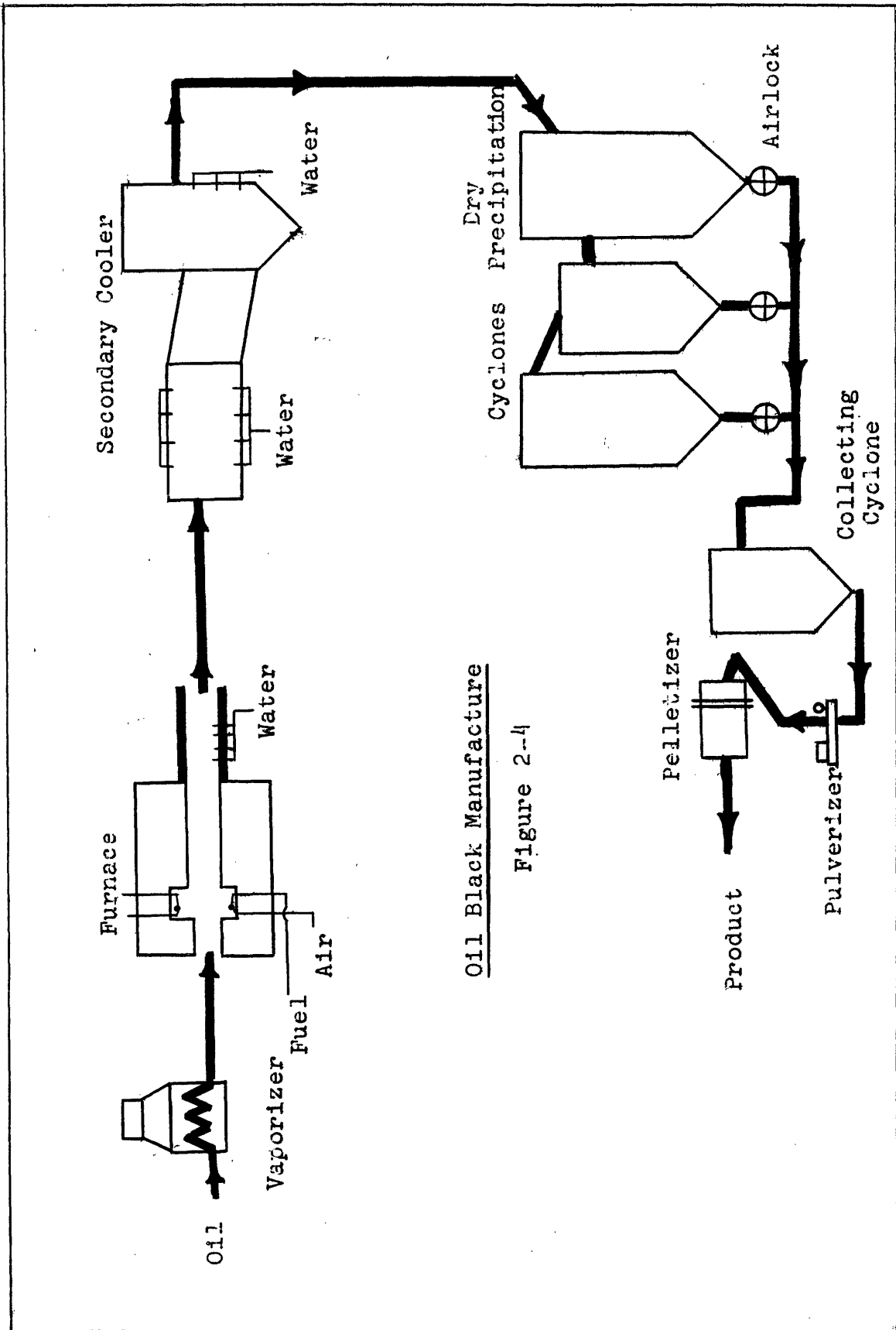
Oil Black Manufacture

Figure 2-4

Patent literature discusses effects of adding O_2 to improve yield (<u>54</u>)

or adding oxygen to a second furnace section to improve properties (<u>55</u>).

But as patent literature is somewhat vague, it is very difficult to

determine what the authors are trying to claim.

In summary, close scrutiny of a typical process flowsheet shows

that it is very difficult to separate the effects of drop size, residence

time and reactor temperature on the final carbon black product. This

separation of interactions is one of the primary goals of this thesis.

Since atomization is a major problem, tne next section will review some

of the pertinent literature.

2.24 Atomization of Liquids

In most gas-liquid chemical reactions, one of the important

parameters is the amount of liquid surface available for reaction.

A review of comustion literature indicates that a considerable amount

of effort has been expended on finding methods of providing initmate

contact between a liquid fuel and the oxidizer. The equipment used to

generate those surfaces is called an atomizer. Atomizers can generally

be classed according to the primary source of the energy which causes the

disintegration of the liquid. Thus, one can distinguish between

pressure atomizers, in which pressure energy is used; rotary atomizers,

where centrifugal energy causes disintegration; and bi-fluid atomizers,

where a gas impinges on a liquid and shearing causes the drops to form.

In their normal industrial mode of operation, all of these atomizer

types produce a wide distribution of drop sizes.

Since drop size control, as well as a knowledge of the size

distribution, is very important to the understanding of a combustion

process, several investigators have modified the more conventional

atomizers in order to obtain a sharper drop size distribution. Of these atomizers, two types can be operated to produce homogeneously sized drops.

First is the dropper technique used by Chang (56) and Gerald (57). Here oil is forced, under pressure, through a small capillary (0.003 to 0.006" O.D.) which is centered in a small orifice. High velocity air flowing around the capillary and through the orifice controls the size of the drop. Recent modifications of this idea have led to a needle which is vibrated to control the drop size. This type of atomizer (58) has been used to produce a stream of drops with a controlled diameter of 25 to 500 microns.

The spinning disk is a modification of the rotary atomizer. In 1950 Hinze and Milborn (59) carried out a theoretical experimental analysis on a rotary cup atomizer. They found that for a given liquid and cup geometry, three distinct types of atomization exist over definite ranges of disk speed. At low liquid feed rates, a liquid torus is formed around the edge of the cup. The torus is deformed and has a series of bulges around the edge of the cup. Liquid drops are thrown off the cup from these bulges. They called this a region of direct drop formation. At higher flows, the bulges transform into ligaments, which disintegrate into a series of drops. Thus the drops are formed in the second region by ligament breakup. Finally, at high flows the torus leaves the disk and breakup is by way of sheet disintegration. Of these regions, only the first produces drops of a single size.

The region of direct drop formation probably describes earlier work done by Walton and Prewitt (60). They were the first to recognize the importance of the spinning disk as a tool for producing a cloud of

uniformly sized drops. Two sizes of drops, instead of one, are formed in this type of atomizer. As the drop is thrown from the disk, a satellite drop is formed, which is approximately one-fourth the diameter of the primary drop. Owing to this difference in size, the satellites are projected a shorter distance from the disk and thus can be separated from the main droplet stream. In their experimental work, they operated low speed motor diven disks and high speed air tops. This experimental program included disks with diameters from 2 to 8 centimeters, disk speeds up to 50,000 radians per second, liquid densities of 0.9 to 13.6 g/cc and surface tensions of 31 to 465 dynes/cm. Over this range of operating conditions, they obtained drops of from 12 to 3,000 microns in diameter.

If one looks at the disk atomizer to determint the controlling parameters, one sees that the liquid collects on the edge of the disk and remains there until the centrifugal force acting on the bulge is greater than the retaining force of surface tension. Therefore, one would expect a proportionality between the product of the drop mass and the accelerating force and the product of surface tension and linear dimension of the drop.

$$\frac{\pi d^3 \rho}{6} \cdot \frac{\omega^2 D}{2} \propto \sigma \cdot d \qquad (2\text{-}10)$$

Rearranging

$$d\omega \left(\frac{D\rho}{\sigma} \right)^{1/2} = \text{const.} \qquad (2\text{-}11)$$

The experimental data of Walton and Prewitt gave values of the constant of about 3.3 to 4.5. The higher values correspond to the high speed air driven tops.

At about the same time, May [61] developed an improved air driven

top in which the driving air sucked the satellite drops from the main

stream. This unit produced drops of 20 to 100 microns and gave a value

for the constant of 4.7. The homogeneity of the spray from this unit

was very good. The standard deviation in drop size was 2.3% of the

mean drop size with 95% of the drops lying within 5% of the mean. A

distribution of the drops from one of May's runs is given in Figure 2-5.

May found that the general criteria for smooth operation of a spinning

disk are: (1) the disk surface must be wetted by the liquid; (2) the

liquid should be fed to the center of the disk; (3) the disk surface

should be smooth, and, finally, (4) feed rates should be low enough to

remain in the region of direct drop formation.

More recently, Renier [62] and Simpson [63] have worked with disk

atomizers. Renier determined the point of transition from direct drop to

ligament drop formation for six liquids and three sizes of disks. These

liquids covered a variation in density (ρ) of 1.03 to 2.13 g/cc, in

surface tension (σ) of 36-63 dynes/cm, and in viscosity μ) of

1.4-324 centipoises. Operating at speeds of 3,000 to 15,000 RPM, he

produced drops of 75 to 400 microns in diameter. Renier represented

his data by the following equation:

$$D = a(\omega)^{-1.01} (\rho)^{-0.68} (\sigma)^{31} (d)^{-.43} (\mu)^{.06}$$ (2-12)

This variation of drop diameter (D) is very similar to that found by

Prewitt and Walton, except for the effect of viscosity μ). Simpson

used the same atomizer on residual fuel oils, but he found that they

could not be atomized satisfactorily until heated to approximately 200°F.

Therefore, the exponent on μ) in equation (2-12) must be viewed with

suspicion. For a rough sizing of experimental equipment, equation (2-11)

should be satisfactory.

SIZE DISTRIBUTION OF DIBUTYL PHTHALATE - MAY -

Figure 2-5
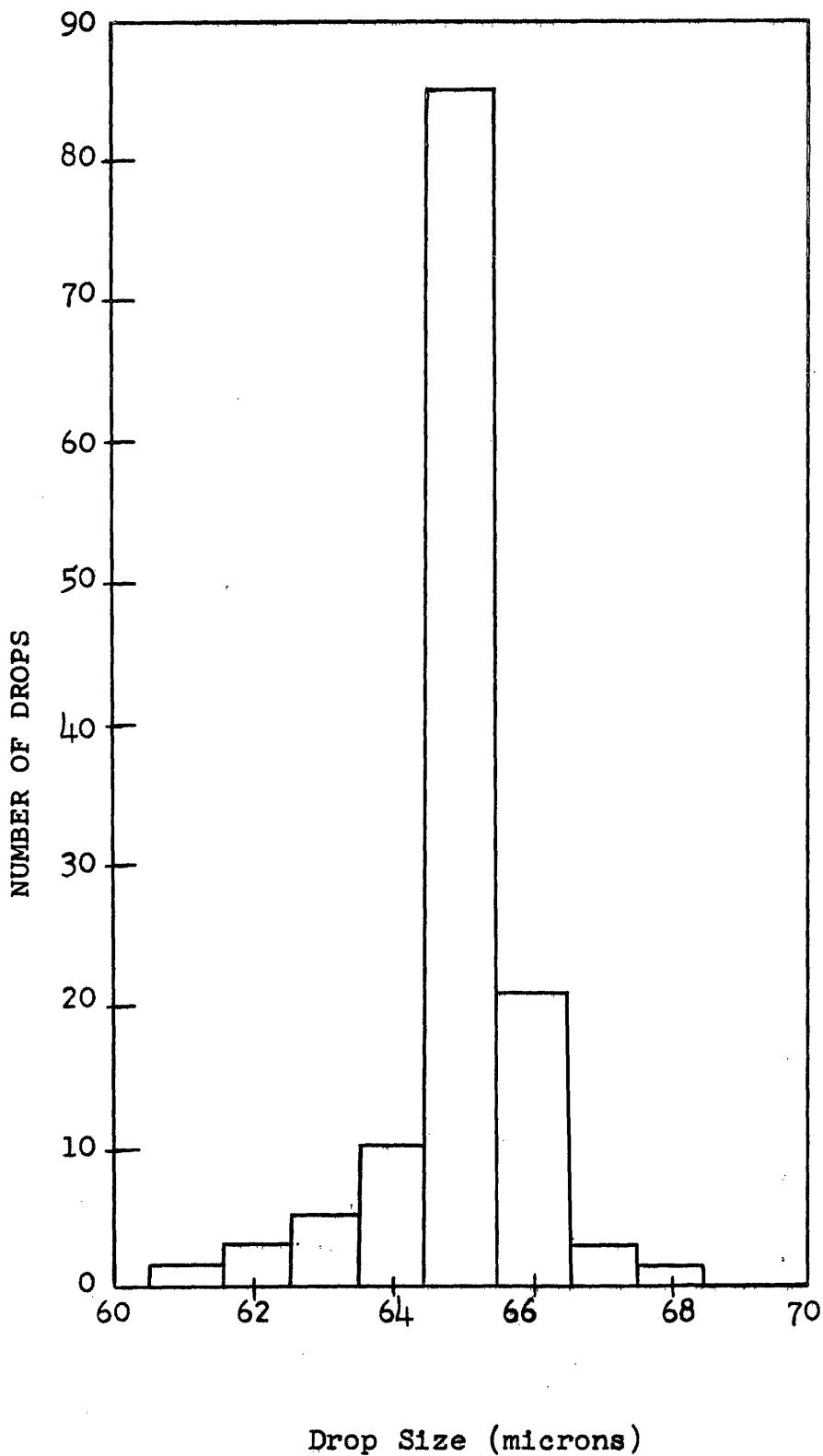
Now that the state of the art of carbon formation and atomization have been briefly described, it is time to outline the goals and approach of the present experimental program.

2.3 Specific Goals and General Approach

The primary goal of this work was to determine the important process variables and then to determine how they influence the physical properties of the carbon black. In addition, efforts were made to shed more light on the mechanism of the nucleation and growth processes.

The process variables considered in this study were drop size, reactor temperature and residence time. With the present experimental apparatus, all of these parameters can be altered independently. In addition to these variables, three different feed stocks were utilized. They include two commercial feed stocks (Aromatic Concentrate and Cosden Tar), and a pure material (Naphthalene). Properties of the feed stocks are given in Appendix A. A summary of the experimental conditions is given in Table II.

Detailed testing was carried out on Cosden Tar (CT). With this oil, drop diameters of 28, 64, and 100 microns were investigated at temperatures of 2000, 2300, 2600, and 2900°F. Only the long residence time was investigated at temperatures of 2000 and 2300°F because of the very low yields at these conditions. At 2600 and 2900°F, three residence times were studied. Aromatic concentrate (AC) and Naphthalene (N) were run at all the above temperatures and residence times with drops of 64 microns.

After each run, the solid carbon was first weighed to determine the yield, then the solid product was analyzed. These tests included tint, extract, scale, surface area, and electron micrographs. Details on these tests are given in Appendix C.

The reaction gas from each run was analyzed for CO, CO_2, C_2H_2, CH_4, O_2, N_2 and H_2. The water content of the exit gases was determined by a material balance around the system. These data also gave the amount of oil and carbon that had been gasified. The next section will describe the equipment and its operation in depth.

Table II

Experimental Program

Key:

   Drop Size:

      100 microns +

      64 microns 0

      28 microns -

   Probe Position (Residence Time)

      Fully extended +

      1/3 Inserted 0

      2/3 Inserted -

Test Number:	1	2	3	4	5	6	7	8	9
Drop	+	0	-	+	-	0	0	+	-
Probe	+	+	+	-	-	-	0	0	0

| Temp. °F	Series Number	Test Number								
		1	2	3	4	5	6	7	8	9
Cosden Tar (CT)										
2000	I	x	x	x						
2300	II	x	x	x						
2600	III	x	x	x	x	x	x	x	x	x
2900	IV	x	x	x	x	x	x	x	x	x
Aromatic Concentrate (AC)										
2000	V		x							
2300	VI		x							
2600	VII		x				x	x		
2900	VIII		x				x	x		
Naphthalene (N)										
2000	1		x							
2300	2		x							
2600	3		x				x	x		
2900	4		x				x	x		

III. PROCEDURE

3.1 Equipment Description

Since this work was primarily an experimental investigation, a considerable amount of time and effort was expended on the design, construction, and debugging of the experimental equipment. Whenever possible, available information on actual "black making" conditions was taken into account. For example, according to the literature, the normal "make-temperature" is from 2400 to 2900°F at a residence time of 5/100 to 15/100 of a second (64). In addition, good conversion is favored by high temperature and short reaction times. After the desired residence time, the hot gas and solid stream is quenched to 800°F with nitrogen or water to stop gasification reactions which deplete the yield. In general, only a limited amount of information is available on actual process conditions and even less is known about the interaction of the various process parameters. Whenever possible, the apparatus was designed to encompass production conditions.

Figure 3-1 is a schematic of the experimental equipment, while the actual apparatus is shown in the photographs on Figure 3-2. Starting at the top of the figure, residual oil was fed through a nozzle to a spinning disk, where it was disintegrated into small drops by the centrifugal force of the disk. The disk speed and temperature were controlled so that a stream of uniformly sized drops, of a known size and at a controlled feed rate could be mixed with the combustion products of a natural gas-air flame.

The exhaust temperature of the burner gas was controlled by the air to fuel ratio and the amount of preheat in the fuel and air streams. The stream of drops were conveyed with nitrogen from the atomizer into

APPARATUS

Figure 3-1
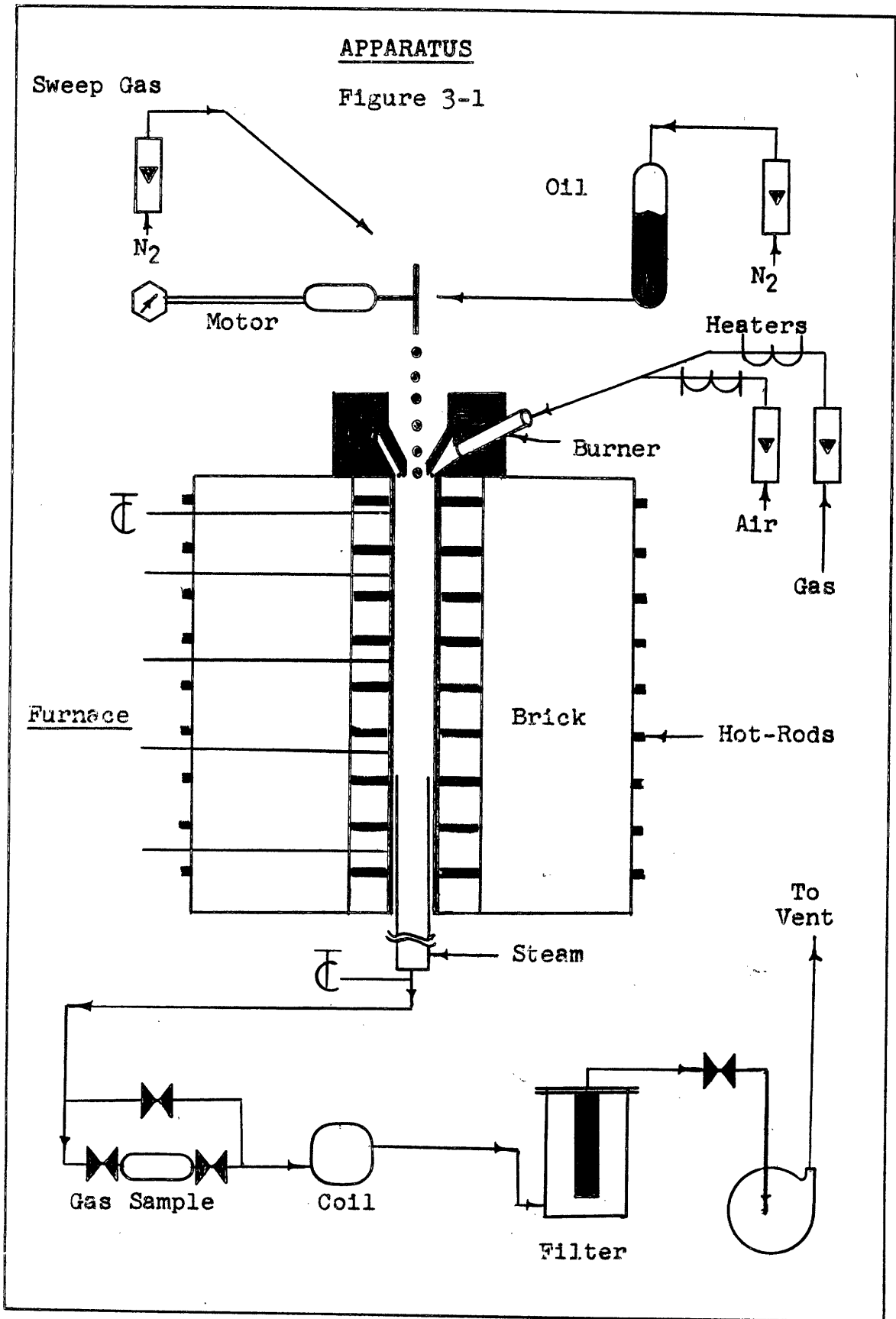
APPARATUS

Figure 3-2
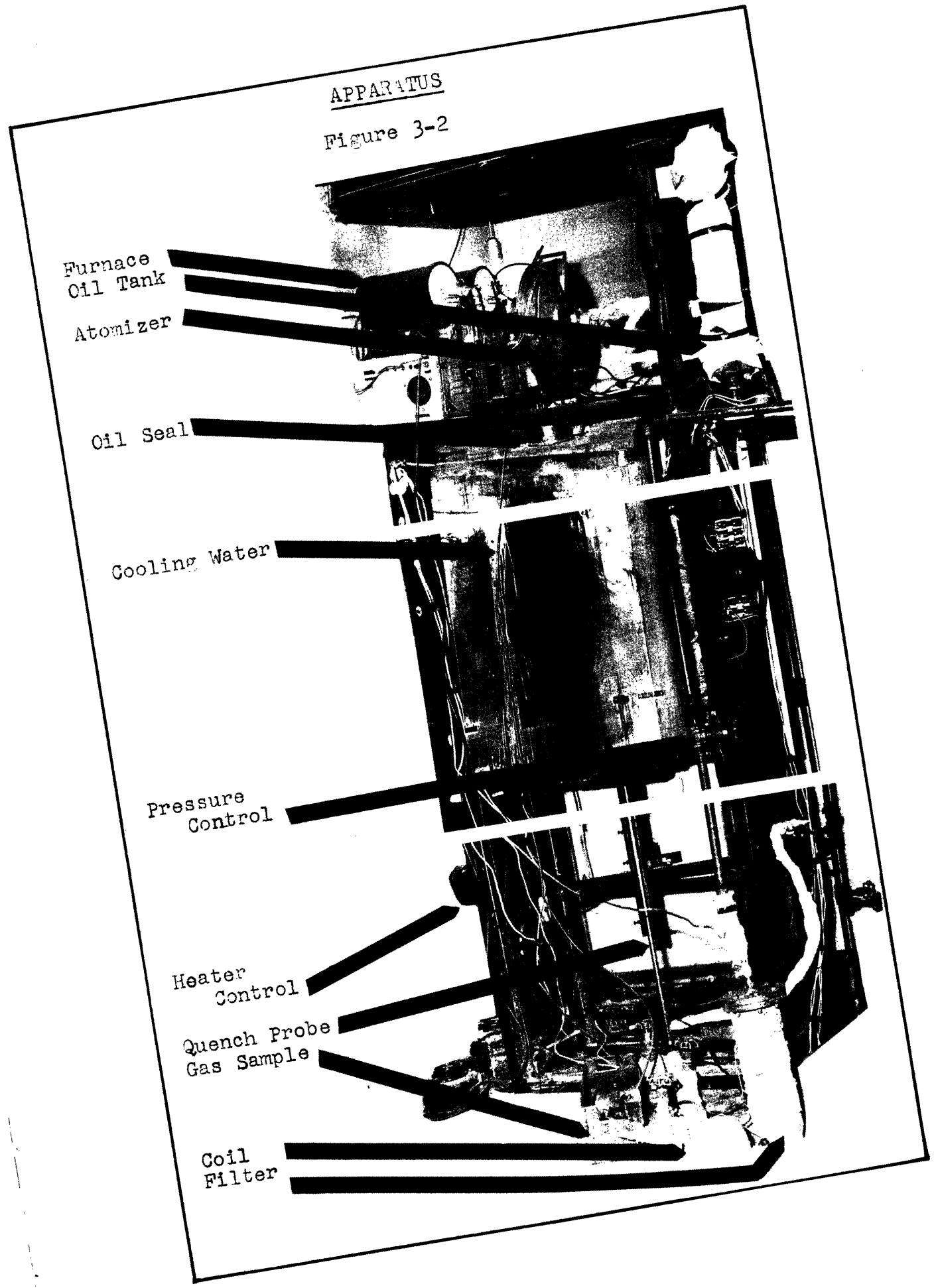

Furnace
Oil Tank

Atomizer

Oil Seal

Cooling Water

Pressure
Control

Heater
Control

Quench Probe
Gas Sample

Coil
Filter

the exhaust gases of the burner. The gas-oil stream then flowed downward

through a vertical reactor which was held at the desired temperature.

When the predetermined reaction time had elapsed, the gas stream was

quenched with steam to approximately 800°F before passing through the

collection system. The next few pages will describe the specific equipment

items and their function in more detail. A more complete equipment

description is located in Appendix H.

3.11 Oil Feed System

The most attractive starting materials from the standpoints of

availability and cost were the "Bunker C" type oils. Residual fuels are

generally composed of hydrocarbons boiling above 700°F. A major portion

of the residual oil consists of polynuclear aromatic and Naphthalene

hydrocarbons with long paraffinic side chains. The asphaltenes and resins

of the crude oil are found in this fraction of the oil. Details of the

composition of the residual oil depend markedly on the source of crude

and its processing history. Table III gives some of the properties of

the two "Bunker C" type fuel oils and the Naphthalene that were used as

starting materials for this study.

Table III

Feed Materials

	Aromatic Concentrate (AC)	Cosden Tar (CT)	Naphthalene (N)
% Asphaltenes	1.6	4.9	0.0
% H	9.08	8.72	0.25
% C	88.1	87.58	93.8
Atomic H/C Ratio	1.23	1.19	1.25

These oils are typical of materials used industrially for carbon black

manufacture and were furnished by Curt Beck of Cabot Corporation. A more

complete description of the starting materials is located in Appendix A.

The oil was fed to the disk by a pressurized nitrogen system as shown on Figure 3-3. Nitrogen from a cylinder first flowed through a regulator, two control valves, and then a four foot long glass capillary with an internal diameter of 0.25 mm to 0.75 mm. Pressure drop across the capillary was read from an oil manometer and total system pressure was indicated on a mercury manometer. These two quantities provided an indication of the oil feed rate. From the capillary the nitrogen flowed to the heated oil tank and forced oil to flow to the atomizer.

3.12 Atomization System

The different types of liquid atomizers were discussed in section 2.24. A spinning disk atomizer was selected for use in the present investigations because it readily provided a cloud of uniformily sized particles. The critical parameters for disk operation are given in equation (3-1) (65).

$$d\omega \left(\frac{D\rho}{\sigma}\right)^{1/2} = \text{const.} \tag{3-1}$$

This equation shows that at constant oil properties and disk size, the drop diameter is inversely proportional to disk speed. A three inch diameter disk was constructed to produce drops of from 25 microns to 100 microns in diameter. In order to maintain a uniform centrifugal stress on the disk (Figure 3-4), the design thickness, t, of the disk was varied according to the following equation (66).

$$t = t_o \exp \ (-\rho\omega^2 r^2)/2gf \tag{3-2}$$

t_o = thickness of radius = 0
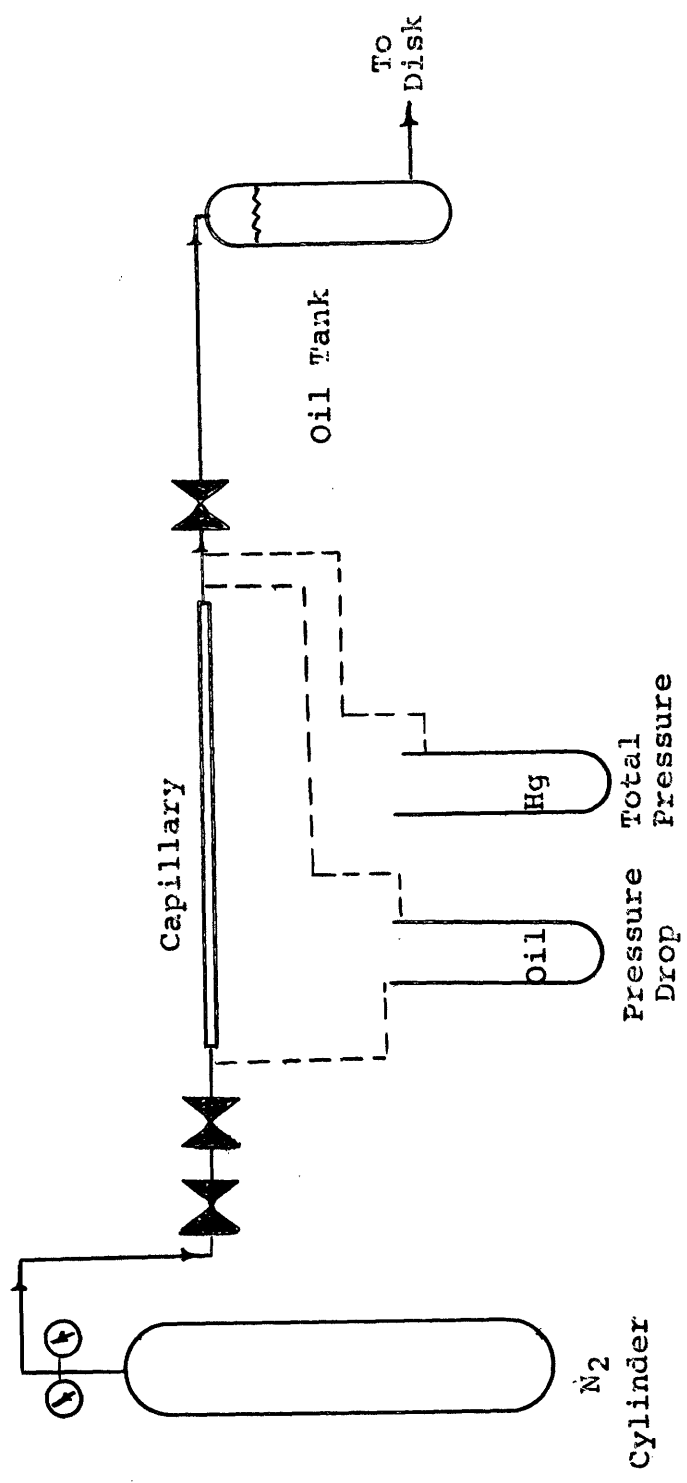
ρ = density

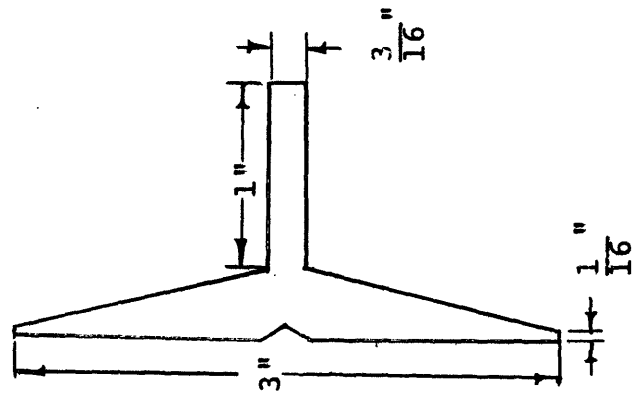r = radius

ω = speed

f = allowable stress

OIL FEED SYSTEM

Figure 3-3

DISK

Figure 3-4

For ease of construction, the shallow exponential curve of this equation was approximated by a conical shape. Power for driving the disk was supplied by a 1/5 hp Precise Electric Grinder with a maximum speed of 45,000 rpm. The speed of the disk was controlled by a variac on the motor primary. Since one of the critical variables was disk speed, it was necessary to monitor accurately and control the disk speed. This was accomplished by combining a photoelectric pick-off, an oscilloscope, and an oscillator. Briefly, a light beam from the pick-off was bounced from a narrow reflector strip on the disk shaft to the photocell in the pick-off. The resulting voltage pulse was then fed to the vertical plates of a dual-beam oscilloscope, while the signal from an audio oscillator was fed to the horizontal plates of the scope. When a simple Lissajous figure (in this case a stationary straight line) was obtained, the frequency of the oscillator was matched to the pulses from the pick-off and the disk speed was then known. Details of the disk speed measurement system are given in Appendix I.

Having developed an atomizer capable of producing the proper sized drops, it was next necessary to provide a means of conveying these drops to the furnace. Figure 3-5 shows a schematic of the disk housing developed to accomplish this. This housing was designed by successive experimentation; the details of its evolution are discussed in Appendix J. The important features of the disk housing are: (1) The nitrogen sweep gas inlet at A. (This gas flow helps to move the drops from the housing to the reactor.) (2) The gas flow baffle. (This was necessary to prevent the gas in the housing from rotating with the disk.) (3) A small flow of bleed nitrogen entering behind the baffle. (This prevents the formation of low pressure region which could cause vortex flow.) Oil drops that hit the wall of the

ATOMIZER

Figure 3-5
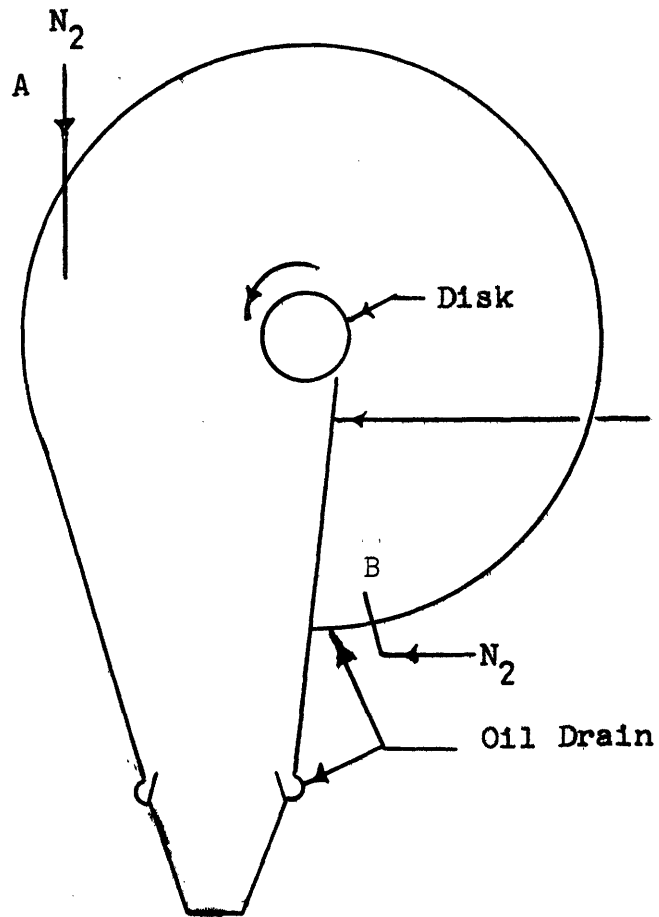
housing into the trough system and were collected on the outside of the housing. An oil seal was used on the oil collector to prevent the loss of process gas.

3.13 Burner

A burner of the can type was chosen because this design has good stabilization properties, a high throughput, and very little axial recirculation. This unit, shown in Figure 3-6, premixes natural gas and air before they enter the burner throat through 28 small jets. The resulting flame stabilized in the center of the burner. The air and gas streams were provided with electric furnaces to permit the addition of preheat. .
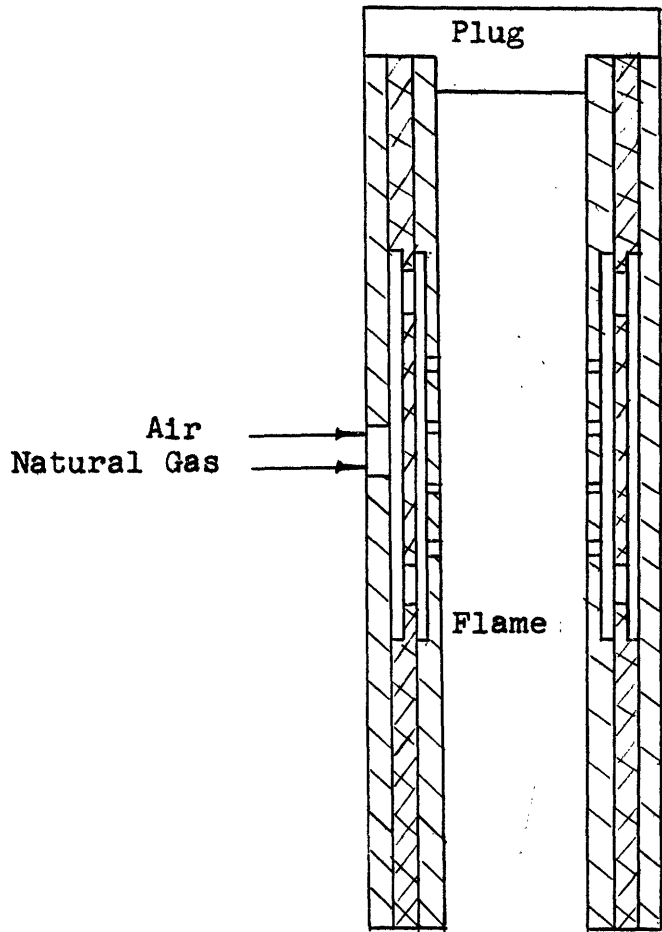
3.14 Reactor System

As the drops leave the disk housing, they enter the transition piece shown in Figure 3-7. Here they contact the combustion products from the burner and enter the reactor. The reactor was a one-inch inside diameter by three foot long silicon carbide tube. As shown in Figure 3-8, this tube was positioned in the center of the 4 inch by 5 inch rectangular opening in the furnace. Electrically heated silicon carbide rods were provided to compensate for heat losses from the furnace and to maintain a flat temperature profile along the reactor wall. Nine inches of zirconia brick and two inches of block insulation were located around the reactor tube. Five Pt,Pt -13% Rh thermocouples were attached to the outside of the reactor to provide the reactor temperature. This furnace could be operated at temperatures of up to 2900°F.

3.15 Quench and Product Collection System

In order to quench the reactions, a water and steam cooled probe (Figure 3-9) was inserted into the reactor to the desired height, and the reaction mixture was quenched with steam. Steam was used instead

BURNER

Figure 3-6

TRANSITION PIECE

Figure 3-7

Disk—|

•

•

(Drops)

•

•

•

•

Burner

Al$_2$O$_3$

Al$_2$O$_3$

— SiC Reactor
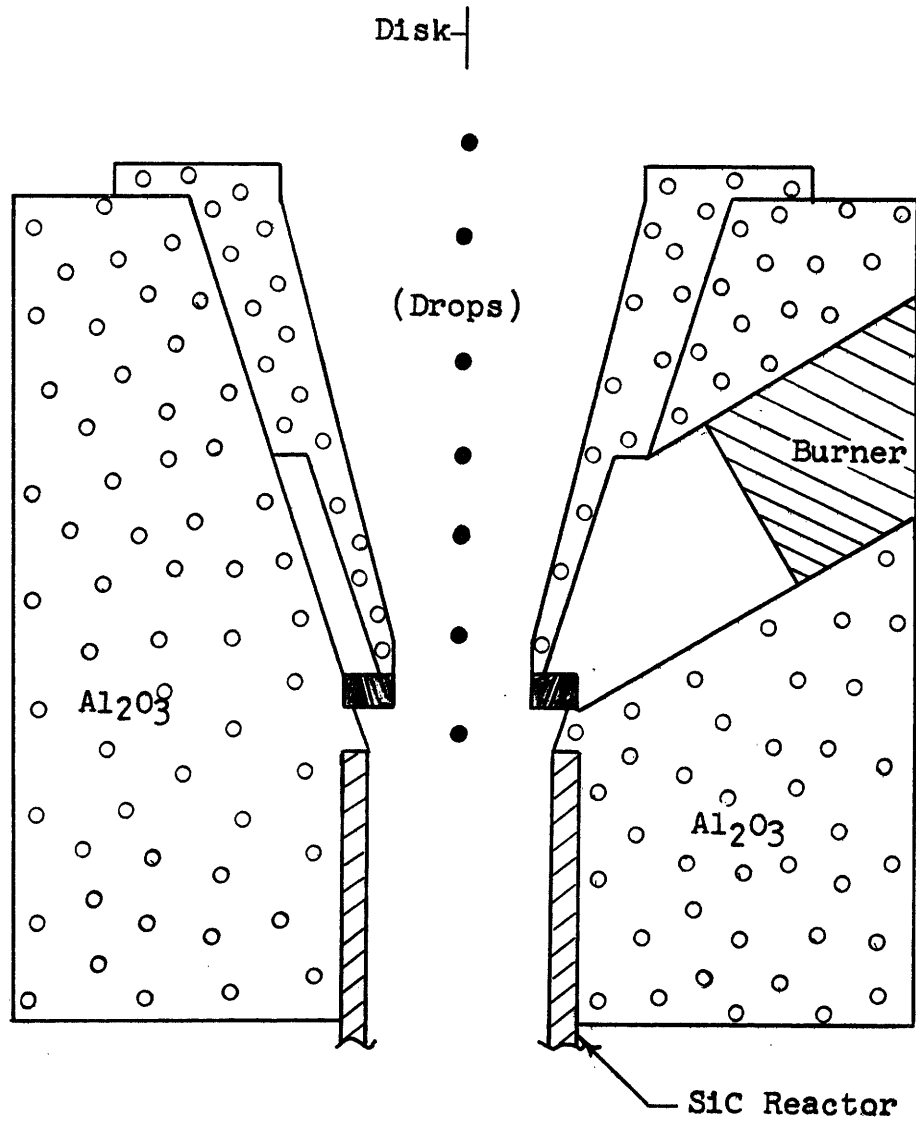
FURNACE
(Top View)

Figure 3-8

Reactor

Hot Rods

$Zr O_2$ Brick

Block Insulation

QUENCH PROBE
Figure 3-9

Steam

Reactor

Gasket

Coolant

Steam

T_o

Product Collection
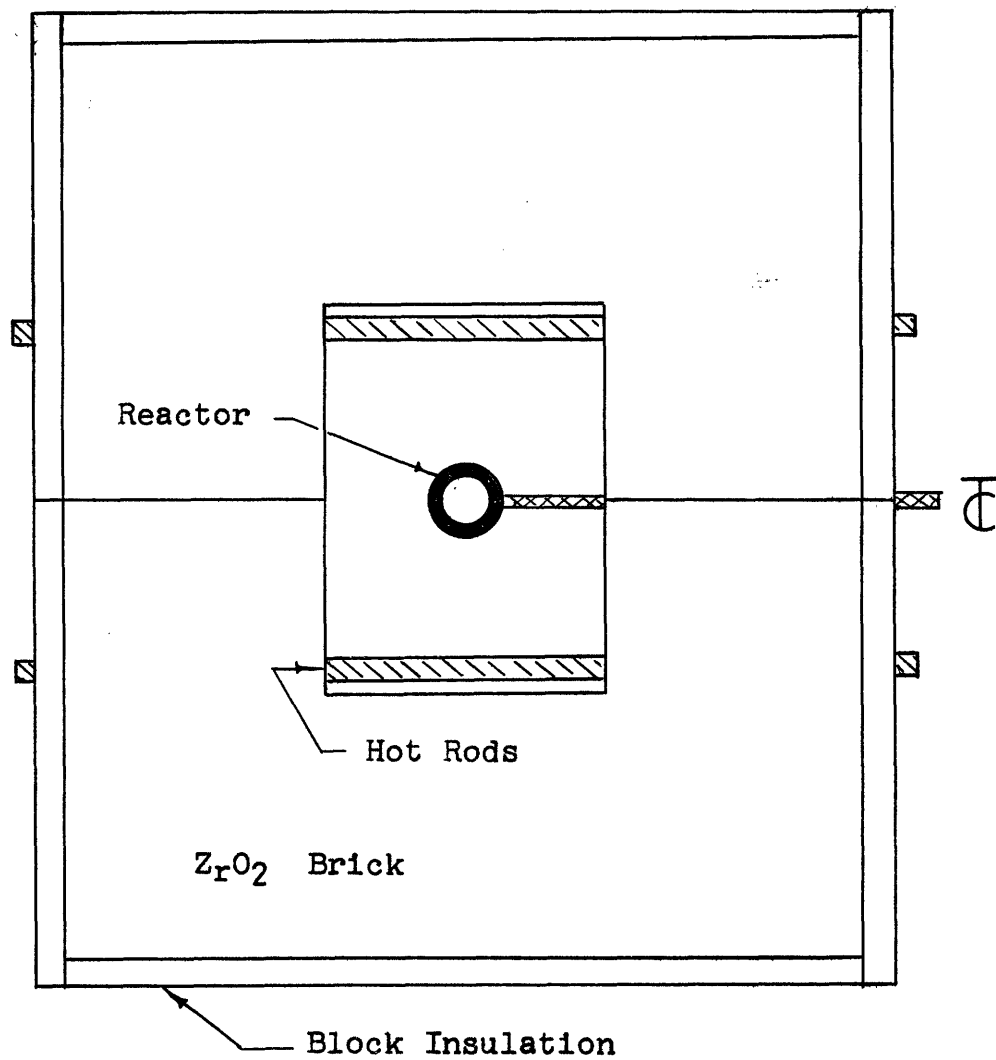
of water because the higher volumetric flows promoted better mixing and hence a quicker quench. A vacuum pump was connected to the end of the collection system and adjusted so that the reactor pressure (slightly above one atomsphere) remained constant and independent of the probe location. After quenching, the gas and carbon black flowed through the sampling system and the agglomerator. The agglomerator coil provided enough residence time for the carbon particles to agglomerate and thus facili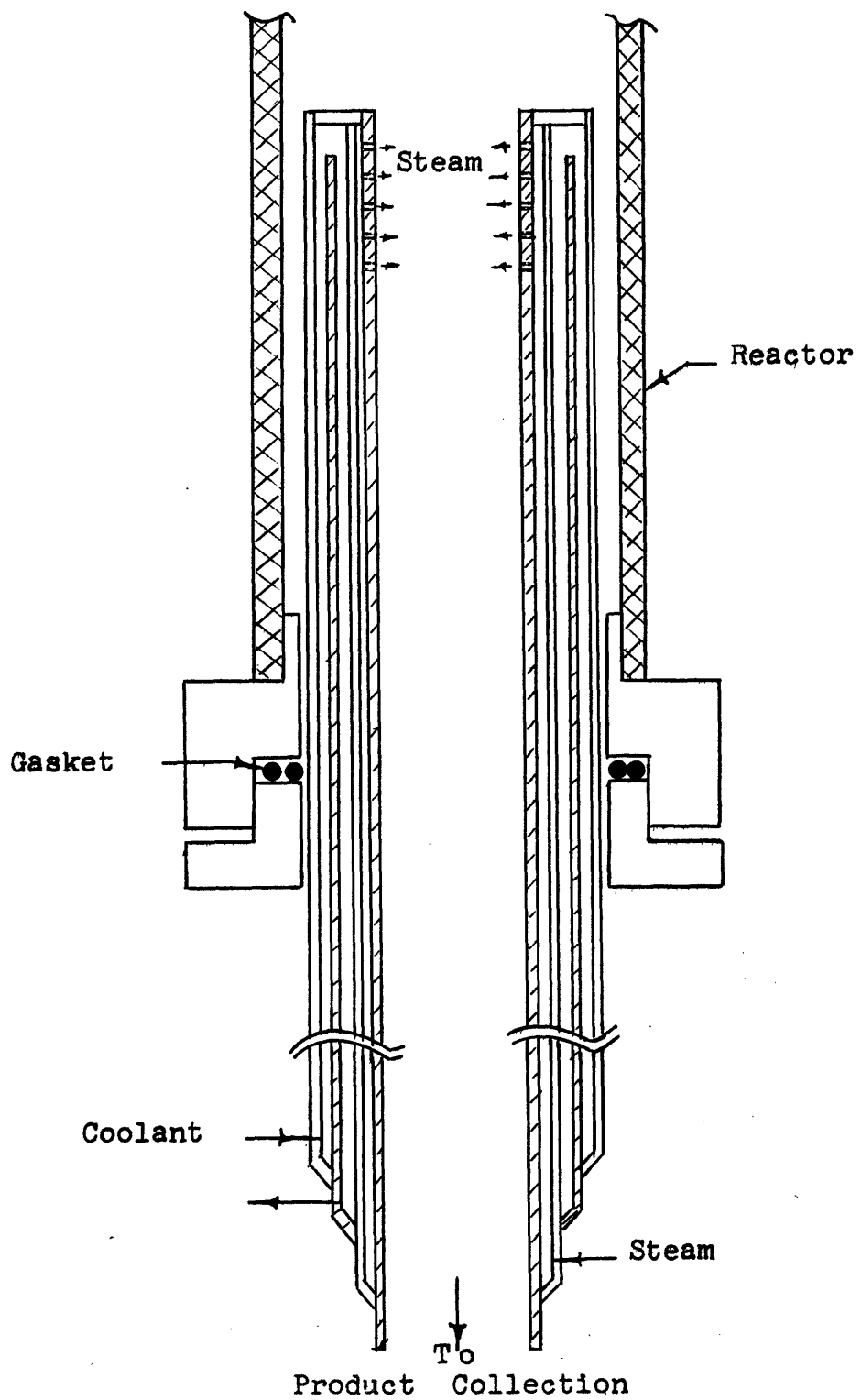tate removal on the sintered metal filter. All equipment items in the collection system were insulated and maintained above 300°F by strip heaters to prevent condensation of water.
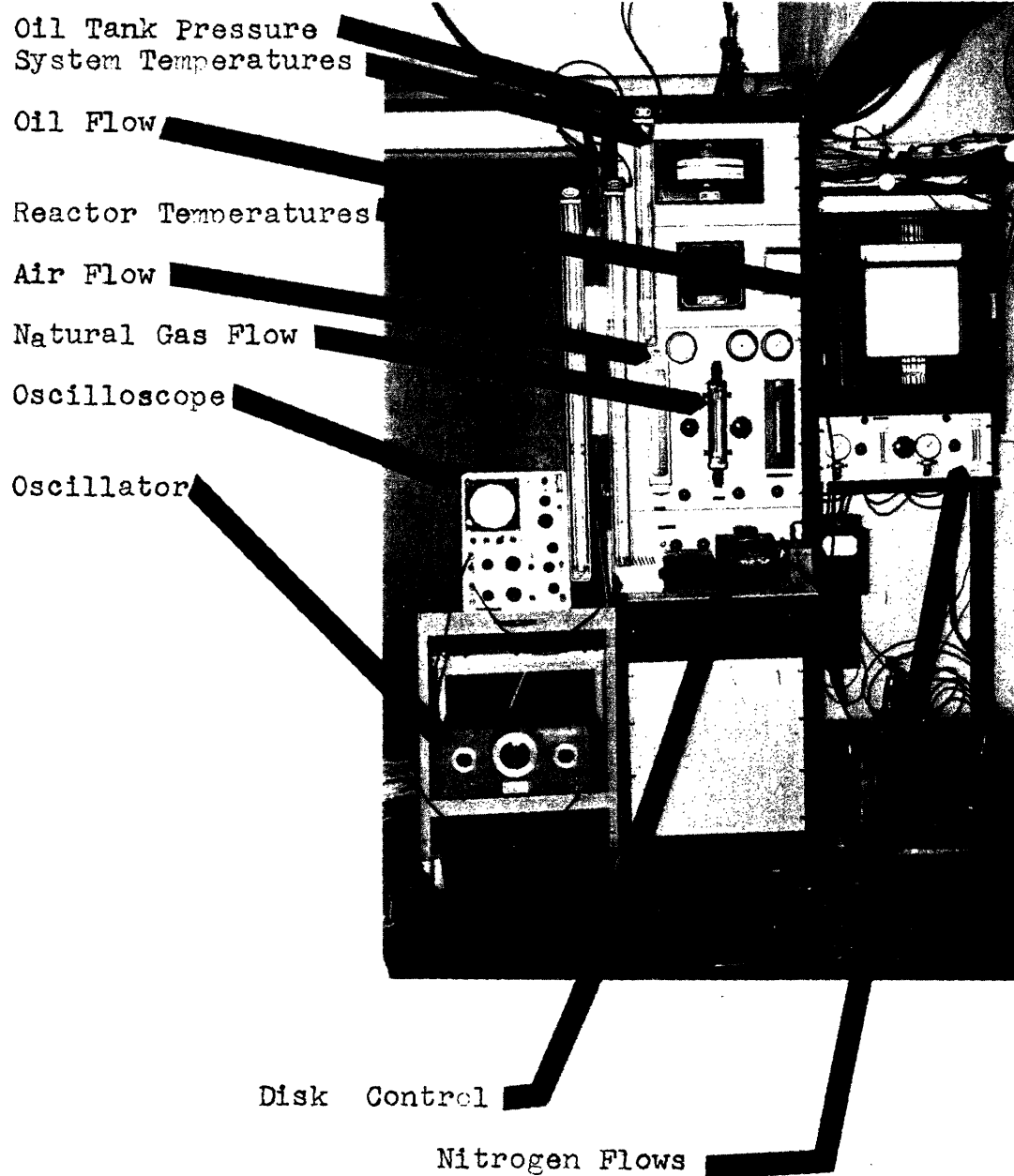
3.16 Data Collection System

Gas flows to the burner and disk housing were measured using the rotameters shown on the flow panel in Figure 3-10. Temperatures in the reactor and transition piece were measured using Pt, Pt-13% Rh thermocouples and recorded on a Leeds and Northrup recorder. Temperatures in the collection system, the oil tank, the disk housing, the fuel preheat furnace, and the quenched gas were obtained with chromel-alumel thermocouples and indicated on a Wheelco pyrometer. Iron-constantan thermocouples, in conjunction with a Honeywell potentiometer, were used to measure cooling water temperatures.

The solid carbon particles were analyzed for extract, scale, surface area, and tint and photographed (using an electron microscope) to determine their size and shape. A sample of the off-gas from the process was collected in a 250 cc gas sample bulb. After the temperature and pressure of the gas in the bulb had been adjusted to room temperature and pressure, a sample of the gas was injected into a two column Fisher-Hamilton gas partitioner for separation. Details of gas and

FLOW PANEL

Figure 3-10

Oil Tank Pressure
System Temperatures

Oil Flow

Reactor Temperatures

Air Flow

Natural Gas Flow

Oscilloscope

Oscillator

Disk Control

Nitrogen Flows

solid analysis are given in Appendices B and C, respectively. The description of the equipment should be clarified somewhat in the next section on equipment operation.

3.2 Equipment Operation

Due to the complexity of the experimental equipment, it was necessary to follow a rigorous operating procedure to minimize product variations caused by slight differences in operating conditions. The overall operation can be broken down into pre-run operations, run operations, and run cleanup operations, which included gas analysis.

3.21 Pre-Run Operations

The major operation in this area was temperature adjustment. During the experimental program the reactor temperature was controlled at four different levels (2000°F, 2300°F, 2600°F, and 2900°F). This control was accomplished using the electrical setup shown in Figure 3-11. Before adjusting the variacs and slide wire resistors, the quench probe was first placed in position. This was necessary since the probe acted as a large heat sink. With the probe in position, it was possible to adjust the power to the hot rods and bring the reactor wall temperatures to the desired level. The L. and N. recorder provided a continuous indication of the reactor wall temperatures.

When the furnace temperature began to level out, the strip heaters on the product collection system were activated to bring temperatures to 300°F (this required approximately three hours). The preheat furnaces on the natural gas and air furnaces were then adjusted to provide enough preheat so that the burnt gas and vaporized oil mixture were at the reactor temperature. The amount of preheat required was determined experimentally.
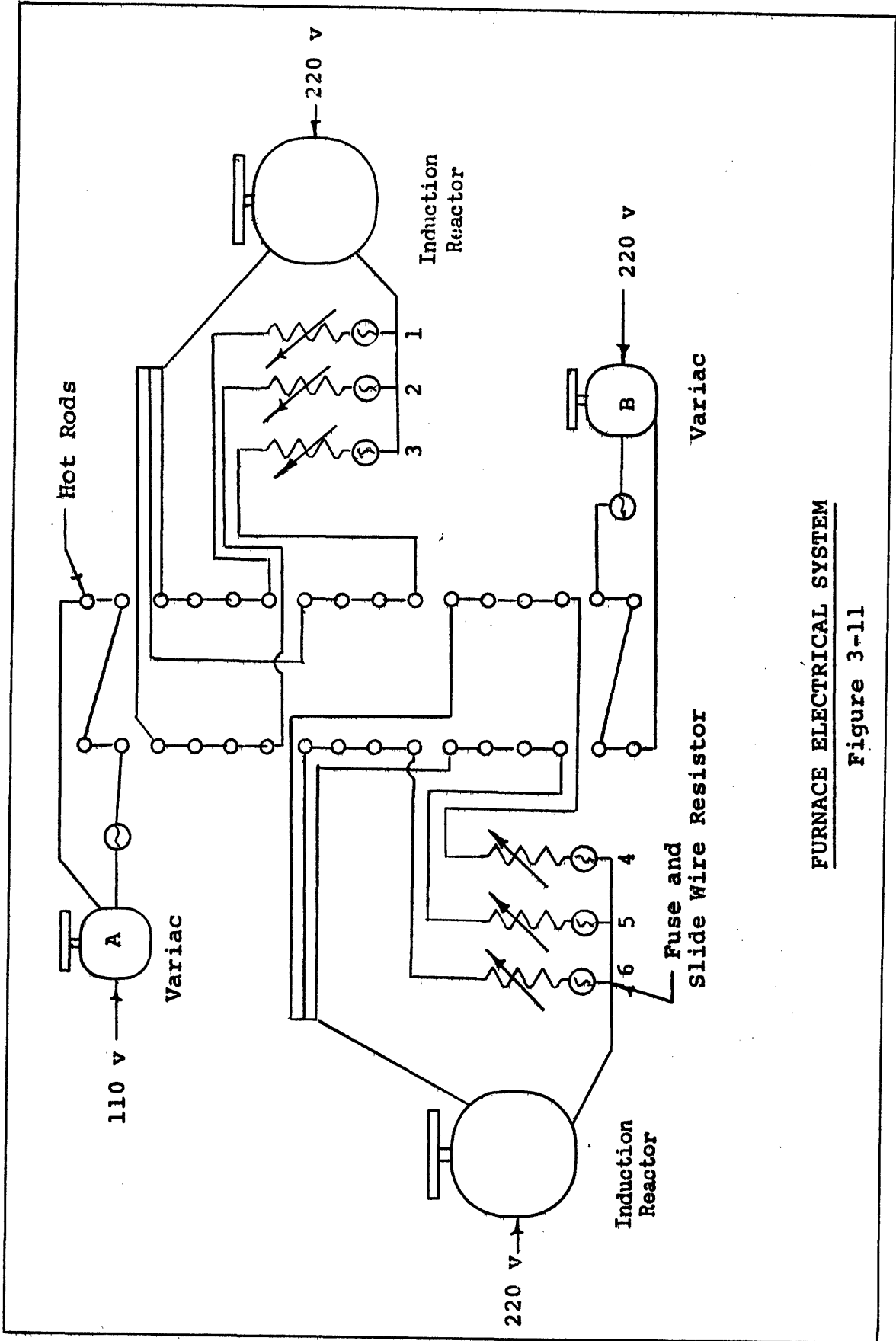
FURNACE ELECTRICAL SYSTEM

Figure 3-11

In the meantime, oil was charged to the reservoir and heated to 230°F. With all auxiliary equipment at temperature, the atomizer was placed on the transition piece and sealed with asbestos tape. The disk housing was then allowed to preheat on top of the furnace for 60 minutes when the furnace was operating at 2000°F or 2300°F and for 30 minutes when the furnace was over 2300°F. At this time, the oil feed nozzle was placed in the housing and 20 minutes were allowed for preheat before starting the run. This brought the nozzle temperature to approximately 230°F.

3.22 Run Operations

When everything was hot, the disk was started and its speed adjusted to approximately the desired level. Then the variac on the disk heater was adjusted to 3-1/2 amps. This brought the disk temperature to approximately 230°F.

Next the natural gas and air flows were set and the burner ignited. As soon as the burner had stabilized, the valve on the vacuum system was adjusted to bring reactor pressure to one atmosphere. This valve was adjusted throughout the run to compensate for the increasing pressure drop due to carbon deposition on the filter. At the same time, steam was added to the probe coolant to bring probe temperature to approximately 2000°F and quench steam was added to bring the gas temperature at the probe exit in the range of 230 to 300°F. This temperature provided a sufficiently rapid quench. At this point, the gas flows to the burner were adjusted and nitrogen flows to the housing were started. With all flows on target, the oil flow was started and the disk speed adjusted to the proper value. This signaled the beginning of the run.

After five minutes of operation, the entire reactor exit flow was valved through the sample bottle for 45 seconds. The flow was then

rerouted around the bottle, but one end of the bottle was left open to the process system for an additional 2-1/4 minutes to allow bottle pressure to equalize with system pressure.

During the run, the following readings were taken:

1. Disk voltage and current

2. Oscillator frequency (disk speed)

3. Oil tank pressure

4. Pressure differential on oil feed capillary

5. Natural gas rotameter setting and pressure

6. Air rotameter setting and pressure

7. Sweep nitrogen rotameter settings and pressures (two)

8. Current flows on: filter heater, steam preheater, sample system heater, and disk heater.

9. Reactor temperatures

10. Temperatures in the oil feed system

11. Quench temperature

12. Preheat temperatures of air and fuel

13. Temperature of gas exiting from the filter

14. The length of the run

After 20 to 30 minutes, the pressure drop across the filter increased due to collected carbon and flows began to decrease. At this time, the run was terminated.

3.23 Run Cleanup Operations

After the run, the disk housing was removed from the furnace and the disk cleaned with solvent. The overflow oil from the housing was measured and the oil tank refilled to determine the exact amount of oil that had been fed to the reactor.

Next, the solid carbon was brushed from the filter and quench probe. The sintered metal filter was then back-flushed with water to prepare it for the next run. Carbon black that had accumulated in the sample system and agglomerator coil was blown into a cloth filter bag. The total weight of product was then obtained and this permitted calculation of the process yield. The solid samples were submitted to Cabot Corporation for analysis. Gas samples taken during the run were analyzed on a gas chromatograph.

Now that one is familiar with the equipment and its operation, the results of the experimental program will be presented.

IV. PRESENTATION OF RESULTS

In this chapter, the experimental data will be presented in graphical form. Tabulations of the data are located in Appendix E. Since drop size is one of the critical variables, it will be discussed first. Next the data on carbon black formation will be reviewed.
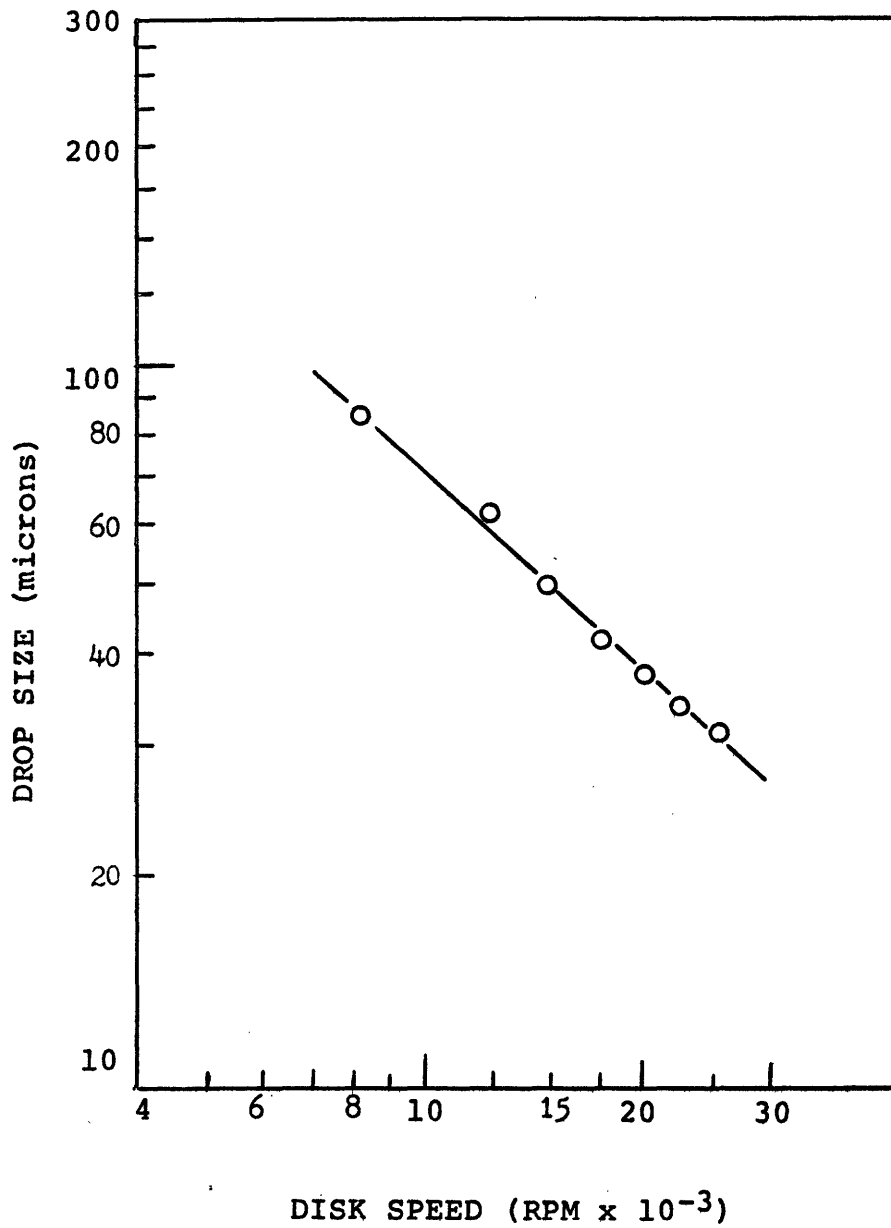
4.1 Atomization

The disk atomizer was operated on four different feed stocks at a feed rate of approximately 25 cc of oil per minute. This gave a drop feed to the reactor of 5 cc per minute. Since the room temperature viscosity of dibutyl phthalate was very close to that of hot oil, it was used to calibrate the disk. It was also used to establish housing design and check disk operation. The results of the initial calibration tests are shown on Figure 4-1. Here the drop size, in microns, is plotted against disk speed.

Next, the disk was calibrated using the two residual fuel oils. There was only a slight viscosity difference between these oils, and, therefore, their atomizing characteristics were very similar. The dependence of drop size on disk speed for Cosden Tar and Aromatic Concentrate is given on Figures 4-2 and 4-3, respectively. The uniformity of these drops can be seen pictorially on Figures 4-4 and 4-5. These figures contain light microscope pictures of the craters (100x) formed by the oil drops on magnesium oxide coated slides.

Naphthalene, a pure material, was used as a control in this study. Its atomization behavior was similar to the residual oils. On Figure 4-6 is presented the relation of drop size to disk speed for Naphthalene, while the magnesium oxide craters are shown on Figure 4-7.

ATOMIZATION OF DIBUTYL PHTHALATE

Figure 4-1

Plot of DROP SIZE (microns) versus DISK SPEED (RPM x 10^{-3}), showing a descending line with data points at approximately 8, 12, 15, 18, 20, 22, and 25 on the horizontal axis.

DROP SIZE (microns)

DISK SPEED (RPM x 10^{-3})

ATOMIZATION OF COSDEN TAR

Figure 4-2

DISK SPEED (RPM x 10⁻³)
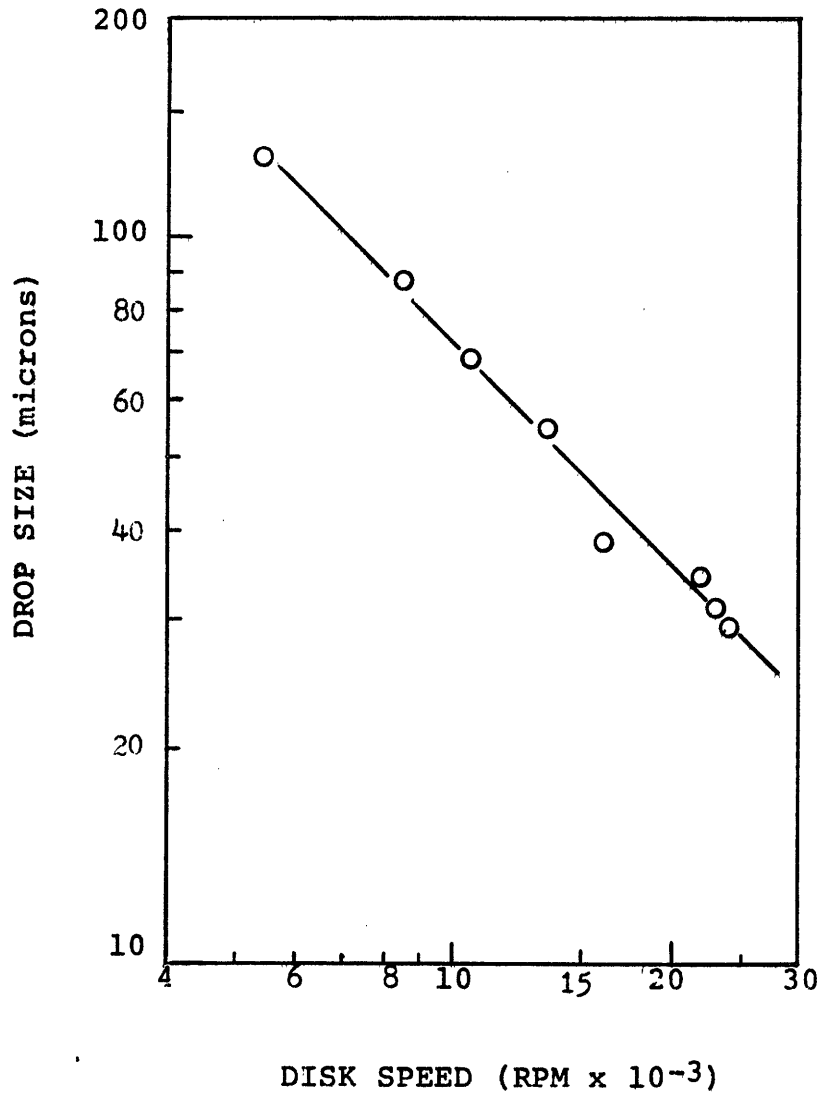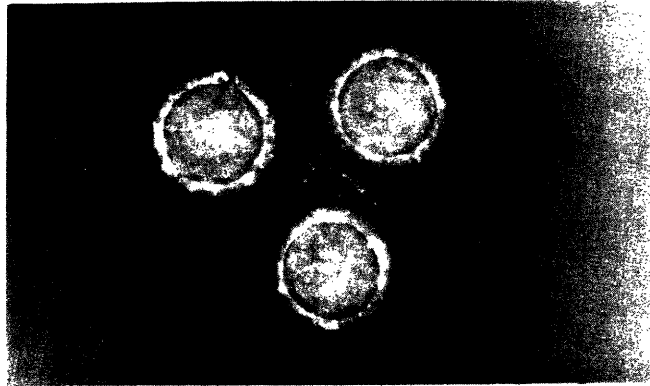
ATOMIZATION OF AROMATIC CONCENTRATE
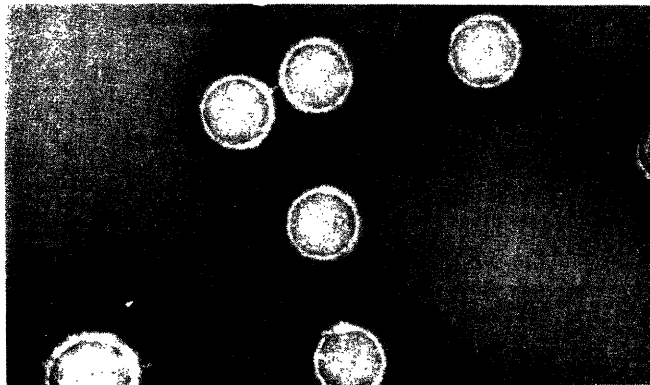
Figure 4-3
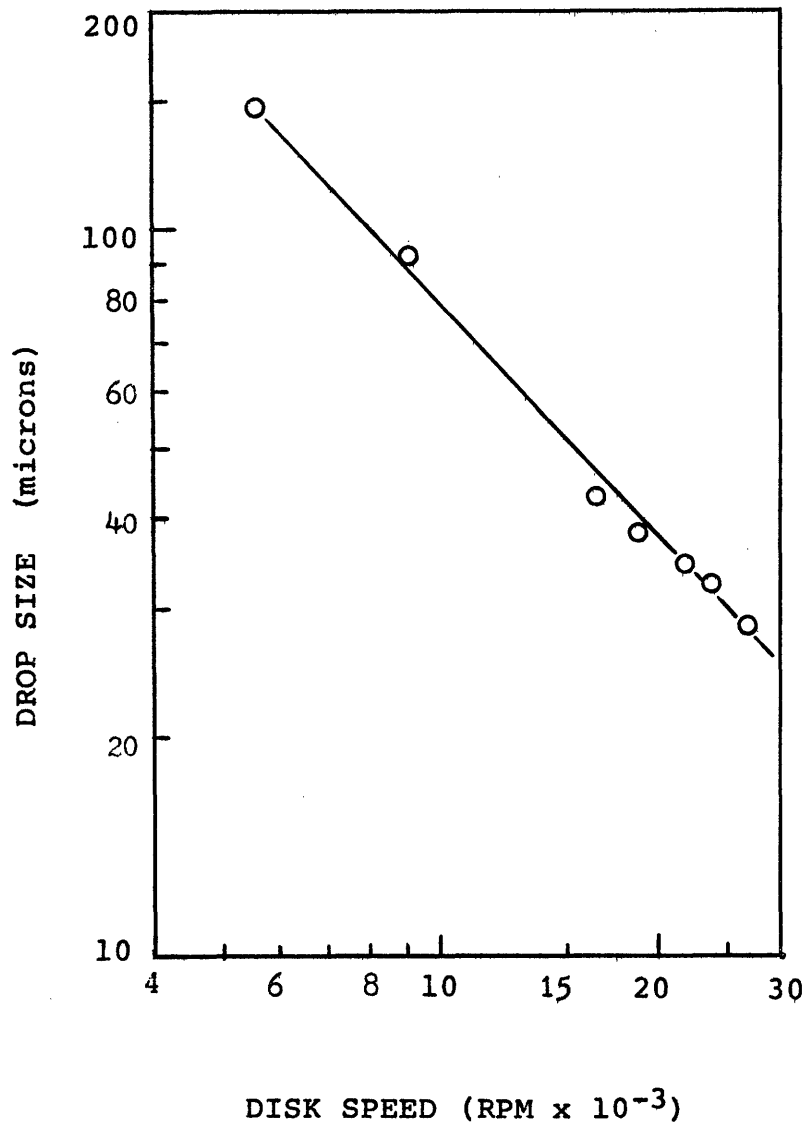
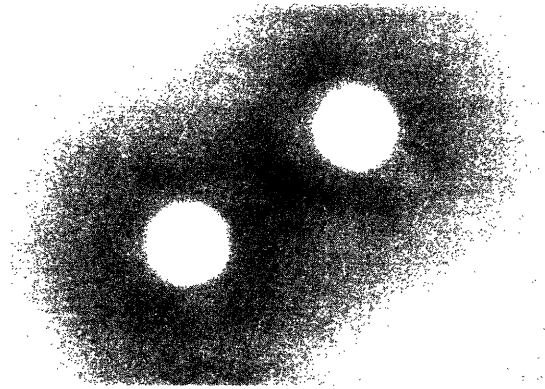# COSDEN TAR CRATERS

Figure 4.4
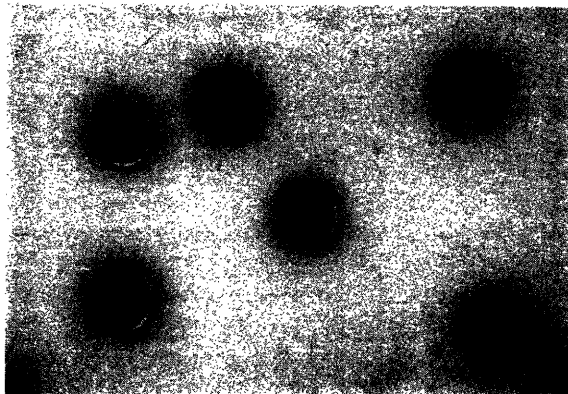

90 microns

54 microns

34 microns

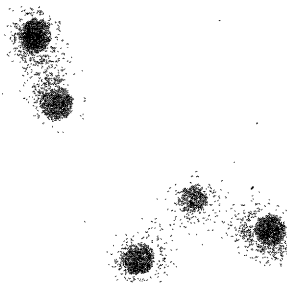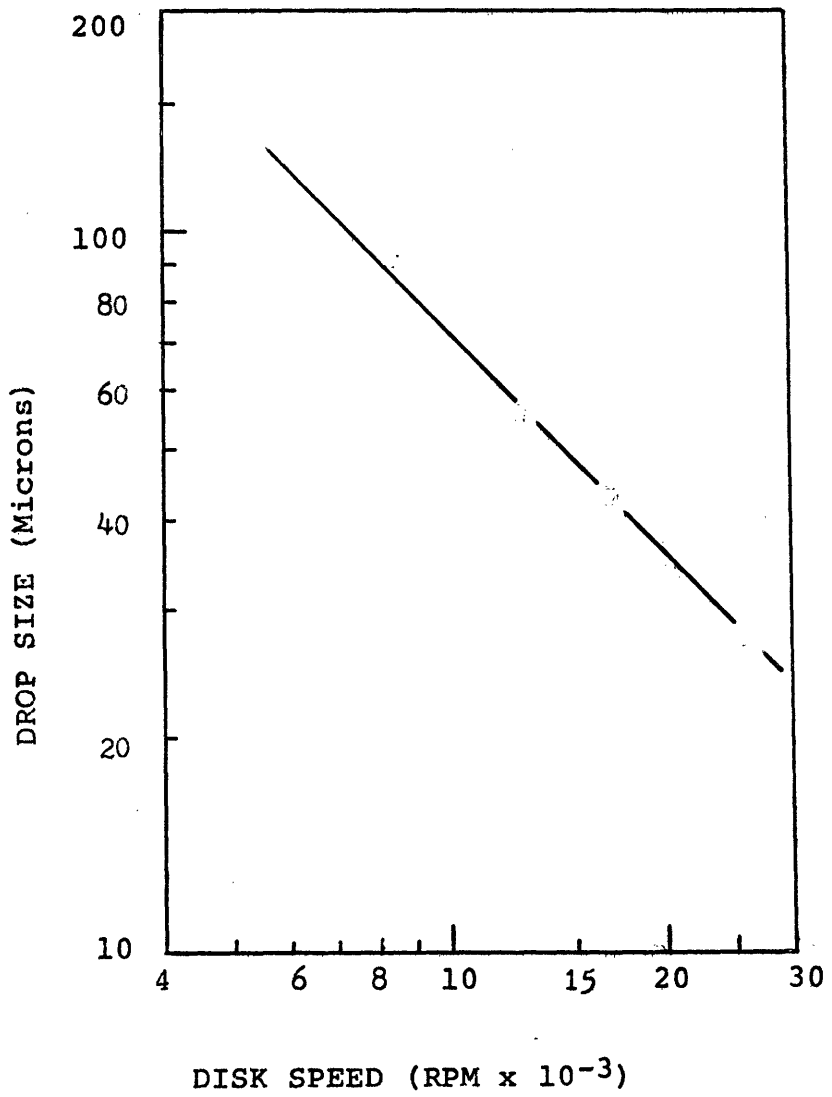# AROMATIC CONCENTRATE CRATERS

Figure 4.5

94 microns

63 microns

32 microns

ATOMIZATION OF NAPHTHALENE
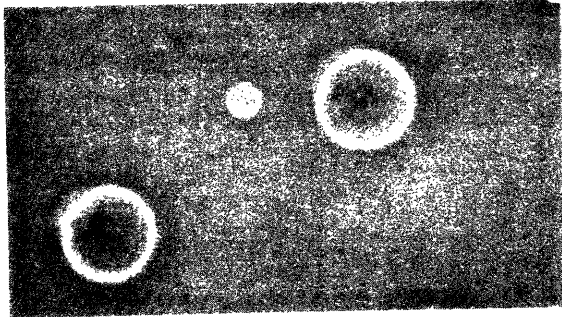
Figure 4-6

DROP SIZE (Microns) vs DISK SPEED (RPM x 10^{-3})
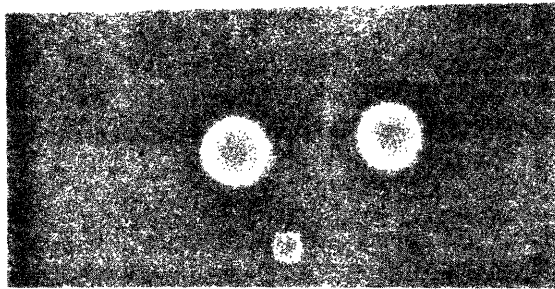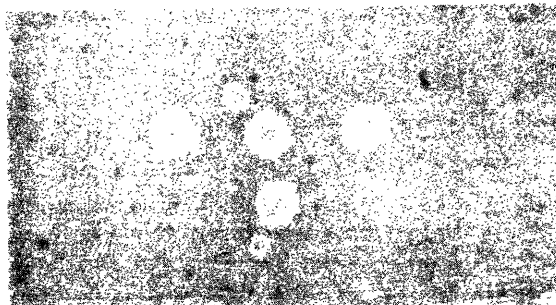
NAPHTHALENE CRATERS

Figure 4.7

95 microns

56 microns

34 microns

4.2 Formation of Carbon Black

This section will consist of a graphical presentation of the carbon formation data from this investigation. As the results are described, pertinent trends will be pointed out, but the development of a model which will attempt to explain the results will be left for Chapter V. The parameters for which the carbon black was analyzed were yield, surface area, scale, tint, extract, and particle size. These tests are described in Appendix C. This section will be composed of three parts. In the first part, the effect of temperature and drop size of the above-mentioned parameters will be presented. The following two parts will show how these parameters change as function of residence time at temperatures of 2900 and 2600°F.

4.21 Temperature Effect

The reactor wall temperature was maintained at four levels during the course of this program. These levels were: 2000, 2300, 2600 and 2900°F. The aluminum oxide reactor used during initial testing had thermowells inserted into the gas stream in addition to those attached to its walls. Since the wall and gas stream thermocouples registered very little temperature difference and responded rapidly to changes in reactor operating conditions when a high conductivity silicon carbide reactor was installed in place of the alumina reactor, the thermocouples were cemented to the wall, and it was assumed that the wall temperature was close to the gas temperature. The temperature effect was determined using the full length of the reactor and three different feed stocks. Cosden Tar (CT) was investigated in depth, with drop diameters of 100, 64, and 28 microns. Only 64 micron drops were used with the Aromatic Concentrate (AC) and the Naphthalene (N).

Yield is defined as the grams of carbon black produced per gram of oil fed. These data have been normalized to a constant residence time of 91 milliseconds. Figure 4-8 shows how yield from Cosden Tar was affected by temperature and drop size. All three drop sizes behaved approximately the same at temperatures of 2000 and 2300°F. Between 2300 and 2900°F a rapid increase in yield was obtained from the 100 micron drops. The yields at the highest temperature, 2900°F, were in the order of increasing drop size. That is, the drops requiring the longest time to vaporize give the highest yields and drops requiring the least time to vaporize produced the lowest yield. A similar performance is presented on Figure 4-9 for 64 micron drops of the three different oils. Again, yield was approximately the same at the lower temperatures, while at 2900°F the last material to completely vaporize gave the highest yield.

After weighing, the carbon black was analyzed for surface area by the method of Brunauer, Emmett, and Teller (B.E.T). In all solids analysis of low temperature carbon black (2000°F), the reader should keep in mind that this material contains from 5 to 45% of a benzene-extractable hydrocarbon. It is not known if and how this extractable may have altered the various analyses. The variation of surface area with temperature is indicated on Figure 4-10. Looking at plot a, and keeping in mind that a high surface area means a small particle size, for black made from Naphthalene a steady increase in surface area was observed with increasing temperature, whereas the surface area of both Aromatic Concentrate and Cosden Tar black passed through a maximum. The curves on graph b show that the surface area of black from both 64 micron and 28 micron drops of Cosden Tar passed through a maximum while the surface area of black from the 100 micron drops steadily
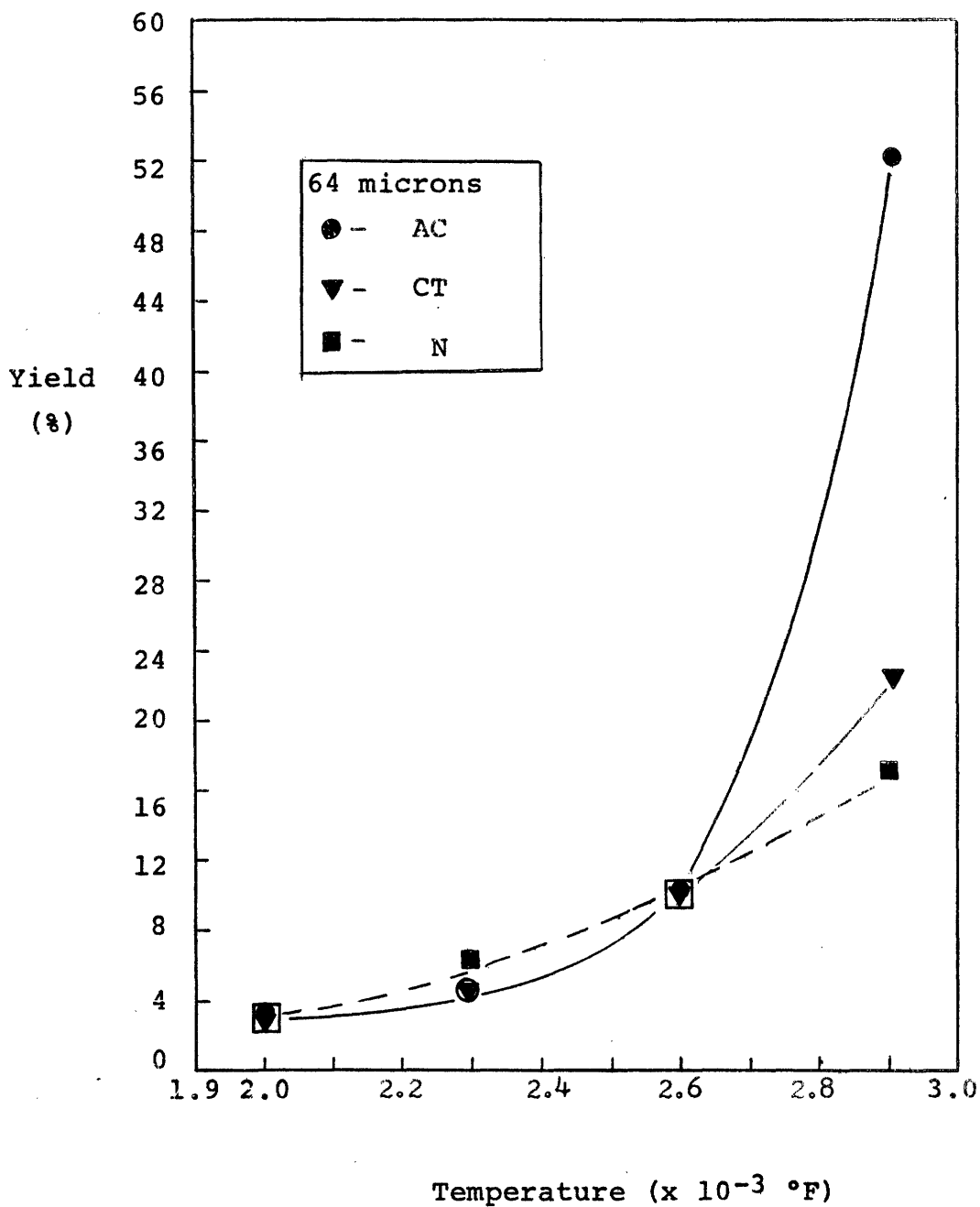
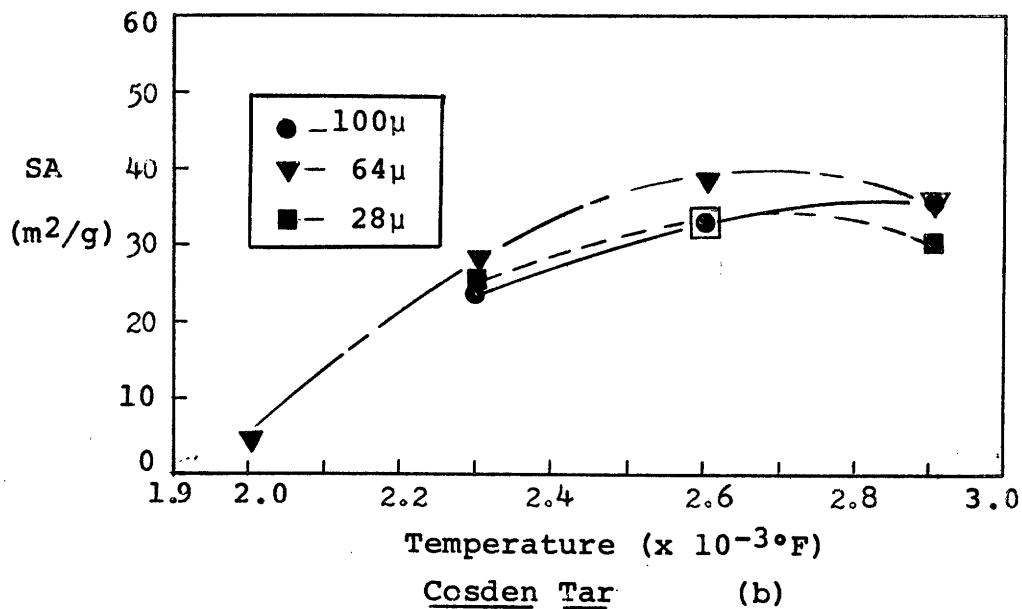EFFECT OF TEMPERATURE ON YIELD

Figure 4-8
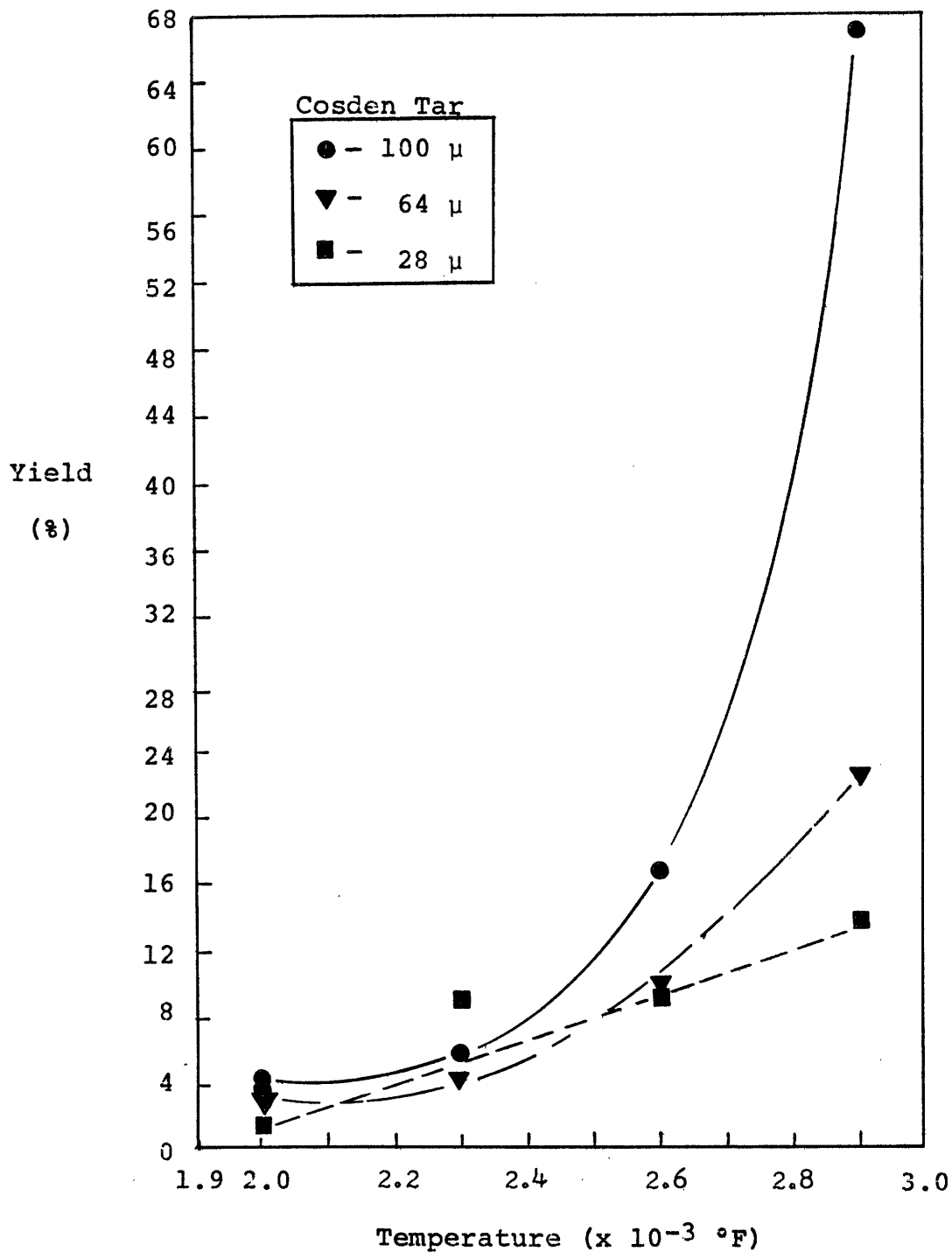
EFFECT OF TEMPERATURE AND
FEED STOCK ON YIELD

Figure 4-9

EFFECT OF TEMPERATURE ON SURFACE AREA

Figure 4-10

64 micron Drops   (a)

Cosden Tar   (b)
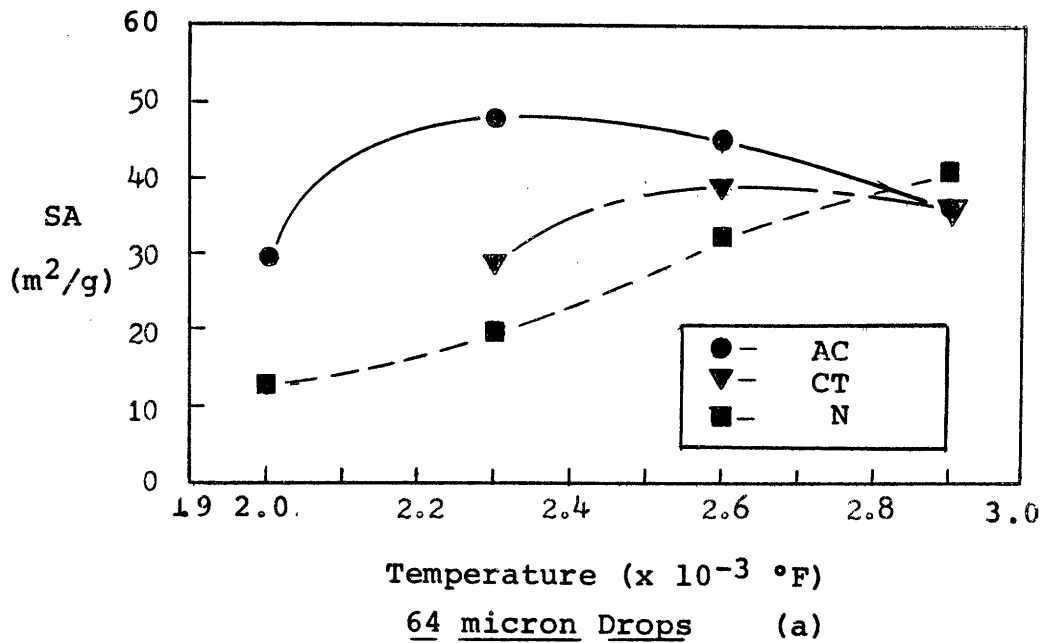
increased with temperature. In all cases at 2900°F, where vaporization time was only a small part of total residence time, the surface areas were nearly the same.

Scale, at least for the present, will be considered as a measure of the blackness or absorptivity of the particles. It should be kept in mind that a change in hydrogen-to-carbon ratio, for the same size carbon particle, could change its absorptivity and the value of scale. The variation in scale with temperature is depicted on Figure 4-11. In both plots (a and b), a general decrease in scale was found between 2000°F and 2600°F. The scale remained essentially constant between 2600 and 2900°F. One should note on plot b that 28 micron drops produced black with the highest scale, while 64 micron drops produced the lowest scale black.

In the discussion of results (Chapter V), an attempt will be made to attach a physical significance to the value of percent tint. At the present time, let us consider the tint as a hiding power of the carbon black and keep in mind that it should be related to the size and general structure of the carbon black chain. The variation of tint with temperature for Cosden Tar black is shown on Figure 4-12. With this oil, and 64 micron drops, the tint steadily increased with temperature, while for black from 100 and 28 micron drops, the tint passed through a maximum near 2600°F. Sixty-four micron drops of all three feed materials demonstrated a similar behavior, and the results are indicated on Figure 4-13.

The variation of particle size with temperature is plotted on Figure 4-14. These diameter values were taken from electron micrographs, and it should be remembered that they are average values and subject

EFFECT OF TEMPERATURE ON SCALE

Figure 4-11

Temperature (x 10^{-3}°F)
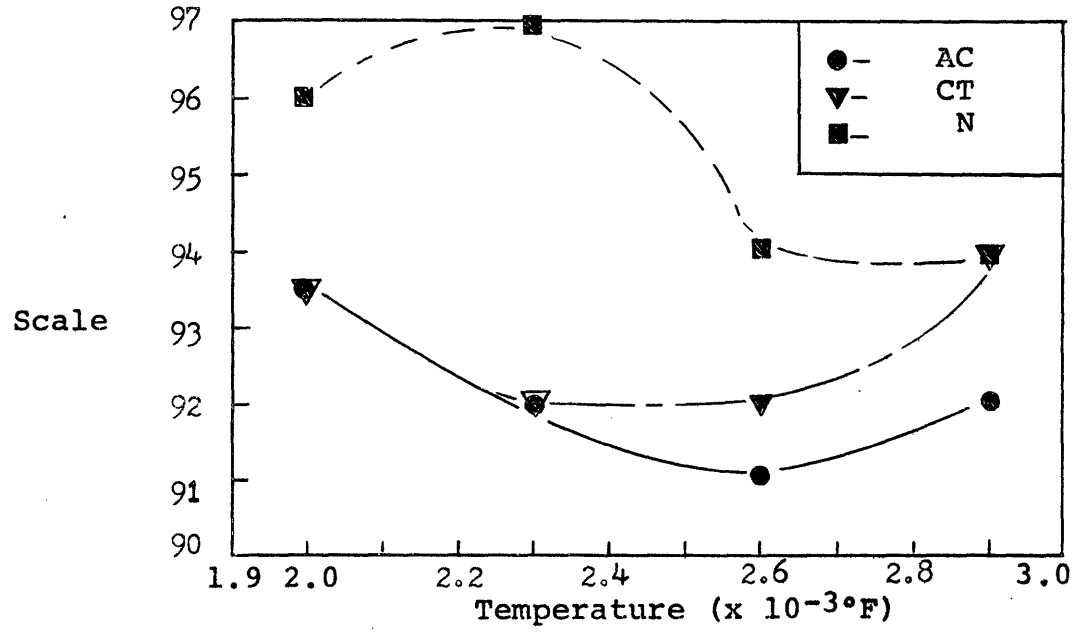
64 micron Drops   (a)
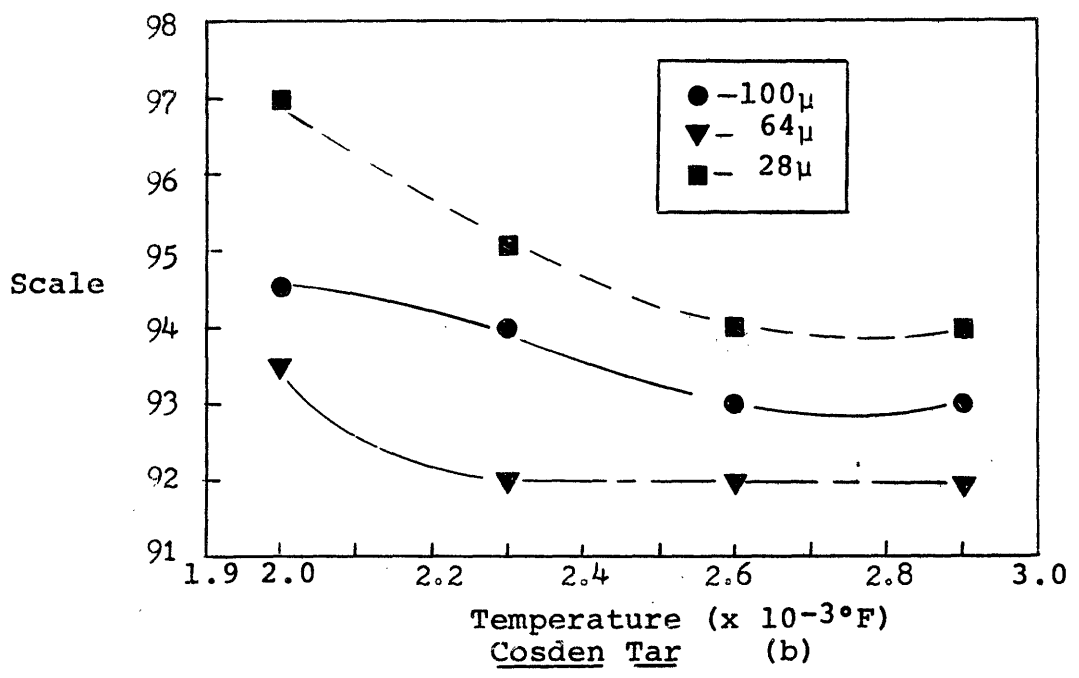
Temperature (x 10^{-3}°F)

Cosden Tar   (b)

EFFECT OF TEMPERATURE ON TINT

Figure 4-12

Cosden Tar

● — 100 μ
▼ — 64 μ
■ — 28 μ

Tint (%)
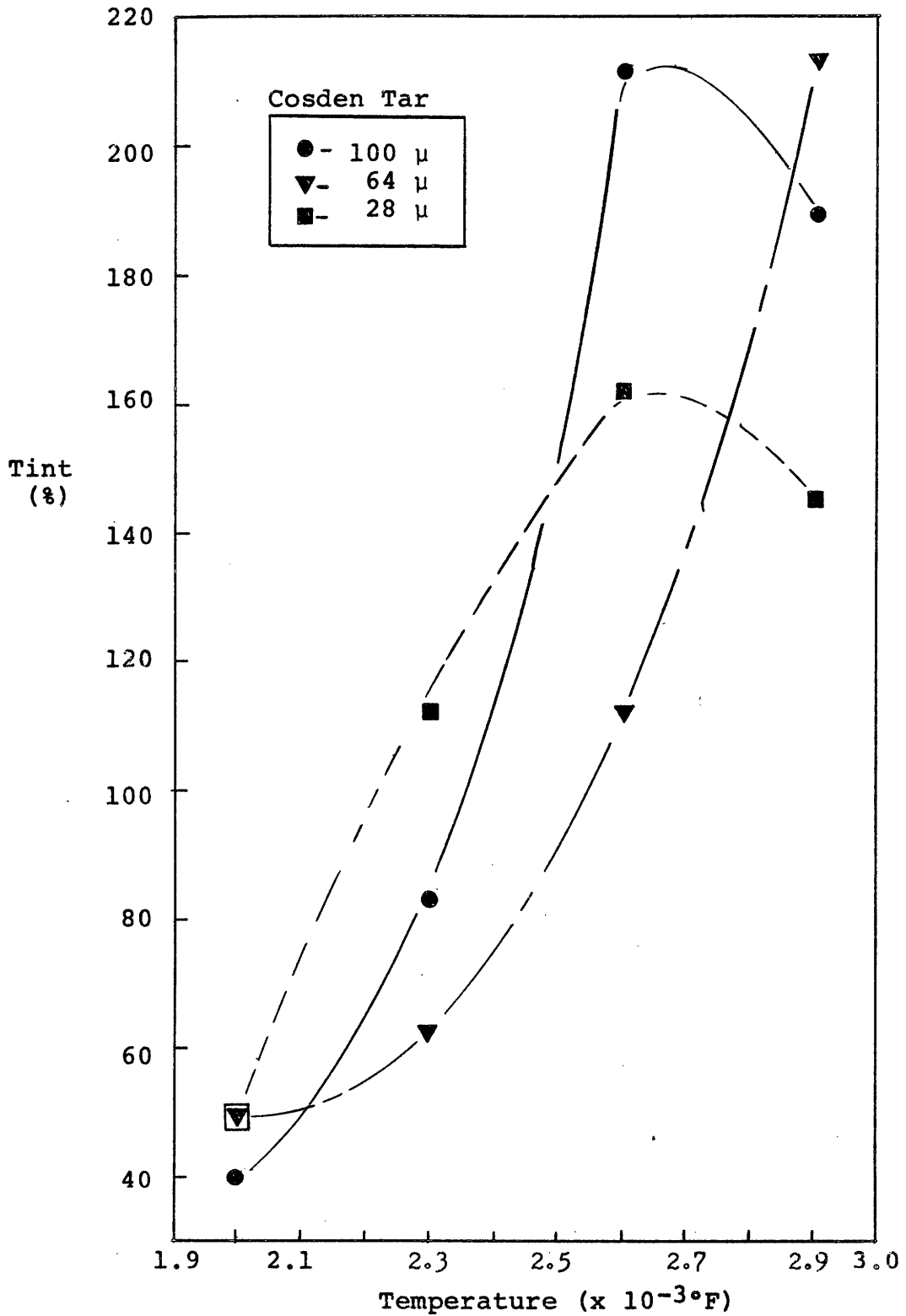
Temperature (x 10^{-3}°F)

EFFECT OF TEMPERATURE AND FEED STOCK ON TINT
Figure 4-13

64 micron Drops

● —	AC
▼ —	CT
■ —	N

Tint (%)
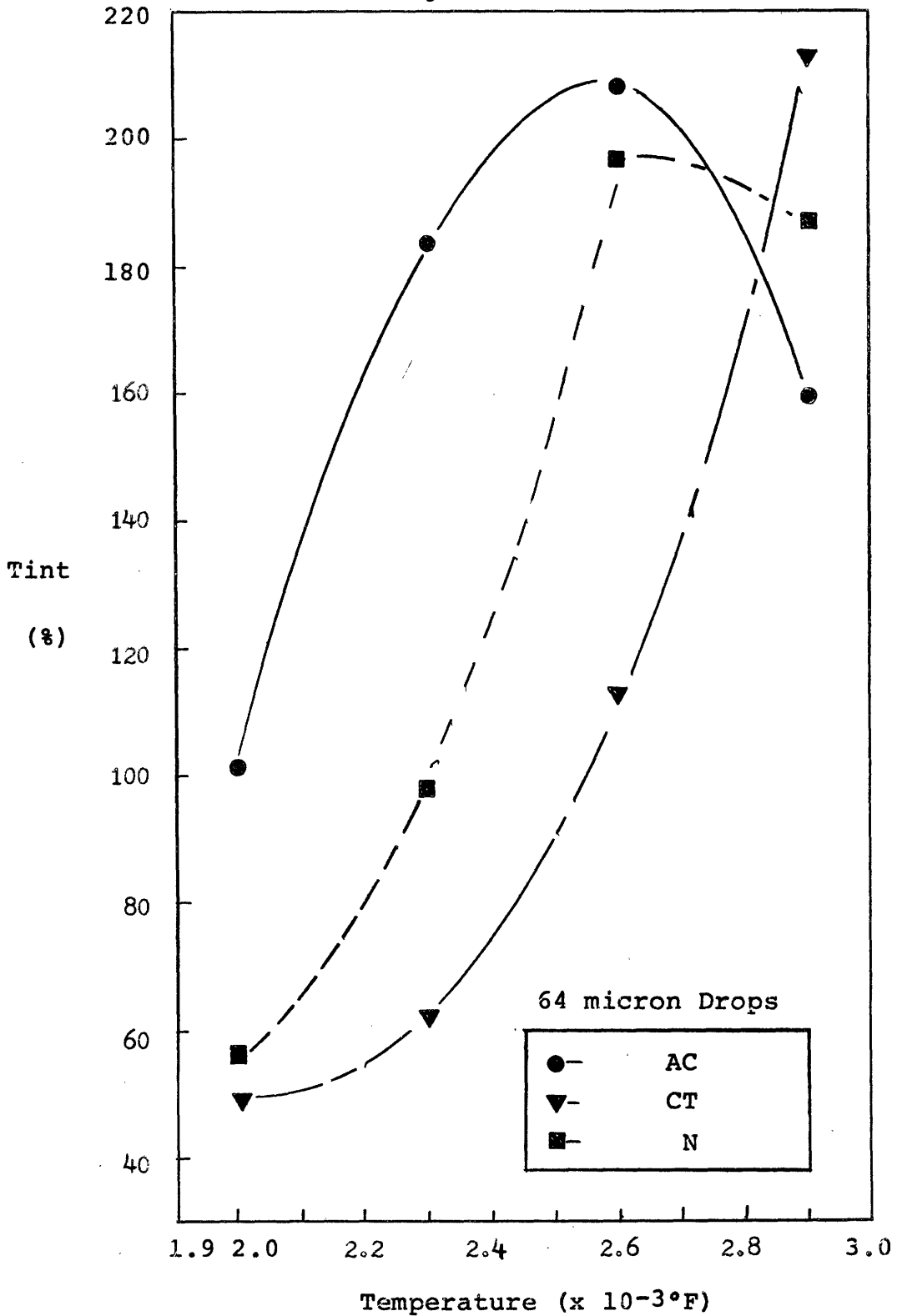
Temperature (x 10-3°F)

EFFECT OF TEMPERATURE ON PARTICLE SIZE

Figure 4-14

64 micron Drops (a)

Cosden Tar (b)
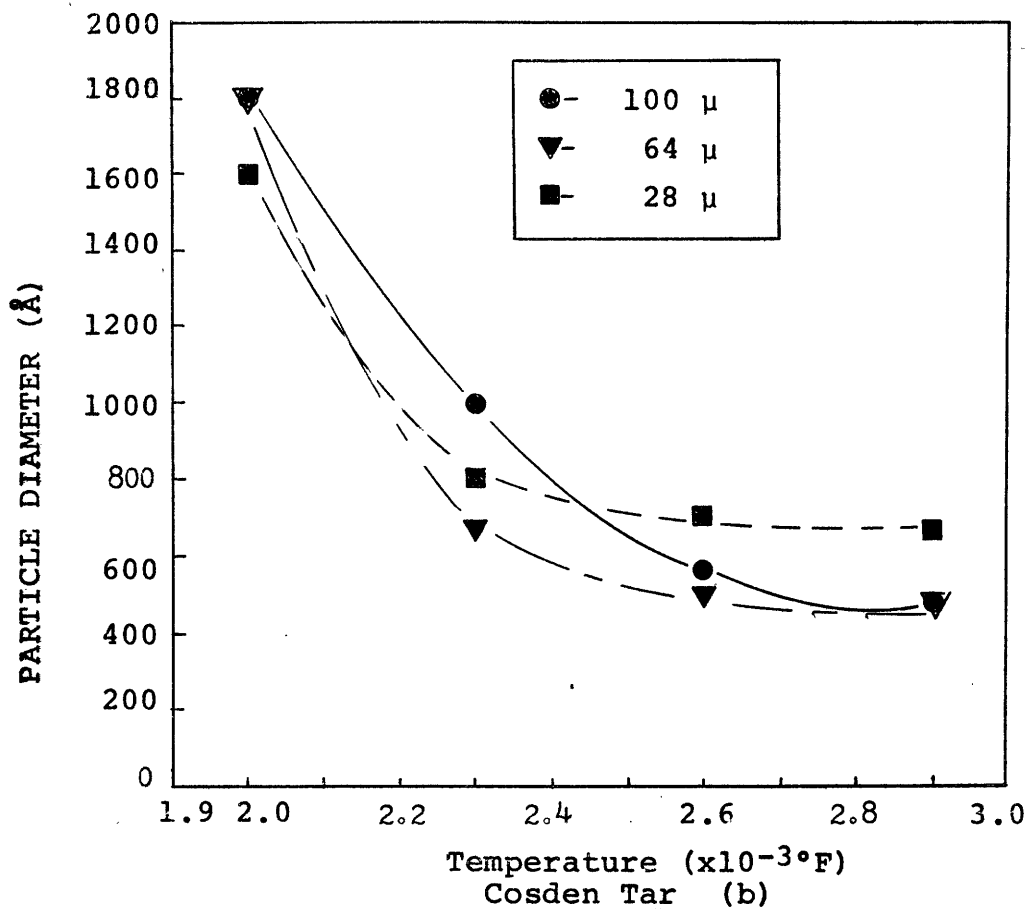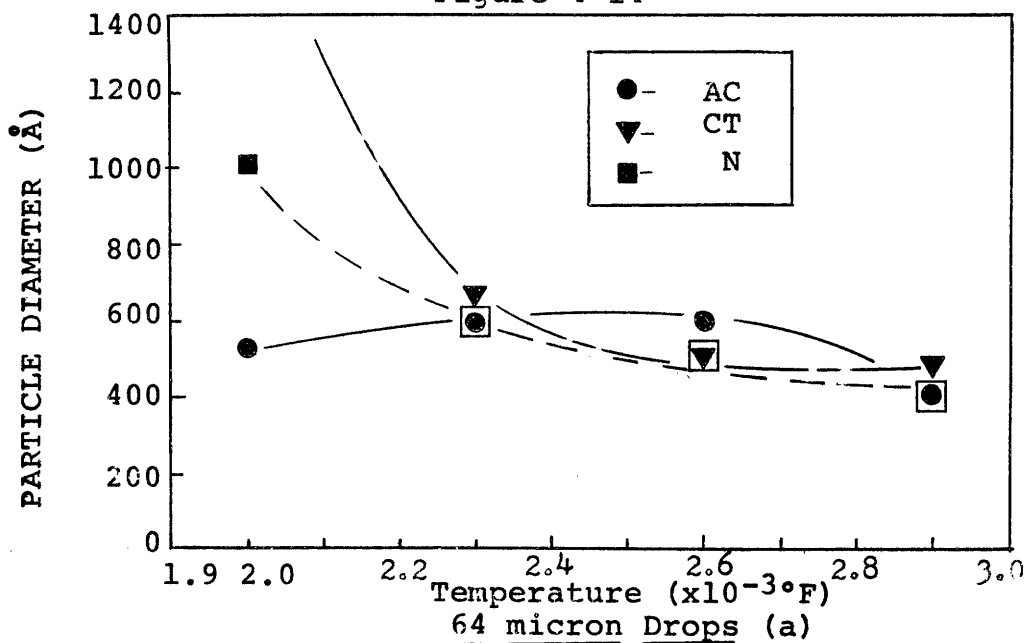
to considerable variation (+30%). In all cases, the particle diameter
decreased as the temperature was increased. Only a small change was
observed between 2600 and 2900°F.

4.22 Residence Time Effect

In order to gain more insight into the growth process, experiments
were carried out at three residence times. The runs were made at the same
conditions as the tests described in section 4.21, except that the residence
time was varied by changing the position of the quench probe. These tests
were made at 2900 and 2600°F, since only these temperatures produced
carbon black at a reasonable rate.

4.221 2900°F. The effect of residence time on the yield of carbon
black from Cosden Tar is shown on Figure 4-15. As noted earlier, the
last material to vaporize completely (100 micron drops) gave the highest
yield. The first material to vaporize completely (28 micron drops)
showed only a gradual increase in yield with residence time. The results
from similar conditions with 64 micron drops and three feed stocks are
depicted on Figure 4-16. In this case, the last material to vaporize
was Aromatic Concentrate (AC), and it gave the highest yield. Naphthalene,
the first material to vaporize, showed a steady increase in yield with
time but had a lower yield than either of the oils at 90 milliseconds.

The general reduction of surface area with residence time is
shown on Figure 4-17. The variation of surface area with feed stock
is depicted on plot a. Except for Naththalene, the smallest particles
were present at approximately 40 milliseconds. This figure indicates
that the particles were steadily growing as the residence time was
increased. In contrast, the size of the black produced from Naphthalene
appeared to pass through a minimum. In a similar manner, the size of

EFFECT OF RESIDENCE TIME ON YIELD
2900°F
Figure 4-15
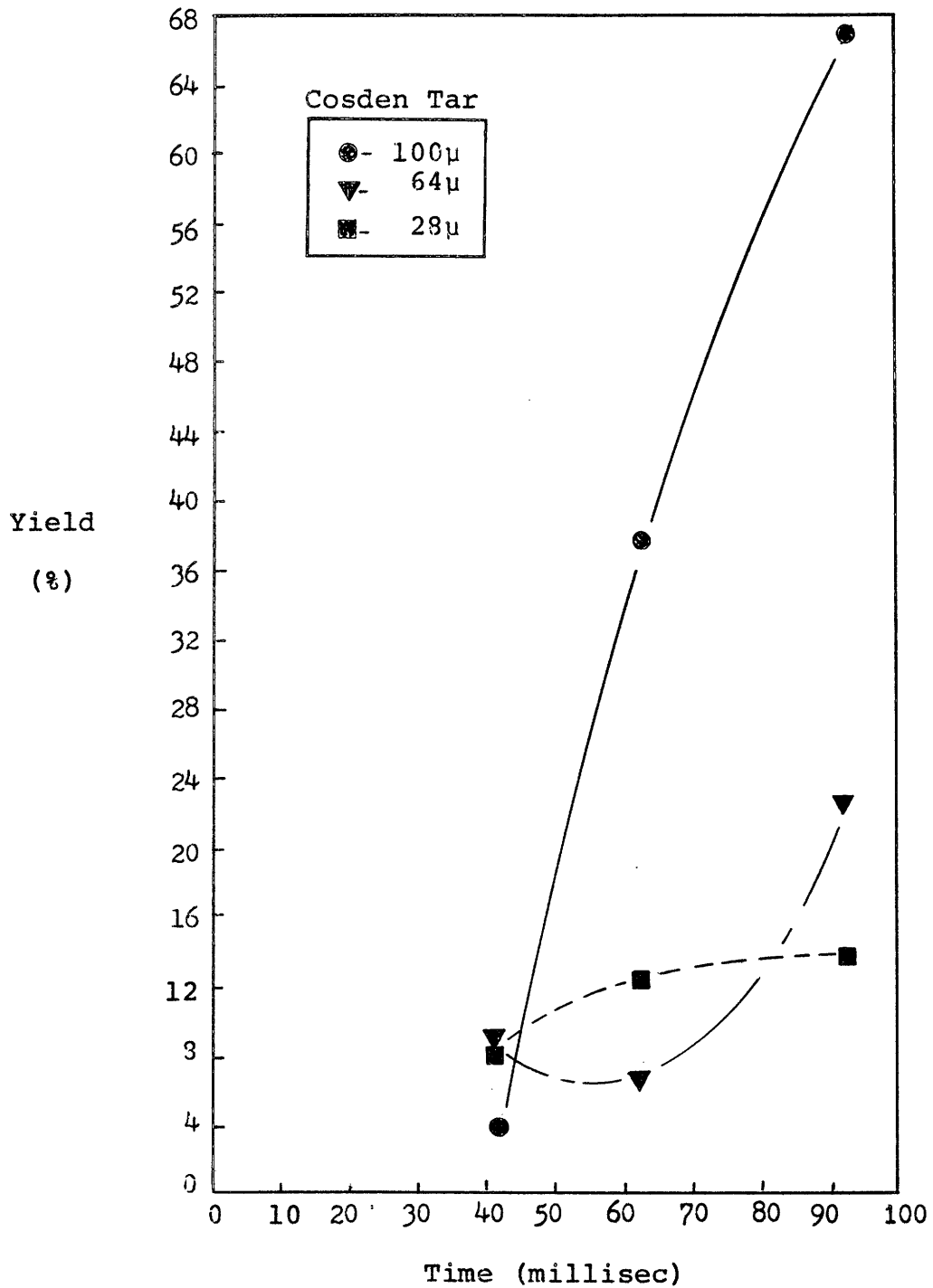
EFFECT OF FEED STOCK ON YIELD

2900°F

Figure 4-16
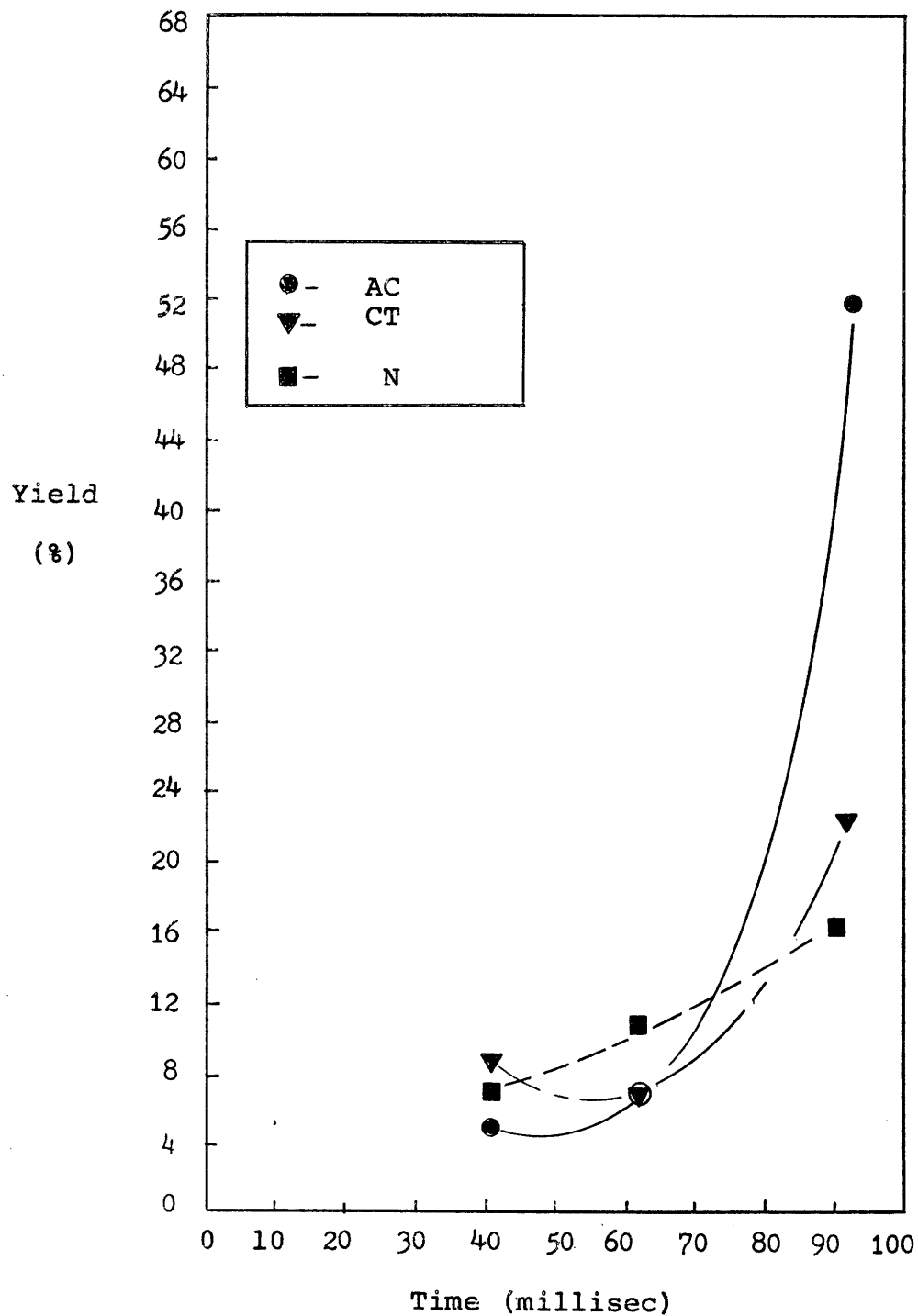
EFFECT OF RESIDENCE TIME
ON SURFACE AREA

2900°F

Figure 4-17
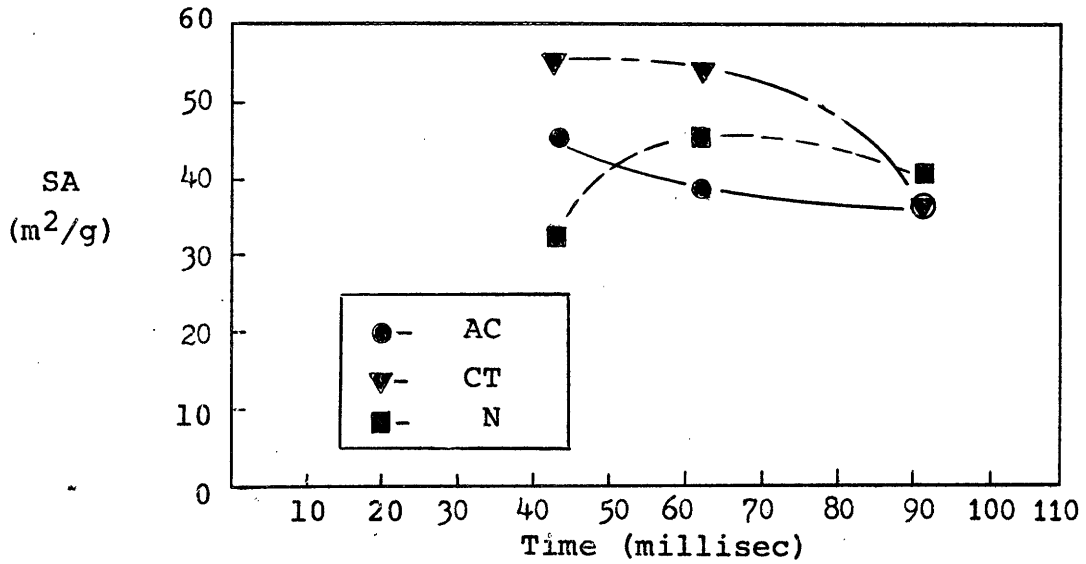
64 micron Drops (a)
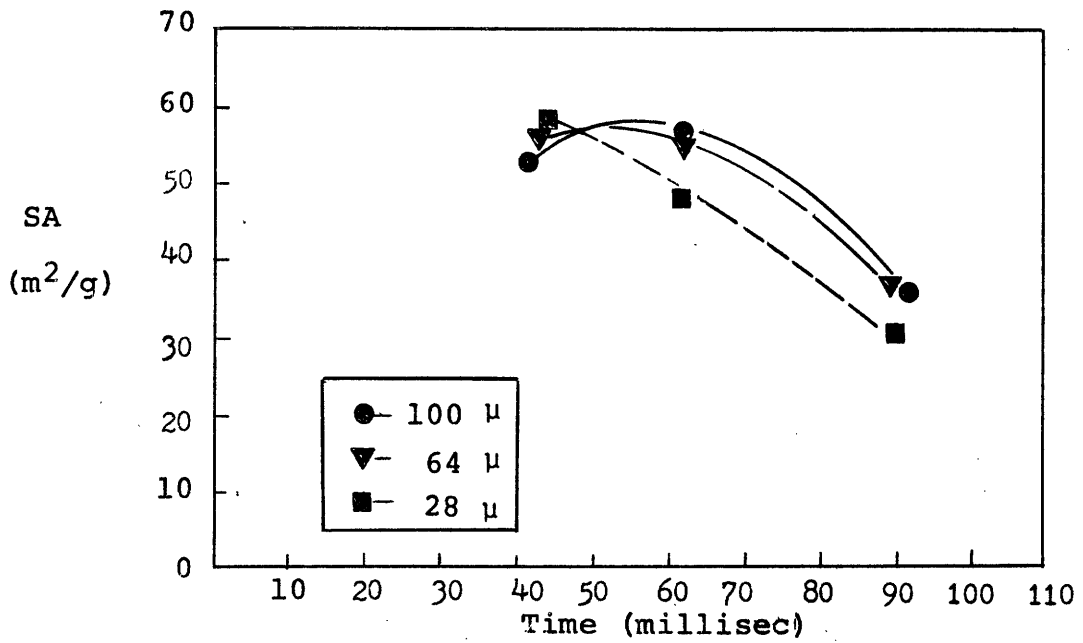
Cosden Tar (b)

the carbon black from 100 micron drops of Cosden Tar (plot b) passed

through a minimum while black from 64 micron and 28 micron drops

steadily increased in size with time.

The variation of scale over the same range of operating conditions

is given on Figure 4-18. On graph (a) is shown how the scale increased

with time, while at 90 milliseconds all three feed stocks produced

blacks with approximately the same scale. The scale of blacks produced

from the three drop sizes of Cosden Tar is shown on graph (b). All

blacks initially had the same scale (89) at 40 milliseconds and increased

in scale to slightly different values at 90 milliseconds.

The change in tint with time is plotted on Figure 4-19. The

black from Naphthalene and Cosden Tar (64 micron drops) passed through

a maximum at 60 milliseconds, while black from Aromatic Concentrate

appeared to have a minimum at 60 milliseconds. The variation of tint

with drop size is depicted on plot b. Here the black from 28 micron

drops showed a steady loss of hiding power with time, while the tint

of the other two materials passed through a maximum at 60 milliseconds.

The actual size of the black particles (determined from electron

micrographs) as a function of time is shown on Figure 4-20. All particles

showed an increase in diameter with time which produced a straight line

when the log of diameter was plotted against time. The black produced

from Cosden Tar was initially smaller than that produced from Aromatic

Concentrate and Naphthalene. After 90 milliseconds, the largest black

was produced from Cosden Tar.

4.222 2600°F. The variation of yield with residence time, at

2600°F, is plotted on Figure 4-21. The different feed stocks (plot a)

show a considerable amount of variation. The yield of black from

EFFECT OF RESIDENCE TIME ON SCALE

2900°F

Figure 4-18

64 micron Drops (a)
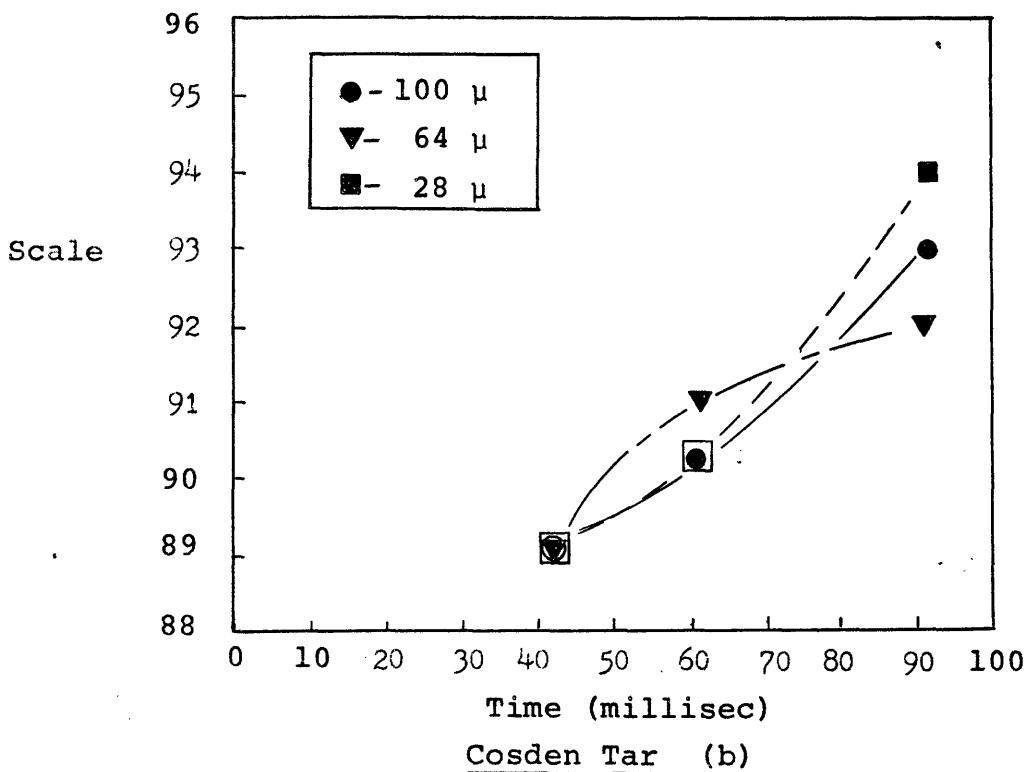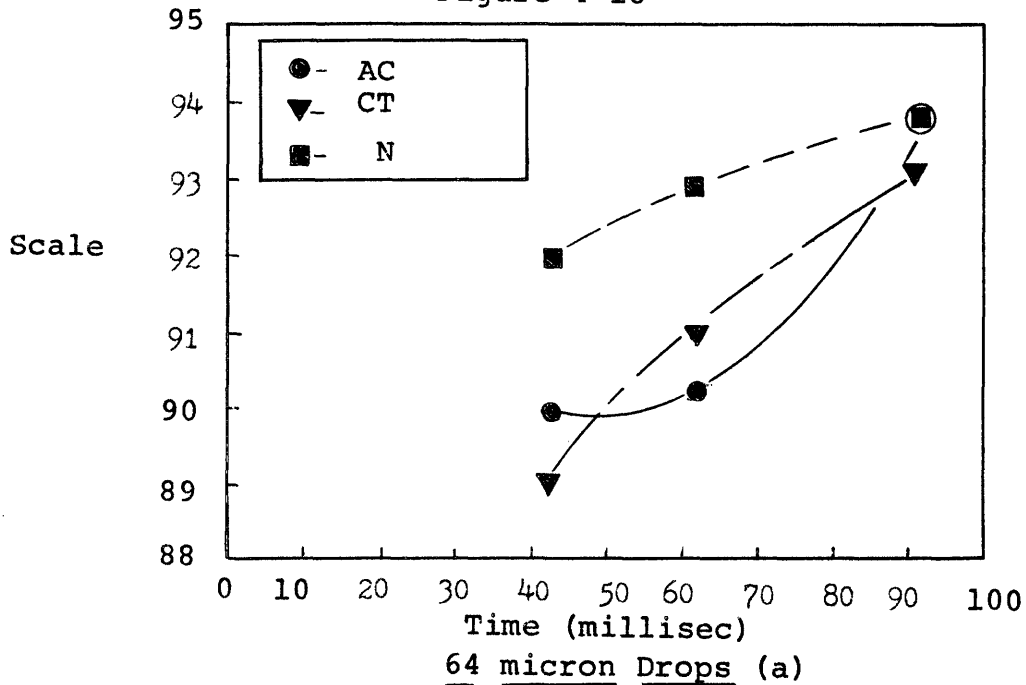
Cosden Tar (b)

EFFECT OF RESIDENCE TIME ON TINT
2900°F

Figure 4-19
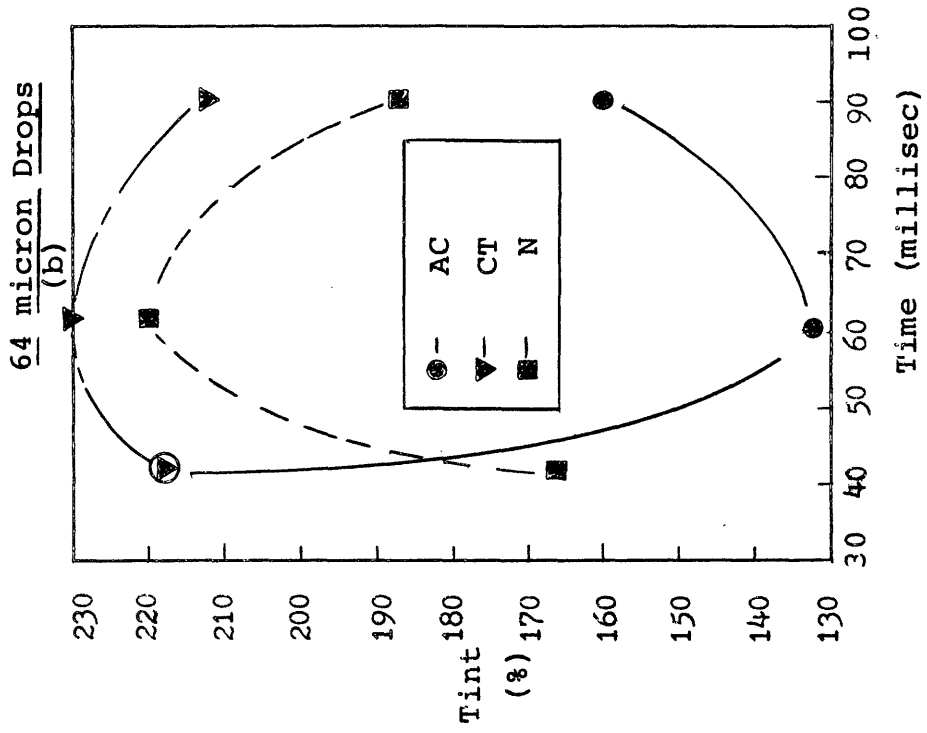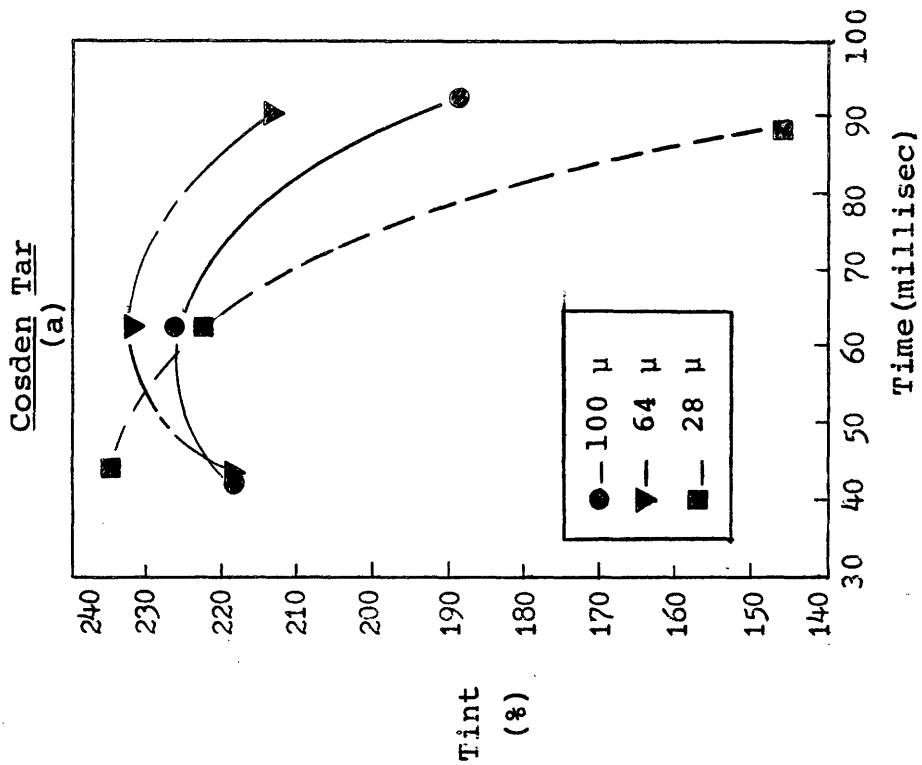
EFFECT OF RESIDENCE TIME
ON PARTICLE SIZE
2900°F

Figure 4-20
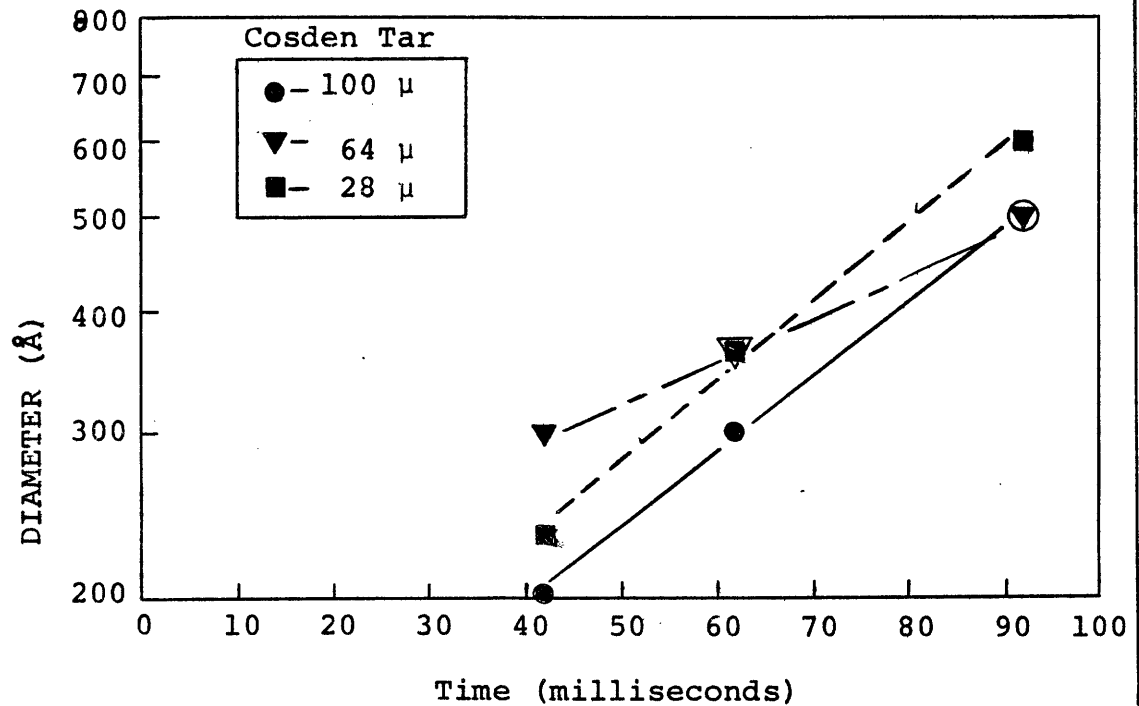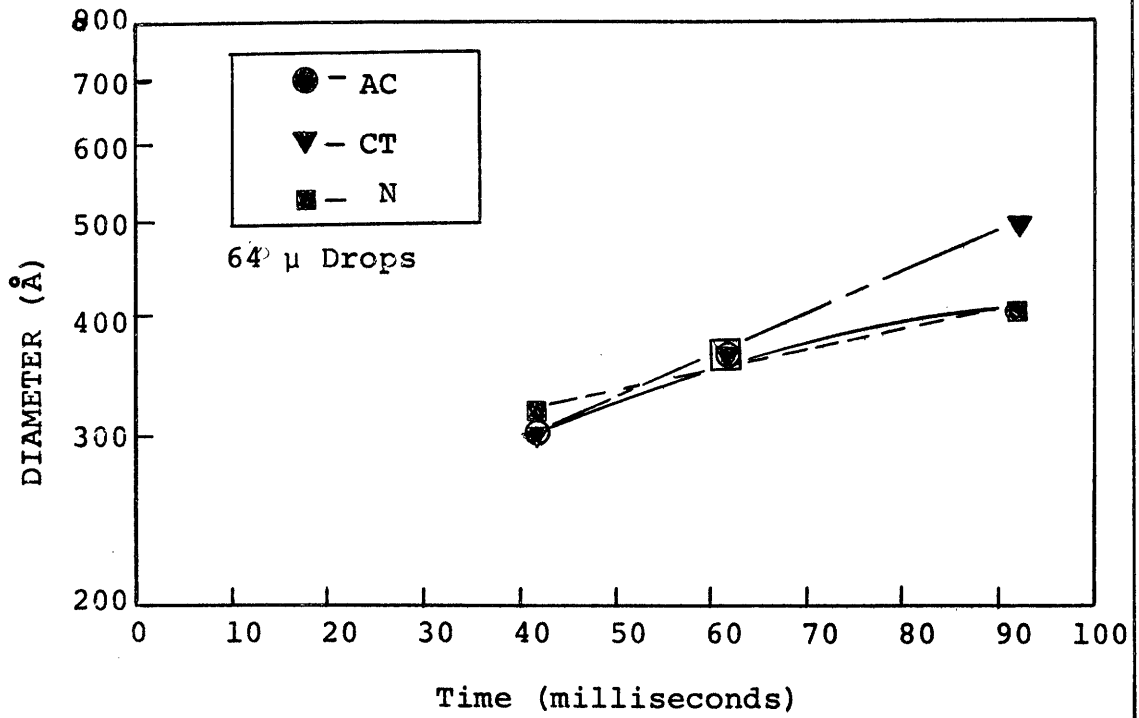
EFFECT OF RESIDENCE TIME ON YIELD

2600°F

Figure 4-21

Cosden Tar
(a)

64 micron Drops
(b)
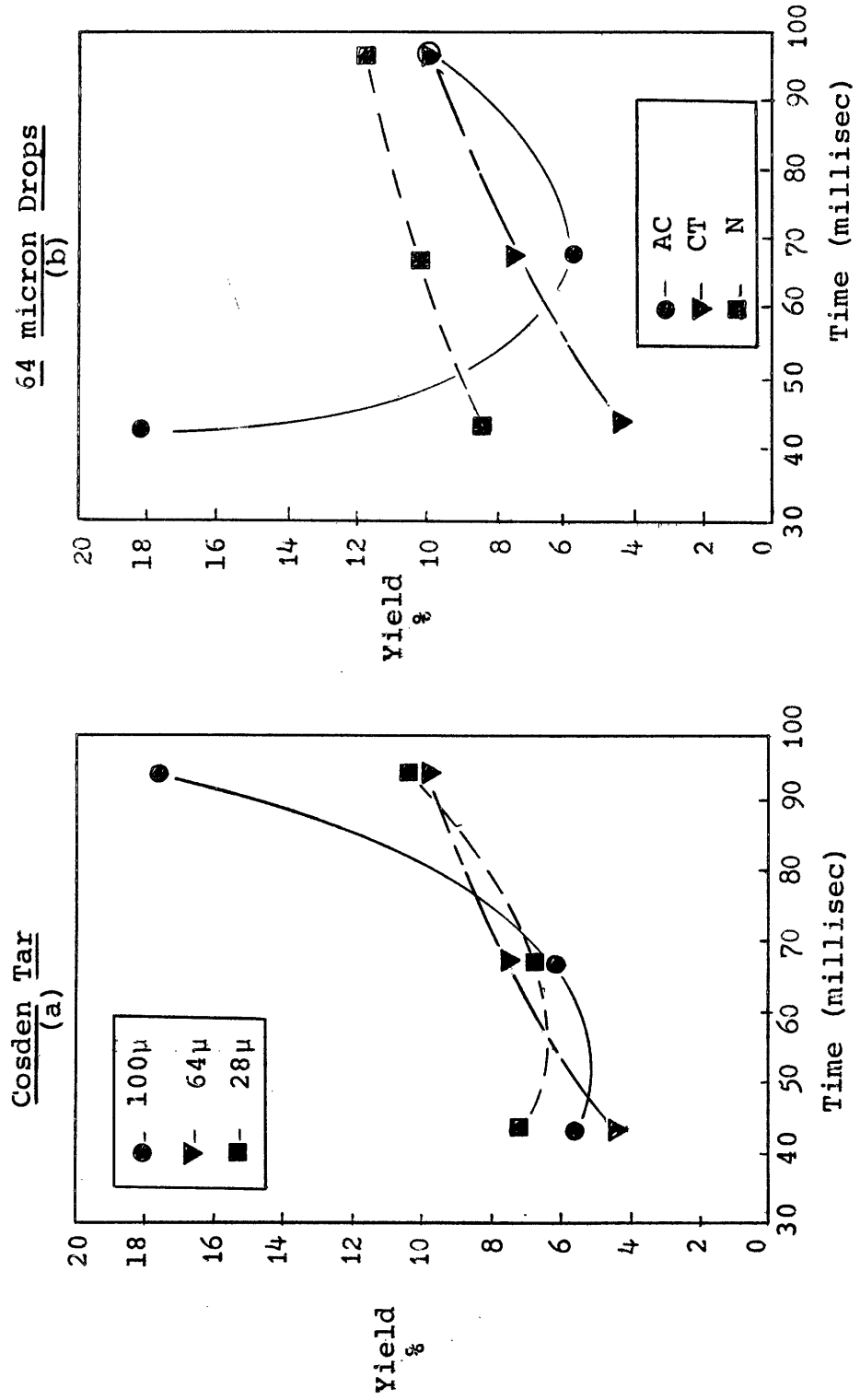
Cosden Tar and Naphthalene increased with time except for the Naphthalene point at 44 milliseconds. Black production from Aromatic Concentrate appeared to pass through a minimum at 70 milliseconds. The yield of black from 64 micron and 28 micron drops of Cosden Tar (plot b) increased gradually with residence time.

Similarly, erratic variations with time were also present in other analyses. The variation of surface area with time is shown on Figure 4-22. The black from different starting materials (plot a) had surface areas at 45 milliseconds ranging from 38 to 60 square meters per gram. As residence time was increased, the black from Naphthalene and Cosden Tar increased in size, while the black from Aromatic Concentrate appeared to have a minimum in size at 70 milliseconds. A similar behavior was noted for the different drop sizes of Cosden Tar (plot b). The black produced from 100 micron drops of Cosden Tar had a maximum surface area or minimum size at 70 milliseconds. Blacks from the other drop sizes had surface areas which decreased with time.

The variation of scale with time is shown in Figure 4-23. The scale of the black from Naphthalene and Cosden Tar increased with time. The scale value appeared to pass through a minimum for black from Aromatic Concentrate. An analogous behavior was noted in the case of the black produced from different sized drops of Cosden Tar. For this material, the scale of the black from 28 micron and 64 micron drops increased with time, while the scale of the carbon black produced from 100 micron drops appeared to pass through a minimum.

Changes in tint as a function of residence time, at 2600°F, are shown in the next two figures. The increase in the tint of the black produced from Naphthalene is shown on Figure 4-24. At the same conditions,

EFFECT OF RESIDENCE TIME
ON SURFACE AREA
2600°F
Figure 4-22

64 micron Drops
(a)
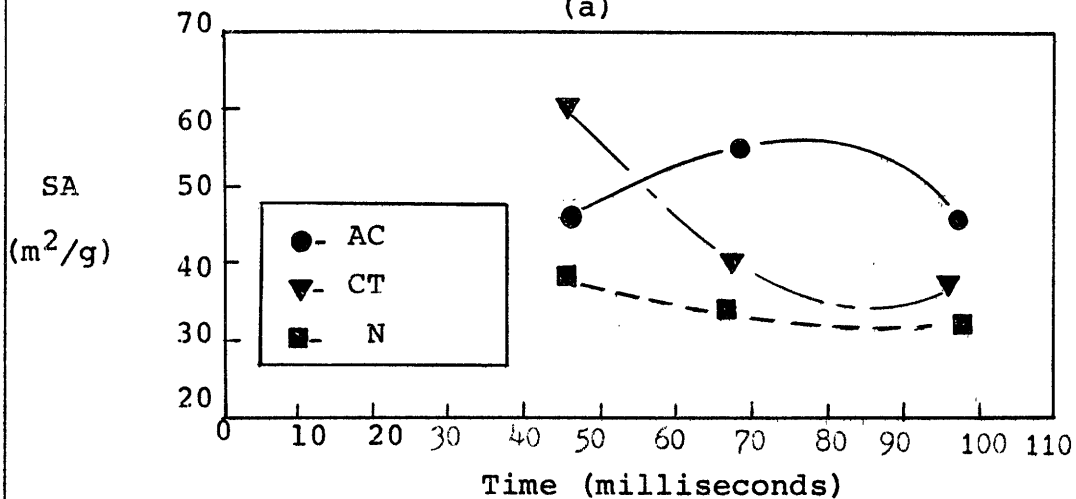
Cosden Tar
(b)
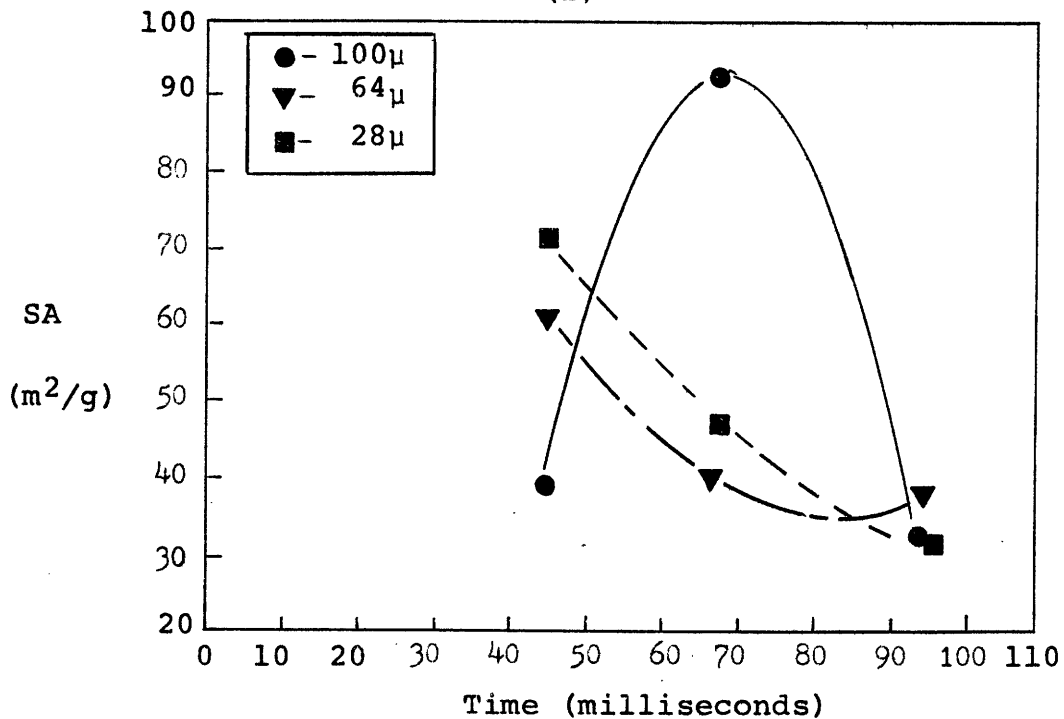
EFFECT OF RESIDENCE TIME
ON SCALE
2600°F
Figure 4-23

(a)   64 micron Drops
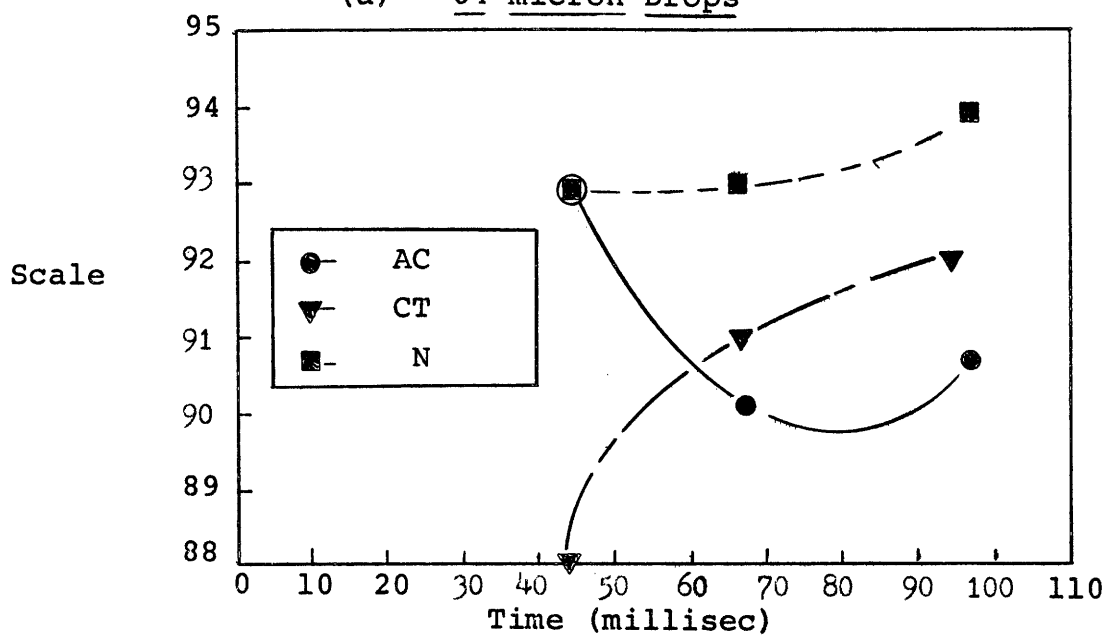
(b)   Cosden Tar
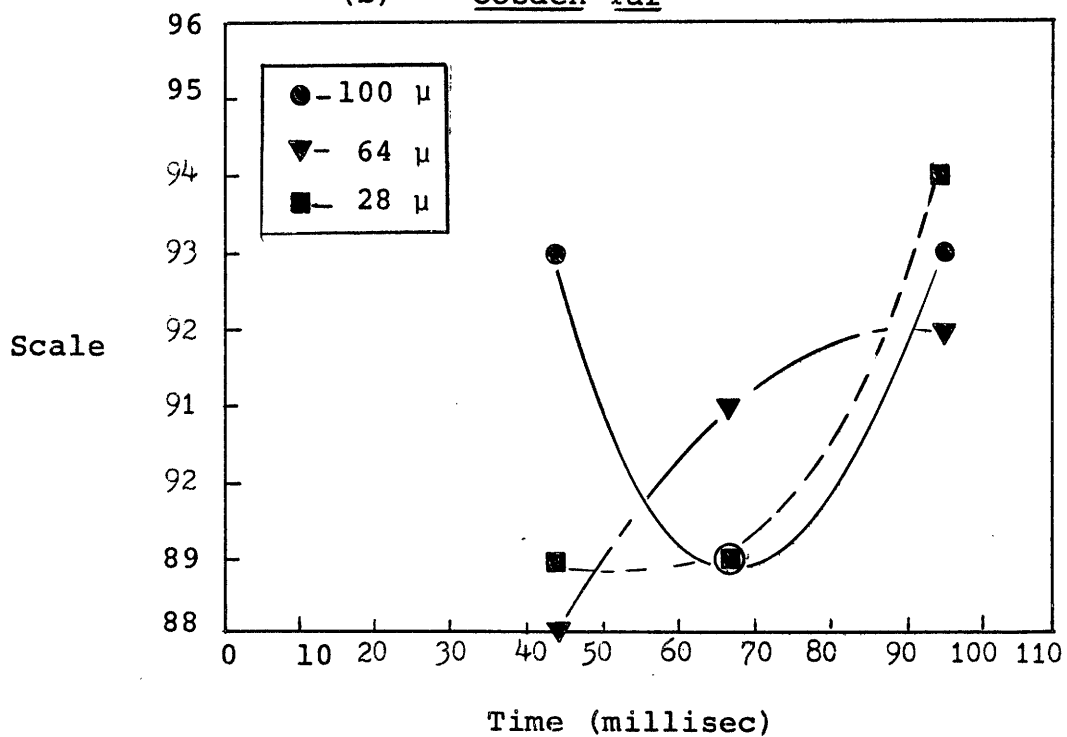
EFFECT OF RESIDENCE TIME

AND FEED STOCK ON TINT

2600°F

Figure 4-24

64 micron Drops
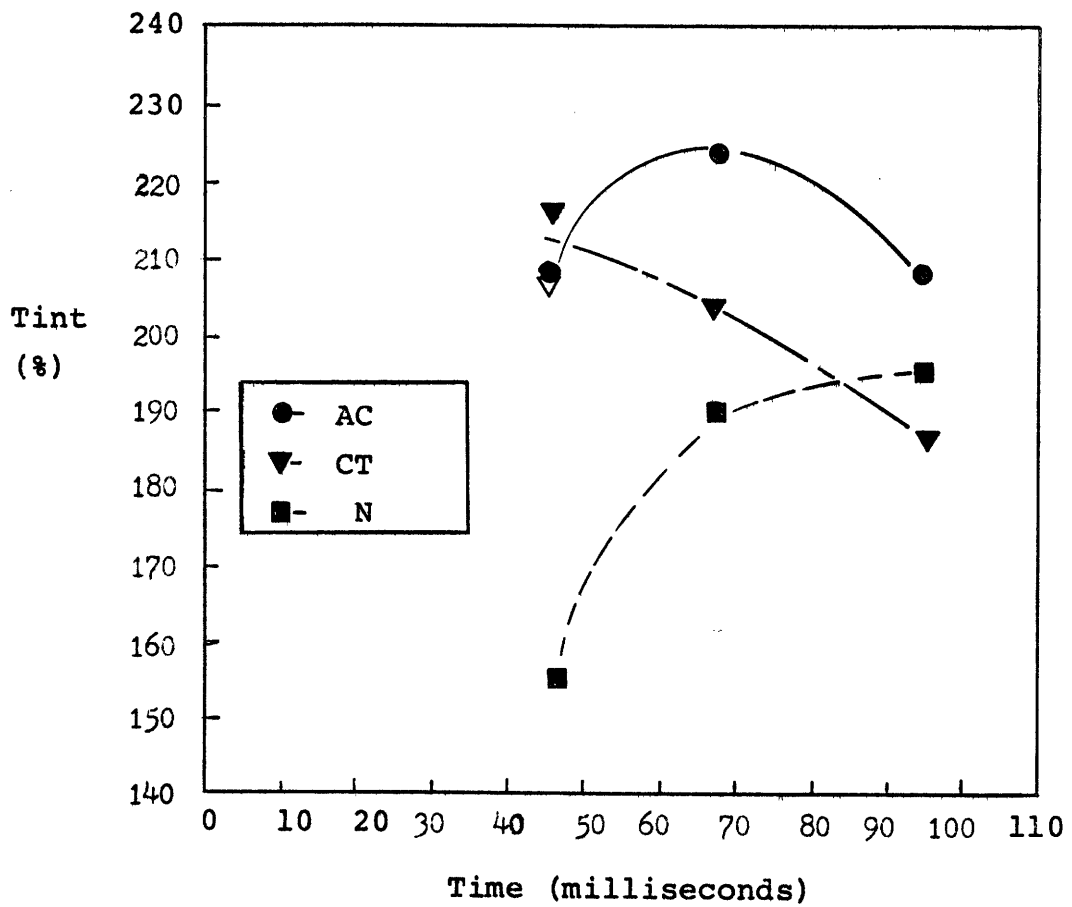
the tint of the black from Cosden Tar decreased with time, while the
tint of black from Aromatic Concentrate went through a maximum. The
behavior of the different sized drops of Cosden Tar was slightly
different (Figure 4-25). The black from both the 28 micron and 100 micron
drops showed a minimum tint with residence time while the tint of the black
from 64 micron drops steadily decreased with time.

The variation of particle size with residence time at 2600°F is
shown on Figure 4-26. In all cases, a plot of the log of diameter against
time produced a straight line. At 44 milliseconds, Cosden Tar produced
the smallest particles and at 94 milliseconds the largest particles.

EFFECT OF RESIDENCE TIME

AND DROP SIZE ON TINT

2600°F

Figure 4-25

Cosden Tar

Time (milli-sec)
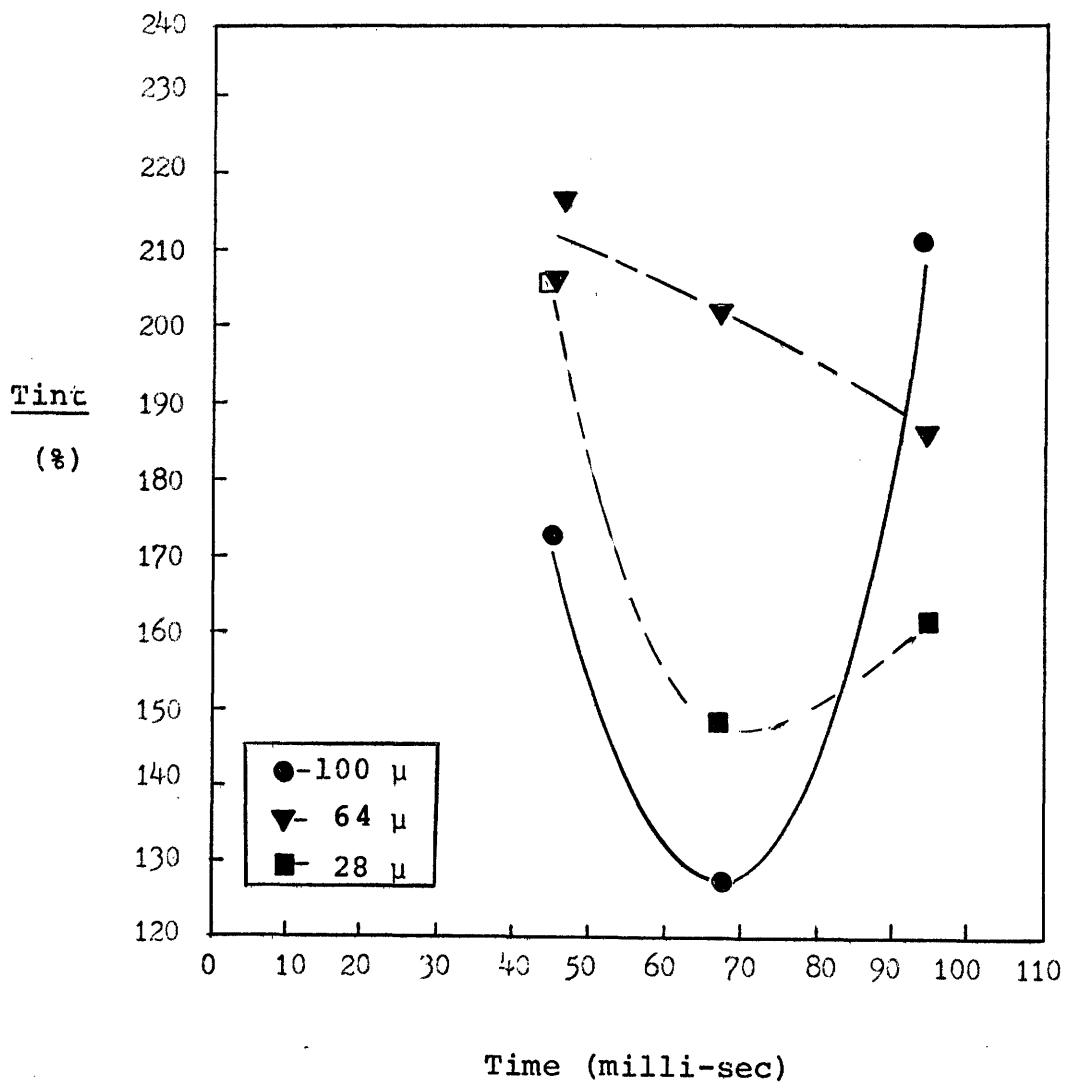
EFFECT OF RESIDENCE TIME
ON PARTICLE SIZE

2600°F

Figure 4-26
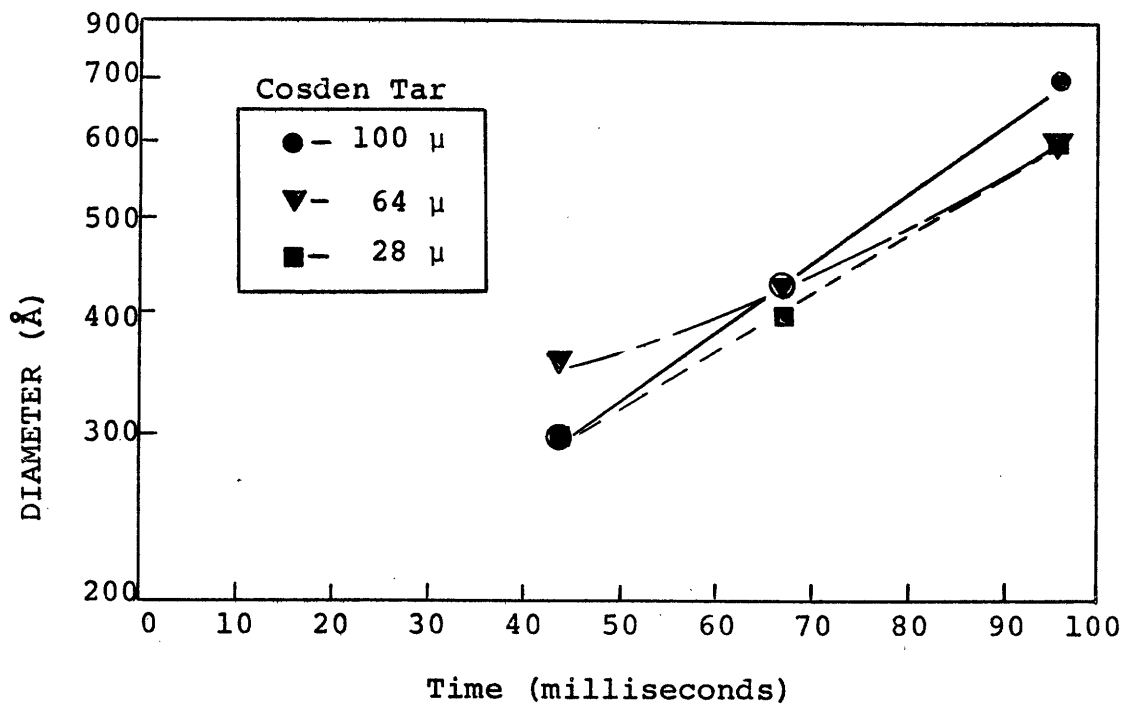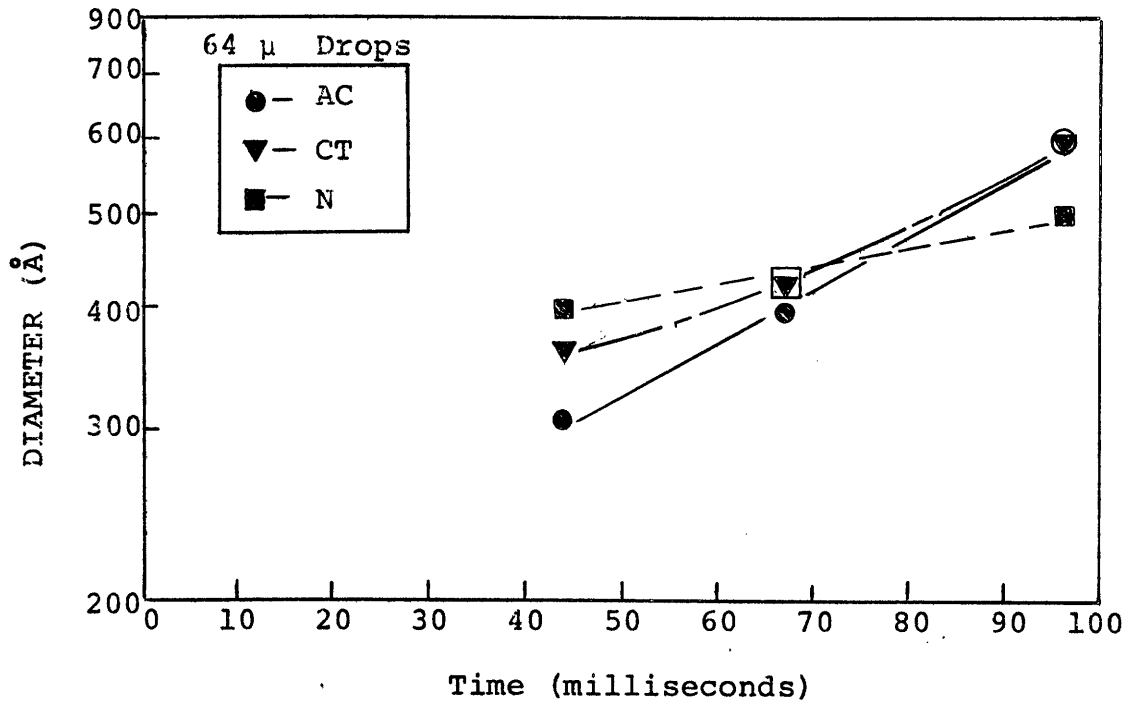
V. DISCUSSION OF RESULTS

This section consists of a discussion and evaluation of the results
presented graphically in Chapter IV. First will be described the results
of preliminary tests which showed that the equipment operated consistently.
Then, the experimental data will be evaluated and compared to a three-step
model for carbon black formation.

5.1 Preliminary Measurements

Before beginning the full-scale experimental program, it was necessary
to evaluate the equipment operation as well as the operating procedure in
order to establish reliability and reproducibility. Some of the most
important areas were: the uniformity of drops, the flatness of the
temperature profile, and the closing of the material balance.

5.11 Atomization

The atomizer described in Appendix H is far from optimum, but with
good control of the oil feed rate and sweep gas flows, it produced a
clean stream of drops (no drips). The results of the calibration tests
on this atomizer were presented in section 4.1. Disk atomizer operation
is described by (67):

$$d\omega \left(\frac{D\rho}{\sigma} \right)^{1/2} = \text{const.} \qquad (5-1)$$

According to this equation, if oil and disk properties are constant,
then a log-log plot of drop size against disk speed, should produce
a straight line with a slope of -1.0. The corresponding plots shown in
Figures 4-2, 4-3 and 4-6 contained lines with slopes of -1.0 to -1.02.
These slopes indicate that the atomizer was operating in the region
of direct drop formation where the most homogeneously sized drops are
formed. Further verification of homogeneity was shown by the photographs
of the craters contained in Figures 4-4, 4-5 and 4-7. These photographs

also indicated the presence of a few satellite drops. In the analysis

of the data, the satellites were neglected since they were generally

one-fourth of the diameter of the primary drop and, therefore, 64 small

drops are required to equal the mass of one large drop.

5.12 Temperature Control

It was desirable, from a kinetic standpoint, to maintain a flat

temperature profile in the reactor. The two typical reactor temperature

profiles shown in Figure 5-1 demonstrate the degree of success obtained

in temperature control. Some problem was encountered at the bottom of

the reactor due to the presence of the probe. Since the probe acted

as a heat sink, it had to be accurately centered in the reactor and

had to have a clean reflective surface in order to minimize heat losses.

With these criteria fulfilled, it was possible to maximize the temperature

gradient in the gas, at the probe entrance, and the indicated profiles were

obtained.

The large heat losses at the top of the furnace made it necessary

to adjust the preheat furnaces to maintain a uniform temperature profile

throughout the reactor. The point to note is that extra energy, above

the combustion energy, was added so that the mixed oil-gas stream was

heated to the desired level.

5.13 Material Balance

The problem of accounting for all of the carbon fed to the reactor

as oil was not completely resolved. From Figures 4-8 and 4-9 which show

the effect of temperature on yield, it was noted that yields are generally

below a normal oil black yield of approximately 50%. The first thing

that came to mind was that the unaccounted for carbon was present in the

gas phase as CO_2, CO, C_2H_2, or CH_4. But, according to the gas analysis,

REACTOR TEMPERATURE PROFILE

Figure 5-1
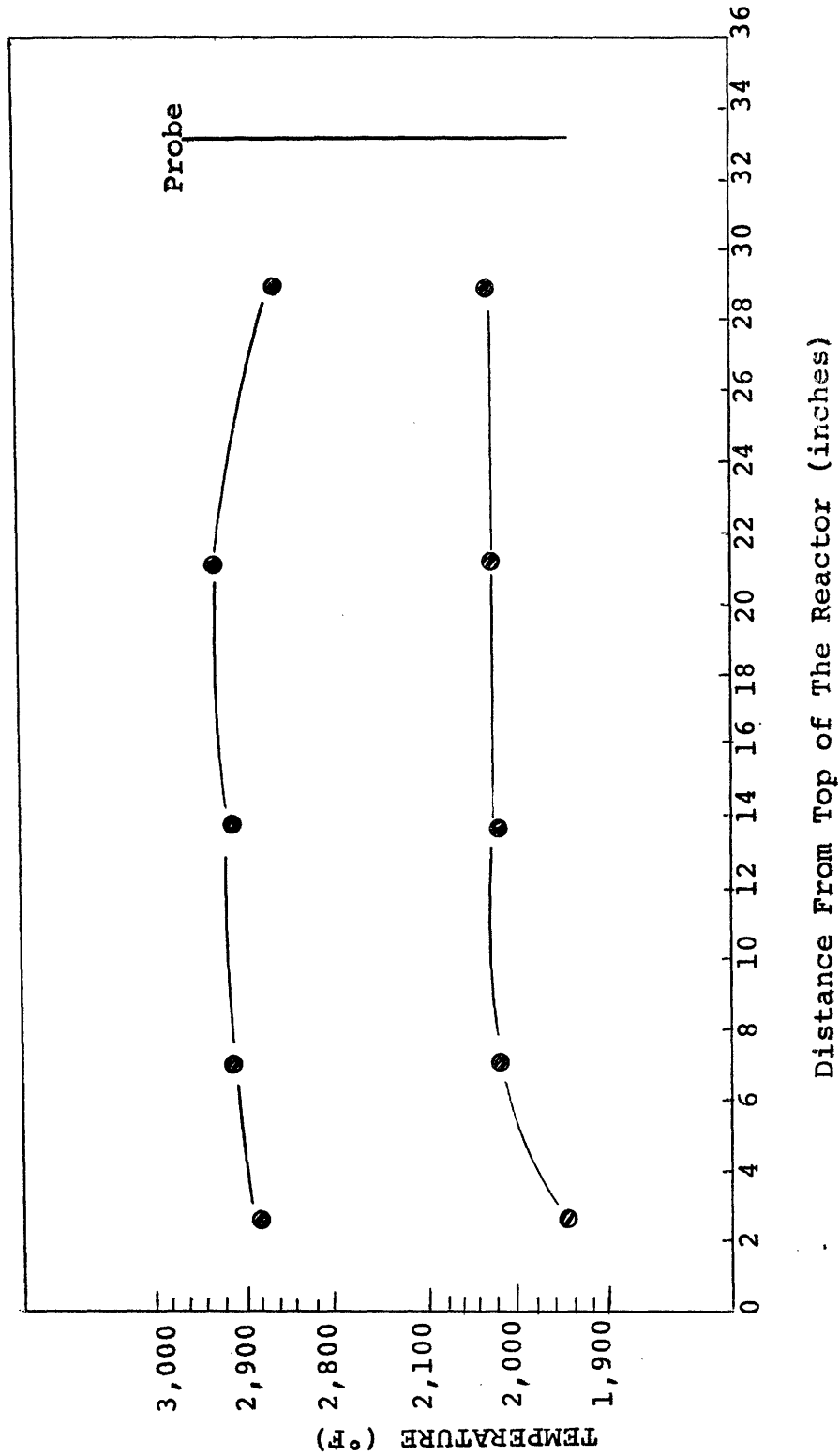
this was not the case. At this point, the flow system was recalibrated, but still only 11.8% (2000°F) up to 20.6% (2900°F) of the carbon fed as oil ended up in the gas phase. An additional point is that oil leaks, either as liquid or vapor, are readily visible as smoke or fire. They did not exist. Finally, the amount of carbon collected from runs made at similar conditions was reproducible, i.e., a 3.7 and 4.3% or a 3.1 and 3.1% yield. The fact that yield was also a function of the time required for vaporization, i.e., the largest drops or highest boiling oil gave the largest yields, indicated the possible formation of a gas phase species, which was a slow carbon former.

Since the carbon collection system was held over 300°F, any such materials present must have been vaporized at 300°F because they were not found in the collection system. In addition, they must be liquid at room temperature because the gas analysis (which would include the unknown if it were a vapor) totaled from 98 to 102%. On this basis, a cold trap was designed to quench all of the gas leaving the filter. The trap was cooled with liquid nitrogen and, therefore, collected water plus other condensables. The amount of the water collected was calculated from a hydrogen and oxygen balance around the system. Next, from the change in weight of the cold trap, and assuming that the gas phase material had the same carbon-to-hydrogen ratio as the oil, the amount of residue was determined. In two runs, this weight accounted for 69% (60.8 grams total) and 80% (78 grams total) of the carbon fed and the material balance was within 8% and 5% of closing. The resulting trap residue was cloudy, brownish liquid with a strong odor (similar to Naphthalene). This material was submitted to Cabot for analysis. The only positive results obtained were from a spectrophotometer

which showed absorption bands at 224, 275, 286, 297 millimicrons and
indicated the possibility of methyl-napthalene being present in a
concentration of 20-30 ppm, and obviously this does not quantitatively
explain the difficulty. However, a sample held at the Fuels Research
Laboratory for the same period of time had lost most of its characteristic
odor and, therefore, possibly a large portion of the sample which Cabot
analyzed had evaporated before analysis. Physically, this is not too
satisfying, but it is obvious that an unknown material was present and
that its identity is still a mystery. Close examination of Russian data
indicates that they experienced a similar problem. Tesner (68) states
that essentially no carbon from the oil was gasified and also that 80%
of the carbon in the oil which was converted to carbon black appeared
during the nucleation period. However, a material balance using his
stated carbon black concentrations and gas flows accounted for only
16% to 38% of the carbon fed as oil. In Foster's (69) well-mixed reactor,
only 85% of the input carbon was accounted for as carbon, CO_2 and CO.
On this basis, it would seem obvious that this apparent loss of carbon
needs to be investigated further and that possibly the identification
of the species may shed some light on the formation process.

5.2 Carbon Formation

In the following section, the data from this work will be analyzed
and compared to existing experimental work and theory. At the same time,
an attempt will be made to clarify the literature on carbon black formation
and to integrate this information with the present work in order to
develop the proposed picture of a three-step process for dispersed carbon
formation.

For the purposes of this discussion, it will be assumed that the
ideal carbon black process will be the one which has a high yield and

produces small uniform particles (diameter of around 150 angstroms).
These particles should be as black as possible, i.e., low in scale, and
have a high hiding power, i.e., high in tint. In addition, the amount
of extractable in the black should be low since the extract affects
the dispersion characteristics of the black. Since in most applications
the black is dispersed in another medium, dispersibility is an important
parameter. As the results of this work are discussed, an attempt will be
made to predict methods of approaching the ideal black process.

5.21 Overall Model of Formation Process

In Chapter II, the various theories of carbon formation were briefly
reviewed. There it was mentioned that activation energies of 120, 57,
30-40, and 5-9 Kcal per gram mole had been reported for the carbon
formation process. In addition, one research group believes that the
number of particles is constant after nucleation while another group
reports a decreasing number of particles.

The first step in clarification of this picture is to look at the
part of the process that each group has investigated in depth and their
methods of approach. Table IV shows a comparison between the basic
approaches of the different investigators.

Table IV

Carbon Black Investigators

Investigator	Feed Stock Form	Type of Reactor	Feed Stock	Residence Time Time Range (milliseconds)
Tesner, Surovikin and Snegyreua	Vaporized and Atomized	Turbulent	Green Oil and Toluene	0.1-80
Surovikin	Vaporized	Turbulent	Green Oil and Toluene	2.2-80 14-80
Bass	Dropper	Laminar	Green Oil	?
Homann and Wagner	-	Flame (Low pressure)	Benzene and Acetylene	0.2-30
Foster and Narasimham	Gas	Turbulent	CH_4	10-30
Present Work	Drops	Laminar	Residual Oils and Naphthalene	40-100

The important points to be noted in the table are: (1) most work has been carried out in a turbulent reactor, (2) the present work was done in a laminar reactor, and (3) the work of Homann and Wagner was carried out in a low pressure flame. The relative temporal positions of these investigations as compared to the important events in the process of carbon formation are shown in Figure 5-2. Here a normalized number of carbon particles is plotted against residence time. Close examination of this figure points out a possible reason why these investigators appear to describe different processes. Tesner and the other Russian investigators have looked very closely at the early stages of carbon formation (0.1 to 5 milliseconds). This is the region of carbon nucleation, followed by a short growth region. They obtained only one point per run at the relatively long time of 80 milliseconds. It is obviously difficult and dangerous to extrapolate the number of small carbon particles over such a range on the basis of one point per run. On the other hand, Foster covers a short intermediate time period and even though he assumes constant particle number he cannot prove it. Homann and Wagner cover the widest time span but they could resolve the initial regions as well as Tesner. Most of the first particles Homann and Wagner collected were around 50 angstroms in diameter and collected after a time of about 2 milliseconds. Even at this point in time they still found a significant number of particles with diameters of from 100 to 175 angstroms. These latter must have been growing for some time. Tesner and co-workers describe dispersed carbon formation as a two-step process consisting of nucleation followed by growth. They believe that after nucleation the number of particles is constant. Homann and Wagner describe growth as a combination of agglomeration and surface growth with a decreasing number of particles.

TEMPORAL VARIATION OF NUMBER OF PARTICLES

Figure 5-2
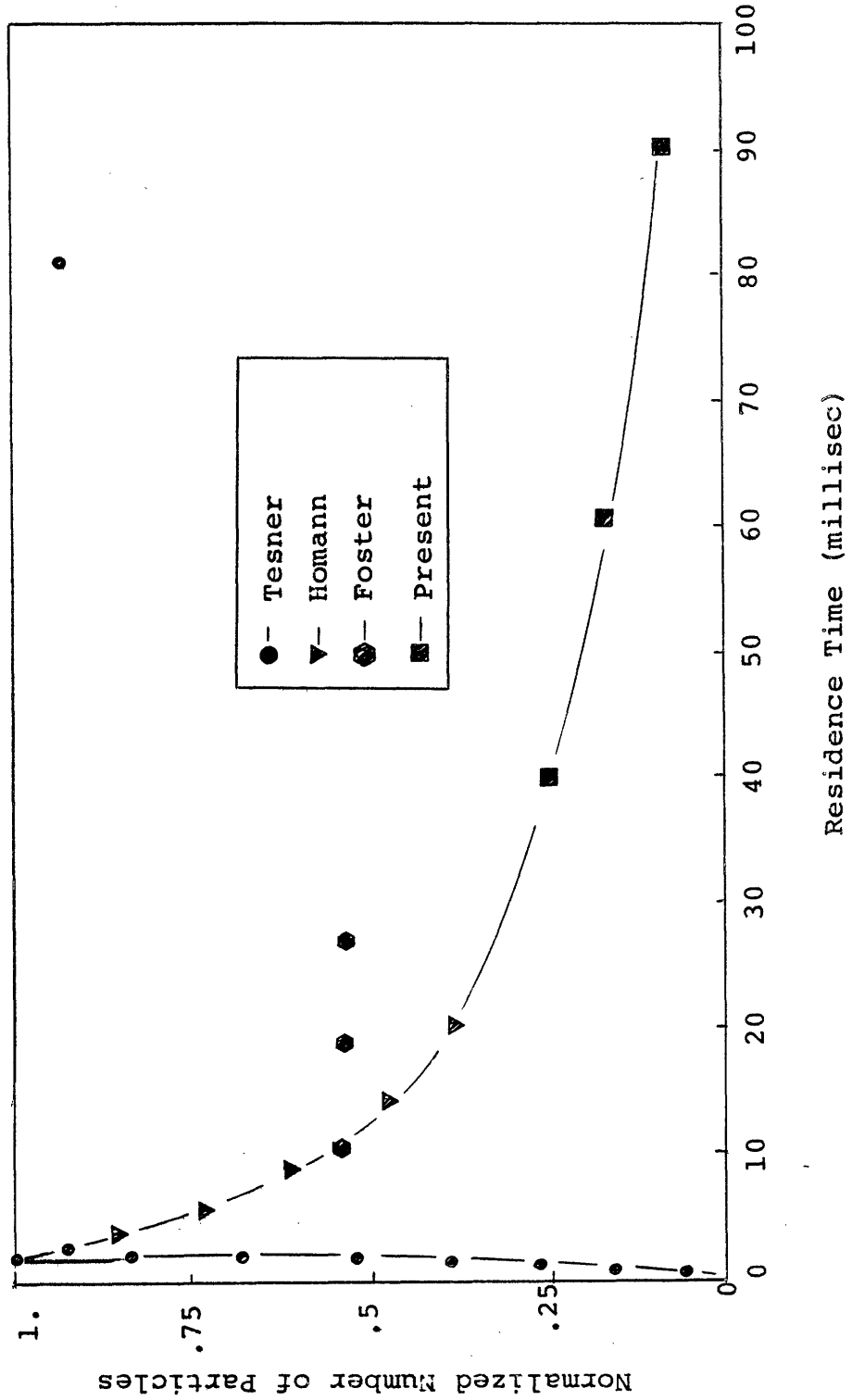
It is the belief of this author that the observations of these
investigators are all consistent within the time regions where their data
are the most accurate. Furthermore, it is felt that the process of
dispersed carbon formation can be better described by considering three
steps in the formation process. The first is the production of nuclei
described by Tesner. The second and third steps consist of a gas phase
reaction which produces active species which then deposit on the surface
of the existing carbon particles, causing growth. These last two steps
occur simultaneously and have different temperature dependences. This
scheme schematically is:

Nucleation$\rightarrow$Gas Phase Reaction$\rightarrow$Surface Growth

In the next few sections, the experimental data from this work and those
of other authors will be compared to this model.

5.22 Analysis of Nucleation

Since most of Tesner's data was taken during the period of nucleation,
his interpretation of this step and the comparison of his data to those
of the present work will be discussed first. Before proceeding, it
should be pointed out that many free radical or bond-breaking reactions
have high activation energies. For example, the generation of the C_2
radical requires 150 Kcal per mole, or the rupture of the carbon-hydrogen
bond in acetylene or methane requires 125 and 101 Kcal per mole,
respectively. In addition, the removal of a hydrogen atom from ethane
requires 98 Kcal per mole. In this light, if nuclei are formed by a
free radical process, then one would expect a high activation energy.

Tesner and co-workers noted a sharp maximum in the rate of particle
formation as a function of time, which occurred at a time when the
hydro-carbon concentration was still high. If one assumes that nuclei

are formed by a radical process, then a logical reason for the sudden

decrease in the rate of particle formation is that the radicals decay

on the large amount of surface presented by the new carbon black

particles. In this light, Tesner analyzed his data according to

Semenov's (70) equations for a chain branching explosion with a

quadratic termination step. Semonov's equation assuming a uniform

particle size and the destruction of radicals by their mutual interaction

is:

$$\frac{dn}{d\gamma} = n_o + (f - g)n - g_o n^2 \qquad (5-2)$$

In this equation, n is the number of carbon particles and $dn/d\gamma$ is

the change in the number of particles with time. f and g are constants

for the kinetic rates of chain branching and chain termination, resp-

ectively, and g_o is the geometrical factor for radical destruction.

With data on particle size (surface area and electron micrographs) and

carbon concentrations, Tesner calculated the number of particles as a

function of time. With this information and equation (5-2), he calculated

n_o which he called the initial number of active centers. This number

seems to be the same as the number of critical nuclei, which one would

calculate from nucleation theory. With values for n_o and n, Tesner

calculated the activation energy for nucleation (E_n) from the following

equation:

$$n_o = N \ 10^{13} \ exp(\frac{E_n}{RT}) \qquad (5-3)$$

This equation assumes that the active center is formed by a monomolecular

reaction involving bond rupture of the initial hydrocarbon (N). Tesner

also calculated E_n from the temperature dependence of n_o, i.e., a plot

of log n_o vs 1/T. In both cases, he obtained values of E_n of 122-126 Kcal

per mole for toluene and 118 to 122 Kcal per mole for green oil. These
values of E_n are in reasonable agreement with the before-mentioned values
of activation energies for radical reactions of approximately 100 Kcal
per mole. This analysis does not prove the existence of a branched
chain or radical process but it does seem plausible and it helps one
to gain insight into the process of nucleation.

The question at this point is: Can the current experimental
results be compared with this work, and if so, do they agree? First
of all, it should be remembered that the data of the current work must
be extrapolated back to the nucleation region, and this is as uncertain
as Tesner's prediction of long time results from his data. Even though
the author sees no reason that his data should fit Semonov's equations,
for comparison's sake the analysis was made on one run and the calculated
activation energy was 100 Kcal per mole. The apparent concordance of this
value with those of Tesner is interesting but may be of no significance.
Due to the large differences in residence times between this work and
that of Tesner, direct comparison of the two may not be very meaningful
in a quantitative sense, but several interesting comparisons can be made.
First, Tesner states that nucleation begins in around 10^{-4} seconds
and is complete in approximately 5×10^{-4} seconds. In no case in the
present work did the electron micrographs contain small particles which
would indicate a secondary nucleation. This is shown in Figure 5-3
which contains electron micrographs of the carbon produced from 100 micron
drops, with a furnace temperature of 2900°F and at residence times of
42, 64, and 92 milliseconds. A further indication of the speed of the
nucleation process can be seen from a comparison of the carbon black
produced under similar conditions. In Figure 5-4 are shown two samples

ELECTRON MICROGRAPHS of CARBON BLACK

(Cosden Tar 50,000x)

Figure 5.3
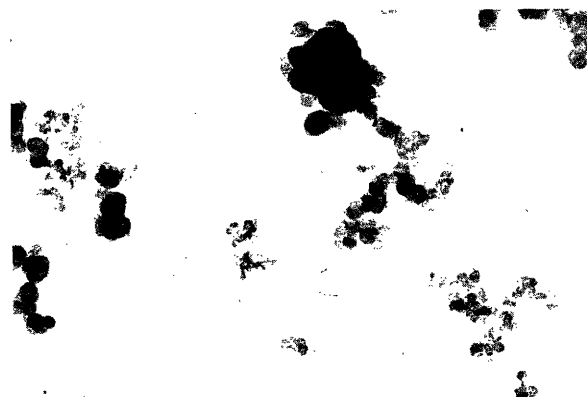
42 Milliseconds
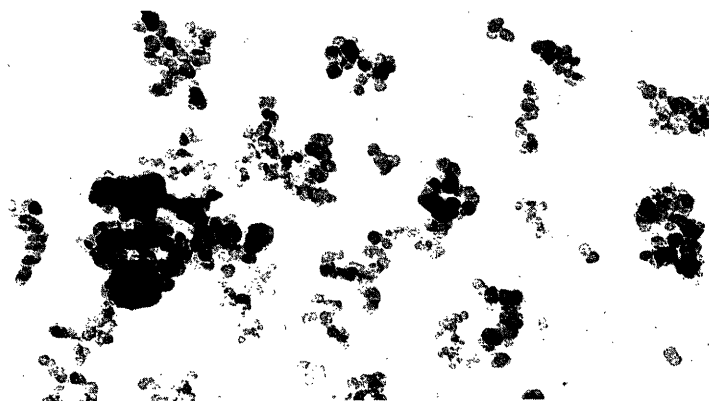
62 Milliseconds

92 Milliseconds

EFFECT of VAPORIZATION TIME on SIZE DISTRIBUTION
Figure 5.4

a
Naphthalene
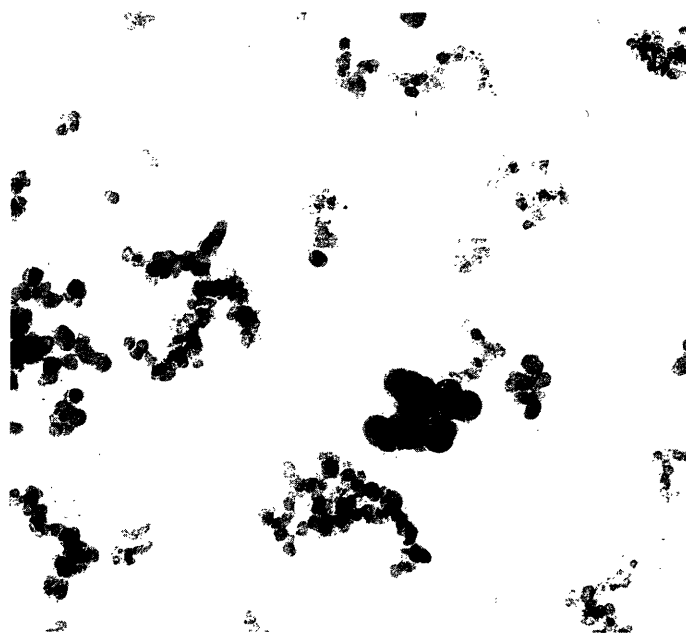
b
Cosden Tar

of carbon black produced from 64 micron drops at 2900°F with a residence time of 42 milliseconds. Figure 5-4(a) is an electronmicrograph of carbon black from Naphthalene which vaporized in approximately 1.8 milliseconds while Figure 5-4(b) is of carbon black from Cosden Tar which vaporized in approximately 7 milliseconds. Note first the range of sizes which indicates that carbon is being formed while vaporization is still going on and, secondly, that the size variation is much larger in the carbon black made from the Cosden Tar. This indicates a wide range in the growth time for this material. The variation in hydrocarbon concentration around the drop (laminar reactor) could account for some of this variation but not all of it.

A further indication that the nucleation which occurred in Tesner's work was similar to the nucleation which occurred in the present work comes from the comparison of the temperature dependence of the total number of nuclei. In this calculation, the particle diameter (electron micrographs) and the total amount of carbon black collected, at the end of Tesner's reactor or the present system, were used to calculate the total number of particles. The dependence of total number of particles on temperature is shown on Figure 5-5. Here the slope of Tesner's data is 1.3 which compares favorably to a value 1.1 for the 64 micron drops of the three materials from the present work. The closeness of these values adds credence to the idea that we have a similar nucleation process. A similar plot of number of particles from the different sized oil drops of Cosden Tar is shown on Figure 5-6. Here it should be remembered that there is a large difference in the number of nuclei produced from different sized drops. The slope of the lines decreases from 1.5 for 100 micron drops to 0.5 for 28 micron drops. This can be understood if one remembers that carbon nuclei form before vaporization

PARTICLE FORMATION
Figure 5-5
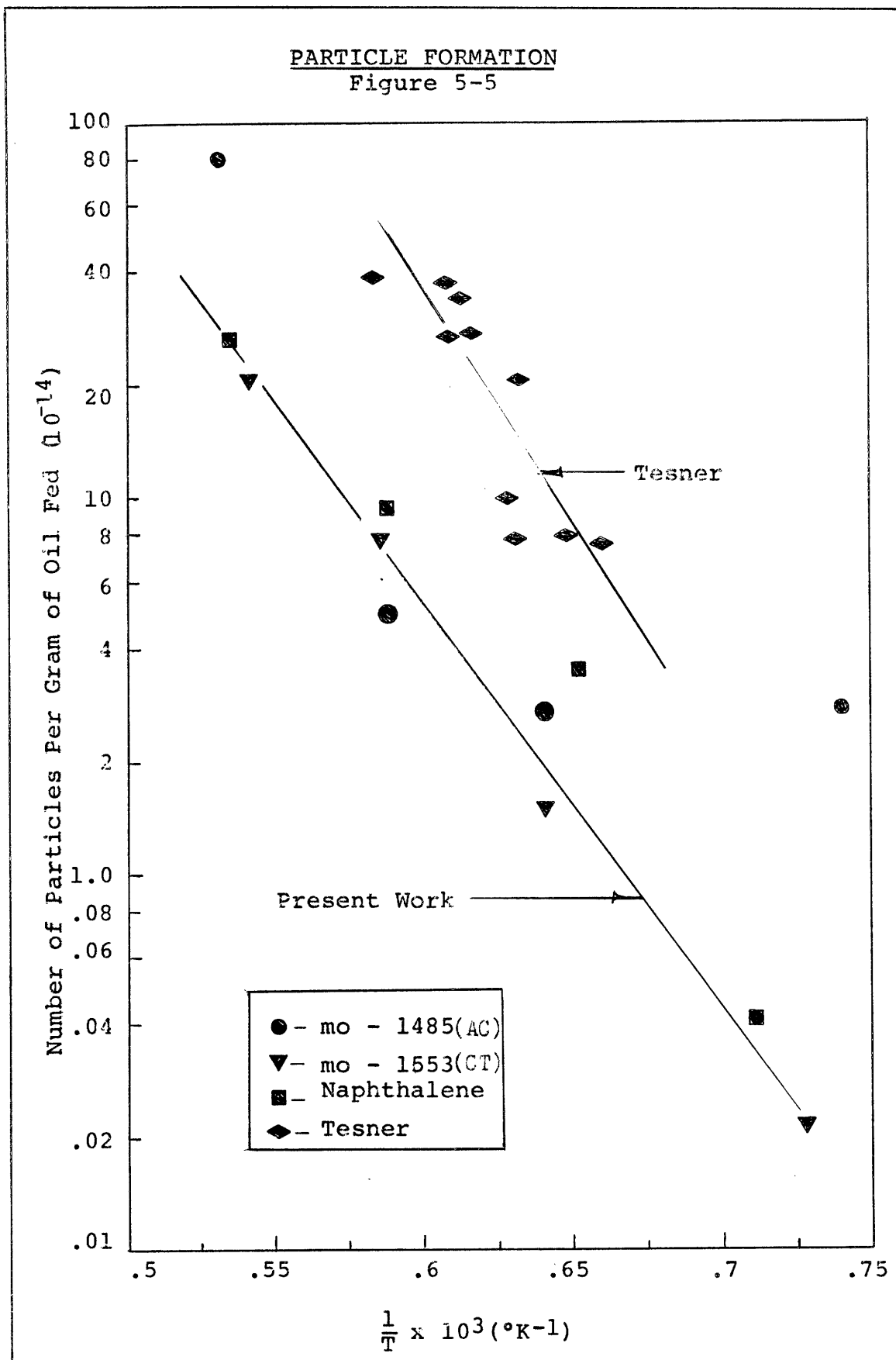
EFFECT OF TEMPERATURE ON THE
NUMBER OF PARTICLES
Figure 5-6
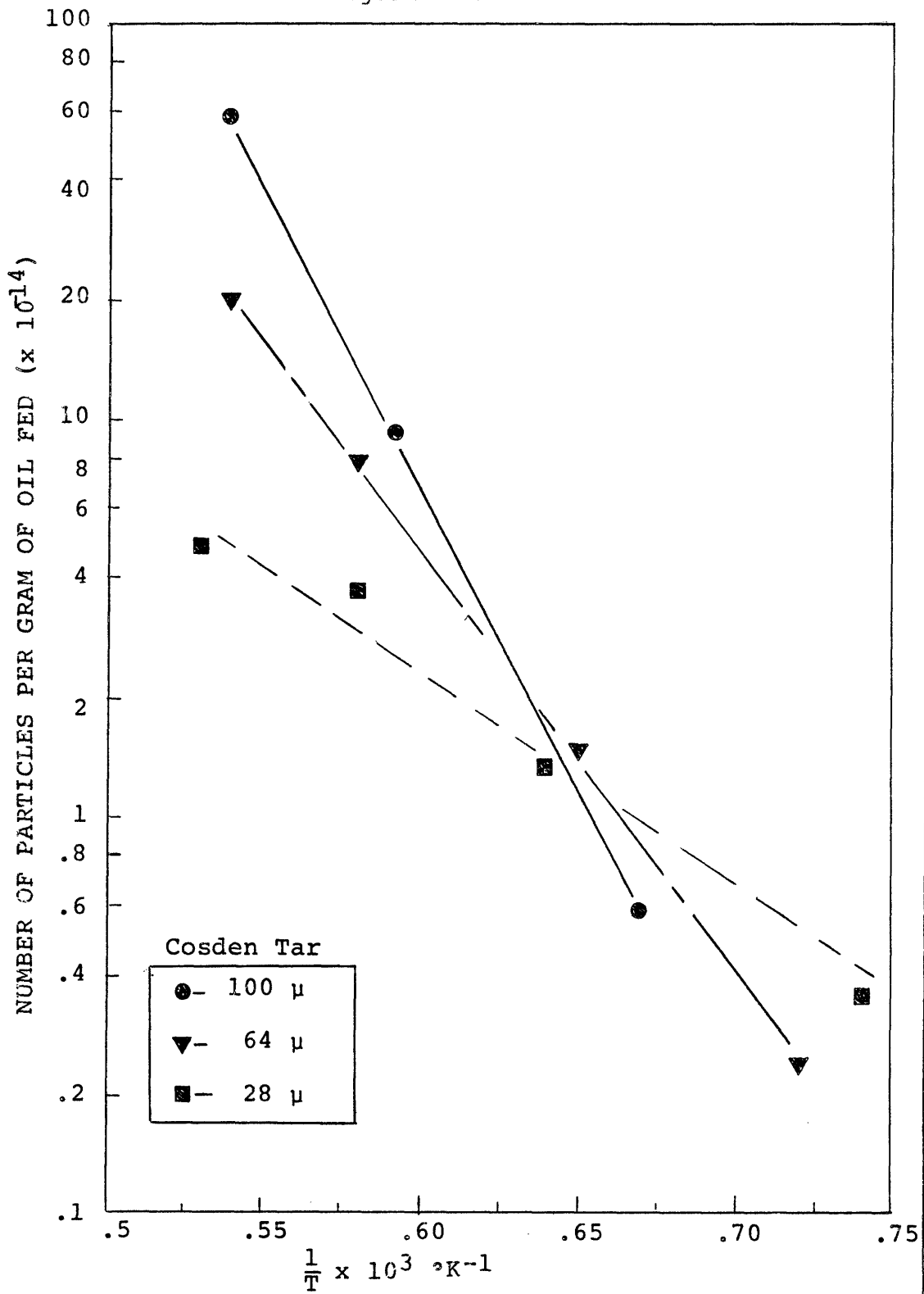
is complete and that the vapor around the large drop is more concentrated, and, therefore, nucleation is taking place in a region of higher concentration and thus more nuclei are formed. This variation will be discussed again under growth. The present work showed a slow decrease in the number of particles with time. (Possible reasons for this decrease will be discussed in a later reaction.)

Still another method of looking at nucleation is through classical nucleation theory, using the concept of the critical nucleus and assuming an incompressible solid. The critical nucleus is defined as the smallest particle that is stable as a solid at system conditions. If one assumes that embryos of all sizes and all structures are in equilibrium, the number of critical nuclei, n_i, is given by ($\underline{71}$):

$$n_i = n \exp\left(\frac{-\Delta G^*}{kT}\right) \tag{5-4}$$

where G^* is the excess free energy of the critical nucleus. ΔG^* is defined by:

$$G^* = \frac{16\pi\sigma^3}{(L\Delta T/T_\ell)^2} \tag{5-5}$$

where σ is the surface free energy and L is the latent heat of vaporization. ΔT is the temperature difference between the sublimation temperature and the system temperature, while T_ℓ is the sublimation temperature. A similar relationship can be developed to determine the radius, r_i, of the critical nucleus. In this equation,

$$r_i^* = \left(\frac{2\sigma}{L\Delta T}\right)T_\ell \tag{5-6}$$

Here it is seen that r_i^* also depends on σ and L. The values of σ and L are not well established for carbon black, and since ΔG^* and r_i^* are very sensitive to these number, a precise answer cannot be

obtained. Yet, it is interesting that, depending on the values chosen

for   and L, values of r_i* of from 20 to 40 angstroms and $G*$ from 20 to

100 Kcal per mole can be calculated. Considering the inaccuracy of the

physical property data, these are not unreasonable numbers and are within

the range of what has been observed experimentally.

5.23 <u>Nucleation Summary</u>

It is obvious from this discussion that nucleation is a high energy

barrier process. The species which produce the critical nucleus have not

been identified, but the process appears to be a chain reaction or free

radical type of process.

From the standpoint of the ideal black process, a maximum amount of

nucleation over a short time interval is desirable. In order to obtain

this process, several alternatives present themselves. The first is to

maximize temperature. Since conventional furnaces are near the maximum

temperature obtainable with a natural gas air flame, an obvious improve-

ment is to eliminate nitrogen and combust with pure oxygen, although

it may still be possible to improve nucleation by improving the initial

mixing of the oil and burnt gases. Still another approach is to move

into a second temperature regime and use an electrically augmented

burner to boost the energy content of the flame. An even higher temp-

erature could be obtained in a plasma arc where residence times can be

reduced to microseconds. The utility of this approach will depend to a

large extent on energy costs. Even with a higher temperature, it is

important from the standpoint of yield and size distribution to provide

rapid mixing and a uniform vaporization time. Rapid mixing is

accomplished commercially using turbulent flow systems. Ideally, the

residual oil should have a narrow boiling range and the drop size

distribution should be uniform. Practically, the boiling range criterion cannot be reached, but an improvement in degree of atomization is attainable. From the present study in a laminar flow system, it was not possible to determine if an optimum drop size exists since there appears to be interaction of drop size and mixing. In practice, a balance will have to be established between the economics of obtaining a more uniform drop size and the end effect on the carbon black properties.

Another possibility is to add a species to the gas which will act as nucleation sites and hence promote faster nucleation. Tesner obtained smaller particles with a lower activation energy from green oil than toluene. In this study, smaller particles were obtained from the residual oils. Green oil, like the residual oils used in this study, should contain small carbon particles which are a result of the manufacturing steps, and it is possible that these particles act as nucleation sites. A few of the larger particles of this type are shown in Figure 5-7 which contains photomicrographs of the residual oil. Another point along this line is that Tesner found an induction period for nucleation when using toluene, and this was not the case with green oil. Weinberg and Place (72) have found that cesium ions increase the number of nuclei. Therefore, it is possible that nucleation can be improved by seeding the gas stream with a suitable material.

5.24 Growth of Carbon Particles

All workers in the field appear to believe that after the formation of 40 to 50 angstrom particles no new particles are formed. Homann and Wagner believe that existing particles grow by agglomeration, and surface reaction to particles as large as 2000 angstroms in diameter. It is for this growth region that reported activation energies range from

RESIDUAL OIL

(610x)
Figure 5.7

a
Cosden Tar

b
Aromatic Concentrate

5 Kcal per gram mole to 57.6 Kcal per gram mole. It is the opinion of this author that this region can best be described by a gas phase reaction which produces a hydrocarbon species that in turn adds to the surface of the carbon particles in a rapid reaction.

5.241 <u>Gas Phase Reaction</u>. First let us consider the work of Homann and Wagner, which was carried out in a low pressure flame. They observed the formation of gas phase species which act as building blocks by adding to small carbon particles, causing growth. For acetylene and benzene flames the active species were polyacetylenes and polycyclic aromatics, respectively. They feel that these species decompose on the surface of the particle with an activation energy of 30 to 40 Kcal per mole. It is important to note that the important species were different for two different fuels.

On the other hand, Foster and Narasimhan envisioned carbon growth as a bi-molecular collision between a carbon particle and a methane molecule. This is reasonable if one considers that the concentration of the molecule which is actually causing growth is probably proportional to the methane concentration. From kinetic theory the collision rate between carbon particles and an active gas species is given by

$$z = N_s N_m \left(\frac{d_s + d_m}{2} \right)^2 \times \left(8 \pi R T \left[\frac{m_s + m_n}{m_s + m_n} \right] \right)^{1/2} \qquad (5\text{-}7)$$

where d, N, m are the diameter, number, and mass, respectively of the carbon, s, and methane, m, particles. The number concentration, N, mass concentration, c, and soot particle diameter, d_s, are related by

$$d_s = \frac{1}{10} \left(6 \ C/N_s \ \pi \rho \right)^{1/3} \qquad (5\text{-}8)$$

These relations can then be combined with an Arrheius factor into a
growth equation:

$$\frac{dC}{dt} = \text{constant } (N_s)^{1/3}(C)^{2/3}(X/T^{0.5})\exp(-E/RT) \qquad (5-9)$$

Here X is mole fraction of methane, and it is assumed that the concentration
of the species causing growth will be proportional to the methane
concentration. From data on the mass of carbon produced and particle
size as a function of time and temperature, all of the numbers in
equation (5-9) can be calculated except for the constant and the
activation energy. Foster, from his data, calculated these parameters
assuming N_s to be constant and plotted the log of:

$$\frac{dC}{dt} \quad T^{0.5}/X(N_s)^{1/3}(C)^{2/3}$$

against 1/T. From this plot he calculated an activation energy of
57.6 Kcal per gram mole.

The data of the present work were evaluated in a similar manner
using the value of mole fraction of oil for X. One should remember
that data were taken on particle size and concentration at three
residence times. These data are generally quite consistent and fit
an equation of the form

$$d = ke^{kt} \qquad (5-10)$$

as shown in Figures 4-20 and 4-26. However, these data were taken only
at two temperatures and thus a small variation in temperature could
significantly affect the calculated value of E. The results of this
calculation are shown in Table V.

Table V

Activation Energy for Growth

Oil	Drop Size microns	E_g Kcal/mole
Naphthalene	64	41
Aromatic Concentrate	64	45
Cosden Tar	100	50
Cosden Tar	64	35
Cosden Tar	28	18
Foster and Narasimhan (methane)	--	57.6
Homann and Wagner		30-40

It is interesting to note that all of these values are below the 57.6

value obtained by Foster. This one would expect, since the methane

molecule is much more stable than the large oil molecules used in this

study. The closest value is the 50 Kcal per mole which was obtained

from the 100 micron drops of Cosden Tar. One would expect this value

to be higher because, as mentioned in the last section, the number of

nuclei depends strongly on drop size and temperature, and the large

number of small particles produced from Cosden Tar would then influence

the activation energy determined from equation (5-9). Due to this strong

influence of number, this author does not believe that this activation

energy can be called an activation energy for growth. It really reflects

the combined influences of nucleation, gas phase reaction, and surface

growth. If one compares the activation energy for 64 micron drops of

Naphthalene and Aromatic Concentrate, where the number of particles is

essentially the same, then a variation of an activation energy of

nucleation is not present and the values should be relatively cose,

if the gas phase and surface reactions are similar. As will be seen in

the next section, the surface reactions are similar, and, therefore, the

gas phase activation energies should be nearly the same, as is indicated

by the values of 41 and 45 Kcal per gram mole. Looking closer at this value,
and assuming that the surface reaction is very fast (i.e., low activation
energy), then these values should be indicative of the magnitude of the
activation energy for a gas phase reaction, such as breaking up a poly-
acetylide molecule (30-40 Kcal).

5.242 <u>Surface Reaction.</u> In this section, the above assumption of
rapid surface reaction will be justified. Tesner used his data on
concentration and size of carbon black particles as a function of time
and temperature to calculate an activation energy for growth. He reports
a value of three Kcal per mole for green oil and six to seven Kcal per
mole for toluene. Since this value is based on the actual change of
particle diameter, it should approximate the activation energy
(E_s) for the surface reaction.

The data of the present investigation were treated in a similar
manner and produced values of three Kcal per mole for Cosden Tar,
six Kcal per mole for Aromatic Concentrate, and seven Kcal per mole
for Naphthalene. Granted, the absolute magnitudes of these numbers
are not precise since they are based on average particle sizes from
electron micrographs, and these are hard numbers to obtain; however, the
low value indicates that roughly one of every three surface collisions
is an effective contributor to growth and hence there is a rapid reaction.

The form of equation (5-10) suggests that growth rate is proportional
to the amount of material present. This would suggest that the carbon
black particles contain active centers or sites for the addition of a
gas phase species.

The precision of particle size data, from electron micrographs,
does not allow one to differentiate between diffusion limited, surface-

area limited, or volume limited growth models. A statistical study of many particles will be required to establish the true mechanism of surface growth process.

5.243 Growth Summary. The growth of carbon black particles occurs by the surface addition of a species that as yet is unknown. But, this reaction is fast and tends to be limited by the gas phase reaction. Not enough is known about the composition of the residual oils to enable one to explain the differences between oils or between the oils and Naphthalene. But the fact that Naphthalene had a higher growth activation energy is consistent with Tesner's work. This analysis again pointed out that nucleation is the important factor and that for the ideal black process the initial few milliseconds, when mixing and nucleation occur, are the most important. It is felt that the activation energy for growth as determined by Foster includes the effect of nucleation (E_n), gas phase reaction (E_g), and surface growth (E_s), although E_s is so small that it probably contributes very little to the overall E. The present experimental results do not allow one to determine all of these numbers, but they suggest that both E_n and E_g may be important.

5.25 Evaluation of Measured Parameters in Light of the Proposed Model

During the discussion of nucleation and growth, the analysis made use of particle size (electron microscope), the variation of particle size and the yield. In this section, the variation of the parameters surface area, scale and tint will be compared to the predictions of the proposed model.

5.251 Nitrogen Surface Area. The nitrogen surface area of the carbon black gives an average particle size for the carbon black. Generally, the particle size from surface area measurement is larger than the size determined from the electron micrographs (often a factor

of 2). This is probably due to an interacting affect of chaining, porosity, and the amount of extractable material left on the black surface. Generally, if the chains are very short, the two particle sizes are in good agreement. Keeping in mind that a high surface area means a small particle, Figure 4-10 showed that the particle size of the black formed with a residence time of approximately 91 milliseconds decreased as the temperature was increased from 2000 to 2600°F. Since nucleation is a strong function of temperature, as the temperature was increased, the number of nuclei increased and smaller particles resulted. Also, as the temperature increased, the rate of the growth reaction or the production of gas phase species increased rapidly. From 2600°F to 2900°F, even though the number of nuclei had increased, the growth reaction was fast enough that the surface area decreased. This was true for all materials except Naphthalene, which continued to increase in surface area between 2600 and 2900°F. This is reasonable since Naphthalene also had the highest activation energy for growth. On Figure 4-17 the change in surface area with time at 2900°F was presented. For Cosden Tar all drop sizes showed an increase in size with time, and the largest growth occurred between 62 and 90 milliseconds. This region of accelerated growth agrees with the yield data. If one assumes that the gas phase reaction is controlling at 62 milliseconds, the number of active species in the gas phase must be very high, causing a large number of collisions and hence a rapid growth rate. The only exception is one low surface area point for the 100 micron drop at 42 milliseconds. This black contained 2.2% extractable, which one would expect to decrease the surface area.

A similar behavior was exhibited by the Aromatic Concentrate, although the drop in surface area between 60-90 milliseconds was not

as great. But in this case, both of the intermediate points contained over 1% extract and, therefore, the reported surface areas are probably low. The erratic short-time point for Naphthalene is not as easy to understand. In the first place, extract data are probably not really comparable to the residual oils, since if Naphthalene were on the black surface most of it would not be found by the extract measurement (see Appendix C). Secondly, the particle size of this material from the electron micrographs is much smaller, which would indicate that the surface area should be around 50 m^2/gram.

At 2600°F, extracts are generally higher and surface areas do not behave as regularly as at 2900°F. But as time increases, the surface decrease is in agreement with the change in yield over the same region. In all cases where surface area behavior is erratic (for example, when Aromatic Concentrate showed an apparent decrease in size with time), the behavior is not confirmed by the electron micrographs. That is to say, particle size increases as one would predict.

In summary, the surface area measurement, which indicates the size of the particles, agrees with the picture of growth presented in the previous sections. For example, as the temperature increases and the rate of growth increases, then the rate of decrease of surface area increases. In the ideal carbon black process, it is desirable to produce a very high surface area material (i.e., over 100 m^2/gram) at a high yield. Therefore, it is necessary to minimize growth time. Actually, it would be best to allow only enough growth time to boil off the extractable material. Again, this goes back to the desirability of having the best possible nucleation conditions to produce many small articles and thus it would take less time to meet extract requirements, and a high surface area black could be maintained.

5.252 <u>Scale</u>. It is not really clear what a variation in scale means. As was pointed out in Appendix C, the scale is a measurement of the light absorption by the black particles. Cabot has been able to correlate the scale measurement with particle size for black from production furnaces. But on many pieces of experimental equipment, the correlation does not hold. A possible explanation for this is that in the small scale equipment, the temperature history of the black is different from that in production, and probably chemical composition also varies. Since a change in the carbon-to-hydrogen ratio changes the absorptive properties of the black, the size correlation should not be expected to hold. Another factor that may influence the scale measurement is the amount of extractable. An absorbed layer of some high molecular weight hydrocarbon should influence the absorptivity measurement.

The variation of scale with temperature was shown on Figure 4-11. These plots showed a decrease in scale from 2000 to 2300 °F, while the scale remained essentially constant for one oil and drop size between 2600 and 2900°F. At the low temperatures, extracts were generally over 2%. The electron micrographs of the 2000°F carbon black showed the particles to be contained in a film of oil. Therefore, the accuracy of the scale value is doubtful. In addition, the black at 2600 and 2900°F which have identical scales are about 100 angstroms different in diameter. This difference may be within the accuracy of the scale measurement for determining size. But at any one temperature, the variation between the black made from different drop sizes or starting materials is opposite to what one would expect. That is, the smallest particles have the highest scale.

At 2900°F, as shown in Figure 4-18, scale increases with time. That is what would be predicted for a growing particle. Again, the position of these lines cannot be explained on the basis of size. They are probably strongly influenced by the amount extractable and chemical composition.

At 2600°F (Figure 4-23), the variation of scale is more erratic. For the Cosden Tar, at 44 milliseconds the variation in scale (88 to 93) does not agree with an observed size variation of 0 to 60 angstroms from electron micrographs. Along the same line, the scale of the black from Aromatic Concentrate appears to go through a minimum with time. But according to the electron micrographs, this is not the case.

In summary, it would appear that for experimental programs of this type, scale at best provides a reference with production material. If one were analyzing the black for chemical composition, then this number could be of more value. In addition, the change of chemical composition might also be very helpful in determining more precisely how the particles are growing.

5.253 _Tinting Strength_. The analysis of the tinting strength brings one to the area of most confusion in carbon black formation. That is, does the number of individual particles change? If so, when and how do these small particles get together? Before discussing the present results, a brief review of current theory and fact is in order. Tesner and co-workers (73) do not mention the chaining of the particles but do state as one of their prime assumptions that the number of particles is constant during growth. Close examination of their data shows a decrease in number of particles of from 10-27%. The larger losses in number correspond to regions of a large amount of growth. On the other

hand, Homann and Wagner (74) (75) describe growth as a combination of agglomeration and surface reaction, hence, a large decrease in number of particles would be expected. They feel that chaining takes place in a region of slow growth after the particles have reached a round 250 angstroms in diameter. The present author, in a previous work (76), found chained particles of 60-75 angstroms. One prevalent argument is that the particles chain after they leave their growth environment. The fact that almost all of the particles are in chains leads one to believe that chaining occurs before quenching. In addition, Harling and Heckman (77) have found that particle-to-particle bonds in the chain are as strong as the crystallite bonds in the particle. It is the present authors belief that chains are forming and breaking in the growth environment. This would mean that the particle-to-particle bonds in the reactor must be weak (i.e., Van der Waals Forces) and must strengthen during quenching. The length of the chain is probably strongly affected by the changes in chemical composition of the particle (off gassing), rate of growth, and the movement of the chain, as a function of the temperature.

In the present work, it was found that over regions where a large amount of growth took place, the number of particles decreased by as much as a factor of two. Also, over the same region the particles tended towards a uniform size. Von Smoluchowski has developed a theory of rapid coagulation of particles. He felt that rate of coagulation was determined by the Brownian motion of the particles and their interaction when they were close together. It is well to note that temperature would affect the motion of the particles, while off gassing could strongly affect particle-particle interactions. Smoluchowski describes the time of coagulation according to (78):

$$T = \frac{1}{4\pi D_1 R \nu_o} \qquad (5\text{-}11)$$

where T is the time required for the number of particles to decrease by 50%. In this equation, D_1 is the diffusion constant for the particles, R is the radius of interaction while ν_o is the original number of particles. This relation assumes all collisions result in growth. If this is not the case, ν_o must be multiplied by an effectiveness factor (α). Muller (79) extended this theory to systems with a range of particle sizes. He found that with a wide size range, the number of large particles does not change but the number of small particles decreases rapidly. Hence, it appears that the large particles capture the smaller ones. The larger the initial size variation, the more rapid is the approach to one size or constant particle number. Since the residence time in the present experiments were relatively long compared with coagulation times predicted by Muller's results, this theory can be applied quantitatively to the present work. Figure 5-8 shows that for constant conditions, the carbon black approaches a uniform diameter with time. This discussion also introduces a possible area of doubt in the previous statement that there was no evidence of a secondary nucleation. According to this approach, if secondary nucleation had occurred, it would have been difficult to determine since the tiny particles would rapidly attach themselves to the large particles. In any event, this agglomeration could account for the observed decrease in particle number. It would be very difficult to prove or disprove this, since growth occurs simultaneously.

Now, the variation in tinting strength will be analyzed. Figure 5-9 shows how the tint compares to chain length. This relation suggests that tint is a measure of an average chain length. Figures 4-12 and

SIZE VARIATION of CARBON BLACK PARTICLES

Figure 5.8
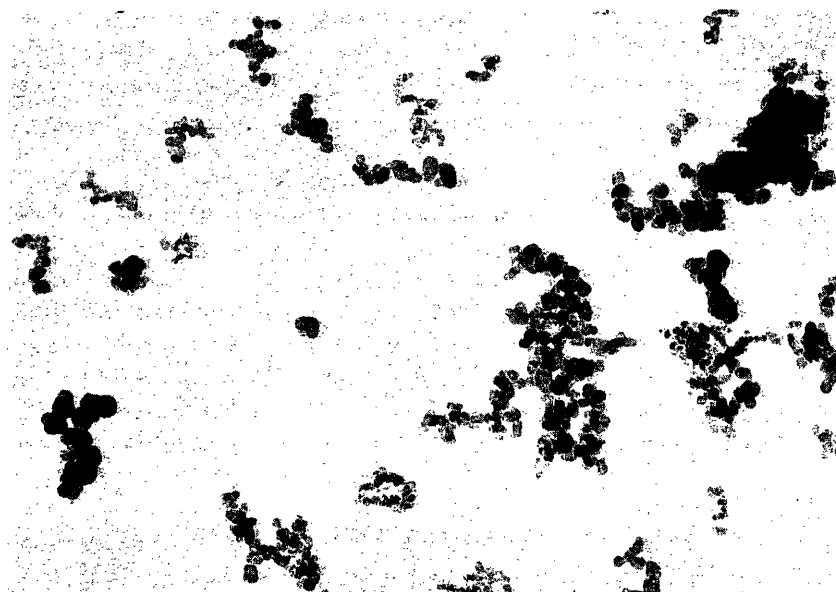
a
42 Milliseconds
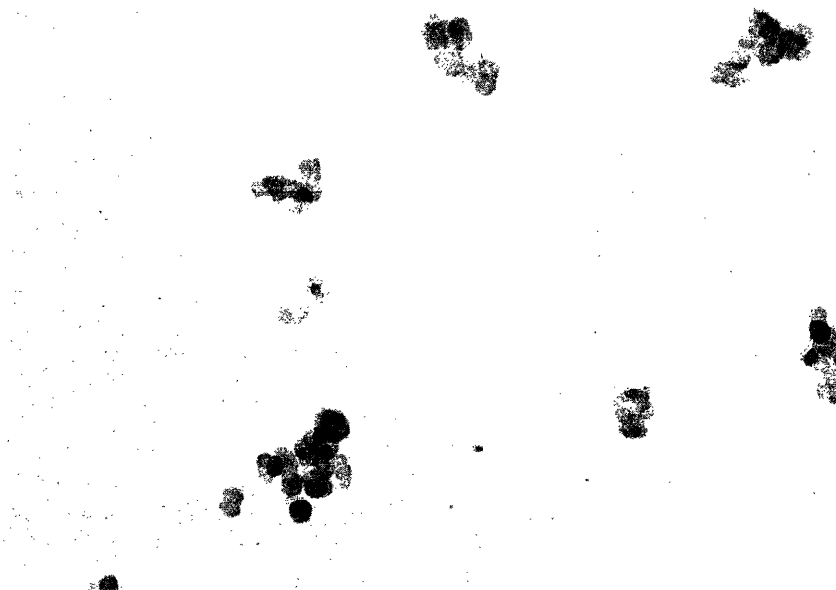
b
92 Milliseconds

A COMPARISON OF TINT TO CHAIN LENGTH

Figure 5-9
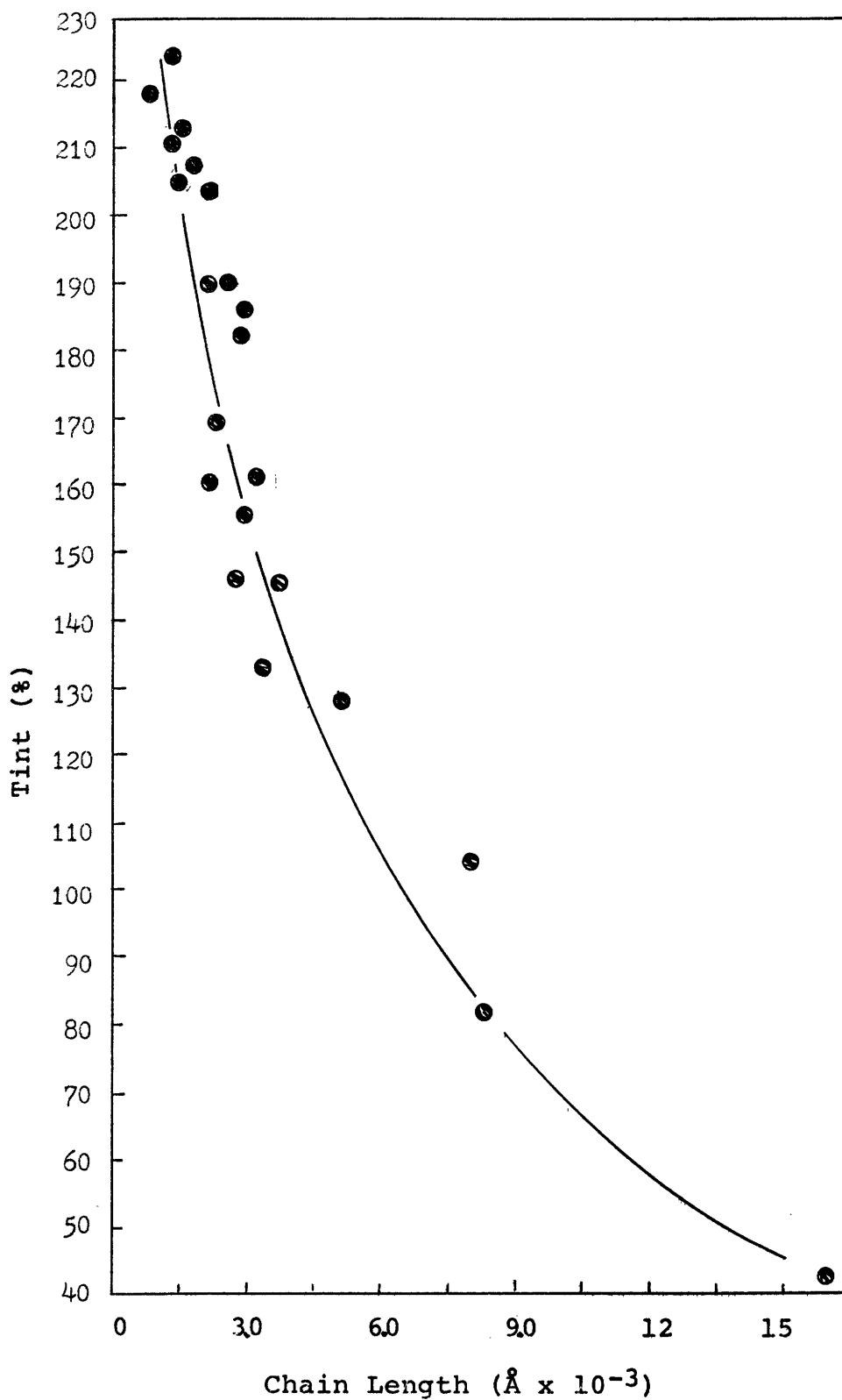
4-13 depicted the variation in chain length with temperature. This change in length is shown more dramatically by the electron micrographs in Figure 5-10. Here one finds very long chains at 2000°F. For all cases, except the 64 micron drops of Cosden Tar, chain length goes through a maximum around 2600°F. For the different drop sizes of Cosden Tar, the shortest chain length corresponds to the material with the highest extract. Since this material should be off-gassing the most, this gas flow would hinder the collision and sticking of the particles. Also, since these particles contain a large amount of extract, the particle-to-particle bonds could be fairly soft and easily fractured by a collision. It is quite possible that when the system is at 2900°F, the thermally induced movement of the chains would make long chains unstable.

This possible interaction of off-gassing, bond strength, and thermal movement was shown again in Figure 4-19. This figure showed how chain length varied with time at 2900°F. Generally, the residual oils which have around 1% extract at 42 milliseconds decrease in chain length from 42 to 62 milliseconds. After 62 milliseconds, there is very little off-gassing, and chain length increases. Naphthalene behaves in a similar manner, but its measured extract changes only slightly. The region of increasing chain length is also a priod of rapid growth, and this deposition of fresh material could help stick colliding particles together.

The picture is not nearly as clear at 2600°F (Figure 4-24). This is also the region mentioned earlier where chain length went through a maximum with temperature. One tends to doubt the apparent minimum in chain length at 67 milliseconds that was exhibited by 100 and 28 micron drops of Cosden Tar since these tints do not correlate with the length of the chains as measured from the electron micrographs.

CHAIN LENGTH

Figure 5.10

2,000 °F
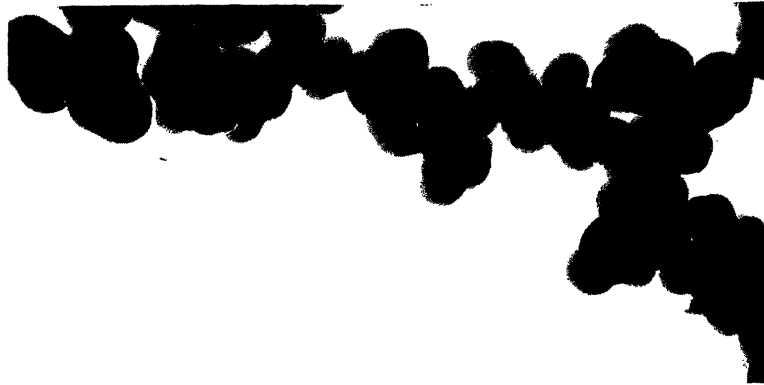
2,300 °F
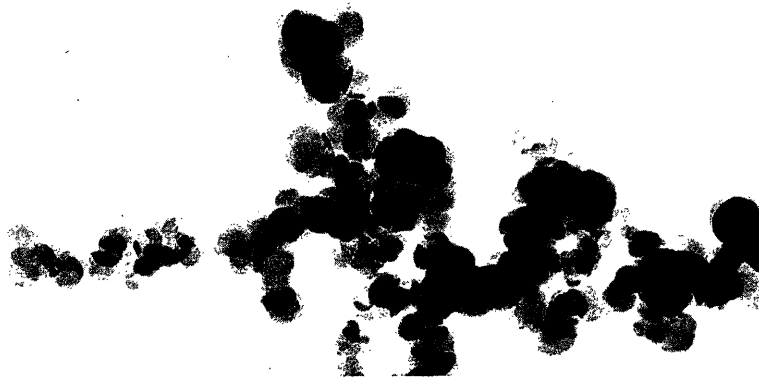
2,600 °F

2,900 °F

In summary, it was shown that chain length was affected by temperature and the amount of extractable. Again, it was seen that from the ideal black standpoint (high tint), it is desirable to have small particles (i.e., rapid nucleation) with a rapid quench to minimize growth and chaining. From the variations in chain length with time and temperature, it would seem that the black is chained during growth but that the chains are continually making and breaking. This would be possible if the "at temperature" bonds are relatively weak compared to the room temperature bonds. No good explanation has been found for why the particles in one chain are nearly all the same size or why unchained particles are almost never found. It is possible that colliding particles are near each other, nucleated at the same time, and grew in the same environment; hence, one would expect them to be nearly the same size. In addition, coagulation times are very short, and this would minimize the number of individual particles.

5.3 Comparison of the Experimental Black to Production Carbon Black

During the discussion of the data from this program, extrapolations were made toward the design of an ideal black process. This extension can only be valid if the blacks have similar properties. In all cases it was necessary to provide long residence times to reduce the extract level to less than one percent. This long time produced large particles, but they were of the same size as some commerical blacks. They are comparable to the coarse blacks, which are designated by Cabot as F.E.F. The properties of (FEF) black are compared to the 2900°F blacks from this program in Table VI.

Table VI

Comparison of Experimental and FEF Carbon Black

	FEF	Experimental
Scale	95.0	92-94
Surface Area (m^2/gm)	42.0	31-37
Size (Electron Microscope) A	410.0	400-660
Tint (%)	200.0	160-224
Extract (%)	0.06	0.58-0.00

The only long time black which did not meet the extract criterion was the material made from Aromatic Concentrate which contained 0.58% extractable and had the low tint value of 160%. The electron microscope examination showed the experimental blacks to have a similar microstructure and morphology (80) to those of production blacks. A further piece of evidence was the result of dispersion tests which were made on two samples. Figure 5-11 shows a dispersion of the experimental blacks which is very similar to production material. Many black spots would indicate a poor dispersion. All of these tests indicate that the experimental black is similar to production material, and, therefore, the predictions on the effects of process parameters should be meaningful.

DISPERSION TESTS

Figure 5.11

Cosden Tar
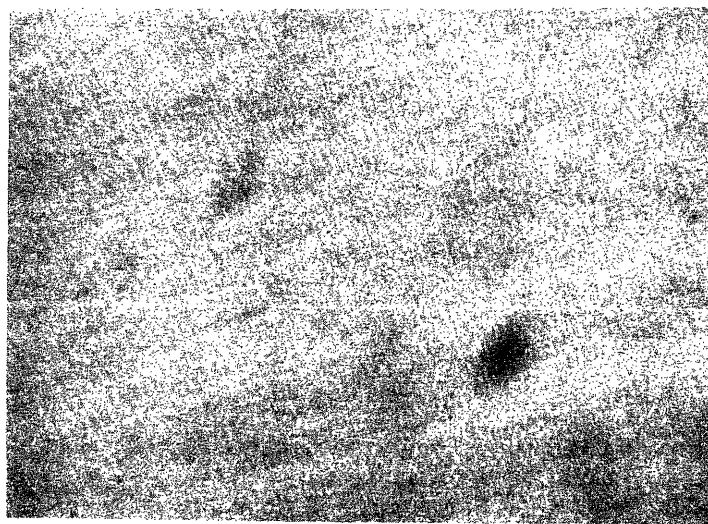
Aromatic Concentrate

VI. CONCLUSIONS

Nucleation:

1. The process of carbon formation and growth can be considered as a nucleation step followed by simultaneous gas phase and surface reactions.

2. Nucleation is the most important step in carbon formation. The rate and homogeneity of nucleation influences the final size, surface area, extract, and chain length of the carbon black particles.

3. Nucleation is a high activation energy process and therefore is very temperature dependent.

4. Nucleation occurs in a period of time which is short compared to the one to seven milliseconds required to vaporize the oil drops.

5. Nucleation appears to occur in one burst, with no secondary particle formation.

Growth:

1. The apparent activation energy for growth for the gas phase reaction varies with feed material and is in the range of 35 to 45 Kcal per mole.

2. The surface reaction has an apparent activation energy of 3 to 7 Kcal per mole which depends on the feed material.

3. Pure materials have a higher activation energy for growth than do residual oils.

General:

1. The carbon black produced in the experimental equipment was similar to production material.

2. The industrially important empirical test for tint is a
   measure of the chain length of the particles.

3. The linkage between carbon particles in the chains are for
   some time in the growth process alternately breaking and making
   chains.

4. Scale does not correlate with carbon particle size for this system.
   Scale probably depends on the chemical composition of the particles.

5. Larger fuel drops produce more varbon particles per mass of fuel,
   but this effect may be markedly modified by variations in the
   speed of mixing fuel with hot gases.

6. Rapid mixing and short vaporization time are important factors
   in obtaining a uniform product.

VII. RECOMMENDATIONS

The present study indicated several areas where more detailed investigations are required.

7.1 Nucleation

Since nucleation is one of the most important steps in carbon black formation, it should be investigated in depth. The apparatus for this work should be capable of turbulent flow, temperatures to at least 2900°F, and residence time resolution of 10^{-4} seconds. Initially, vaporized fuel should be used to eliminate variations due to drop size and to circumvent the problem of obtaining high throughput from disk atomizers. A great deal of information could be obtained from the yield data and from a statistical study on the electron microscope to determine particle number, particle size, and particle size variation. Possibly a mass spectrometer could be used to identify important species (similar to Homann's work).

It would be desirable at a later time to use a system with high temperature capabilities. This temperature could be obtained with a combustion flame (oxygen) or by utilizing an electric arc.

Possibly the seeding of the nucleation zone with small particles or ions (such as cesium) would provide insight into the nucleation process.

7.2 Growth

Once nucleation is better understood, the optimum nucleation conditions could be used to study growth. A detailed electron microscope examination of the particles would provide valuable information on coagulation, growth, and chaining.

With the above information on nucleation and growth, it would then be appropriate to vary the feed stock and drop size. At this point, one

could incorporate tests such as tint, surface area, and scale. Then, an overall model could be formed to predict the carbon black properties which would result from a specific set of processing conditions.

A program for determination of the important gas phase species which contribute to growth would be very interesting but difficult to accomplish.

VIII. APPENDIX

APPENDIX A

Properties of Feed Materials

One of the primary goals of this work was to study carbon formation from residual oils; therefore, two commercial carbon black oils were chosen as starting materials. Naphthalene was used as a third feed stock. This pure material then acted somewhat like a control in the evaluation of experimental results.

In general, one can class residual oils as hydrocarbon mixtures with a major fraction boiling above 700°F. These hydrocarbons contain small amounts of normal paraffins above $C_{22}H_{46}$, but a large fraction is composed of polynuclear aromatic and naphthalene hydrocarbons with long paraffinic side chains. If cracked oil was included in the residual oil, then olefins and diolefins will be present along with other polynuclear aromatics. The asphaltenes and resins are also concentrated in this fraction of the crude. These oils, as shown earlier, also contain colloidal asphaltene particles which may affect the carbon formation process. Actual details of the composition of the residual oil depends strongly on the source of the crude and its processing history.

Some of the properties that are normally measured on production oils are given for this program's starting materials in Table A-1. Comparing the two residuals, it is worthwhile to note that Cosden Tar contains 4.9% asphaltenes as compared to the 1.6 asphaltenes in the Aromatic Concentrate. The asphaltenes may have a tendency to coke during carbon formation, and this could cause a gritty carbon black if the coke balls are not removed. In addition, Cosden Tar contains 0.004% ash. Some oils contain as much as 0.06% ash, and it is possible that this material could have some effect on the nucleation process. A critical parameter for carbon formation

Table A-1

Feed Stocks

	Cosden Tar MO-1553	Concentrate MO-1485	Naphthalene
Sp. Gg.	1.06	1.05	1.0
Viscosity (s.s.u.)			
130°F	112	483	-
210°F	47	68	-
% Asphaltenes	4.9	1.6	0.0
% Ash	0.004	0.0	0.0
% Sulfur	2.6	0.0	0.0
% Carbon	87.58	88.17	93.75
% Hydrogen	8.72	9.08	6.25
H/C ratio	1.19	1.23	1.25
Mean Boiling Point °F	693	790	410
% Water	0.0	0.5	0.0

is the hydrogen-to-carbon ratio which was 1.19 and 1.23 for the two residual oils and 1.25 for the naphthalene.

The boiling curves for the two residual oils are given on Figure A-1. These data show that the Cosden Tar has about 15% more low boilers than the Aromatic Concentrate and its mean boiling point is 690°F while the mean boiling point of Aromatic Concentrate is 790°F.

In summary, the major differences between the two residual oils is that the Cosden Tar contains 3% more asphaltenes, 2.6% more sulfur, a small amount of ash, and has a mean boiling point that is approximately 100 degrees lower.

BOILING POINT CURVES

Figure A-1
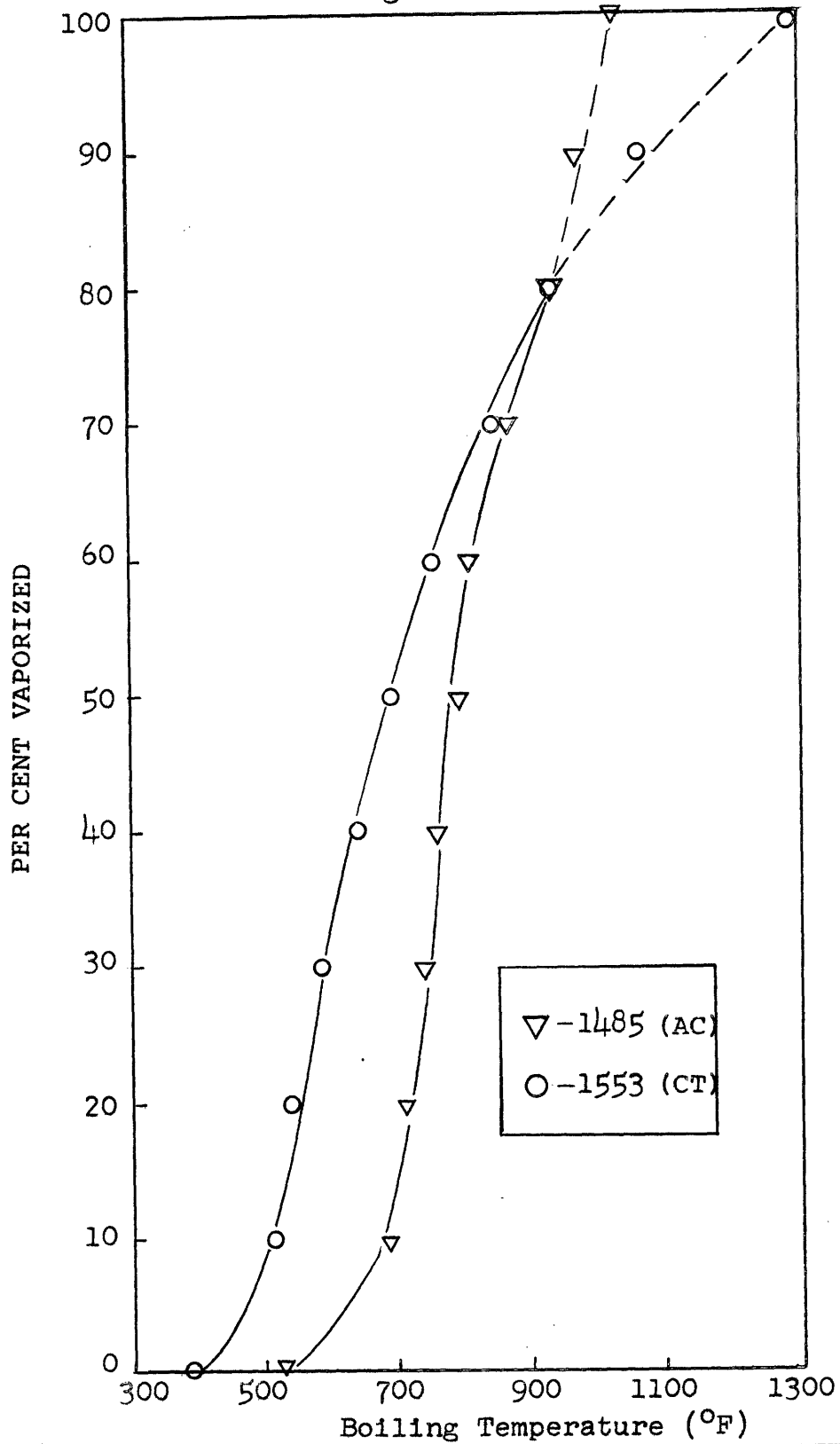
APPENDIX B

Gas Chromatographic Analysis

All gas samples were analyzed on a Fisher-Hamilton Model 29 Gas Partitioner. This dual-column, dual-dector system was used to separate carbon dioxide, carbon monoxide, acetylene, methane, oxygen, nitrogen, and hydrogen. The first column in this unit was a six foot long by 1/4 inch diameter tube packed with Di-2-ethylexylsebacate (DEHS) on 60 to 80 mesh Columpak. The second standard column was 6-1/2 feet long by 3/16 inches in diameter and packed with 42 to 60 mesh molecular sieves. With this column system, acetylene could not be separated from oxygen. Therefore, a six foot long by 3/16 inch column of silica gel was added ahead of the molecular sieve column.

The resulting system gave separation, as shown schematically on Figure B-1, when operating with a helium carrier. Each sample required approximately seven minutes for separation. For hydrogen determination only the second column was used and argon was the carrier gas.

Concentrations of the various gases were determined by comparing the peak heights of the reactor gas sample with peak heights obtained from a bottle of Matheson Standard Gas. The analysis of the standard gas is given in Table B-1.

Table B-1

Gas Analysis

Compound	Concentration (%)
CO	11.6
CO_2	9.98
O_2	1.17
CH_4	3.14
N_2	63.12
C_2H_2	0.98
H_2	9.98

SAMPLE CHROMATOGRAM

Figure B-1
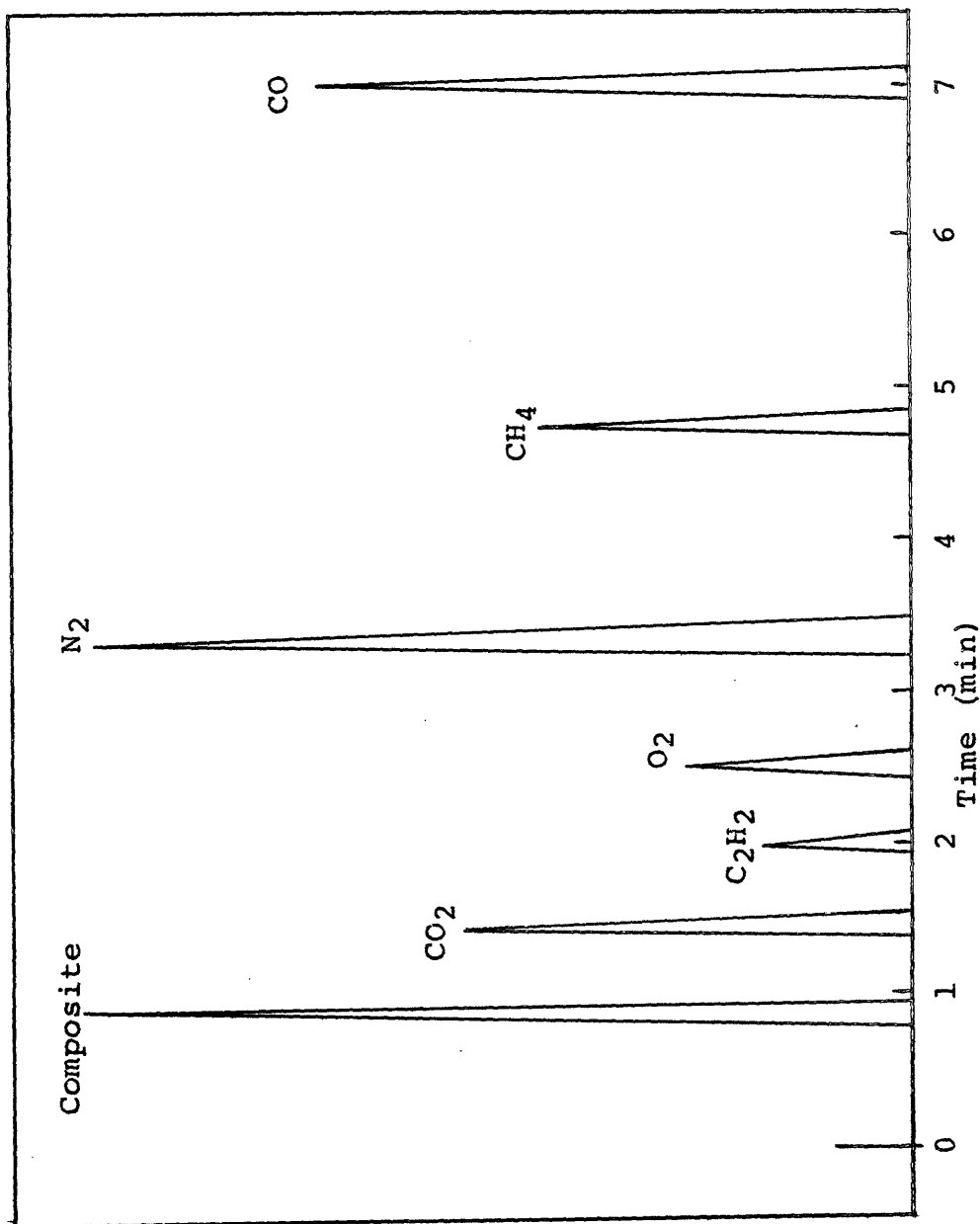
APPENDIX C

Analysis of the Solid Product

All of the analyses of the carbon black were carried out by the
laboratories of Cabot Corporation. The following sections contain
brief descriptions of their procedures.

C.1 Scale. The Cabot Nigrometer Scale is a relative measurement of
the diffuse reflectance from a carbon black-varnish dispersion. The scale
provides an indication of the blackness of the particles.

To prepare carbon black for scale determination, the black is first
dried at 230°F for one hour. Then 0.25 grams of the black are intimately
mixed into 3 cc of 00 Linseed Oil Varnish by mulling in clockwise, counter-
clockwise, and then clockwise directions. The resulting black paste is
smeared on a glass slide to a thickness of approximately 1/8 of an inch.
This sample is then placed into the Nigrometer which has been calibrated
on a Standard Black Tile, and the reflectance of monochromatic light from
the sample is determined as a percentage of an arbitrary scale. Generally,
the smallest blacks give the lowest scale reading. For many carbon blacks,
Cabot has been able to correlate the scale with the actual particle size.
Figure C-1 shows this relationship.

C.2 Tinting Strength. The percent tint is a whiteness test that
appears to be a measure of the hiding power or chaining of the carbon
black particles. For this test, 0.2 gram of the paste from the scale
measurement is mixed with 10 grams of white paste. The white paste is
65% lithopone (white printing ink) and 35% 00 Linseed Oil Varnish. After
mulling, the paste is placed on a slide and positioned in an I.D.L. color
EYE. This instrument indicates the reflectance from the sample as a
percentage of the reflectance from a white standard. This value is then
compared to the value from a standard carbon black.

RELATION OF SCALE TO PARTICLE SIZE
FOR PRODUCTION BLACKS

Figure C-1

PARTICLE DIAMETER ($\overset{\circ}{A}$)

Scale
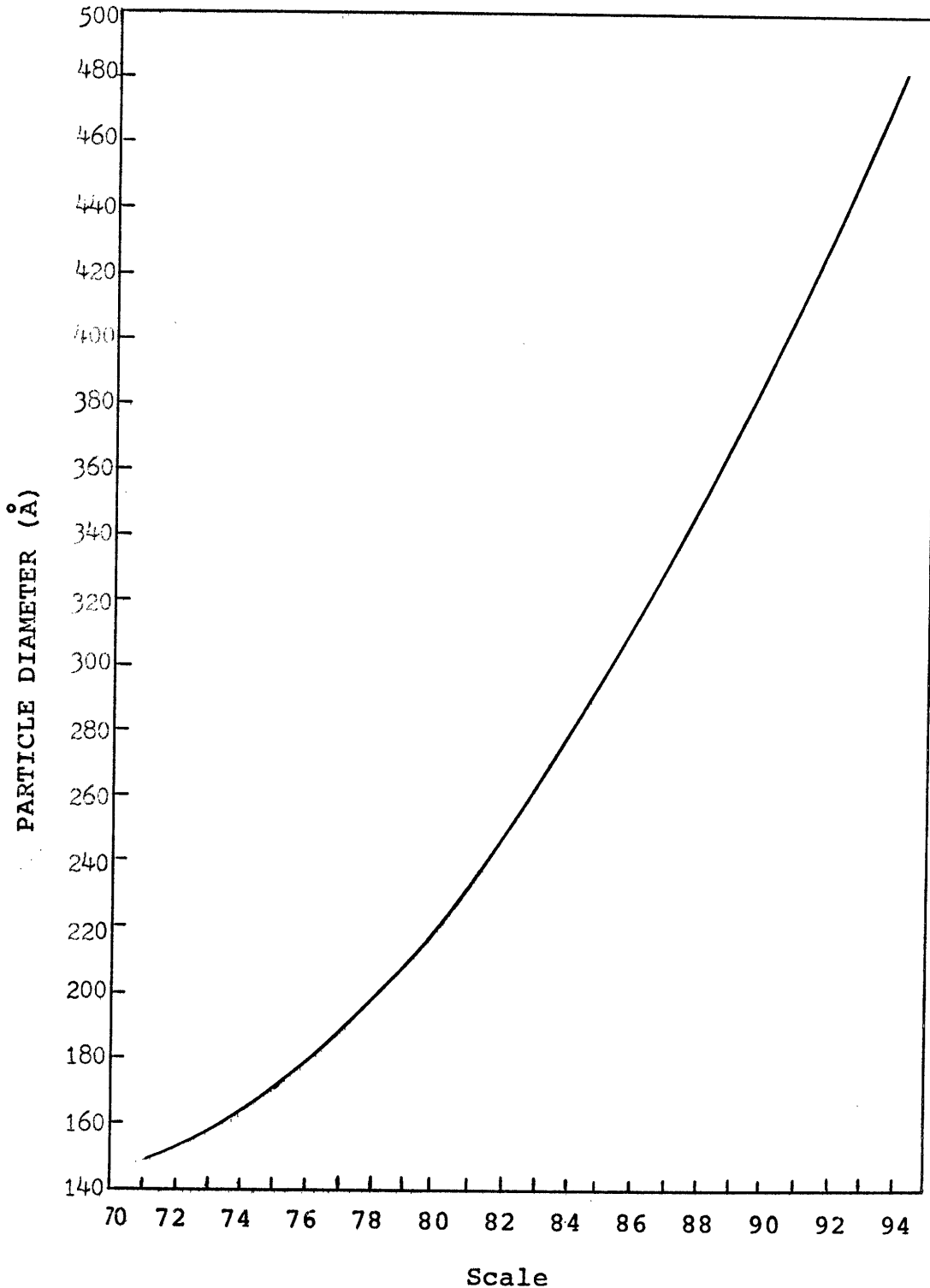
C.3 <u>Benzene Extract</u>. For this test, a weighed amount of carbon black is placed in the thimble of a Soxhlet Extractor and the sample is extracted with benzene for eight hours. After this time, the benzene is evaporated to dryness, and the residue is weighed to determine the amount of material extracted from the carbon black.

C.4 <u>Nitrogen Surface Area</u>. This is the standard B.E.T. analysis which determines surface area from the volume of nitrogen required to form an absorbed monolayer on the surface of the carbon black particles.

C.5 <u>Dispersion Test</u>. This test developed by L. Doppler of Cabot Corporation, provides an indication of how well the black can be dispersed in a medium. First, a sample of carbon black is mulled into varnish with an automatic muller and then the paste is smeared between two glass plates and photographed at 100x under a light microscope. The uniformity of the dispersion on the resulting picture provides a rapid visual indication of the mixability of the carbon black. A large number of black spots or carbon agglomerates is an indication of a poor dispersion.

C.6 <u>Electron Microscope</u>. The secret to a good electron microscope picture lies in the dispersion technique. F. A. Heckman and D. F. Harling of Cabot Corporation have developed a good, reproducible ultrasonic dispersing technique. In this technique, carbon black is first placed in a vial of acetone at concentrations of 0.2 to 0.5%. The mixture is then sonified for three minutes at the maximum intensity of a Branson Model S-75 Sonifier equipped with a Step-horn and a flat tip. Immediately after sonifing, a carbon or SiO substrate grid is dipped into the acetone. Excess liquid is blotted from the grid. After drying, the grid is placed in the electron microscope and photographed at 10,000x and 60,000x. The resulting pictures are then blown up to 50,000x and 300,000x before printing.

APPENDIX D

Drop Size Determination

In order to correlate disk speed with drop size, it was necessary to calibrate the atomizer. The Magnesium Oxide Method of May (81) was chosen because it was relatively rapid and reasonably accurate. In this technique, clean microscope slides were coated with magnesium oxide by moving them back and forth in the tail flame of a burning magnesium ribbon. In this manner, the slide was coated with a soft smooth layer of particles which had a grain size of approximately 0.5 microns. In order to obtain a good crater, the layer of magnesium oxide should be at least twice as thick as the diameter of the particles to be measured. When an oil drop struck the surface of the slide, it left a well-defined circular impression. The diameter of this crater was then measured by illuminating the sample with strong transmitted light and using a microscope with a calibrated eyepiece.

In his work, May carried out a set of experiments in which he measured the size of drops coming from a spinning disk by both the crater and the absolute method. In the absolute method, the drops were caught and mounted in a second liquid. This liquid was immiscible with the oil, it had a high viscosity, a different index of refraction, and a density similar to the droplets. With this technique, the drops were preserved in spherical form and could be measured using a light microscope. May compared drops with diameters ranging from 200 microns down to 20 microns and found the ratio of the true drop size (Absolute method) to the crater size equal to 0.86. This conversion factor was then used to calibrate the present disk. An additional important fact was that the crater diameter was found to be independent of the impact velocity of the drop.

APPENDIX E

Experimental Data

The raw data and some of the calculated results are included in this section. The outline of the experimental program and run conditions was given in Section 2.3. The following code was used to number the experimental runs.

```
        1 - 1 - 1
        ↓   |   |
   Series Number
            ↓   |
        Test Number
                |
                ↑ Run Number
```
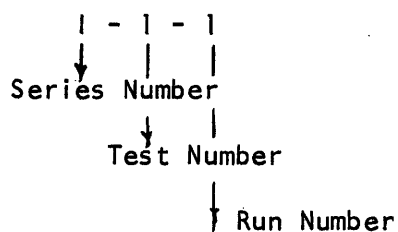
The Series Number provides the type of oil and temperature level, while the Test Number indicates the drop size and probe position. The Run Number labels the different runs made with the same series and test numbers. Normal air flows were 0.93 SCFM and natural gas flows were 0.089 SCFM. The pertinent experimental data are given in the following tables E-I, E-II, E-III and E-IV. Figures E-1 through E-10 contain representative electron micrographs. All micrographs are magnified 50,000 times.

Table E-1

Run Data

Run	Temperature (°F)	Run Length (min)	Total Gas Flow (SCFM)	% Yield (grams C per gram of oil fed)
I-1-1	2003	16	1.34	3.7
I-1-3	2026	15	1.34	4.3
I-2-5	2050	12	1.37	3.1
I-2-7	2060	25	1.45	3.1
I-3-1	2010	22	1.34	1.4
II-1-1	2230	22	1.45	5.8
II-2-4	2340	21	1.4	4.3
II-3-1	2360	11	1.4	10.4
III-1-1	2570	17	1.45	17.2
III-3-1	2600	15	1.4	6.2
III-4-1	2600	13	1.4	5.7
III-2-4	2600	20	1.4	9.67
III-7-1	2620	14	1.4	8.5
III-7-2	2590	10	1.4	7.7
III-6-1	2590	20	1.4	-
III-6-2	2590	20	1.4	4.25
III-3-1	2640	17.5	1.4	10.5
III-9-1	2600	22	1.4	6.5
III-9-2	2580	30	1.4	6.9
III-5-1	2600	25	1.4	7.5
IV-1-1	2880	17.5	1.31	67.2
IV-8-1	2860	10.5	1.4	37.6
IV-4-1	2900	15	1.4	4.1
IV-2-1	2860	25	1.4	22.8
IV-7-1	2860	24	1.4	7.2
IV-6-1	2900	16	1.4	9.8
IV-3-1	2930	14	1.4	13.8
IV-9-1	2900	19	1.4	12.6
IV-5-1	2900	20	1.4	8.0
V-2-1	2000	30	1.4	4.2
VI-2-1	2340	30	1.4	5.68
VII-2-1	2600	20	1.4	10.3
VII-7-1	2600	13	1.4	5.7
VII-6-1	2580	20	1.4	18.4
VIII-2-3	2900	22	1.4	52
VIII-7-1	2900	15	1.4	6.8
VIII-6-1	2900	15	1.4	5.1
1-2-2	2080	10	1.4	4.1
2-2-1	2300	16	1.4	7.8
3-2-1	2600	15	1.4	11.7
3-7-1	2600	13	1.4	10.2
3-6-1	2600	10	1.4	8.5
4-2-1	2900	11	1.4	16.7
4-7-1	2900	12	1.4	11.7
4-6-1	2900	10	1.4	6.5

Table E-11

Carbon Black Analysis

Run	Scale	Tint (%)	Surface Area (m²/gram)	Extract (%)
I-1-1	89	~20	-	10.3
I-1-3	94-1/2	~40	53.9	45.3
I-2-5	98	50	-	9.5
I-2-7	93-1/2	~40	4.9	15.9
I-3-1	97	49	-	1.1
II-1-1	94	83	23.6	3.2
II-2-4	92	62	28.3	0.7
II-3-1	95	112	25.2	13.8
III-1-1	93	212	32.7	0.1
III-8-1	89	128	94.2	0.68
III-4-1	93	173	38.6	1.16
III-2-4	92	187	38.5	0.0
III-7-1	93	178	36.6	0.58
III-7-2	91	202	40.1	1.06
III-6-1	92	206	41.5	0.55
III-6-2	88	219	62.6	1.62
III-3-1	94	162	32.6	0.05
III-9-1	-	-	45.8	-
III-9-2	89	148	63.8	0.0
III-5-1	89	206	72.3	1.29
IV-1-1	93	190	35.6	0.0
IV-3-1	90-1/2	227	57.2	0.45
IV-4-1	89	219	53.0	2.18
IV-2-1	92	214	36.6	0.05
IV-7-1	91	232	55.8	0.0
IV-6-1	89	219	56.1	0.98
IV-3-1	94	146	30.6	0.05
IV-9-1	90-1/2	224	48.1	0.53
IV-5-1	89	235	58.6	1.81
V-2-1	93-1/2	102	29.9	9.3
VI-2-1	92	184	48.2	1.8
VII-2-1	91	208	45.6	1.15
VII-7-1	90	224	55.8	0.58
VII-6-1	93	208	45.1	0.54
VIII-2-1	94	160	36.7	0.46
VIII-7-1	90-1/2	133	39.0	1.82
VIII-6-1	90	218	45.5	1.36
1-2-2	96	57	13.0	5.48
2-2-1	97	98	20.2	0.57
3-2-1	94	197	32.8	0.97
3-7-1	93	190	34.3	0.49
3-6-1	93	156	38.8	0.43
4-2-1	94	187	41.0	0.28
4-7-1	92	220	46.2	0.89
4-6-1	93	167	32.9	0.39

Table E-III

Calculated Results

Run	Residence Time (milli-seconds)	Reactor Velocity (ft/sec)	Shift Temp. (°F)	N_{re}	Average Diameter $\overset{\circ}{A}$	Range of Diameters $\overset{\circ}{A}$
I-1-1	124	22	2660	878	-	-
I-1-3	118	23	2275	916	1800	-
I-2-5	123	22	2106	852	-	-
I-2-7	-	-	-	-	1800	-
I-3-1	125	22	2230	858	-	-
II-1-1	107	26	1880	879	1000	-
II-2-4	105	26	2590	859	667	-
II-3-1	101	27	2390	859	800	-
III-1-1	94	29	2930	825	700	400-800
III-8-1	67	28	2800	799	430	370-450
III-4-1	46	28	2360	798	300	200-600
III-2-4	94	29	2700	820	600	500-800
III-7-2	67	28	3560	794	430	330-660
III-6-1	47	28	2920	797	-	-
III-6-2	47.5	27	2820	795	360	200-800
III-3-1	96	28	2990	790	600	400-800
III-9-1	67.5	28	2450	797	-	-
III-9-2	69.2	27	3540	797	400	200-800
III-5-1	47.5	27	3240	794	300	200-400
IV-1-1	92.4	29	3870	713	500	430-530
IV-8-1	62	30	3040	756	300	160-430
IV-4-1	42	31	2860	758	200	120-530
IV-2-1	89	31	2880	764	500	400-600
IV-7-1	62	30	3080	764	370	200-700
IV-6-1	43	30	3620	758	300	160-800
IV-3-1	87.5	31	2990	756	600	500-1000
IV-9-1	62	30	3120	760	370	220-1000
IV-5-1	44	30	3970	758	230	160-400
V-2-1	123	22	4410	886	530	300-830
VI-2-1	109	25	3130	830	600	300-670
VII-2-1	100	27	3000	796	600	200-800
VII-7-1	69	27	2680	794	400	100-1000
VII-6-1	46.6	28	2510	799	310	100-800
VIII-2-3	91.5	30	2180	759	400	160-1200
VIII-7-1	62	30	3010	758	370	300-800
VIII-6-1	43	30	2980	758	300	160-600
1-2-2	120	22	2220	-	1000	800-1200
2-2-1	108	25	4000	-	600	400-800
3-2-1	92	30	4000	-	500	300-800
3-7-1	63	30	3500	-	430	400-800
3-6-1	44	29	3140	-	400	300-800
4-2-1	81	34	4010	-	400	300-1000
4-7-1	62	32	3400	-	370	300-800
4-6-1	41	36	3300	-	320	200-830

Table E-IV

Gas Compositions

Run	N_2	O_2	CO_2	CO (%)	CH_4	C_2H_2	H_2O	H_2
I-1-1	74.7	0.23	4.29	2.17	0.46	0.09	15.1	2.32
I-1-3	76.3	0.14	5.48	2.88	0.53	0.09	11.68	2.3
I-2-5	73.8	-	4.6	3.38	-	0.16	13.27	4.25
I-3-1	73.8	0.28	4.11	3.03	0.21	0.16	13.85	3.98
II-1-1	72.97	0.83	3.5	2.57	0.51	0.19	13.44	5.41
II-2-1	76.47	0.34	4.56	1.98	0.11	0.09	14.02	1.79
II-3-1	72.67	0.21	3.2	3.23	0.36	0.18	14.53	5.04
III-1-1	72.66	0.39	2.27	2.54	0.19	0.15	16.71	4.51
III-8-1	72.4	0.05	3.47	4.14	0.17	0.26	14.5	4.5
III-4-1	72.3	0.06	3.56	3.27	0.18	0.20	14.97	4.83
III-2-4	74.08	0.03	2.66	1.94	-	0.14	17.12	3.13
III-7-2	74.11	0.11	3.50	3.05	0.15	0.13	15.82	2.51
III-6-1	74.8	0.24	4.04	2.38	0.08	0.14	15.4	2.2
III-6-2	77.5	0.25	6.07	1.42	0.01	0.03	13.2	0.8
III-3-1	72.65	-	2.89	2.72	0.11	0.11	17.14	3.8
III-9-1	73.7	0.29	4.0	3.45	0.03	0.12	13.9	3.9
III-9-2	76.5	0.15	4.85	1.58	0.02	0.04	15.4	0.92
III-5-1	77.3	0.23	5.65	1.32	0.01	0.03	14.13	0.68
IV-1-1	67.7	-	1.69	3.81	0.16	0.13	19.03	0.13
IV-8-1	75.4	0.28	4.43	2.72	0.04	0.10	14.4	2.02
IV-4-1	72.8	0.23	2.78	2.39	0.08	0.19	17.2	3.74
IV-2-1	72.1	0.25	2.81	2.91	0.13	0.09	16.36	4.72
IV-7-1	73.3	0.08	3.2	2.84	0.10	0.15	16.4	3.26
IV-6-1	77.3	0.24	5.48	1.13	0.0	0.04	14.6	0.54
IV-3-1	72.58	0.26	2.83	3.93	0.07	0.06	16.25	4.22
IV-9-1	75.1	0.24	4.26	2.88	0.04	0.09	14.6	2.2
IV-5-1	78.4	0.25	6.69	0.77	-	0.01	12.97	0.23
V-2-1	75.6	0.22	3.97	1.64	0.2	0.13	16.6	0.96
VI-2-1	76.2	0.24	4.56	1.37	0.06	0.08	15.8	1.05
VII-2-1	76.1	0.24	4.58	1.46	0.04	0.06	15.7	1.18
VII-7-1	77.4	0.26	5.88	1.16	-	0.04	13.8	0.76
VII-6-1	73.7	0.12	3.81	2.41	0.22	0.26	15.7	3.12
VIII-2-3	77.8	0.23	6.47	0.98	-	0.04	13.03	0.80
VIII-7-1	73.1	0.24	3.01	3.3	0.10	0.13	15.9	3.58
VIII-6-1	77.3	0.27	5.71	1.38	0.27	0.03	13.9	0.79
1-2-2	74.1	0.85	2.55	1.12	0.20	0.13	17.88	3.19
2-2-1	75.3	0.12	2.46	1.46	0.14	0.10	18.4	1.28
3-2-1	72.8	0.29	2.57	7.10	0.16	0.20	11.4	4.86
3-7-1	71.63	-	1.77	2.99	0.49	0.40	17.4	5.81
3-6-1	73.9	0.26	3.07	3.38	0.29	0.31	14.5	3.52
4-2-1	70.4	0.10	1.34	4.66	0.10	0.20	15.8	7.96
4-7-1	73.0	0.13	2.78	4.66	0.56	0.30	13.8	4.34
4-6-1	66.3	-	2.95	3.80	0.65	0.70	16.4	10.5

ELECTRON MICROGRAPHS

Figure E-1
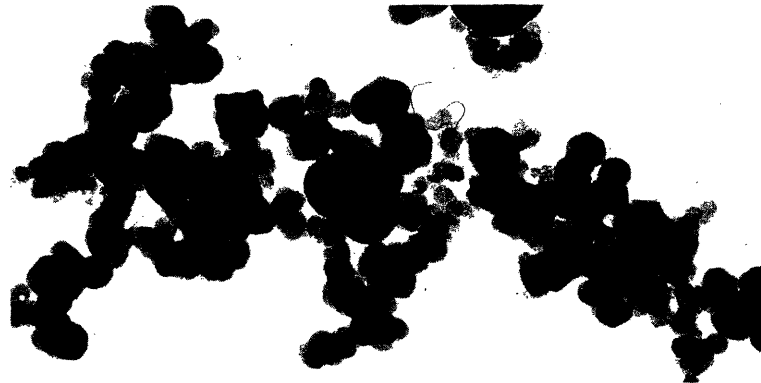
I-1-3
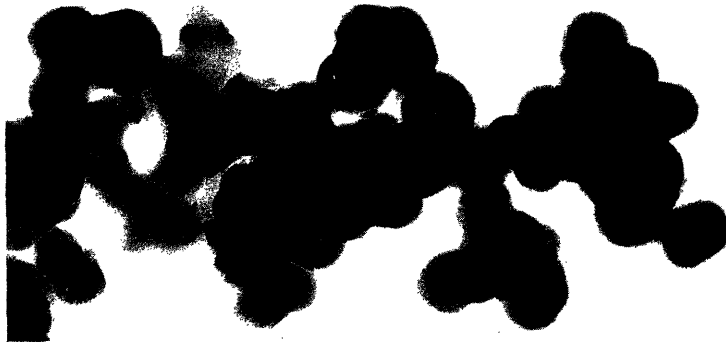
I-2-7

I-3-1

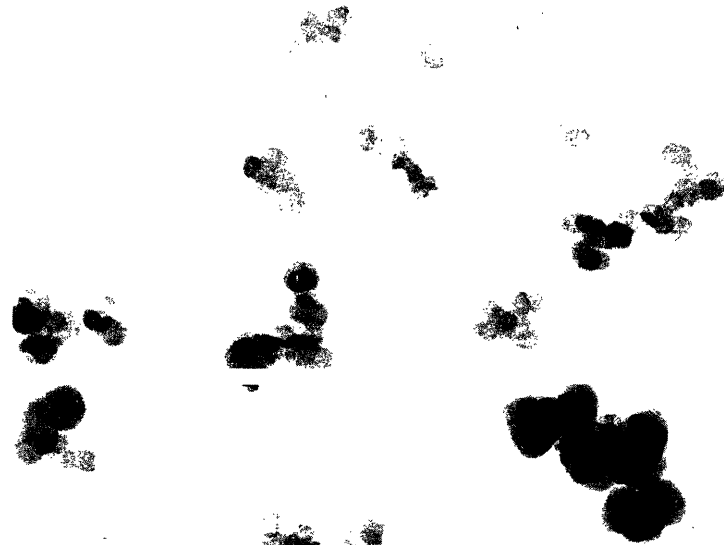II-1-1

ELECTRON MICROGRAPHS
Figure E-2

II-2-1

II-3-1
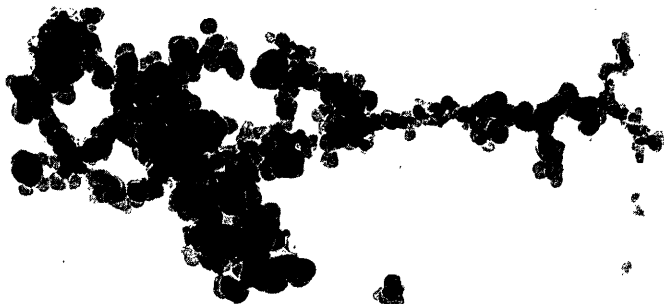
III-1-1

III-2-4

ELECTRON MICROGRAPHS

Figure E-3

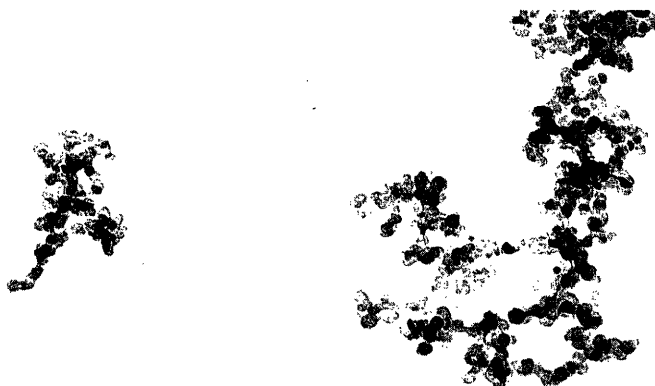III-3-1

III-4-1

III-5-1

III-6-1

ELECTRON MICROGRAPHS
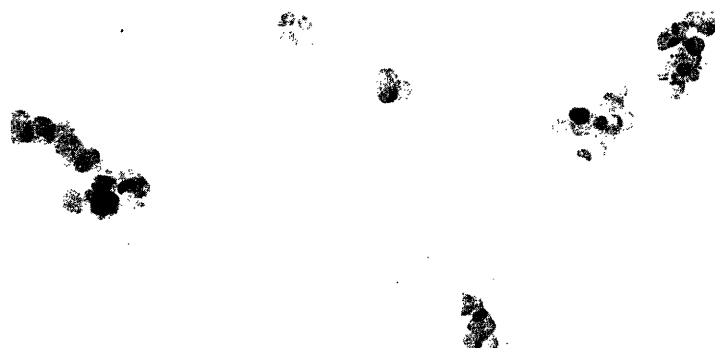## Figure E-4

III-7-2

III-8-1

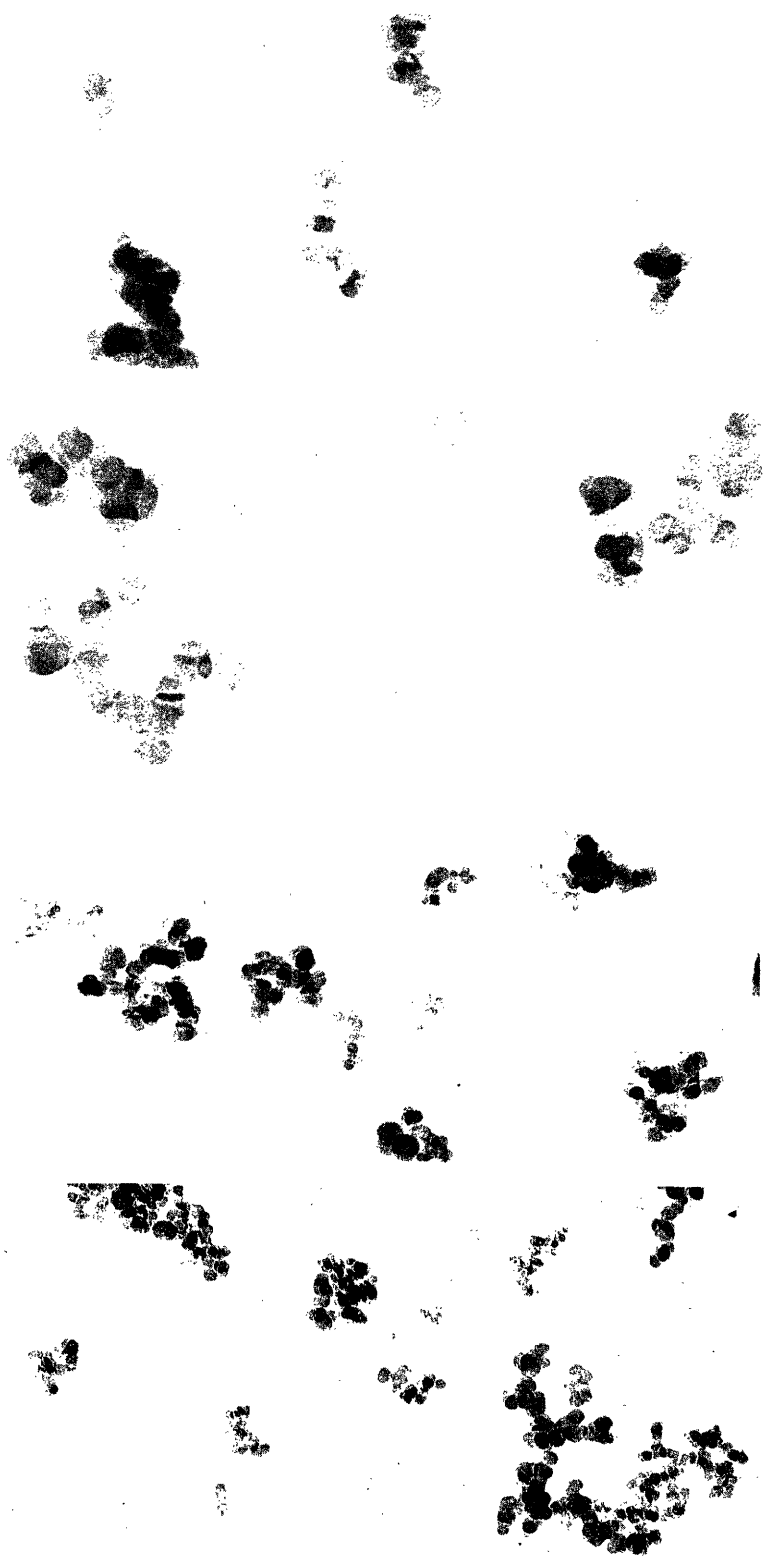III-9-2

IV-1-1

ELECTRON MICROGRAPHS

Figure E-5

IV-2-1
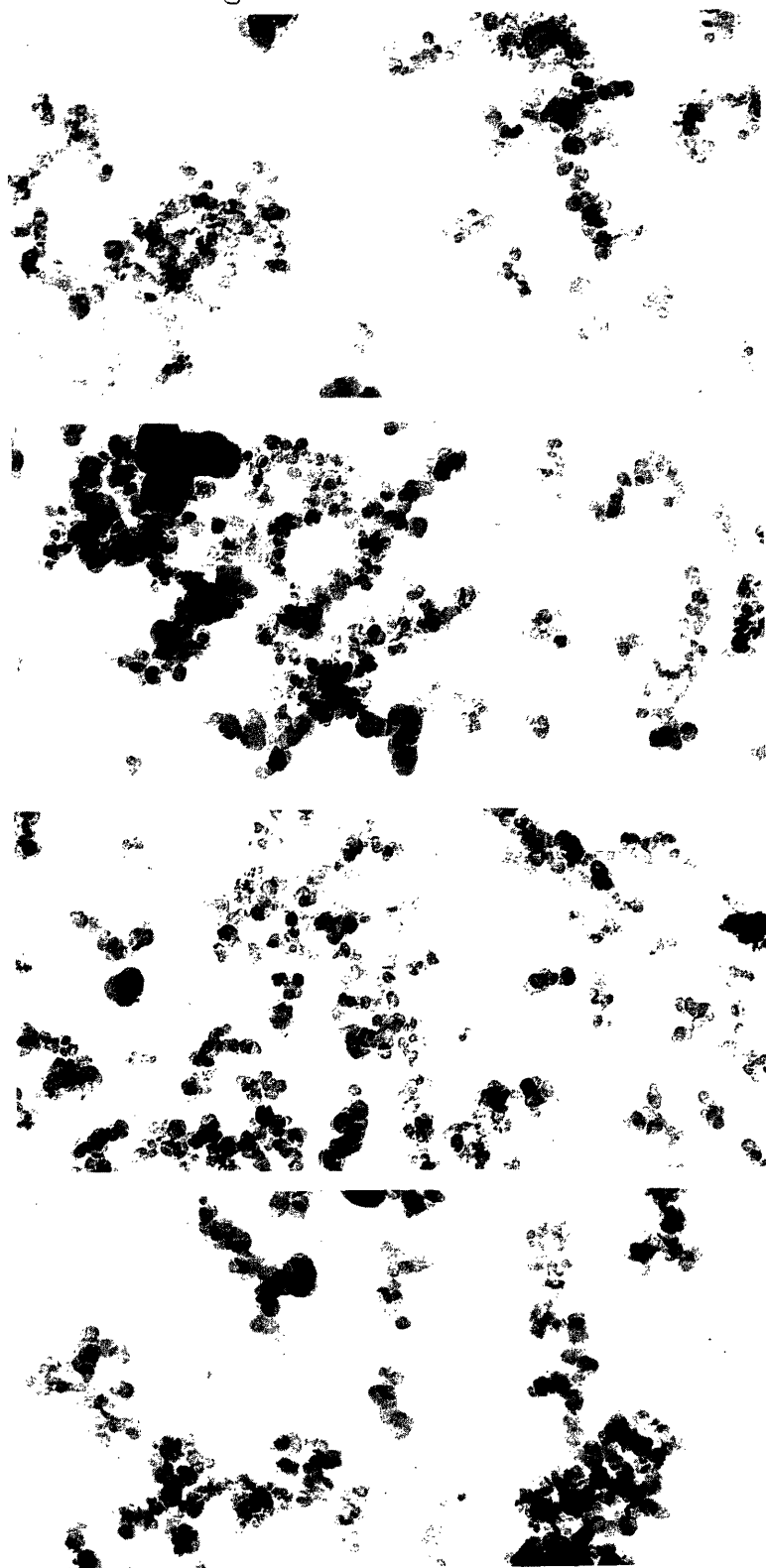
IV-3-1

IV-4-1

IV-5-1

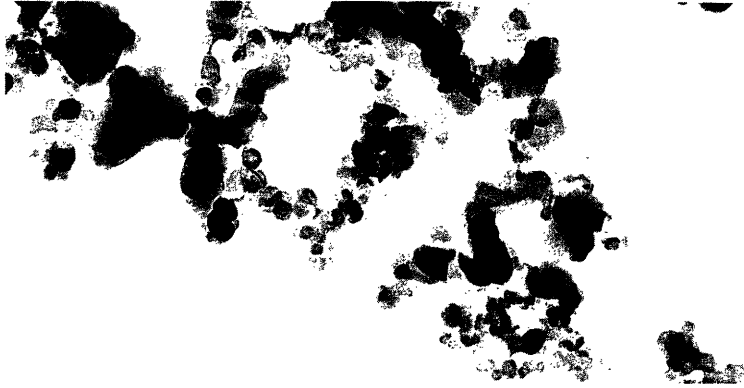# ELECTRON MICROGRAPHS

Figure E-6

IV-6-2

IV-7-1

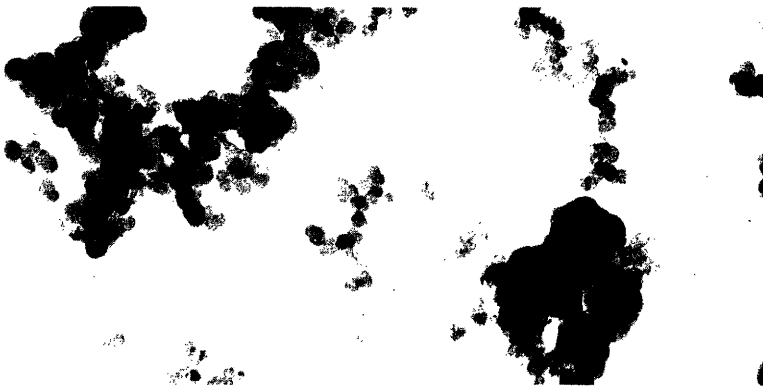IV-8-1
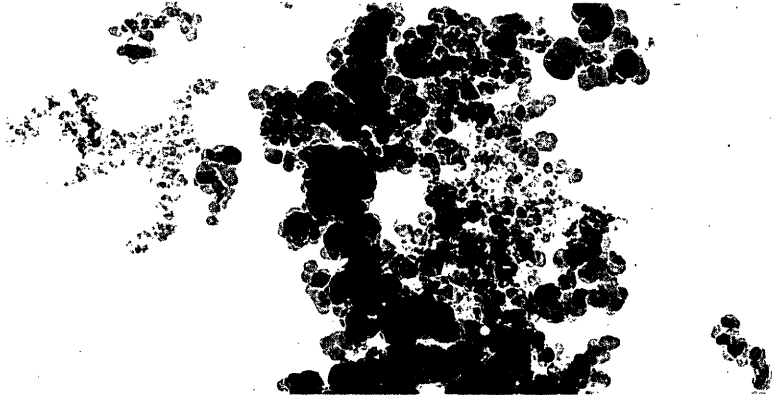
IV-9-1

ELECTRON MICROGRAPHS
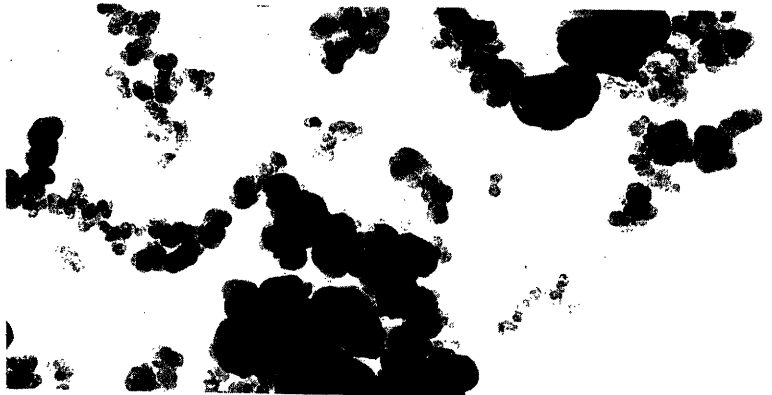
Figure E-7

V-2-1

VI-2-2
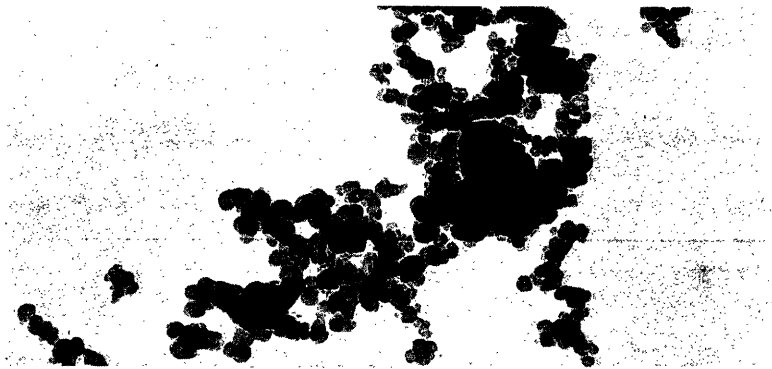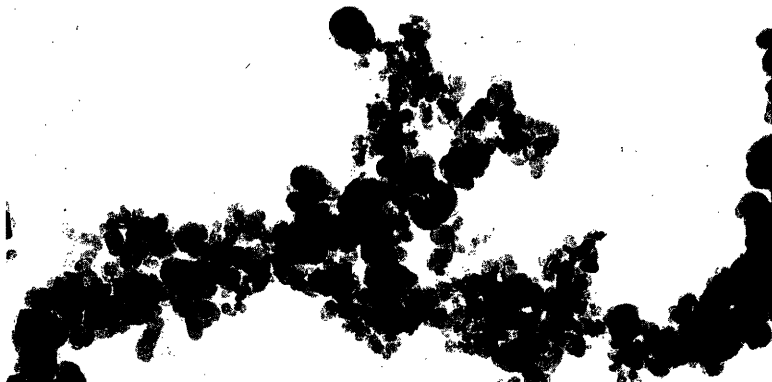
VII-2-3
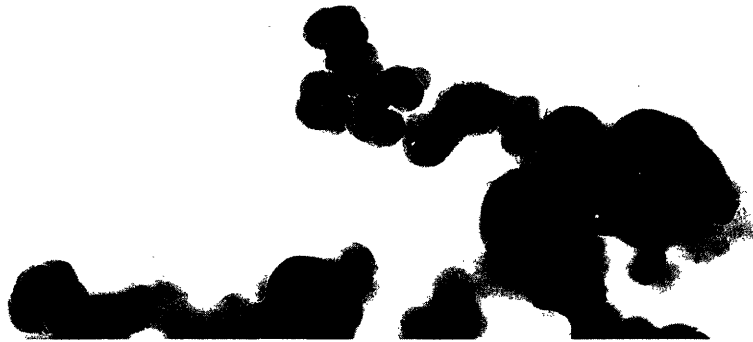
VII-6-1

ELECTRON MICROGRAPHS

Figure E-8

VII-7-1

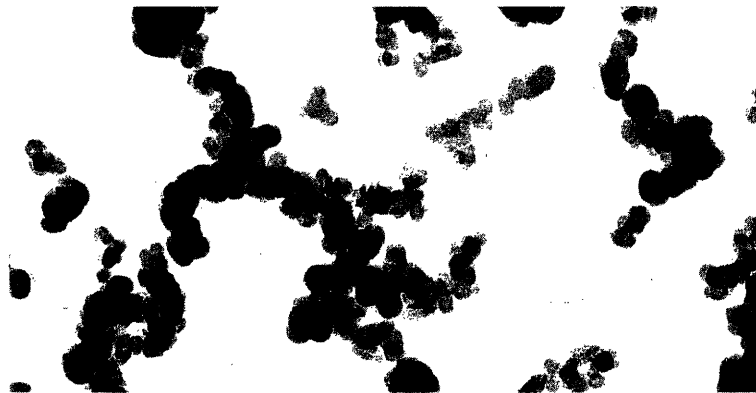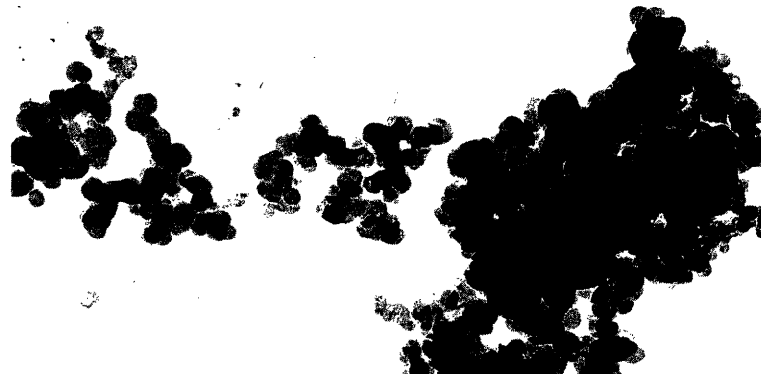VIII-2-3

VIII-6-1

VIII-7-1

ELECTRON MICROGRAPHS

Figure E-9
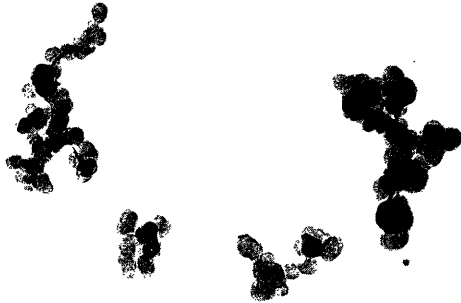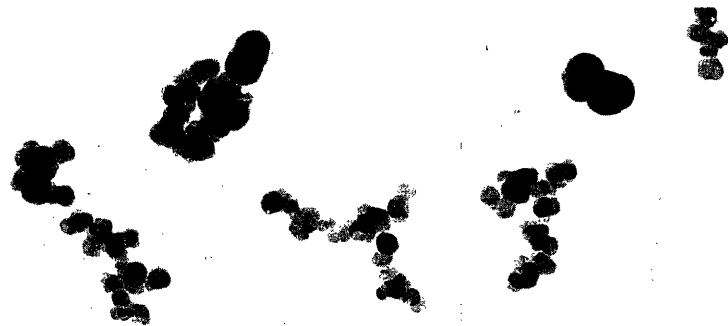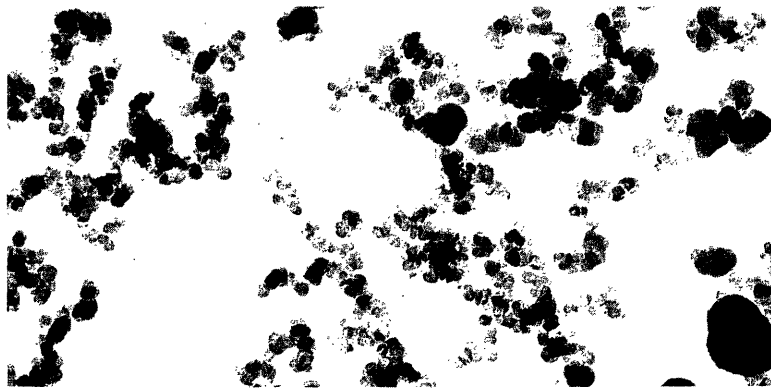
1-2-2

2-2-1

3-2-1

3-6-1

ELECTRON MICROGRAPHS

Figure E-10

3-7-1

4-2-1

4-6-1

4-7-1

APPENDIX F

Droplet Vaporization

When the drops were mixed with the hot gases in the furnace, heat was transferred to them by radiation and conduction. It was desirable to know the differences in vaporization times of the different sized oil drops. This permitted the determination of the effect of drop size on carbon black properties.

In general, the steady state heat transfer to a sphere is a function of the Reynolds and Prandtl numbers of the gas stream. In this case, the Reynolds number corresponding to the difference between the velocity of the oil drop and gas medium was less than one. Therefore, it was assumed that the Nusselt number was equal to 2.0. This value was used, with the realization that 2.0 is only correct for steady state heat transfer from a stationary gas to a sphere.

One can consider the radiation from the reactor tube as black. Therefore, the rate energy of impingement on the drop surface due to radiation is given by:

$$gr = \pi D^2 h_r (T_\infty - T_1) = \pi D^2 \sigma T_\infty^{\,4} \tag{F-1}$$

Here, T_1 is the drop temperature, T_∞ is the gas and wall temperature. The radiation heat transfer coefficient h_r is then defined as:

$$h_r = \left(\frac{T_\infty^{\,4}}{T_\infty - T_1} \right) \tag{F-2}$$

For the conduction transfer, it was assumed that the Nusselt number N_u [defined by equation (F-3)] was equal to 2.0.

$$N_u = \frac{h_c D}{K_2} \tag{F-3}$$

Finally, the ratio of the two heat transfer coefficients
was given by

$$\frac{h_r}{h_c} = 1/2 \left(\frac{\sigma\, T_\infty^{\,4}}{T_\infty - 1}\right) \frac{D}{K} \tag{F-4}$$

The vaporization time was split into two portions to simplify the
analysis. The first time period consisted of the time up to a point
where vaporization became appreciable. It was assumed that during this
time heat was transferred to the drop by radiation from the walls and
the gases as well as by conduction from the hot gases. In addition, it
was assumed that no appreciable vaporization took place during this
period. The second time period was the vaporization time. Here it
was assumed that all heat transferred to the drop caused vaporization
of the oil. Furthermore, a constant drop diameter was assumed since
the work of Gerald (82) has shown that with residual oils the drop
diameter remains constant during 90% of the vaporization time.

The method of calculating the lifetime of the drops was based
on the work of Simpson (83) and much of the data he obtained for Residual
Fuel Oils was used. Simpson first defines three special parameters which
he terms the conduction, radiation, and absorptivity groups.

$$A = \frac{h_c R_1}{K_1} \qquad\qquad \text{Conduction Group} \tag{F-5}$$

$$B = \frac{h R_1}{K_1} \qquad\qquad \text{Radiation Group} \tag{F-6}$$

$$C = k' R_1 \qquad\qquad \text{Absorptivity Group} \tag{F-7}$$

These three groups account for the heat conveyed to the drop by
conduction, radiation and the amount of radiation absorbed by the
drop. Using an approximate kg, calculated at the mean temperature

of the gas and the drop, it was possible to calculate A according to

$$A = \frac{h_c R_1}{k_1} = (Nu)c \frac{Kg}{2k_1} \qquad \text{(F-8)}$$

For the oils used in this program, A was calculated to be 1.6. Simpson recommends a correction on the dimensionless temperature θ for this value of A. θ is defined by

$$\theta = \frac{T - T_1}{T_\infty - T_1} \qquad \text{(F-9)}$$

Here, T is the final surface temperature of the drop and T_1 is the initial drop temperature. In these calculations, instead of T_∞, T_∞^* was used to compensate for the high value of A.

$$T_\infty^* = 2A\, T_\infty \qquad \text{(F-10)}$$

For an A equal to 1.0, Simpson solved the governing equations for various values of B and C and presented this data in graphical form.

All of the pertinent data on Simpson's charts was put into equation form, along with the relevant equations, and programmed for the IBM-360 computer. This program then generated preheat times and vaporization times for the various feed materials and drop sizes as a function of temperature. As an example, for CT the calculated values for B for a 130 micron drop and a 25 micron drop are 0.25 and 0.055, respectively. In addition, a 130 micron drop has a C value of 0.25 as compared to a value of 0.05 for the 25 micron drop. Using these values and Simpson's charts, it is possible to calculate θ, which enables one to calculate a dimensionless time of preheat J, as defined by:

$$J = \frac{k_L t}{C_a \rho_\ell R_1^2} \qquad \text{(F-11)}$$

Generally, the preheat time accounted for approximately 20% of the total vaporization time.

PAGE MIS-NUMBERING — FROM ORIGINAL

NO # PG. 179

The vaporization period was approached by considering that the total heat which reached the drop was the sum of the radiative and conductive energy. The resulting equation was:

$$\frac{dm}{dt} \Delta H_v + \frac{C \rho \pi D^3}{6}(1-f) \rho \frac{dT}{dt} = h_c \pi D^2(T_\infty - T_1) + h_r d^2(T_\infty - T_1)\alpha \qquad \text{(F-12)}$$

or rearranging,

$$t = \frac{\Delta H_v \rho D \Delta f + C_f D\rho(1-f)\Delta T}{6(h_c + h_r \alpha)(T_\infty - T)} \qquad \text{(F-13)}$$

This equation accounted for the fact that the boiling point of the oils was not constant. Here Δf represented the fraction of oil vaporized during any one interval and $(1-f)$ represented the average amount of liquid which remained in liquid form during the interval. In this manner, the vaporization period was broken up into five or six time periods. The term hc + hr was evaluated at an average temperature equal to $\frac{T_\infty + \text{Average } T \text{ over the Interval}}{2}$. Values of Δf and $(1-f)$ were obtained from the boiling point data given in Appendix A.

α, the overall absorptivity of the drop was calculated from the following equation:

$$\alpha = \frac{a}{2k'R^2}\left[(2k'^2R^2-1) + (2k'R+1)^{-2k'R}\right] \qquad \text{(F-14)}$$

This relationship assumes no refraction and no external reflection. Simpson found these assumptions to be adequate for low values of C.

Since, according to Gerald's work, the diameter of the drop remained constant for 90% of the vaporization time. Equation (F-13) was solved on the computer for 90% vaporization using a constant diameter. For the last 10% of the vaporization, the program took into account the

variation in D. Figures F-1, F-3, F-3 give the total vaporization time

for the drops of Naphthalene, Aromatic Concentrate, and Cosden Tar as a

function of temperature and drop size.

NAPHTHALENE VAPORIZATION
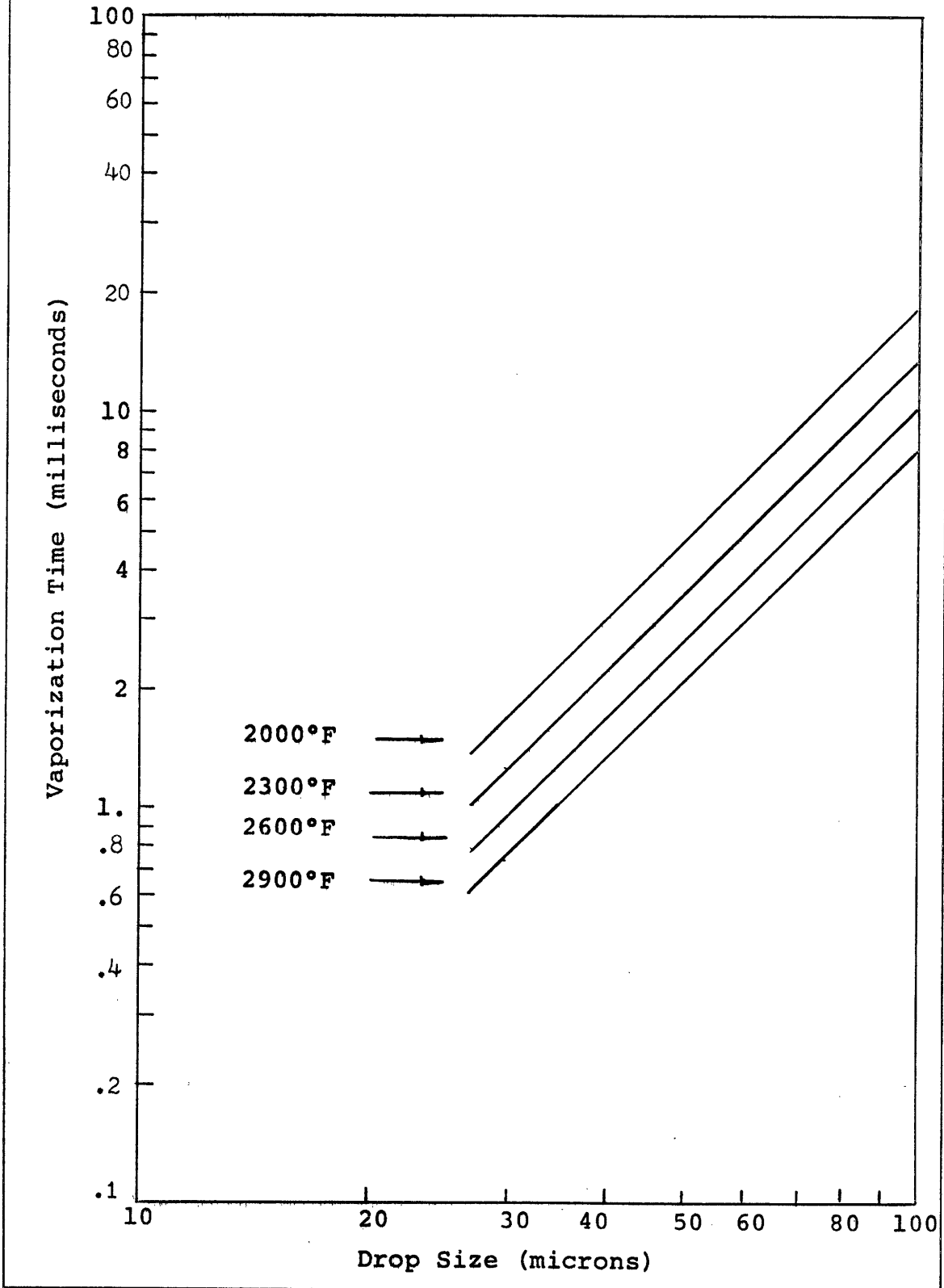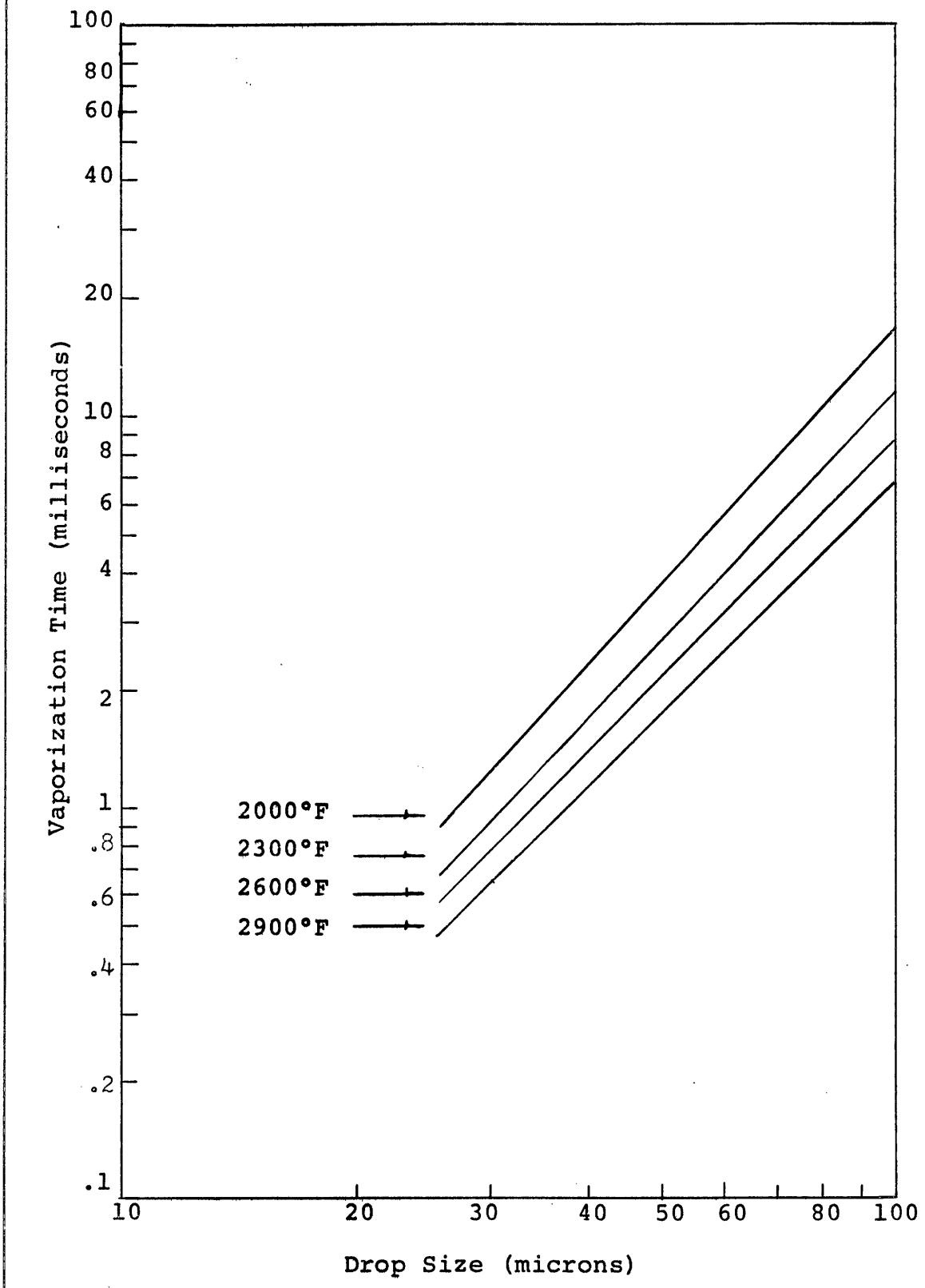
Figure F-1
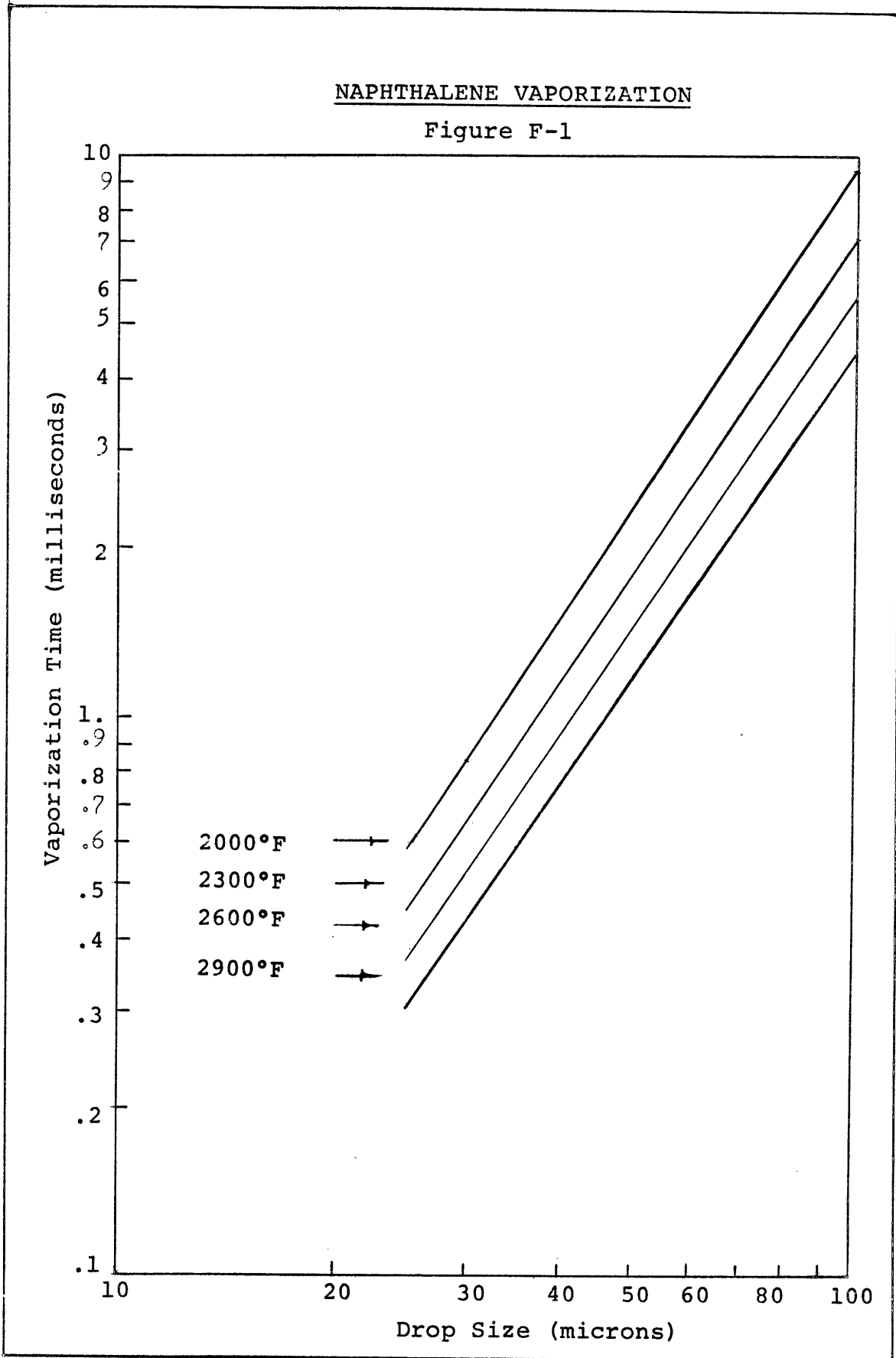
AROMATIC CONCENTRATE VAPORIZATION
Figure F-2

COSDEN TAR VAPORIZATION

Figure F-3

Vaporization Time (milliseconds) vs Drop Size (microns) for 2000°F, 2300°F, 2600°F, and 2900°F

APPENDIX G

Data Processing

The raw data from each run was punched onto cards and processed on the IBM-360 computer. The calculations performed by the machine were straight forward and, therefore, will not be described in detail.

Input information for the program:

1. Gas Analysis (dry basis)

2. Air and Nitrogen Flows

3. Natural Gas Flow

4. Oil Feed Rate (type of oil)

5. Average Reactor Temperature

6. Probe Position

The computer carried out the following calculations:

1. Using N_2 flow as a basis, it computed flow rates of the other gases.

2. Made an O_2 balance.

3. Made an H_2 balance

4. Calculated Water Content of of exit gases from the O_2 and H_2 balance.

(5.) Computed concentrations of CO, CO_2, CH_4, O_2, N_2, C_2H_2, H_2, H_2O.

(6.) Calculated gas velocity.

(7.) Calculated Reynolds Number.

(8.) Calculated Residence Time.

9. Made a carbon balance.

(10.) Calculated the theoretical yield of carbon black.

(11.) Computed the equilibrium temperature for the water gas shift reaction.

The information in brackets was printed out and used in the evaluation of the experimental results.

APPENDIX H

Equipment Details

The flow system was described in the body of the thesis. This section contains more details on the various items which might be of interest to an experimenter working on a similar problem. This description will start at the top of the apparatus and work down to the vacuum pump.

H.1 Oil Feed System. The details of the nitrogen flow measurement system were covered in Section 3.11. Nitrogen from this system flowed to the oil tank shown in Figure H-1. This insulated tank was maintained at the desired temperature (approximately 230°F) by a Chromalox 2.5 kw immersion heater that screwed into the two inch pipe coupling on the top of the tank. The temperature of the oil was measured by two chromel-alumel thermocouples inserted into the thermowells on the side of the tank. The oil was pushed from the tank, through the 1/2 inch coupling, the valve, and then a small screen filter (from an oil burner), the 3/8 inch heated copper line and then a nozzle, before impinging on the center of the spinning disk. The nozzle had a 0.0013 inch diameter hole for the Cosden Tar and an 0.0021 inch diameter hole for Naphthalene and Aromatic Concentrate.

H.2 Atomizer. The heart of the atomizer was the Precise Super 30 Grinder Motor. The speed of the motor was controlled by a variac on the primary of the motor. A Sola voltage regulator was used to maintain constant line voltage. A volt meter and amp meter were used to provide operating information on the motor. In the grinder chuck was placed the shaft of the aluminum disk that was shown in Figure 3.4. The motor and disk were then mounted in the atomizer housing as shown in cross-section on Figure H-2. The large sides of the housing were 17 inches in diameter by 1/4 inch thick aluminum plates. These plates were positioned
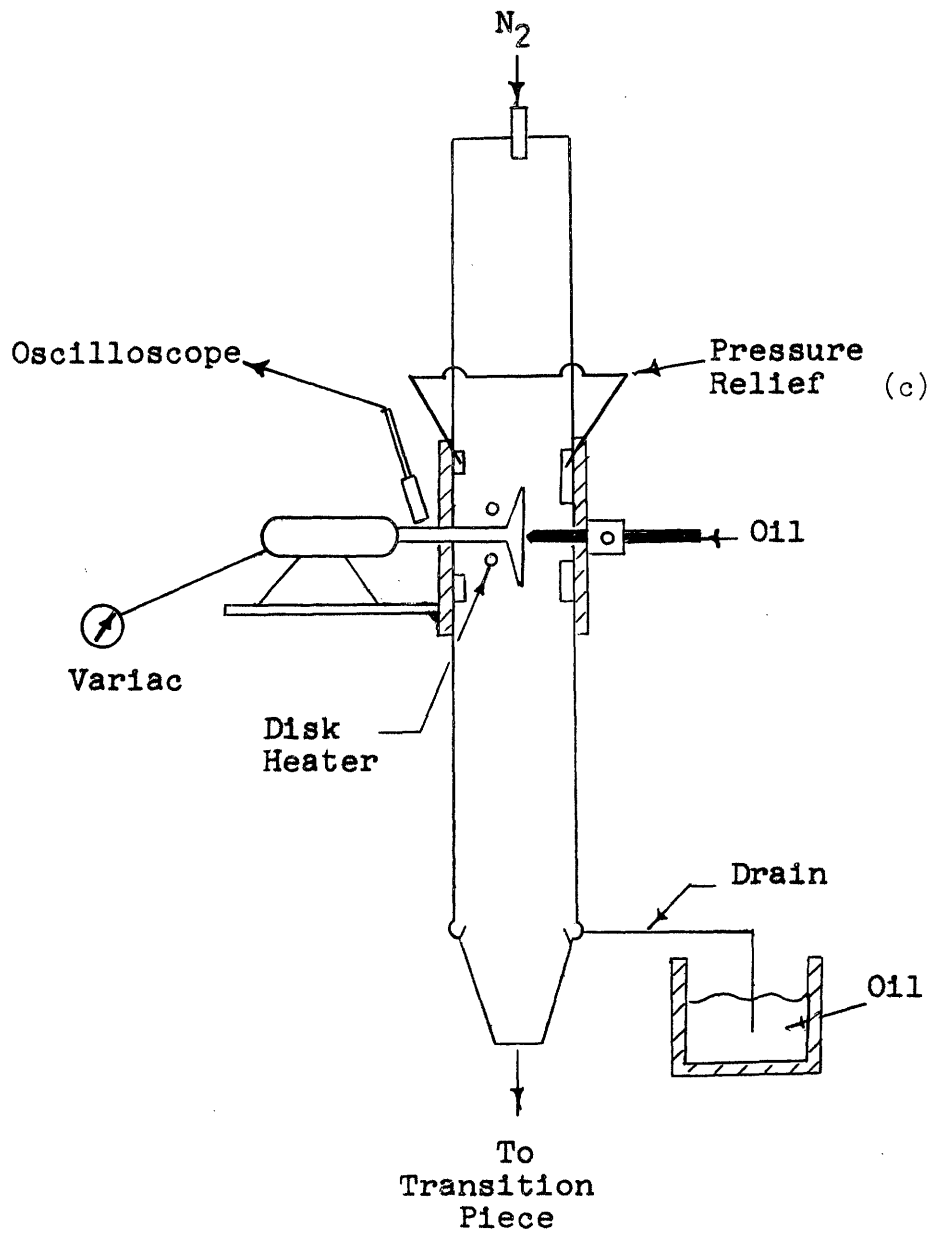
OIL TANK

Figure H-1

Heater

Oil

N₂

Screen

To Disk

Filter

Drain
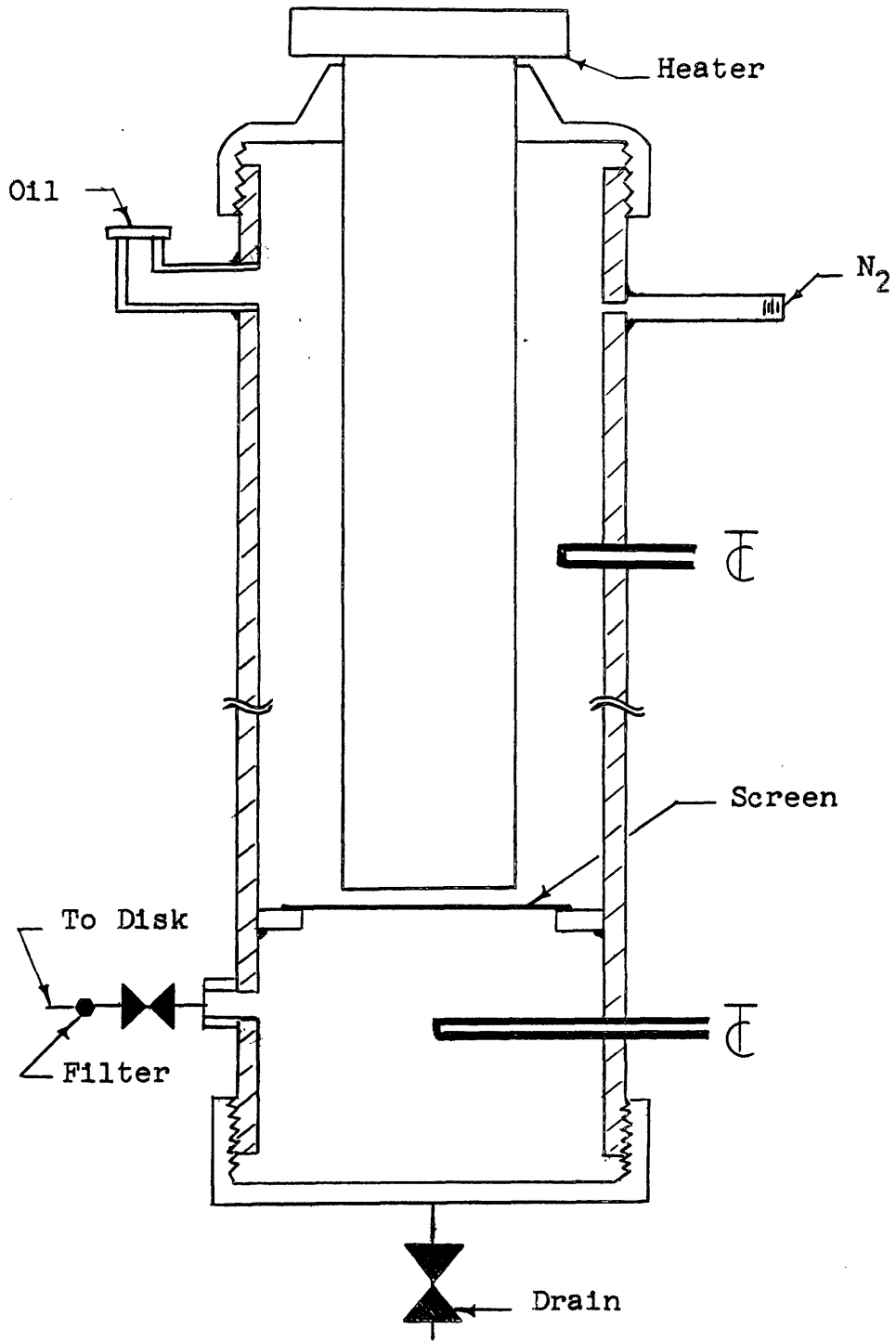
Atomizer Housing

Figure H-2

by means of a 1/8 inch by 3-1/2 inch wide brass spacer. Steel supports, positioned the motor and oil feed nozzle on the sides of the housing. A 300 watt radiant heater was positioned 1/2 inch behind the disk to maintain disk temperature at 230°F. Porous metal rings were located on both sides of the disk. These rings were interconnected on the outside of the housing and helped to damp out the pumping action of the disk. Oil that hit the walls of the housing was collected by the lips at the bottom of the housing. This liquid then flowed outside the housing and through a liquid seal to a collection vessel. The liquid seal prevented gas loss from the housing. This figure also shows the approximate position of the photo-cell that was used to determine disk speed (Appendix I).

H.3 Burner System. The burner system is shown schematically in Figure H-3. Air from the building supply and natural gas from a 200 cubic foot cylinder flowed through rotometers and 400 watt preheat furnaces before mixing outside of the burner. Temperatures in the furnaces were controlled by temperature controllers. The temperature of the gases before and after mixing was measured using chromel-alumel therocouples.

The burner itself was of the can type, which provided good stabilization with very little axial recirculation. The burner was shown schematically in Figure 3-6. Air and fuel first enter the burner through a 1/4 inch diameter pipe and pass into a two inch by 0.025 inch channel. They then pass through four 1/8 inch holes into a two inch by 0.020 inch distribution channel. Finally, the gases jet into the burner through twenty-eight 0.025 inch diameter holes which caused rapid mixing and stabilized the flame.

H.4 Reactor System. The reactor system was composed of the transition piece, the furnace itself, and the furnace controls. The transition

BURNER SYSTEM

Figure H-3
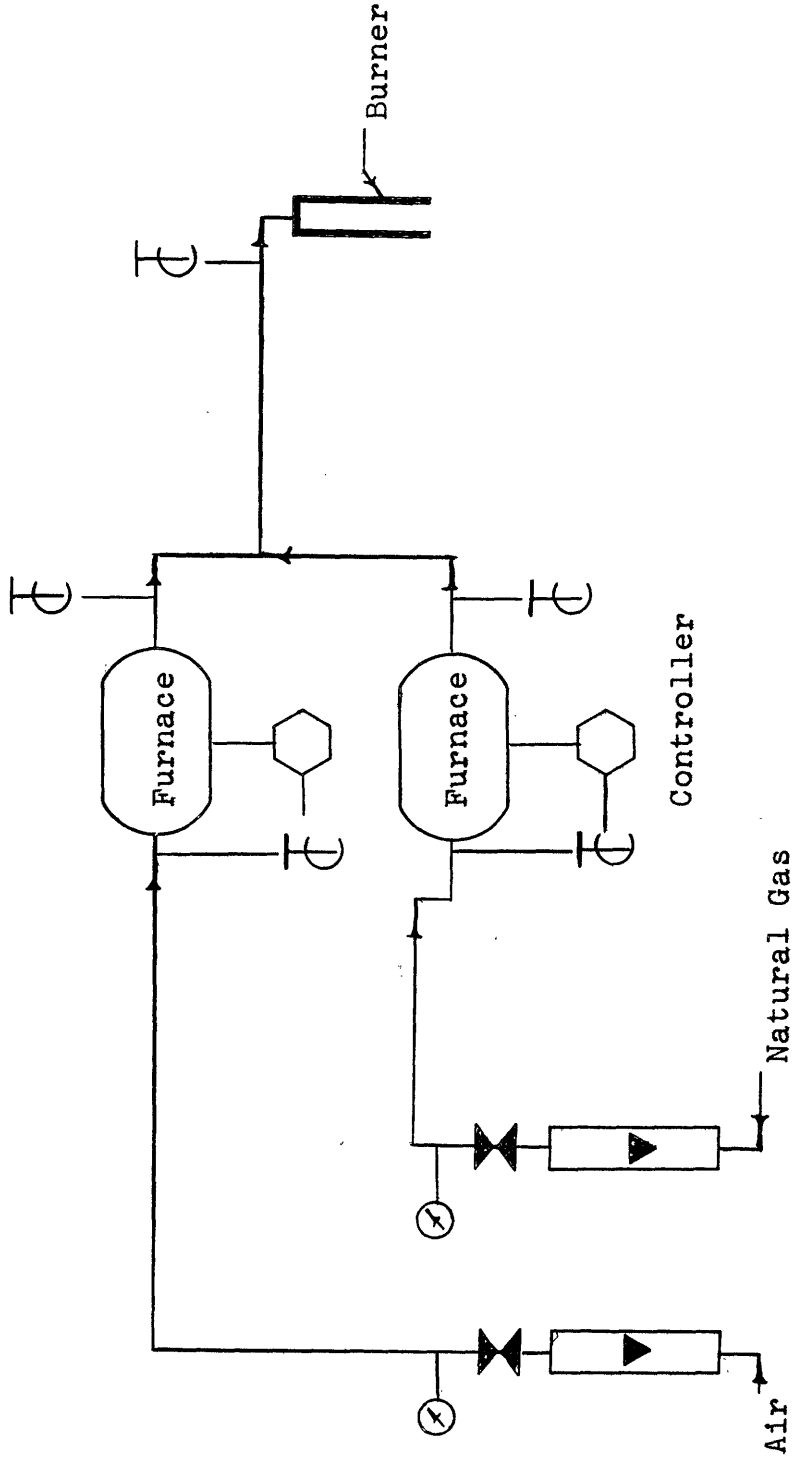
piece was shown in Figure 3.7. This piece was cast from A. P. Green

high density castable aluminum oxide. As shown in this figure, the burner,

atomizer, and reactor are sealed into the transition piece. In addition,

the transition piece provided for distribution of the burnt gas around the

outside of the drops. The gas jetted into the reactor through sixteen

0.040 inch diameter holes, which were inclined 45 degrees to the horizontal.

The silicon carbide reactor tube was 36 inches long with a one inch

inside diameter and had a 1/4 inch thick wall. Aluminum oxide was

originally used, but the thermal shocks from the probe caused it to

crack. As shown in Figure 3.1, the reactor tube connected to the

transition piece at the top, the quench probe at the bottom, and was

contained in an insulated furnace. This figure also shows the approximate

location of the 32 hot rods (7/16 inches in diameter x 24 inches long with

a 5 inch hot zone) and 5 thermocouples (Pt-Pt 13% Rh). All of the hot rods

are not shown on the figure. They were spaced as much as possible to

compensate for high heat losses at the top and bottom of the furnace.

The thermocouples were located at distances of two 3/4 inches, six

7/8 inches, thirteen 7/8 inches, twenty-one 1/4 inches and twenty-three

7/8 inches from the top of the reactor. The 4 inch wide by 5-1/2 inch

long furnace zone was surrounded by 9 inches of zirconia brick insulation

($k = 4$ B.T.U./ft^2 - Hr - °F - in) and 2 inches of block insulation

($k = 0.63$ B.T.U./ft^2 - Hr - °F - in). In addition, one half of the

furnace was on rollers to permit access to the reactor tube and thermowells.

Figure 3.11 shows the controls used to provide a flat temperature

profile in the reactor. The top zone was composed of four elements

connected in series and connected to the 110 volt AC line. A variac

was used to control the current between 4 and 14 amperes. Zones 1

through 3 were each composed of 4 elements connected in series with a variable resistor of approximately 18 ohms. The three zones were then connected in parallel and controlled by an induction reactor fed from 220 volt AC line. Total current flow varied from 15-45 amperes for the bank of 3 zones. A similar arrangement was used for zones 4, 5 and 6. Zone B consisted of four elements, in series, and controlled by a power-statt on the 220 volt AC line. Currents on all lines were measured using an Amprobe tong meter.

H.5 <u>Product Collection System</u>. This system shown schematically in Figure H-4 included the quench probe, the crossover line, the sample bottle, the agglomerator coil and the filter. Normal flow was through the probe, the main crossover line, the coil and then the filter. For sampling, valve A was closed and the entire flow passed through valves B and C.

A cross-section of the quench probe was shown on Figure 3-9. This unit consisted of four concentric stainless steel tubes. The outer two tubes carried a mixture of water and steam for cooling the probe. Steam flowed through the third tube and then jetted into the reaction mixture through twenty-eight 0.025 inch diameter holes. The quenched reaction mixture then flowed down the probe and through the crossover. The probe was sealed to the bottom of the reactor with a packing gland which contained asbestos packing.

The agglomerator coil consisted of an eleven foot long coil of 3/8 inch diameter copper tubing. This insulated coil provided a residence time of approximately 0.2 seconds. This time allowed the carbon black to agglomerate before it contacted the filter.

After the coil, the carbon black laden stream flowed to the filter shown in Figure H-5. This unit consisted of a two inch diameter by

PRODUCT COLLECTION SYSTEM

Figure H-4

FILTER ASSEMBLY

Figure H-5

To Vent

S. Steel
Filter

From
Cross-Over
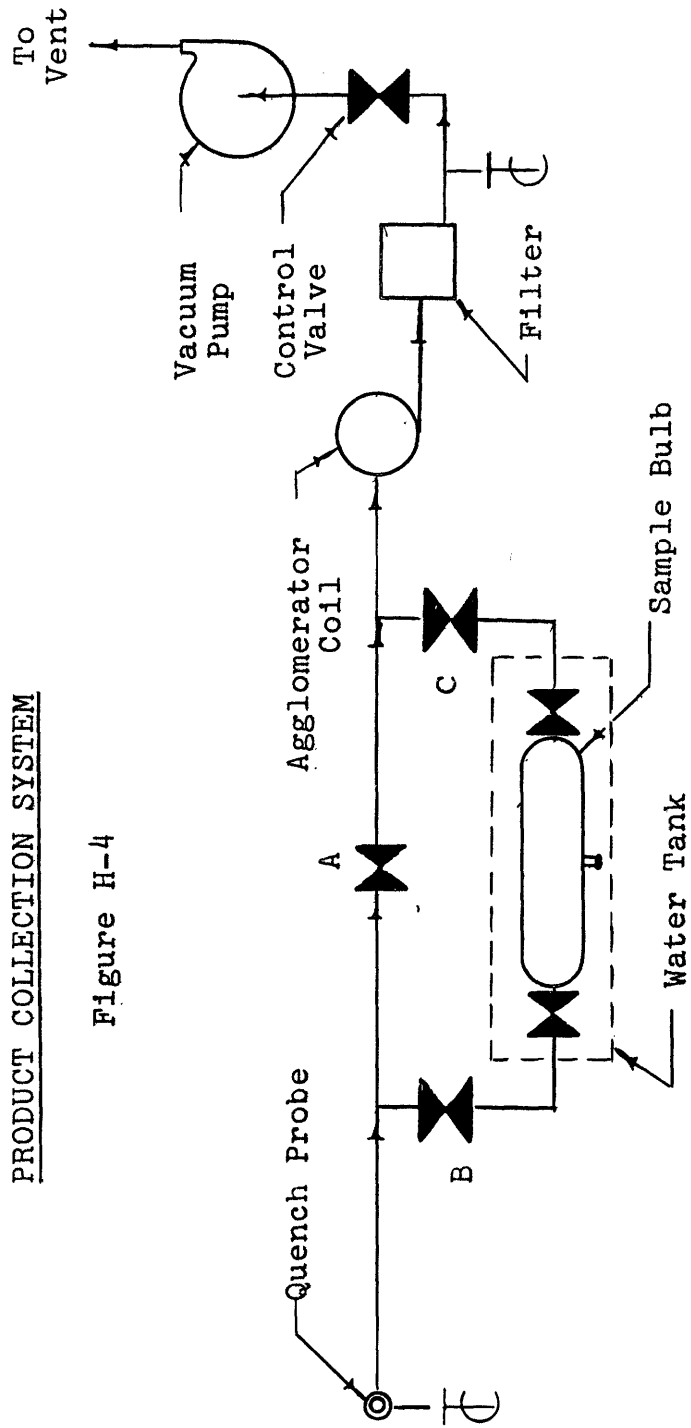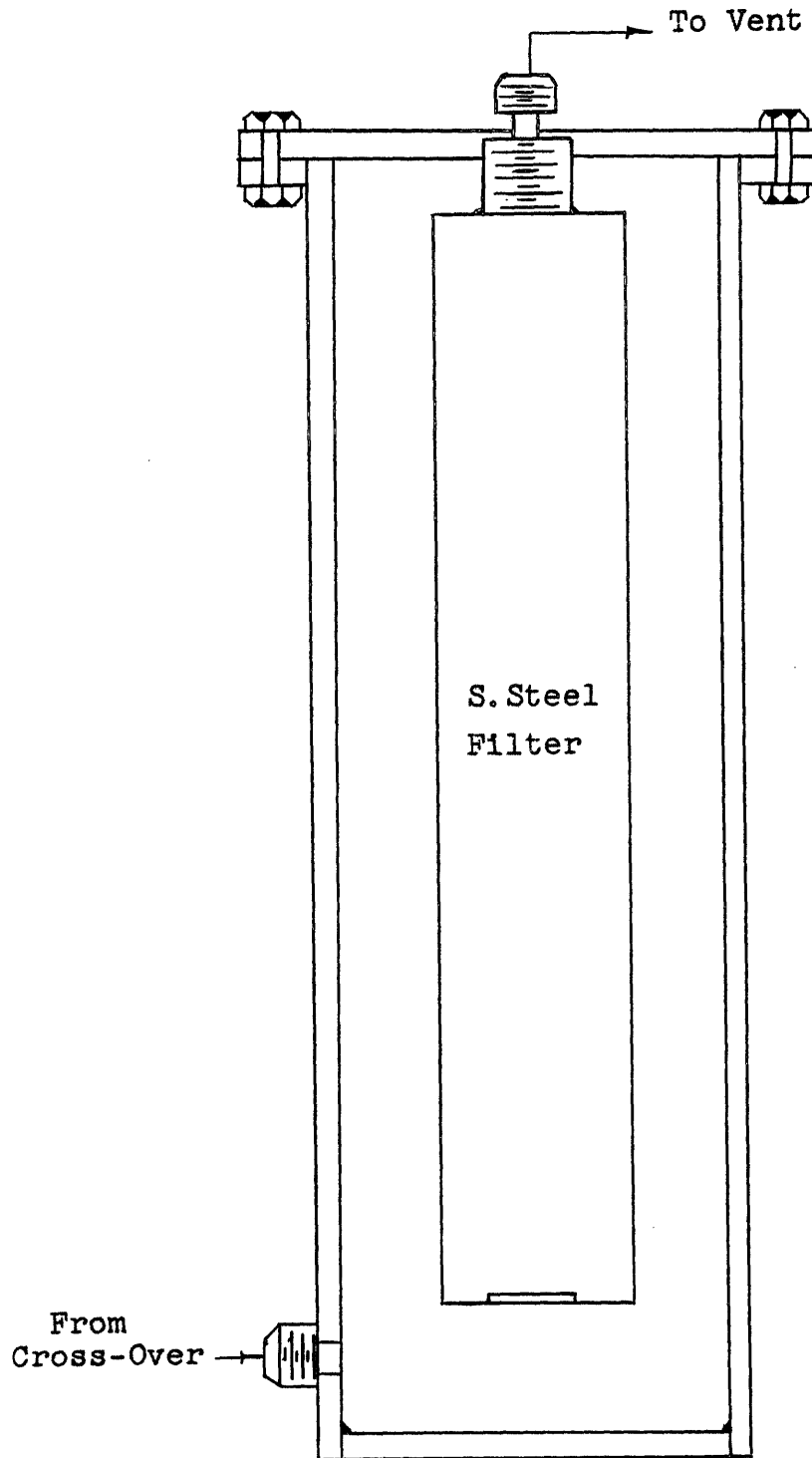
FILTER ASSEMBLY

Figure H-5
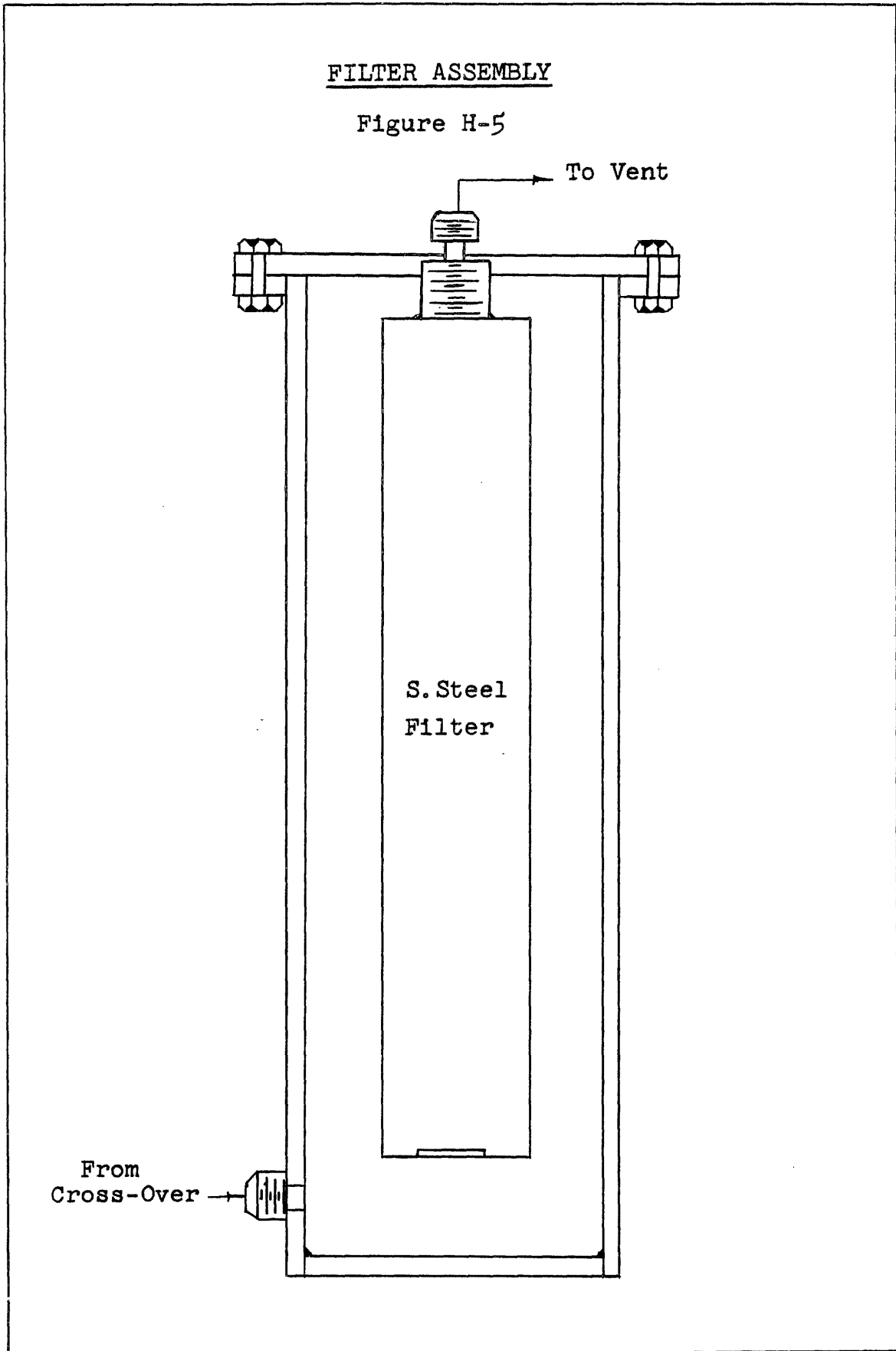
twelve inch long sintered stainless steel filter which was contained in a four inch diameter steel pipe. The pipe was wrapped with a 340 watt heating tape and insulated with asbestos tape. This combination maintained filter temperature at approximately 300°F. Filters with 5 and 40 micron pore diameters were used, but the 40 micron filter gave better overall performance. Flow through the reactor and quench system was maintained by a Stokes Rotary Vacuum Pump attached to the exit of the filter.

APPENDIX I

Disk Speed

Since disk speed was one of the most important variables in
determining drop size, it was necessary to accurately moniter the speed
of the disk. Initially, speed determinations were made by using the
calibrated sweep on the oscilloscope and then measuring the distance
between the peaks. Figure I-1 shows how the distance between peaks
varied with disk speed. This technique proved to be very time consuming.
An audio-oscillator (Hewlett Packard Model 200C) was then added to
improve the system. Then when the frequency of the oscillator was
matched to the frequency of the voltage pulses from the phototube,
a stationary Lissajous-figure was displayed on the screen. In this case,
the Lissajous-figure was a straight line. Thus, if the oscillator
frequency was known, one could obtain directly the disk speed. In
addition, any variation of disk speed could easily be seen on the scope.

The final scheme for disk speed measurement is shown in Figure I-2.
The key component in this system was the General Radio Model 1536-A
Photoelectric pick-off. This pick-off directed a beam of light to the
disk shaft. The shaft was completely black except for a small strip of
silver. The light was reflected from the strip, back to the phototube
in the pick-off, which in turn sent a voltage pulse through the flash
delay to the Tetronix 502 Dual Beam Oscilloscope. This pulse rate
was then matched to the signal from the oscillator. Figure I-3 shows
how the speed of a 3 inch diameter disk varied as a function of the
voltage applied to the disk motor.

DETERMINATION of SPEED

Figure I-1
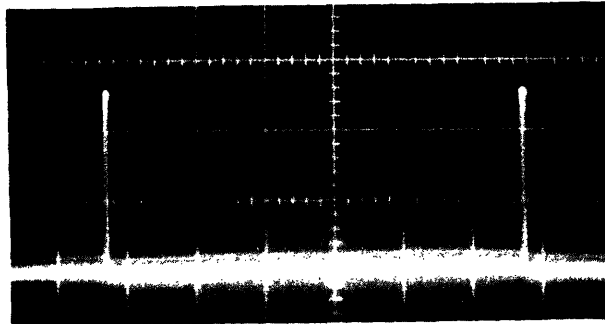
17,000 RPM
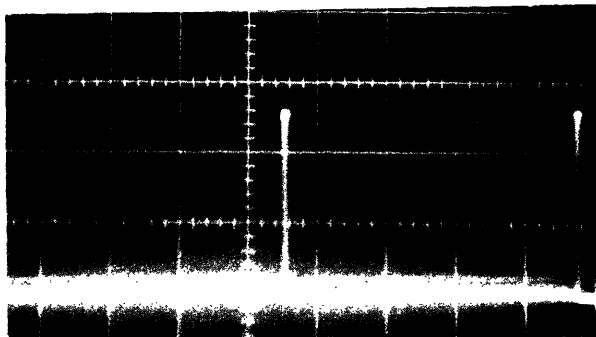
24,000 RPM

29,000 RPM

DISK SPEED DETERMINATION SYSTEM

Figure I-2

DISK SPEED
Figure I - 3

APPENDIX J

Disk Housing Evolution

The disk housing was one of the most critical pieces of equipment.
It had to convey approximately 5 cc per minute of atomized oil to the
top of the furnace. Because of the complexity of this unit, a considerable
amount of effort was expended before the final design was reached. This
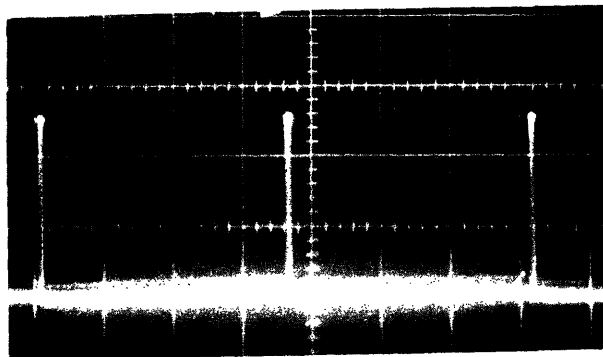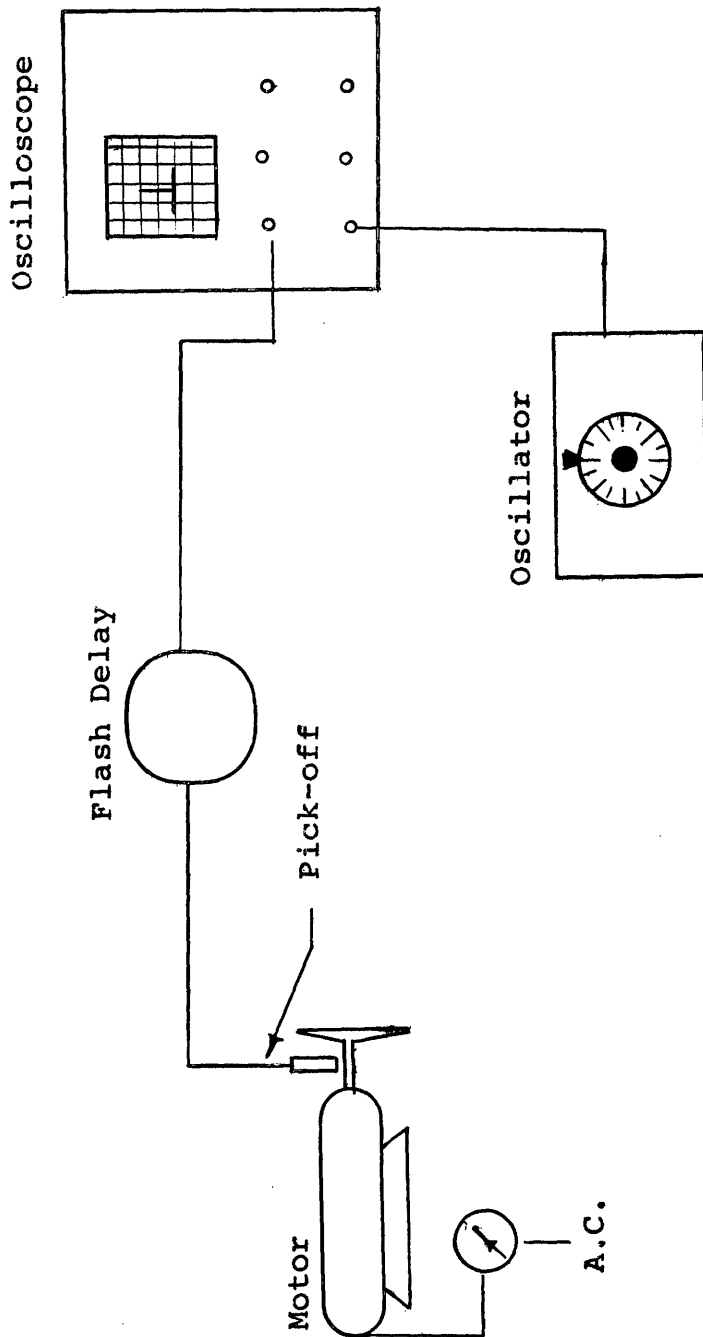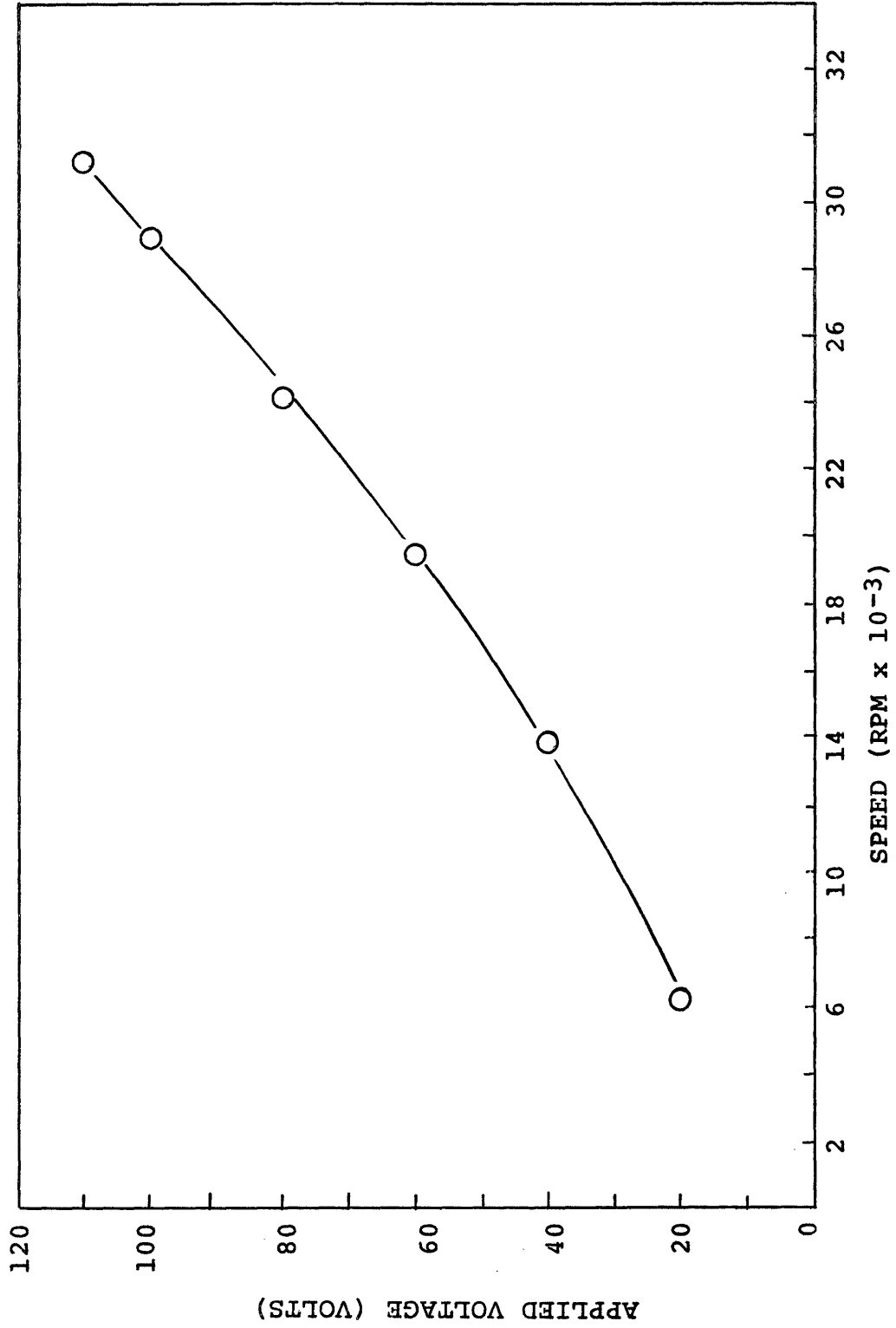unit is by no means optimum, but it will deliver the desired volume of
drops. Figure J-1 depicts the evolution of the atomizer housing.
Figure J-1a was the design used initially for calibration of the disk.
This unit permitted just a small stream of drops to leave the housing.
After calibration, the involute shown in J-1b was constructed. It was
felt that the circular motion of the disk combined with the flow of the
sweep nitrogen would carry a substantial portion of the drops from the
housing. This was not the case. Several different positions of the sweep
gas inlet were investigated along with a wide range of nitrogen flows.
Over this range, drop production was essentially constant and amounted
to approximately 1% of the oil fed to the disk.

In order to make more effective use of gravity, the housing shown
in Figure J-1c was constructed. This unit was an improvement over its
prececessor, but production was still only a few percent of the atomized
drops. Close examination of the droplet stream showed that all sizes
of drops were rapidly moving to the vicinity of the housing wall. This
indicated that the gas mass in the housing was rapidly rotating and
therefore not slowing down the oil drops. Hence, a baffel was inserted,
as shown in Figure J-1d.

The baffel stopped gas rotation and increased production up to
1/4 to 1/3 of the atomized oil. The operation of this housing is still
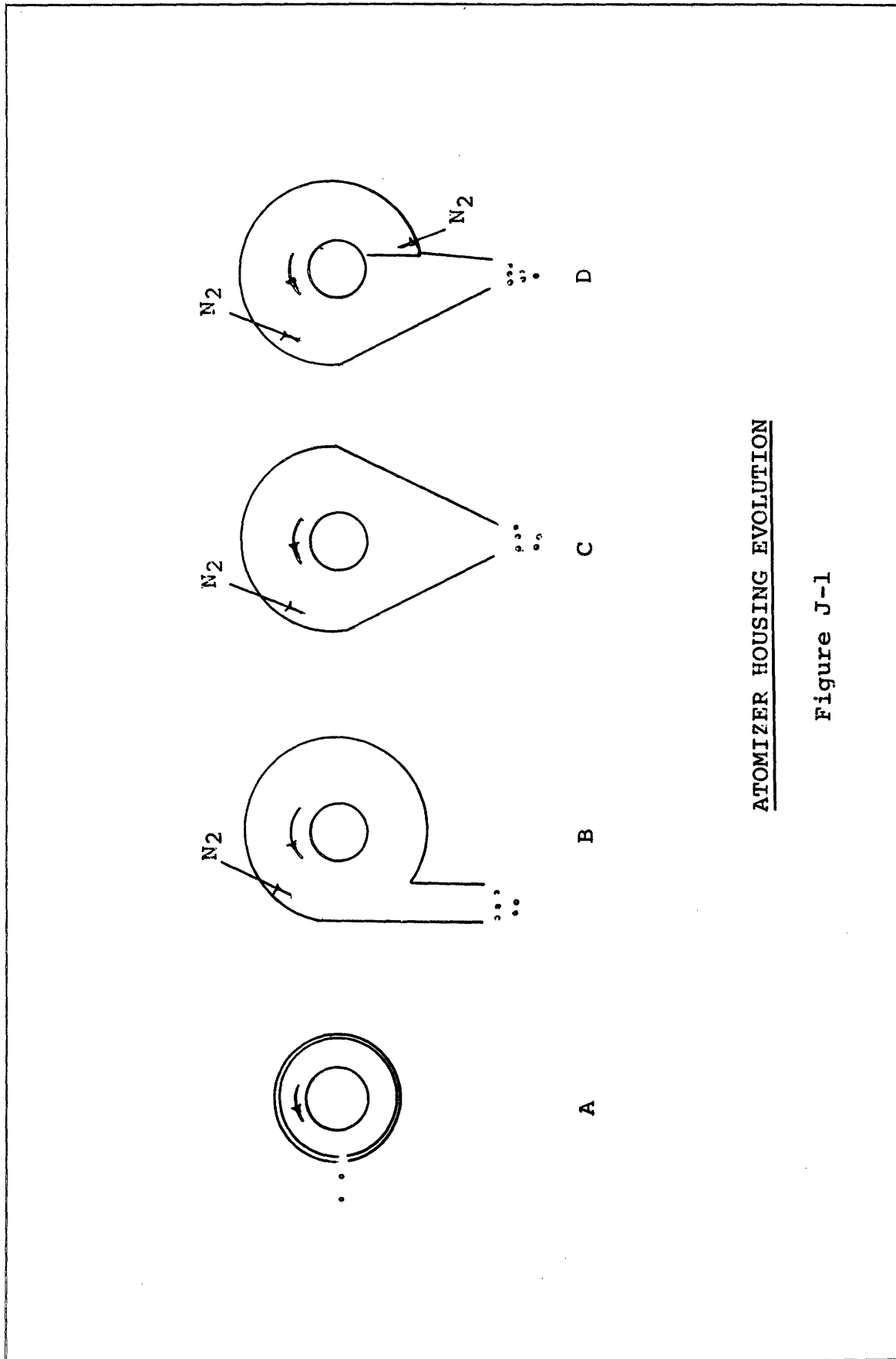
ATOMIZER HOUSING EVOLUTION

Figure J-1

very complicated. The primary sweep gas enters as shown on Figure H-2, the picture of the atomizer. This nozzle must be positioned very accurately since a small movement causes a large decrease in droplet production. It is also necessary to maintain constant pressure around the disk through line C. A bleed flow enters at B, to prevent the establishment of a low pressure area behind the baffel. Even with these flows, drop production depends on disk feed rate and goes through a sharp maximum at approximately 22 cc/min. of oil flowing to the disk. Therefore, production rates are limited to around 6 cc/min.

The lips shown in Figure H-2 were added to prevent oil from dripping into the furnace. Oil striking the baffel or wall runs into the lips and then flows to a chilled container where it is collected. A liquid seal is maintained at this point to prevent gas loss. The oil in this vessel, subtracted from the amount fed to the disk, gave the total amount of oil fed to the reactor. A photograph of the final design of the atomizer is shown on Figure J-2.

FINAL DISK HOUSING

Figure J-2

Pressure Relief

Motor

Feed Nozzle

Heater

Overflow Lips

Sweep Gas

Disk Heater

Disk

Pressure Tap

Oil Drains
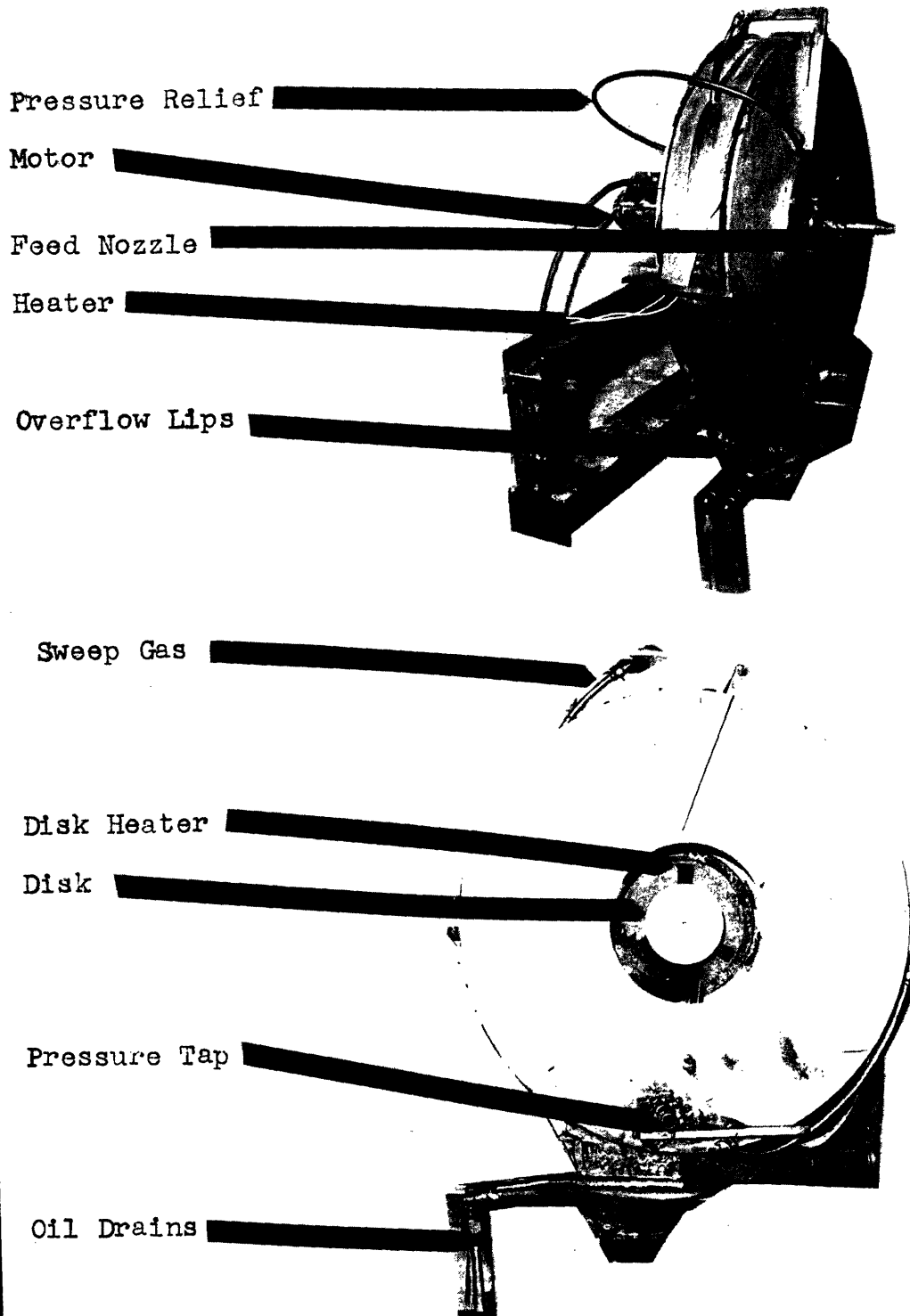
APPENDIX K

Sample Calculations

1. Calculation of Particle Diameter

This calculation is included to illustrate the difficulty of obtaining a precise value for the diameter.

$$D = \frac{\text{Measured Diameter}}{\text{Magnification}} \quad \text{conversion factor}$$

In all cases the magnification was 50,000.

For Run IV-1-1 measured diameter range: 0.22-0.27 cm.

Average diameter was determined by measuring as many particles as possible: 0.25 cm.

$$D = \frac{0.25}{.5 \times 10^5} \times 10^8$$

$$D = 500 \pm 40 \ \overset{o}{A}$$

In many cases, such as Run IV-9-1 where the range of diameters was 220 to 1000 angstroms, the value for average diameter will be less precise.

2. Calculation of the Number of Particles Ns

$$Ns = \frac{(\text{Weight of carbon per gram of oil fed})(\text{oil feed rate})}{(\text{gas flow rate})(\text{weight of single particle})}$$

For Run IV-1-1

Weight of carbon $= 0.672 \ \dfrac{\text{gram}}{\text{gram of 0.1}}$

Oil feed rate $= \dfrac{5}{60} = 0.083 \ \dfrac{\text{grams}}{\text{sec}}$

Gas flow rate $= 7.06 \times 10^2$ cc/sec

Weight of a particle $= 1/6 \ D^3$

$$= 1/6 \ 3.14 \ (5 \times 15^6)^3 \ 1.37$$

$$= 1.2 \times 10^{-16} \pm 0.1 \times 10^{-16} \ \text{grams}$$

$$Ns = \frac{(6.72 \times 10^{-1})(8.3 \times 10^{-2})}{(7.06 \times 10^{2})(1.2 \times 10^{-16})}$$

$$Ns = 6.58 \times 10^{15} \pm .7 \frac{particles}{cc}$$

3. Calculation of Chain Length

Chain length was determined by measuring the length of the backbone, including side chains, of all discrete particles on an electron micrograph (50,000x). This number was then divided by the number of particles and the length converted to angstroms. From Run IV-1-1

$$\text{Chain length} = \frac{Length}{(Number\ of\ Particles)} \frac{(Conversion\ Factor)}{(Magnification)}$$

$$\text{Chain length} = \frac{(25.4)}{(19)} \frac{(10^{8})}{(50,000)}$$

$$\text{Chain length} = 2670 \overset{\circ}{A}$$

4. Calculation of Activation Energy

$$\frac{dc}{dt} = const(Ns)^{1/3}(c)^{2/3} \frac{X}{T^{0.5}} e^{-\frac{E}{RT}}$$

For 100 micron drops of Cosden Tar:

a. Data available at 2600 and 2900°F.

b. Ns calculated as shown in Appendix K-2.

c. $\frac{dc}{dt}$ was obtained from a plot of concentration against time at each temperature.

$$\frac{dc}{dt} = 18.6 \times 10^{-4} \frac{grams}{cc\text{-}sec} \qquad 2900°F$$

$$\frac{dc}{dt} = 3.39 \times 10^{-4} \frac{grams}{cc\text{-}sec} \qquad 2600°F$$

d. X is mole fraction fuel.

$$\frac{X}{T^{0.5}} = 2.31 \times 10^{-4} \qquad 2900°F$$

$$\frac{X}{T^{0.5}} = 2.42 \times 10^{-4} \qquad 2600°F$$

e. Plotted.

$$\frac{dc}{dt} \quad \frac{T^{0.5}}{X} \quad \frac{1}{Ns^{1/3} C^{2/3}} \quad vs \quad \frac{1}{T}$$

f. Slope of the above line.

$$M = \frac{-E}{R}$$

$$E = MR$$

$$= 25.3 \times 1.98$$

$$E = 50.1 \text{ Kcal per mole}$$

5. Calculation of the Apparent Activation Energy for Surface Growth for Naphthalene

Growth rate of the particles was plotted against 1/T. The growth rate was determined by the change in diameter (electron micrographs) as a function of time.

The slope of the above line:

$$M = \frac{E}{R}$$

$$E = (1.98)3.4$$

$$E = 6.8 \text{ Kcal per mole}$$

APPENDIX L

Location of Original Data

The experimental data from this program are contained in two notebooks and on sections of recorder paper. The only analytical data not totally included in this thesis are the electron micrographs. All of the above are in the possession of the author.

APPENDIX M

Nomenclature

A   Conduction group

a   Correction constant for grey body absorbtivity

B   Radiation Group

C   Carbon black concentration

C_1 Absorptivity Group

c_ℓ Heat capacity of liquid drops

D   Disk diameter

D_1 Diffusion constant

d   Drop or particle diameter

E   Activation energy

E_n Activation energy for nucleation

E_g Activation energy for gas phase reaction

E_s Activation energy for surface growth

f   Allowable stress

f   Kinetic constant for chain branching (Equation 5-2)

G*   Excess Free Energy of Critical Nucleus

g   Gravitational constant

g   Kinetic constant for chain termination (Equation 5-2)

g_o Geometrical factor for radical destruction (Equation 5-2)

ΔH Heat of vaporization

h_c Heat transfer coefficient for conduction

h_r Heat transfer coefficient for radiation

K   Correction constant for gray body absorptivity

k   Boltzmans constant

kg   Thermal conductivity of vaporized oil

k_ℓ Thermal conductivity of liquid oil

L Latent heat of vaporization

m Mass

M Complex refractive index

N Concentration of fuel

Ns Number of carbon particles per unit volume

n Number of particles or nuclei

n_o Number of active centers

n Refractive index

n' Absorption

R Gas constant

R Radius (Equation 5-11)

R_1 Original drop radius

r Disk radius

r* Critical radius

T Absolute temperature

T_1 Original oil temperature

T_e Equilibrium temperature

T_∞ Gas temperature

T_∞^* Corrected gas temperature

t Time

X Mole fraction

Greek

α Effectiveness Factor (Equation 5-11)

α Absorptivity

γ Absorption Coefficient

θ Dimensionless temperature

λ Wave length

ν_o Original number of particles

ρ Density

ρ_ℓ Liquid density

σ Surface tension

γ Time

ω Angular velocity

APPENDIX N

Literature Citations

(1)   Tesner, P. A. and V. F. Surovinin, "Formation of Carbon Black by the Decomposition of Hydrocarbons in a High Temperature Stream of Products of Complete Combustion", Gaz. Prom. 10:5, pp 44-50 (1965).

(2)   Homann, K. H. and H. G. Wagner, "Some New Aspects of the Mechanism of Carbon Formation in Premixed Flames", Eleventh (International) Symposium on Combustion, The Combustion Institute, Pittsburgh, Pennsylvania, pp 371-380 (1967).

(3)   Narasimhan, K. S. and P. J. Foster, "The Rate of Growth of Soot in Turbulent Flow with Combustion Products and Methane", Tenth Symposium (International) on Combustion, The Combustion Institute, Pittsburgh, Pennsylvania, p 253 (1965).

(4)   Op. Cit., Homann, K. H.

(5)   Op. Cit., Tesner, P. A.

(6)   Walker, D., "Black Magic", Rubber World, 151:92-95 (1964).

(7)   Heckman, F. A., "Microstructure of Carbon Black", Rubber Chemistry and Technology, Vol. XXXVII, No. 5, pp 1245-1298 (December 1964).

(8)   Palmer, H. B. and C. F. Cullis, "Formation of Carbon from Gases", Chemistry and Physics of Carbon, (edited by P. L. Walker), Vol. I, Marcel Dekker, Inc., New York (1965).

(9)   Milliken, R. C., "Optical Properties of Soot", J. Optical Soc. Am., Vol. 51, No. 6, pp 698-699 (June 1961).

(10) Cabot Corporation, "Typical Properties of Cabot Carbon Black Pigments".

(11) Deckens, J. and A. van Tiggelen, "Ion Identification in Flames", Seventh Symposium (International) on Combustion, pp 254-255, Butterworths' Scientific Publications, Ltd., London (1959).

(12) Calcote, H. F., "Mechanisms for the Formation of Ions in Flames", Combustion and Flame, Vol. 1, No. 4, pp 385-403 (1957).

(13) Thring, M. W., "The Science of Flames and Furnaces", John Wiley & Sons, Inc., New York (1962).

(14) Lewis, B. and G. Von Elba, "Combustion, Flames, and Explosions of Gases", p 585, Academic Press, Inc., New York (1961).

(15) Green, J. A. and T. M. Sugden, "Some Observations on the Mechanism of Ionization in Flames Containing Hydrocarbons", Ninth Symposium (International) on Combustion, pp 607-621, Academic Press, New York (1963).

(16) Knewstubb, P. F. and T. M. Sugden, "Mass Spectrometry of the Ions Present in Hydrocarbon Flames", Seventh Symposium (International) on Combustion, pp 247-253, Butterworth's Scientific Publications, Ltd., London (1959).

(17) Kinbara, Tosiro and Junji Nakamura, "On the Ions in Diffusion Flames", Fifth Symposium (International) on Combustion, pp 285-289, Rheinhold Publishing Corporation, New York (1955).

(18) DeJaegere, S., J. Deckens, and A. van Tiggelen, "Identity of Most Abundant Ions in Some Flames", Tenth Symposium (International) on Combustion, pp 155-160, Williams and Wilkins Co., Baltimore (1962).

(19) Kinbara, T. and H. Ikegami, "On the positive and Negative Ions in Diffusion Flames", Combustion and Flame, Vol. 1, pp 199-211 (1957).

(20) Feugier, A. and A. Tiggelen, "Identification of Negative Flame Ions", Tenth Symposium (International) on Combustion, The Combustion Institute, Pittsburgh, Pa., pp 621-624 (1965).

(21) Palmer, H. B. and C. F. Cullis, "Formation of Carbon from Gases", Chemistry and Physics of Carbon, Vol. 1, pp 265-320, Marcel Dekker, Inc., New York (1965).

(22) Foster, P. J., "Carbon in Flames", J. Inst. of Fuel, 38, p 297 (1965).

(23) Parker, W. G. and H. G. Wolfhard, J. Chem. Soc., p 2038 (1950).

(24) Street, J. C. and A. Thomas, Fuel, 34, p 4 (1955).

(25) Calcote, H. F., "Electrical Properties of Flames Transverse Fields", Third Symposium (International) on Combustion, pp 245-253, Williams & Wilkins Company, Baltimore (1949).

(26) Calcote, H. F. and R. W. Pease, "Electrical Properties of Flames - Longitudinal Fields", I.&E.C., Vol. 43, No. 12, pp 2727-2731 (December 1951).

(27) Payne, K. G. and F. J. Weinberg, "A Preliminary Investigation of Field-Induced Ion Movement in Flame Gases and Its Applications", Proc. Royal Soc. London, A, 250, pp 316-336 (1959).

(28) Place, E. R. and F. J. Weinberg, "The Nucleation of Flame Carbon by Ions and the Effect of Electric Fields", Eleventh Symposium (International) on Combustion, the Combustion Institute, Pittsburgh, Pa., pp 245-256 (1967).

(29) Witt, A. E., S. M. Thesis, Dept. of Chemical Engineering, M.I.T. (December 1965).

(30) Smith, E. C. W., Proc. Royal Soc. A, 174, pp 110 (1940).

(31) Gaydon, A. G. and H. G. Wolfhard, Flames, Second Edition, Chapman
      and Hall, Chapter 8 (1960).

(32) Porter, G., "Combustion Researches and Reviews", p 108, Butterworth's
      (1955).

(33) Tesner, P. A., Seventh Symposium on Combustion, Oxford, 1958, p 546
      (1959).

(34) Tesner, P. A., H. J. Robinovitch and I. S. Rafalkes, "The Formation
      of Dispersed Carbon in Hydrocarbon Diffusion Flames", Eighth Symposium
      (International) in Combustion, Williams & Wilkins Company, p 801-806
      (1962).

(35) Bonne, U., K. H. Homann and H. F. G. Wagner, "Carbon Formation in
      Premixed Flames", Tenth Symposium (International) on Combustion,
      The Combustion Institute, Pittsburgh, Pa., pp 503-542 (1965).

(36) Ibid., pp 503-542.

(37) Porter, G., "Carbon Formation in the Combustion Wave", Fourth Symposium
      (International) on Combustion, Williams and Wilkins Company, Baltimore,
      p 248 (1953).

(38) Op. Cit., Homann, K.H. and G. G. G. Wagner.

(39) Op. Cit., Narasimhan, K. S. and P. J. Foster.

(40) Surovikin, V. F. and E. Y. Pokorskii, "Effect of Hydrodynamic and
      Temperature Conditions of the Furnace Process on the Structure-
      Formation of Carbon", Kauchuk i Rezina, 9 (1963).

(41) Surovikin, V. F., "Kinetics of Carbon Black Formation in Turbulent
      Combustion of Liquid Hydrocarbons", Soviet Rubber Technology, 22,
      pp 35-39 (1963).

(42) Tesner, P. A., T. D. Snegyreua, and V. F. Soorovikin, "Kinetics of
      Dispersed Carbon Formation", Preprint for Eleventh Symposium
      (International) on Combustion.

(43) Op. Cit., Tenser, P. A. and V. F. Surovikin.

(44) Bass, Yu. P., "Investigation of the Process of Formation of Carbon
      Black from Incomplete Combustion of Single Drops with the Assistance
      of High Speed Photography", Gaz. Prom., No. i (1963).

(45) Gallie, J. F., "Carbon Black", Petroleum Refiner, Vol. 23, No. 3,
      pp 97-108 (March 1944).

(46) Shreve, R. N., The Chemical Process Industries, pp 157-160,
      McGraw-Hill, New York (1956).

(47) Walker, D., "Black Magic", Rubber World, 151:92-95 (1964).

(48) Nelson, W. L., "Chemical Composition of Oils Used in Black
      Manufacture", Oil & Gas Journal, 53:145 (March 28, 1958).

(49) Strasser, D. M., "From Hydrocarbon to Oil Black", Petroleum Refiner,
      Vol. 33, No. 12, pp 177-182 (1954).

(50) Reinke, R. A., T. A. Ruble and W. H. Shearon, "Oil Black", I.&E.C.,
      Vol. 44, No. 4, pp 685-694 (April 1952).

(51) "Continental Carbon Process for Oil Black", Oil & Gas Journal,
      62:116 (September 7, 1964).

(52) Edminster, J. W., C. B. Beck, G. F. Friauf, U. S. Patent assigned
      to Cabot Corporation, No. 2,917,370 (December 15, 1959).

(53) Beck, C. B., Cabot Corporation, Personal Communication (May 1967).

(54) Heller, G. L., U. S. Patent No. 2,782,101, February 19, 1957.

(55) Heller, G. L., U. S. Patent No. 2,768,067, October 23, 1956.

(56) Chang, T. Y., "Combustion of Heavy Fuel Oil", Sc.D. Thesis,
      Chem. Eng. Dept. MIT (1941).

(57) Gerald, C. F., "The Mechanism of Cumbustion of a Heavy Fuel Oil",
      Sc.D. Thesis, Ch. Eng. Dept. MIT (1940).

(58) Hedley, A. B., Nuruzzaman, A.S.M., "A Technique for Studying
      Small Freely Suspended Oil Droplet Flames", J. Inst. Fuel, 39(305),
      pp 248-253 (1966).

(59) Hinze, J. O. and H. Milborn, "Atomization of Liquids by Means of
      a Rotating Cup", J. Applied Mech., 17, p 145 (1950).

(60) Walton, W. H. and W. C. Prewitt, "The Production of Sprays and
      Mists of Uniform Drop Size by Means of Spinning Disk Type Sprayers",
      Proceedings of The Physical Society, Series B, Vol. 62, part 6,
      p 341 (June 1949).

(61) May, K. R., "An Improved Spinning Top Homogeneous Spray Apparatus",
      J. Applied Physics, 4, p 167 (1953).

(62) Renier, E. R., "The Spinning Disk Atomizer as a Source of Homogeneous
      Drops", S. M. Thesis, Ch. Eng. Dept. MIT (1952).

(63) Simpson, H. C., "The Combustion of Droplets of Heavy Liquid Fuels",
      Sc.D. Thesis, Ch. Eng. Depts. MIT (1954).

(64) Morgan, A. C., Cabot Corporation, Personal Communication (February 1965).

(65) Op. Cit., Walton, W. H. and W. C. Prewitt.

(66) MacCullough, G. H. and Timoshenko, S., "Elements of Strength of Materials", D. van Nostrand Company, Inc., New York (1955).

(67) Op. Cit., May, K. R.

(68) Op. Cit., Tesner, P. A. and V. F. Surovinin.

(69) Op. Cit., Narasimhan, K. S. and P. J. Foster

(70) Semenov, N. N., "Some Problems in Chemical Kinetics and Reactivity", translated by M. Boudant, Vol. 2, p 115, Princeton University Press, Princeton, New Jersey (1959).

(71) Chalmers, B., "Principles of Solidification", pp 68-90, Wiley and Sons, Inc., New York (1964).

(72) Place, E. R. and F. J. Weinberg, "The Nucleation of Flame Carbon by Ions and the Effect of Electric Fields", preprint for Eleventh Symposium (International) on Combustion.

(73) Op. Cit., Tesner, P. A. and V. F. Surovinin.

(74) Op. Cit., Homann, K. H. and H. G. Wagner (Tenth Symposium).

(75) Op. Cit., Homann, K. H. and H. G. Wagner (Eleventh Symposium).

(76) Op. Cit., Witt, A. E.

(77) Harling, D. F. and F. A. Heckman, Cabot Corporation, Personal Communication (September 1965).

(78) Kruyt, H. R., "Colloid Science", Vol. 1, Elsevier Publishing Company, Amsterdam, p 283 (1952).

(79) Ibid., p 286.

(80) Harling, D. F., Cabot Corporation, Personal Communication (September 1967).

(81) May, K. R., "The Measurement of Airborne Droplets by the Magnesium Oxide Method", J. of Appl. Physics, 27, p 128 (1950).

(82) Op. Cit., Gerald, C. F.

(83) Op. Cit., Simpson, H. C.

APPENDIX O

Biographical Note

The author was born in Kalamazoo, Michigan on July 4, 1938. He attended local schools until graduating from high school in June of 1956.

He entered Michigan State University in September 1956 and received a Bachelor of Science degree in June of 1960.

In June 1960, the author began work as a development engineer for Union Carbide Nuclear Company in Oak Ridge, Tennessee. In September of the same year, he married Barbara Jane Hegarty of Bangor, Michigan.

The author entered Massachusetts Institute of Technology in June of 1964 and received a Master of Science degree in Chemical Engineering in February 1966.

In February of 1966, he began work on his doctoral thesis. During that period he was financed by an N.S.F. Traineeship.

The author has accepted full-time employment with the Nuclear Materials and Equipment Corporation (NUMEC) of Apollo, Pennsylvania.